

# **The environment, diversity and activity of microbial communities in submarine freshwater springs in the Dead Sea**

**Dissertation**

Zur Erlangung des Grades eines  
Doktors der Naturwissenschaften  
- Dr. rer. nat. -

dem Fachbereich Geowissenschaften  
der Universität Bremen  
vorgelegt an

**Stefan Häusler**

Bremen, April 2014

Die vorliegende Arbeit wurde in der Zeit von November 2010 bis April 2014 am Max-Planck-Institut für Marine Mikrobiologie in Bremen angefertigt.

1. Gutachter: **Prof. Dr. Marcel M.M. Kuypers**
2. Gutachter: **Prof. Dr. Thorsten Dittmar**

Datum des Promotionskolloquiums: 16. Mai 2014

# Contents

<b>Summary</b> .....	<b>1</b>
<b>Zusammenfassung</b> .....	<b>3</b>
<b>Chapter 1</b> .....	<b>7</b>
Introduction.....	7
Motivation and objectives.....	23
<b>Overview of enclosed manuscripts</b> .....	<b>35</b>
<b>Chapter 2</b> .....	<b>39</b>
Microbial and chemical characterization of underwater fresh water springs in the Dead Sea	
<b>Chapter 3</b> .....	<b>105</b>
Microenvironments of reduced salinity harbor biofilms in Dead Sea underwater springs	
<b>Chapter 4</b> .....	<b>125</b>
Spatial distribution of diatom and cyanobacterial microbial mats in the Dead Sea is determined by response to rapid salinity fluctuations	
<b>Chapter 5</b> .....	<b>153</b>
Sulfate reduction and sulfide oxidation in extremely steep salinity gradients formed by freshwater springs emerging into the Dead Sea	
<b>Chapter 6</b> .....	<b>189</b>
Conclusions and perspectives	
<b>Contributed work</b> .....	<b>201</b>
<b>Acknowledgements</b> .....	<b>211</b>



## Summary

The Dead Sea, located at the border between Jordan, Israel and the Palestinian authority is one of the most hypersaline lakes on earth. Its waters contain a total dissolved salt concentration of up to  $348 \text{ g L}^{-1}$ , which is about 10 times higher than regular sea water. The lake is characterized by elevated concentrations of divalent cations ( $\sim 2 \text{ M Mg}^{2+}$  and  $\sim 0.5 \text{ M Ca}^{2+}$ ), which, in addition to the high salinity, form an extreme environment where only highly adapted microorganisms can survive.

This doctoral thesis describes the environment, diversity and activity of microbial communities in a novel ecosystem of submarine freshwater springs in the Dead Sea. These springs allow for the formation of diverse microbial mats in an otherwise hostile environment. Water chemistry analysis showed that these springs originate from the Judean Group Aquifer. However, their chemistry is altered along the subsurface flow path from the Aquifer to the Dead Sea due to microbial activity, mixing with interstitial brine in the sediment and dissolution and precipitation of minerals. Pyrosequencing of the 16S rRNA gene and community fingerprinting methods revealed that most of the spring sediment community originates from the Dead Sea sediments and not from the spring water.

Using a novel salinity mini-sensor and a flume system that simulates the spring water flow into the Dead Sea it was demonstrated in the second study, that microenvironments of reduced salinity are formed in sediments and around rocks in the springs. The presence of microbial mats in these unique microenvironments led to the conclusion that one of the main drivers of the abundant microbial life is a local salinity reduction. However, as shown by flow and salinity microsensor measurements, the locally decreased salinity is unstable due to frequent fluctuations in the spring water flow. Therefore, although the microorganisms inhabiting these environments are exposed to an overall reduced salinity, they have to cope with large and rapid salinity fluctuations in the range of minutes to hours.

The results of the third study showed that some of the microbial mats found in the spring area are either dominated by diatoms or unicellular cyanobacteria and are spatially

separated. Growth experiments showed that the local salinity reduction is sufficient to allow for growth of these phototrophs, however, the salinity fluctuations directly affect their distribution. This could be deduced from the observation that diatoms and cyanobacteria had different *in-vitro* recovery rates of photosynthetic activity following rapid salinity shifts. Furthermore, the high energy demand which is expected to result from the salinity fluctuations, limits phototrophic life to shallow water depths, where enough light is available, in this case less than 10 meters.

As shown in the fourth study, other microbial mats in the spring ecosystems were dominated by sulfide oxidizing bacteria (SOB), which were fueled by a flux of sulfide from the sediment below. However, sulfate reduction rates (SRR) in the spring surface sediment ( $<2.8 \text{ nmol cm}^3 \text{ day}^{-1}$ ), were too low to account for the sulfide flux determined by *in situ* microsensor measurements. In fact, isotopic analysis of coexisting sulfide and sulfate in the spring water showed that the reduced sulfur compounds are instead produced along the flow path. The sulfide flux, in combination with a locally reduced salinity and  $\text{O}_2$  supply from the Dead Sea water column are the driving factors for the abundant microbial biomass of SOB encountered in the springs.

Microbial mats in the Dead Sea are dominated by different types of microorganisms, ranging from different SOB genera, to cyanobacteria or diatoms. Differences in the availability of light, the mean salinity and the scale of salinity fluctuations at different spots are the main factors determining the dominating community and their spatial distribution. As reduced salinity in the spring ecosystems was shown to play an extremely important role in supporting life, it was surprising to discover that SRR in the Dead Sea sediment were higher than in the less-saline springs (up to  $10 \text{ nmol cm}^3 \text{ day}^{-1}$ ). While this indicates the presence of an unexpectedly active, extremely halophilic community of sulfate reducing bacteria (SRB) in the Dead Sea sediments, it also suggests that the extensive salinity fluctuations within the springs may limit the SRB populations due to the high energetic cost of osmoregulation in the dynamic system. Therefore while this thesis shows that the low salinity environment of the Dead Sea springs is advantageous for microbial life, the fluctuations within the environment bring their own set of challenges.

## **Zusammenfassung**

Das Tote Meer ist einer der salzhaltigsten Seen der Erde und liegt an der Grenze zu Jordanien, Israel und der Palästinensischen Autonomiebehörde. Mit Konzentrationen von bis zu  $348 \text{ g L}^{-1}$  an gelösten Salzen ist der Salzgehalt etwa zehnmal höher als in normalem Meerwasser. Der See zeichnet sich durch eine hohe Konzentration an zweiwertigen Kationen ( $\sim 2 \text{ M Mg}^{2+}$  und  $\sim 0,5 \text{ M Ca}^{2+}$ ) aus, die in Kombination mit der hohen Salinität einen extremen Lebensraum bilden, in dem nur sehr speziell adaptierte Mikroorganismen überleben können.

Die vorliegende Doktorarbeit beschreibt den Lebensraum, die Diversität und Aktivität von mikrobiellen Gemeinschaften in einem neu entdeckten Ökosystem von unterseeischen Süßwasserquellen im Toten Meer. Diese Quellen ermöglichen die Entstehung mikrobieller Matten in einer ansonsten lebensfeindlichen Umgebung. Chemische Wasseranalysen ergaben, dass die Quellen aus dem „Judean Group Aquifer“ gespeist werden. Durch mikrobielle Aktivität, die Vermischung mit interstitieller Sole im Sediment, sowie die Ausfällung und Auflösung von Mineralien verändert sich jedoch die chemische Zusammensetzung des Quellwassers entlang des unterirdischen Verlaufs vom Aquifer bis zum Toten Meer. Analysen der mikrobiellen Gemeinschaft durch Pyrosequenzierung des 16S rRNA Gens und Fingerprinting-Verfahren zeigten, dass ein Großteil der Organismen in den Sedimenten der Süßwasserquellen ihren Ursprung nicht im Quellwasser sondern in den Sedimenten des Toten Meeres selbst haben.

Mittels eines neuen Salinitäts-Minisensors und einem System, welches das Einströmen von Quellwasser ins Tote Meer simuliert, konnte in der zweiten Studie gezeigt werden, dass sich in den Sedimenten und um die Steine in den Quellen Mikromilieus mit reduzierter Salinität bilden. Die Präsenz von mikrobiellen Matten in diesen Milieus führt zu der Schlussfolgerung, dass die lokal reduzierte Salinität einer der Hauptfaktoren für das reichhaltige mikrobielle Leben ist. Wie durch Salinitäts- und Strömungsmessungen gezeigt wurde, ist die lokal reduzierte Salinität aufgrund häufiger Schwankungen der Quellwasserströmung jedoch äußerst instabil. Obwohl somit die Organismen einer durchschnittlich geringeren Salinität ausgesetzt sind, müssen sie mit extremen

Salinitätsschwankungen zurecht kommen, die im Bereich von wenigen Minuten bis hin zu Stunden variieren.

Die Ergebnisse der dritten Studie brachten hervor, dass einige der mikrobiellen Matten, die im Bereich der Süßwasserquellen gefunden wurden, entweder von Diatomeen oder von einzelligen Cyanobakterien dominiert werden, jedoch räumlich voneinander getrennt sind. Wie durch Wachstumsversuche gezeigt werden konnte, ist eine lokale Verringerung der Salinität ausreichend, um das Wachstum dieser phototrophen Organismen zu ermöglichen, wobei Schwankungen in der Salinität ihre Verteilung direkt beeinflussen. Dies konnte aus der Beobachtung gefolgert werden, dass Diatomeen und Cyanobakterien unterschiedliche *in vitro* Erholungsraten der photosynthetischen Aktivität nach schnellen Salinitätsschwankungen aufzeigten. Darüber hinaus beschränkt der hohe Energiebedarf, der voraussichtlich aus den extremen Salinitätsschwankungen folgt, phototrophes Leben auf geringe Wassertiefen, in denen ausreichend Licht vorhanden ist, in diesem Fall Wassertiefen  $< 10$  Meter.

Die vierte Studie zeigte, dass andere mikrobielle Matten im Quellökosystem von Schwefelwasserstoff oxidierenden Bakterien (SOB) dominiert sind, die durch einen Schwefelwasserstofffluss aus dem darunter liegendem Sediment gespeist werden. Sulfat-Reduktionsraten (SRR) im Oberflächensediment der Quellen ( $< 2,8 \text{ nmol cm}^{-3} \text{ Tag}^{-1}$ ) waren jedoch zu gering, um den Schwefelwasserstofffluss zu erklären, der mittels *in situ* Mikrosensormessungen bestimmt wurde. Tatsächlich zeigte die Isotopenanalyse von koexistierendem Schwefelwasserstoff und Sulfat im Quellwasser, dass die reduzierten Schwefelverbindungen entlang des Grundwasserflusses zwischen dem Aquifer und dem Toten Meer produziert werden. Die entscheidenden Faktoren, die zu der hohen mikrobiellen Biomasse an SOB führen, die in den Quellen vorgefunden wurde, sind eine Kombination aus der Versorgung mit Schwefelwasserstoff durch die Quellen, einer lokal reduzierten Salinität und der  $\text{O}_2$ -Versorgung aus der Wassersäule des Toten Meers.

Mikrobielle Matten im Quellsystem des Toten Meeres werden von unterschiedlichen Arten von Mikroorganismen dominiert, die von verschiedenen Gattungen von SOB zu Cyanobakterien oder Diatomeen reichen. Die wichtigsten Faktoren,



welche die dominierende Gemeinschaft von Mikroorganismen und ihre räumliche Verteilung an verschiedenen Quellwasseraustritten bestimmen, sind die Verfügbarkeit von Licht, die durchschnittliche Salinität und das Ausmaß der Salinitätsschwankungen. Wie gezeigt wurde, spielt die reduzierte Salinität im Quellenökosystemen eine äußerst wichtige Rolle bei der Unterstützung des Lebens in den mikrobiellen Matten - daher war es überraschend, dass SRR im hypersalinen Toten Meer Sediment höher waren, als im Sediment der weniger salzhaltigen Quellen (bis zu  $10 \text{ nmol cm}^3 \text{ Tag}^{-1}$ ). Dies weist zum einen auf das Vorhandensein einer unerwartet aktiven, extrem halophilen Gemeinschaft von Sulfat reduzierenden Bakterien (SRB) in den Sedimenten des Toten Meeres hin, und verdeutlicht zum anderen, dass die ausgeprägten Salinitätsschwankungen innerhalb der Quellen die SRB-Populationen aufgrund der hohen Energiekosten für die Osmoregulation in diesem dynamischen System begrenzen.

Wie diese Arbeit zeigt, ist der geringe Salzgehalt in den Quellen des Toten Meeres von großem Vorteil für mikrobielles Leben, wohingegen die Schwankungen innerhalb der Umgebung ihre eigenen Herausforderungen mit sich bringen.



# Chapter 1

## Introduction

### **Microbial life in hypersaline environments**

Most of the aquatic ecosystems on Earth are saline. Around 97% of the hydrosphere consists of oceanic waters (Berner 2012), which have an average salinity of about 35 g per liter total dissolved salts (TDS). Exceeding by far the salinity of normal seawater, hypersaline environments such as salt lakes (e.g. Great Salt Lake, Utah), lagoons or man-made evaporation ponds can be found all over the world, and are often a result of seawater evaporation. Thalassohaline brines are normally formed by the initial process of evaporation and therefore the ionic composition of the brines usually reflect the salt composition of seawater, with sodium chloride (NaCl) being the main salt component (Oren, 2013a, 2013c). Changes in the ionic composition occur once the solubility of different salt components has been exceeded. At first, small changes in the ionic composition occur during the precipitation of calcium carbonate as calcite ( $\text{CaCO}_3$ ) which starts at about 6 to 8 % total dissolved salts. Later on, calcium sulfate ( $\text{CaSO}_4$ ) starts to precipitate as gypsum at salt concentrations exceeding 120 to 150  $\text{g L}^{-1}$ , lowering the  $\text{Ca}^{2+}$  and sulfate concentrations in the brines. When evaporation proceeds and the TDS concentrations reach 300 to 350  $\text{g L}^{-1}$ , NaCl starts to precipitate as halite and the ionic composition changes greatly, leaving behind the more soluble  $\text{Mg}^{2+}$  and  $\text{K}^+$  ions. These brines, characterized by a substantially different ionic composition than seawater, are termed athalassohaline brines (Oren, 2013a, 2013c). The prime example of an athalassohaline brine is the Dead Sea, whose origin is discussed later in greater detail.

In the middle of the 19<sup>th</sup> century the possibility of life in such high saline environments was documented. During his cruise on the H.M.S. Beagle, Charles Darwin wrote about a salt lake in Patagonia: *“Parts of the lake seen from a short distance appeared*

---

*of a reddish color, and this perhaps was owing to some infusorial animalcula... How surprising it is that any creatures should be able to exist in brine, and that they should be crawling on crystals of sulphate of soda and lime!... Thus we have a little living world within itself, adapted to these inland lakes of brine”* (Darwin, 1860). Today we know that Archaea are often responsible for the red coloration of extreme hypersaline environments such as evaporation ponds or even the Dead Sea during certain periods (Oren, 2013a). Furthermore, we know that high saline adapted microorganisms are ubiquitous and that diverse prokaryotic and eukaryotic communities can be found in both thalassohaline and athalassohaline brines (Ventosa et al., 1998; Oren, 2002; Oren, 2013a). However, salinity is a strong determinant of microbial community structure and it has in fact been shown that salinity is the most important factor explaining global patterns of bacterial and archaeal distribution (Lozupone and Knight, 2007; Auguet et al., 2010). Although there are few microorganisms that can grow over a large salinity range from 0 to 32 % TDS (e.g. *Halomonas elongata*; Vreeland et al. 1980), the majority of organisms are restricted to grow in a certain salinity range. The most widely accepted classification of salt-loving (halophile) and salt-tolerant (halotolerant) microorganisms was provided by Kushner (1978, 1985) and was slightly modified by Oren (2013b). Depending on the amount of TDS required for growth, organisms are classified either as non- (< 0.2 M TDS), slight- (0.2-0.5 M TDS), moderate- (0.5 to 2.5 M TDS) or extreme-halophiles (2.5-5.2 M TDS). Organisms which tolerate up to 2.5 M TDS, but do not require high salt concentrations for growth are termed halotolerant or extremely halotolerant if they withstand salt concentrations exceeding 2.5 M. Halophilic and halotolerant microorganisms can be found over the complete phylogenetic tree of life in the bacterial, archaeal and eukaryotic domain (Ventosa et al., 1998; Oren, 2002; Oren, 2013a). Non- and slight halophilic organisms are usually represented by freshwater and marine microorganisms, respectively. Most moderate and extreme halophiles are found in subgroups of the *Proteobacteria*, the high and low G+C *Firmicutes* and in branches of *Cyanobacteria*-, *Bacterioidetes*- and *Spirocheates*. The most prominent example of extreme halophiles are Archaea of the order *Halobacteriales*, which are able to grow at salinities of, or close to NaCl saturation level (28-34%), but most of them are unable to grow below 10 to 15% TDS (Kushner, 1985;

---

Oren, 2006c). Within the eukaryotes, the unicellular green alga *Dunaliella* is a prime example of an extreme halotolerant organism, which is often encountered growing in hypersaline environments between 1 to 4 M NaCl (6 to 23 % TDS; Oren 2005).

In addition to the total salt concentration, the salt composition has an effect on microbial life. Divalent cations such as  $Mg^{2+}$  and  $Ca^{2+}$  possess a more destabilizing effect on biological macromolecules than monovalent ions such as  $Na^+$  (Hallsworth et al., 2007; Oren, 2013c). The degree of kosmotropic (stabilizing) and chaotropic (destabilizing) effects on proteins was first described by Hofmeister (1888) who noticed differences in the salting out effect of different ions on egg-white protein. The common view of this process is that competition between the ions and the proteins for water hydration and solvation leads to a higher or lower solubility of the proteins (Oren, 2013c). Chaotropes weaken electrostatic interactions and thereby destabilize biological macromolecules whereas kosmotropes strengthen electrostatic interactions (Hallsworth et al., 2007). Thus, different ions in solution possess antagonistic effects, which are evident when observing the growth tolerance of microorganisms to salt composition. For example, some halophilic Archaea can grow at  $MgCl_2$  concentrations of up to 2.5 M but only in the presence of significant amounts of NaCl (Mullakhanbhai and Larsen, 1975; Oren, 1983a). This demonstrates that not only the salt concentration but also its composition is a strong determinant of whether a microorganism can live in a saline environment. Recent studies of hypersaline brines at the bottom of the Mediterranean Sea suggested that in the absence of kosmotropic ions such as sodium, the upper limit for life in  $MgCl_2$  brines is 2.3 M (Hallsworth et al., 2007). However, microorganisms are exceptional in their ability to evolve mechanisms to cope with stress, for instance by their ability to synthesize compatible organic solutes acting as kosmotropes and thereby counteracting chaotropic effects (Hallsworth et al., 2003).

## **Adaptation to high and changing salt concentrations**

All microorganisms have to maintain a certain water activity in their cytoplasm to ensure proper functioning of their cellular machinery. Since all biological membranes are permeable to water, all microorganisms living in high salt environments have to keep a cytoplasm which is at least in isoosmotic equilibrium with the outer medium to prevent osmotic water loss (Brown, 1990). Therefore, halophilic and halotolerant microorganisms have evolved two very different strategies to equilibrate their cytoplasm to the osmotic strength of the surrounding environment: The “salt-in” strategy and the “compatible osmolyte” strategy.

The salt-in strategy is used by aerobic halophilic Archaea of the order *Halobacteriales* (Oren, 2006c), anaerobic halophilic Bacteria of the order *Halanaerobiales* (Oren, 2006b), *Salinibacter ruber* (Oren, 2006a), and as recently shown, by the purple sulfur bacterium, *Halorhodospira halophila* (Deole et al., 2013). These organisms accumulate high concentrations of inorganic ions (mainly  $K^+$ ) in their cytoplasm to achieve osmotic equilibrium. Generally, the intracellular ion concentrations are regulated by the use of specific ion pumps ( $Na^+/H^+$  antiporters). These pumps are operated over the cytoplasmic membrane, using the proton electrochemical gradient that is normally established by the respiratory electron transport (Oren, 2013a). Species containing bacteriorhodopsins can also use light energy for the direct generation of a proton electrochemical gradient (Oren, 2006b).

The continuous presence of high intracellular concentrations of ions generated by use of the salt-in strategy, interferes with essential electrostatic interactions of proteins and macromolecules, lowers the free water content in cells and increases hydrophobic interactions of proteins (Dennis and Shimmin 1997). Thus, the entire cellular machinery needs to be adapted to function in the presence of high salt concentrations. It appears that the adaptation used for this is an acidic proteome, which has an excess of acidic (aspartate and glutamate) over basic amino acids (lysine and arginine). These act to stabilize the proteins due to interactions of hydrated ions with the acidic side chains (Lanyi, 1974; Madern et al., 2000; Mevarech et al., 2000). An acidic proteome would lead to unstable

---

proteins in the presence of low salt concentrations and accordingly, some proteins of halophiles have been shown to function improperly at low salt concentrations (Lanyi, 1974; Madern et al., 2000; Mevarech et al., 2000).

The presence of an acidic proteome has been attributed to genetic drift (Deole et al. 2013). This means that microorganisms that have been using the salt-in strategy for long time periods (from an evolutionary perspective), such as halophilic Archaea, end up having a very acidic proteome and a strictly halophilic lifestyle. In contrast, organisms who have been utilizing the strategy for less time have varying levels of proteome acidity and maintain a broader range of salinities suitable for life. For example, *Halobacterium salinarum* has a more acidic proteome than *Halorhodospira halophila*, and accordingly can grow in a narrower range of salinities (Deole et al., 2013). This suggests that an extremely acidic proteome results from the use of the salt-in strategy but is not mandatory for its use. This is further supported by the genome analysis of members of the *Halanaerobiales* order, which use the salt-in strategy, but do not possess an unusually high excess of acidic amino acids (Bardavid and Oren 2012). Therefore the correlation between the salt-in strategy and the use of an acidic proteome is still not well understood (Oren, 2013b). Furthermore other factors may combine with an acidic proteomes, for example, proteases and chaperones which modify the proteome upon salt decrease have recently been identified in Archaea using the salt-in strategy (Vauclare et al. 2014).

The second strategy (“compatible osmolyte”) used to prevent water loss and achieve osmotic balance is the accumulation of “compatible” organic osmotic solutes in the cytoplasm. This strategy has been observed in halophilic Bacteria, Eukarya and in halophilic methanogenic Archaea. These osmolytes are compatible with the intracellular machinery and thus it is generally accepted that these organisms do not require the presence of specifically adapted proteins (Galinski, 1995; Ventosa et al., 1998; Oren, 2013a), however extracellular bound proteins may show an excess of acidic amino acids (Oren et al., 2005). These osmotic solutes are usually polar, uncharged, highly soluble or zwitterionic (Fig. 1). The list of such substances known to be synthesized by halophilic organisms is extensive and steadily growing (e.g. Reed 1986; Ventosa et al. 1998; Roberts

---

2005, Roberts 2006). Organic compatible osmolytes are chemically very diverse and belong to polyols, sugars, heterosidases, betains, amino acids, glutamine derivatives and ectoines (Fig. 1; Oren, 2007). Many organisms use a mixture of compatible solutes, rather than depending on a single compound (Galinski, 1995). According to the salt concentration of the surrounding medium the intracellular concentrations of these osmotic solutes can be adjusted as conditions change. Regulation of the solute concentrations can occur by *de novo* synthesis or, if the compounds are available, direct uptake from the medium (Galinski and Trüper, 1994; Oren, 2002; Oren, 2013a). The intracellular sodium concentration is kept low by sodium pumps ( $\text{Na}^+/\text{H}^+$  antiporters), actively pumping out invading sodium ions.

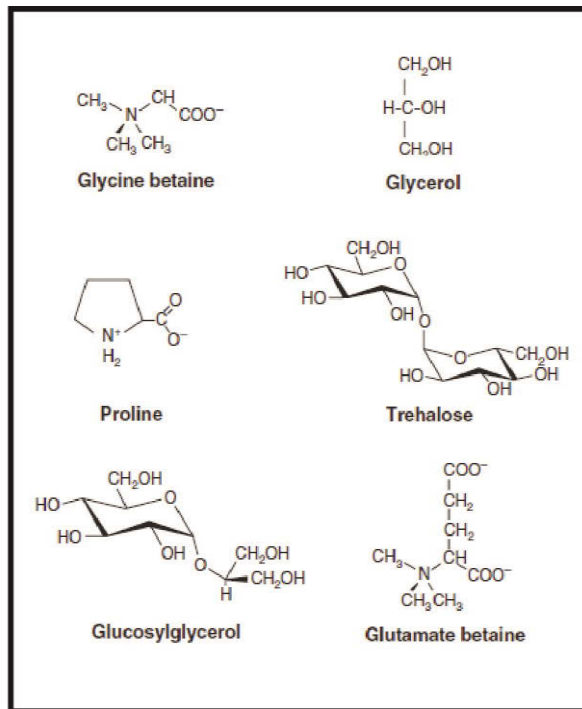


**Figure 1** Examples of common compatible osmolytes found in halophilic prokaryotic and eukaryotic microorganisms. (modified from Oren, 2007)

Life in high salt environments is energetically expensive regardless of the adaptation used. Both strategies involve the active extrusion of invading ions against a concentration gradient. However, organisms using the compatible solute strategy have to invest additional energy for the synthesis or uptake of organic compounds. Thus, the energetic costs of the salt-in strategy are relatively low when compared to the compatible solute strategy (Oren 1999, Oren 2011). Using laboratory and field data Oren (1999, 2011)



summarized the salinity range in which certain microbial processes have been observed to occur. Based on this data he proposed that the main factor determining whether a microorganism can live in high salt concentration is the amount of energy gained by its dissimilatory metabolism relative to the strategy of osmotic adaptation. According to this hypothesis most of the observations regarding the presence or absence of microbial processes can be explained. High energy yielding processes such as oxygenic and anoxygenic photosynthesis, and aerobic respiration can occur up to the NaCl saturation point, irrespective of their osmotic adaptation (Oren, 2011). On the other hand the survival at high salinity of microorganisms performing low energy yielding processes such as fermentation seems to require the use of the lower cost salt-in strategy, as used by Bacteria of the order *Halanaerobiales*. Therefore, organisms which use dissimilatory processes that deliver less energy and also use the high energy requiring osmolyte strategy (as is the case for most organisms), are therefore limited to a lower salinity range.

For instance, autotrophic nitrification seems to be limited to low salinity with the most halotolerant nitrifier described being *Nitrosococcus halophilus* (max. 94 g L<sup>-1</sup> NaCl; Koops et al. 1990). The relatively low energy gain of -274.6 kJ ( $\Delta G^{0'}$ ) of aerobic ammonia oxidation coupled with the high energy requirement for autotrophic CO<sub>2</sub> fixation presumably does not allow for nitrification at high salt concentrations; even though ammonia is abundant in most hypersaline environments (Oren, 1999, 2011). Organisms performing autotrophic oxidation of reduced sulfur compounds (sulfide, sulfur or thiosulfate) are observed to be more halotolerant than nitrifiers (e.g. *Thiohalospira halophila*, max. 290 g L<sup>-1</sup> NaCl; Sorokin et al. 2008) since the aerobic oxidation of H<sub>2</sub>S yields relatively high energy ( $\Delta G^{0'} = -797$  kJ). Another example are sulfate reducing bacteria which are either incomplete oxidizers or complete oxidizers. Incomplete oxidizers gain about 3 times more energy under standard conditions by the oxidation of substrates (e.g. lactate) to acetate ( $\Delta G^{0'} = -160.1$  kJ) when compared to complete oxidizers converting their substrates to CO<sub>2</sub> ( $\Delta G^{0'} = -47.7$  kJ). It makes sense therefore, that incomplete oxidizers are generally found to be more halotolerant than complete oxidizers (Oren, 1999, 2011).

---

Although the thermodynamic hypothesis seems to explain most of the observations of microbial growth at certain salinities there are exceptions (Oren, 2011). For instance, the discovery of a complete oxidizer (*Desulfosalsimonas propionica*; Kjeldsen et al., 2010) which uses propionate and reduces sulfate at a low energy yield ( $\Delta G^0 = -48.7$  kJ per 8 electrons) but still grows at salinities up to 200 g L<sup>-1</sup> TDS. Also the existence of *Natranaerobius*, a halophilic fermentative bacterium, which has increased intracellular K<sup>+</sup> concentrations yet still appears to use organic compatible solutes is hard to explain with thermodynamic considerations (Mesbah and Wiegel, 2008). Complicating matters further, it was recently shown by Deole et al. (2013) that two organisms of the same genus can use different osmoregulation strategies. Thus, thermodynamic calculations and predictions of the salinity growth range for certain metabolic processes might be biased when assuming the mode of osmoregulation from phylogenetically related organisms.

### **Why study hypersaline environments?**

As illustrated above, survival in hypersaline environments presents a number of challenges to organisms. Therefore, the investigation of halotolerant and halophilic organisms surviving in hypersaline environments provides fundamental insights into the understanding of life, as well into how organisms survive in extreme environments. In fact, the possibility that some forms of extremely early primordial life may have evolved in hypersaline environments has been raised (Dundas, 1998). In addition to this, the study of hypersaline environments can also be useful for practical applications. Although so far their use in biotechnological applications is rather limited (Oren, 2010), halophilic and halotolerant microorganisms produce a number of stable and unique biomolecules which can be used commercially. For instance, beta-carotene which is produced by *Dunaliella* strains is used as food additive, or ectoine from moderately halophilic bacteria can be utilized as enzyme protectant or moisturizer in cosmetic industry (Ben-Amotz et al. 1991; Oren 2010b). In addition, due to the halotolerance of many enzymes of halophilic microorganisms, these organisms can be used as source of novel hydrolytic enzymes for enzymatic transformations under extreme physical and chemical conditions (de Lourdes

Moreno et al., 2013). Last but not least, survival in extreme environments can yield insights into the possibility of life on other planets. For example, on Jupiter's moon Europa, it has been suggested that  $Mg^{2+}$  rich sub-surface oceans exist (Marion et al., 2003) and that there was seasonal flow of  $Mg^{2+}$ - $Na^+$ - $Ca^+$ - $Cl^-$  brines on Mars (McEwen et al., 2011). Thus, research in hypersaline environments can yield significant information for disciplines ranging from paleobiology over biotechnology to astrobiology.

In contrast to microorganisms which can adapt to high saline environments as described above, the extreme salinity in hypersaline environments strongly reduces the survival of higher organisms and thus lowers the predation pressure on the microorganisms (Javor and Castenholz 1984; Cohen 1989; Farmer 1992). As a result, microorganisms can create densely populated biofilms which eventually form microbial mats with thickness varying from millimeters to meters (Stal 2012).

### **Hypersaline microbial mats**

Microbial mats are remarkable ecosystems which can be inhabited by diverse functional groups of microorganisms. Modern microbial mats are considered to be recent analogues of lithified ancient microbial mats, which are preserved in the fossil record as stromatolites (Walter 1992). Thus the study of modern microbial mats, their biogeochemistry and community may provide insights into the early stages of life and their environment (Castenholz, 1994; Des Marais, 1995, 2003).

Usually hypersaline microbial mats are dominated by phototrophic cyanobacteria and diatoms, phototrophic and chemolithotrophic sulfur bacteria, heterotrophic bacteria and sulfate reducing bacteria (Van Gemerden 1993; Des Marais 1995). The microorganisms usually show a typical zonation within the microbial mat which is a result of physicochemical gradients developed by the availability of light, supply of substrates and the metabolic activity of the different microorganisms. Insights into the chemical gradients of microbial mats are best obtained by microsensors, small probes with a tip diameter of 1 to 20  $\mu m$  that minimally disturb microenvironments (Revsbech and

---

Jørgensen 1986), and thus have been used in numerous studies on microbial mats (e.g. Revsbech et al. 1981; Wieland and Kühl 2000; Abed et al. 2006).

Figure 2 presents an overview of the major biogeochemical cycles and organisms found in hypersaline microbial mats, focusing on those which lead to steep vertical gradients of oxygen and sulfide. Cyanobacteria and diatoms are usually the main primary producers located at the surface of the mat due to the availability of light. They drive the activities of the remaining microbial community by the process of photosynthesis, producing oxygen and organic matter during day light (Van Gernerden, 1993; Castenholz, 1994). The organic matter is remineralized by aerobic heterotrophic bacteria leading to oxygen depletion and the regeneration of  $\text{CO}_2$  which is subsequently reused by autotrophs. The organic matter produced in the photic zone also fuels the community inhabiting the

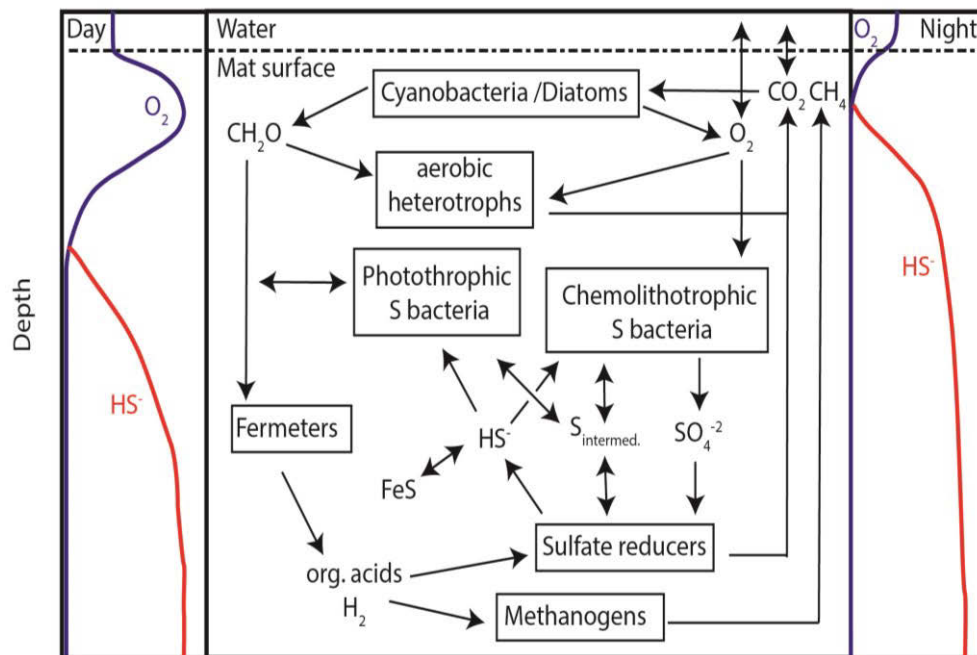


**Figure 2** Scheme of a hypersaline microbial mat with depth gradients of oxygen and sulfide shown in relative concentrations. Boxes represent functional groups of microorganisms, and arrows represent the flow of chemical species produced or consumed by individual groups.  $\text{S}_{\text{intermed.}}$  represents chemical species of sulfur (e.g.  $\text{S}^0$ ). Scheme on the left and right depicts relative oxygen and sulfide depth profiles typically obtained by microsensors measurements during the day and night, respectively. Relative depth can vary between mm to cm depending on the thickness of the microbial mat. Scheme modified from Fenchel and Finlay (1995) and Des Marais (2003).

anoxic layers of the microbial mat where dissimilatory sulfate reduction is the main anaerobic process for carbon mineralization (Jørgensen et al., 1992; Canfield and Des Marais, 1993). Fermentation by anaerobic fermentative bacteria is tightly coupled to dissimilatory sulfate reduction and methanogenesis via the production and consumption of small organic compounds or H<sub>2</sub> (Jørgensen et al., 1992). Hydrogen sulfide produced by the sulfate reducing bacteria is in turn aerobically consumed by chemolithotrophic sulfur bacteria, which occupy the oxygen-sulfide interface. In addition, sulfide can be consumed in the light by photolithotrophic anoxygenic phototrophs (e.g. purple sulfur bacteria, green sulfur and green non sulfur bacteria) leading to light and oxygen controlled competition between chemolithotrophic and phototrophic sulfur bacteria (Jørgensen and Des Marais, 1986). Often, phototrophic sulfur bacteria have a competitive advantage due to their versatile metabolism which can include photoautotrophy and chemoheterotrophy (Hanada and Pierson, 2006). The production and consumption of various intermediate sulfur species (e.g. S<sup>0</sup>, HS<sub>2</sub>O<sub>3</sub>) by different groups of microorganisms and the involvement of various chemical processes, e.g. chemical sulfide oxidation or iron sulfide formation results in a complex sulfur and oxygen cycle within a microbial mat (e.g. Canfield and Des Marais 1993; Van Gemerden 1993). Light plays an important role in determining this complex cycling as it can strongly influence oxygen and sulfide availability and therefore diel variations are commonly observed. During the day, photosynthesis leads to a buildup of oxygen supersaturation and thus, shifts the oxygen-sulfide interface deeper, whereas during night oxygen consumption leads to lower oxygen penetration depths and sulfide accumulates and rises up to the mat surface (Jørgensen et al., 1979). Versatile metabolisms and in some cases the motility of organisms enables the microorganisms to survive in such fluctuating environments.

The zonation of microorganisms is however not strict and overlap between zones can occur. Sulfate reducing bacteria for instance have been shown to be abundant and even active in the oxygen saturated zones of microbial mats (Jonkers et al., 2005; Fourçans et al., 2008). Furthermore, depending on physicochemical parameters, microbial mats can be dominated by different physiological groups. Especially in cold or hot springs, microbial mats may be dominated by chemolithotrophic colorless sulfide oxidizing bacteria or green

---

non sulfur bacteria (e.g. *Chloroflexus*) depending on temperature or sulfide concentrations (Jørgensen and Nelson, 1988; Camacho et al., 2005).

Microorganisms build up extremely high biomass in microbial mats, and as illustrated in the previous sections they are exceptional in adapting to extreme conditions, leading to mats occurring even in fluctuating hypersaline environments such as in intertidal areas (Abed et al., 2006; Kohls et al., 2010). However, there are still environments which so far have been assumed to be too extreme for mat formation to occur. One such example is the Dead Sea, however as this thesis will show, even there, microbial mats can thrive in unusual conditions.

## The Dead Sea

The Dead Sea is one of the most hypersaline lakes in the world as it contains about 347 g L<sup>-1</sup> total dissolved salts with an unusual ionic composition: The main cations are magnesium (about 2 M), sodium (about 1.5 M), calcium (about 0.5 M) and potassium (about 0.2 M) whereas the main anion is chloride (about 6.5 M; Oren 2010a). The water is extremely dense with a specific gravity of 1.24 g ml<sup>-1</sup> (Ionescu et al., 2012). Located in one of the rhomb-shaped grabens of the Dead Sea transform fault, the Dead Sea's geochemical history can be divided into a marine lagoon period and a saline lake period (Katz and Starinsky, 2009). In the lagoon stage, Pliocene Mediterranean seawater entered the Dead Sea basin and was concentrated by evaporation. By the process of dolomitization (exchange of Mg<sup>2+</sup> with Ca<sup>2+</sup> of limestone), most of the Mg<sup>2+</sup> of the Mg<sup>2+</sup>-enriched brines was exchanged with upper cretaceous limestone leaving behind a Ca<sup>2+</sup>-chloridic solution. Frequent mixing with ancient Mediterranean seawater and freshwater led to various chemical changes of the brine. Around 135,000 years before present (BP) the lagoon disconnected from the sea at which point the ongoing lacustrine era began. This resulted in the formation of a Dead Sea basin lake known as Lake Lisan in the period between 70,000 to 15,000 years BP. This lake occupied the area between the Sea of Gallilee and 25 km south of the southern end of the current Dead Sea (Kaufman et al., 1992; Schramm et al.,

2000). During this time the lake level fluctuated between 450 and 160 meters below sea level and reflected the regional climatic and hydrological conditions, with salinities ranging from 90 to 340 g L<sup>-1</sup> (Katz and Starinsky, 2009). Frequent and sometimes long-lasting stratification of the lake as a result of freshwater input was normal and can be seen in the sediment record where aragonite and detritus layers alternate. Dissolved bicarbonate was brought in by freshwater and precipitated in the Ca<sup>2+</sup> saturated brines as aragonite during stages of stratification, whereas detritus was brought in during holomictic (non-stratified) stages. The ionic composition of the lake changed over time, presumably as a result of mixing with freshwater, the precipitation of CaCO<sub>3</sub> and CaSO<sub>4</sub> by the import of HCO<sub>3</sub><sup>-</sup> and SO<sub>4</sub><sup>2-</sup>, and the inflow of saline springs evaporating together with the lake water (Katz and Starinsky, 2009).

Nowadays, the Dead Sea covers an area of about 630 km<sup>2</sup> and consists of a >300 meter deep northern basin and a shallow southern basin, which is occupied by a series of evaporation ponds. The surface of the Dead Sea (currently 423 meters below mean sea level) is the lowest exposed surface on earth. Since the beginning of the 20<sup>th</sup> century the water budget of the lake has been negative and started to decline even more rapidly in the 1960s due to large irrigation projects and the diversion of drinking water from the Jordan river (Oren, 2010). In addition, about 400 to 450 million m<sup>3</sup> Dead Sea water is pumped annually out from the northern basin into evaporation ponds for industrial salt production. After the extraction of potassium and bromide the end-brines mainly consisting of magnesium, calcium and chloride are pumped back into the Dead Sea (Oren, 2010).

The negative water budget of the lake has led to a lake level drop of about one meter per year over the last decades which has only been interrupted by exceptionally rainy winters in 1980 and 1992 (Fig. 3a, Oren 2010). The loss of water has resulted in a change in the physical and chemical characteristics of the lake. In 1976, the shallow southern basin detached from the northern basin and dried out. In 1979, the salinity of the entire lake had increased to about 340 g L<sup>-1</sup>, which caused the lake to overturn. This ended a century long lasting meromictic (stratified) phase of the lake, which was characterized by an oxic upper and anoxic lower water mass (Steinhorn et al., 1979). Since 1983, the lake has been

---

holomictic, with a seasonal stratification in summer due to evaporation and a possible overturn in November when the surface layer cools down (Anati et al., 1987; Anati and Stiller, 1991). As a result of the negative water budget, the ionic composition of the lake has also changed. NaCl has started to precipitate as halite at the lake bottom leaving behind the more soluble  $Mg^{2+}$  ions (Fig 3b, Oren 2010).

### **Microorganisms in the Dead Sea**

Over a vast period of human history the Dead Sea has been considered to be sterile mainly because it was thought to be too saline to sustain any form of life. The Madaba mosaic from the 6<sup>th</sup> century illustrates fish entering the Dead Sea by the Jordan River and either dying or trying to escape the salty water by swimming upstream (Nissenbaum, 1975). During the 19<sup>th</sup> and beginning of 20<sup>th</sup> century no organisms were detected in studies conducted by Gay-Lusac in 1819, Ehernberg in 1848 and Barrios in the mid-1880s (Ventosa et al., 1999). Finally, in the late 1930s, Benjamin Elazari-Volcani (Wilkansky at that time) discovered “Life in the Dead Sea” (Wilkansky, 1936) and later on published a number of studies documenting the presence of the unicellular green algae *Dunaliella*, several types of bacteria, and amoeboid and ciliate protozoans (Elazari-Volcani, 1940, 1943a, 1943b, 1944). Since then protozoa have never been documented again in the Dead Sea, possibly because at the time of those studies the Dead Sea was about 20 % less saline than today (Oren, 2010). Since Elazari-Volcani’s investigations, a number of halophilic Archaea, aerobic and anaerobic fermentative Bacteria from the water column and sediments of the Dead Sea have been isolated and characterized. Among these are a number of representatives of the extremely halophilic Archaea of the order *Halobacteriales* and anaerobic fermentative Bacteria of the order *Halanaerobiales* (Oren, 2010). Recent metagenomic studies in the water column of the Dead Sea have shown that the resident community consists mainly of halophilic Archaea, whereas no Bacteria were detected (Bodaker et al., 2010).

Some patterns of microbial community development have been documented in the Dead Sea, for example the exceptionally rainy winters in 1980 and 1992 led to a lake level

---



increase (Fig. 3a) and a dilution of the upper water layer. These dilution events were followed by the development of dense *Dunaliella* blooms (Fig. 3c) in which cell densities of  $8.8 \times 10^3$  (1980) and  $1.5 \times 10^4$  (1992) cells per mL were reached (Oren and Shilo, 1982; Oren and Gurevich, 1995). Except for these dilution events, *Dunaliella* cells have never been detected again since systematic monitoring started in 1980 (Oren, 2010). The cause of these algal blooms has been attributed to the dilution of Dead Sea water to at least 90% of its original salinity coupled to the input of phosphate which is considered to be the limiting nutrient (Oren and Shilo, 1985). The blooms of *Dunaliella* were followed by blooms of red halophilic Archaea, which lived on the organic substances produced by the photoautotrophic algae (Fig. 3d). Thus, peak densities of  $1.9 \times 10^7$  (1980, Oren 1983) and  $3.5 \times 10^7$  (1992, Oren and Gurevich 1995) developed a few weeks after the *Dunaliella* blooms (Fig. 3d). Nowadays the cell densities in the lake are low, with the latest determination showing a density below  $5 \times 10^4$  cells per mL (Ionescu et al., 2012).

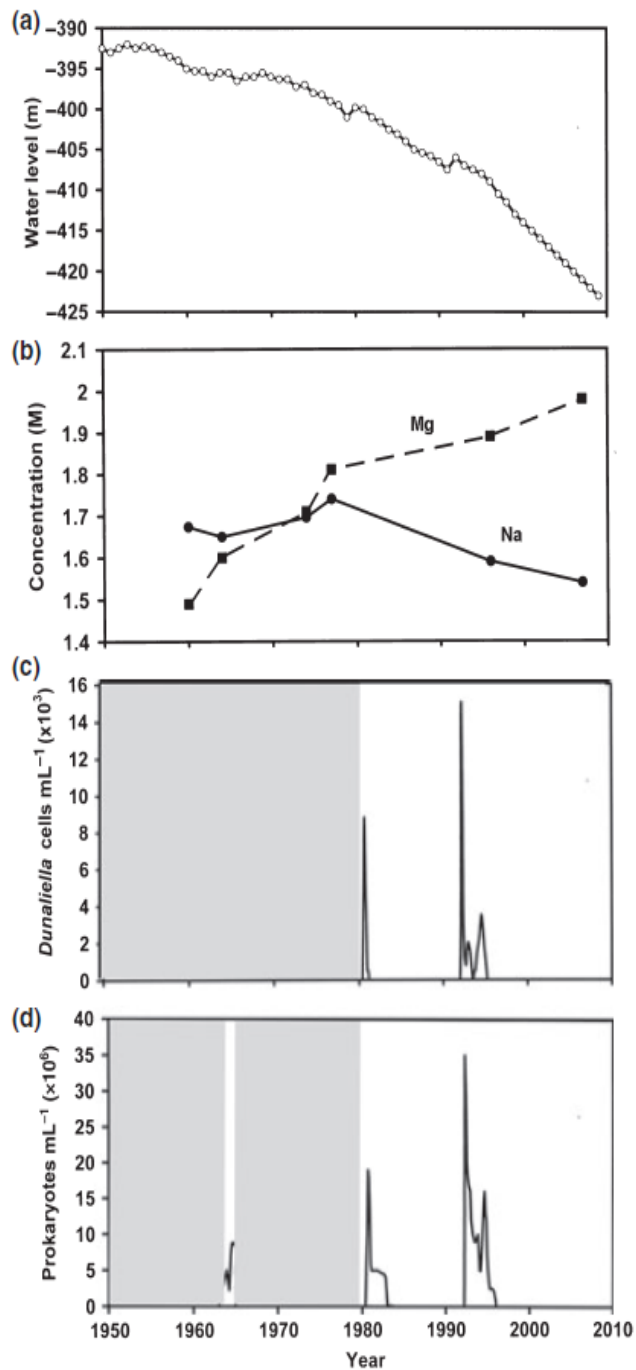


**Figure 3** (a) Surface water level, (b) magnesium and sodium concentrations in the surface water, (c) number of *Dunaliella* cells and (d) number of prokaryote cells in the surface water of the Dead Sea from 1950 to 2010. No data is available for some parts (shaded areas). Adapted from Oren, 2010.

## Motivation and objectives of this thesis

The Dead Sea area is generally rich in thermal springs which emerge along the shores of the lake (e.g. Qedem and Ein-Gedi springs). These include freshwater, saline and hypersaline springs, some of which harbor dense cyanobacterial communities (Ionescu et al., 2007, 2009). Observations of water ripples on the Dead Sea water surface in certain areas on the west coast indicate that subsurface groundwater discharge also occurs in the Dead Sea (Fig.4).



**Figure 4** Image showing the surface view on submarine water discharge taken from the shore of the Dead Sea.

Thus, considering that surface springs of the Dead Sea are inhabited by microbial communities and also that microbial blooms can develop on occasions when the hostile brines are diluted; it was intriguing to search for microbial life at the sites of submarine groundwater discharge. Following preliminary results obtained during the first discovery of the springs in 2009 and 2010 by Danny Ionescu, the following questions were developed and addressed in this thesis:

---

- 1) What is the source and the chemical composition of the spring water and what kind of microorganisms inhabit the spring ecosystems? (Chapter 2)
- 2) Is life in the springs supported by a local reduction in salinity? (Chapter 3)
- 3) Are the phototrophic organisms detected in the system active and what determines their spatial distribution? (Chapter 4)
- 4) Are the sulfide oxidizing and sulfate reducing bacteria in the spring system active and do they maintain an internal closed cycle? (Chapter 5)

These research questions were addressed using a combination of different techniques: Microbial community structure was assessed by molecular tools including 16S rRNA gene pyrosequencing, ARISA fingerprinting and as well as Fluorescent *In Situ* Hybridization (FISH). This data was analyzed in light of the hydrology and biogeochemistry of the system. Salinity microenvironments were measured with a novel salinity mini-sensor, both *in situ* as well as within a flume mimicking spring water flow. In combination with these, cultures of diatoms and cyanobacteria from the spring system were enriched. These allowed the metabolic activity and the response of photosynthesis to fast salinity fluctuations to be investigated using microsensor measurements. The biogeochemistry of the spring water was determined by chemical water analysis including the analysis of sulfur stable isotope composition. To determine the sources and sinks of sulfur compounds, sulfide was measured *in situ* with microsensors, while sulfate reduction rates were determined with radioisotopes *ex situ*.

## References

- Abed, R.M.M., Polerecky, L., Al Najjar, M., and De Beer, D. (2006) Effect of temperature on photosynthesis, oxygen consumption and sulfide production in an extremely hypersaline cyanobacterial mat. *Aquat. Microb. Ecol.* **44**: 21–30.
- Anati, D.A. and Stiller, M. (1991) The post-1979 thermohaline structure of the Dead Sea and the role of double-diffusive mixing. *Limnol. Oceanogr.* **36**: 342–354.
- Anati, D.A., Stiller, M., Shasha, S., and Gat, J.R. (1987) Changes in the thermo-haline structure of the Dead Sea 1979-1984. *Earth Planet. Sci. Lett.* **84**: 109–121.
- Auguet, J.-C., Barberan, A., and Casamayor, E.O. (2010) Global ecological patterns in uncultured Archaea. *ISME J.* **4**: 182–190.
- Bardavid, R. E., & Oren, A. (2012). The amino acid composition of proteins from anaerobic halophilic bacteria of the order Halanaerobiales. *Extremophiles*, **16**: 567–572
- Bodaker, I., Sharon, I., Suzuki, M.T., Feingersch, R., Shmoish, M., Andreishcheva, E., et al. (2010) Comparative community genomics in the Dead Sea: an increasingly extreme environment. *Isme J.* **4**: 399–407.
- Brown, A.D. (1990) Microbial water stress physiology. Principles and perspectives. John Wiley & Sons, Chinchester.
- Camacho, A., Rochera, C., Silvestre, J.J., Vicente, E., and Hahn, M.W. (2005) Spatial dominance and inorganic carbon assimilation by conspicuous autotrophic biofilms in a physical and chemical gradient of a cold sulfurous spring: the role of differential ecological strategies. *Microb. Ecol.* **50**: 172–184.
-

- 
- Canfield, D.E. and Des Marais, D.J. (1993) Biogeochemical cycles of carbon, sulfur, and free oxygen in a microbial mat. *Geochim. Cosmochim. Acta* **57**: 3971–3984.
- Castenholz, R.W. (1994) Microbial mat research: the recent past and new perspectives. In, *Microbial Mats*. Springer, Berlin-Heidelberg, pp. 3–18.
- Darwin, C. (1860) Naturalist's Voyage round the World. *J. Res. into Nat. Hist. Geol. Ctries. Visit. Dur. Voyag. HMS Beagle Round World.*, Random House LLC, New York, 2010
- Deole, R., Challacombe, J., Raiford, D.W., and Hoff, W.D. (2013) An extremely halophilic proteobacterium combines a highly acidic proteome with a low cytoplasmic potassium content. *J. Biol. Chem.* **288**: 581–588.
- Dundas, I. (1998) Was the environment for primordial life hypersaline? *Extremophiles* **2**: 375–377.
- Elazari-Volcani, B. (1944) A ciliate from the Dead Sea. *Nature* **154**: 355.
- Elazari-Volcani, B. (1943a) A dimastigamoeba in the bed of the Dead Sea. *Nature* **152**: 301–302.
- Elazari-Volcani, B. (1940) Algae in the bed of the Dead Sea. *Nature* **145**: 975.
- Elazari-Volcani, B. (1943b) Bacteria in the bottom sediments of the Dead Sea. *Nature* **152**: 274–275.
- Fenchel, T. and Finlay, B.J. (1995) Ecology and evolution in anoxic worlds. Oxford University Press, Oxford.
- Fourçans, A., Ranchou-Peyruse, A., Caumette, P., and Duran, R. (2008) Molecular analysis of the spatio-temporal distribution of sulfate-reducing bacteria (SRB) in Camargue (France) hypersaline microbial mat. *Microb. Ecol.* **56**: 90–100.
-

- 
- Galinski, E.A. (1995) Osmoadaptation in bacteria. *Adv. Microb. Physiol.* **37**: 273–328.
- Galinski, E.A. and Trüper, H.G. (1994) Microbial behaviour in salt-stressed ecosystems. *FEMS Microbiol. Rev.* **15**: 95–108.
- Van Gemerden, H. (1993) Microbial mats: a joint venture. *Mar. Geol.* **113**: 3–25.
- Hallsworth, J.E., Prior, B.A., Nomura, Y., Iwahara, M., and Timmis, K.N. (2003) Compatible solutes protect against chaotrope (ethanol)-induced, nonosmotic water stress. *Appl. Environ. Microbiol.* **69**: 7032–7034.
- Hallsworth, J.E., Yakimov, M.M., Golyshin, P.N., Gillion, J.L.M., D’Auria, G., De Lima Alves, F., et al. (2007) Limits of life in MgCl<sub>2</sub> containing environments: chaotropicity defines the window. *Environ. Microbiol.* **9**: 801–813.
- Hanada, S. and Pierson, B.K. (2006) The family chloroflexaceae. In, *The prokaryotes*. Springer, pp. 815–842.
- Hofmeister, F. (1888) Zur Lehre von der Wirkung der Salze. *Arch. für Exp. Pathol. und Pharmakologie* **25**: 1–30.
- Ionescu, D., Oren, A., Hindiyeh, M.Y., and Malkawi, H.I. (2007) The thermophilic cyanobacteria of the Zerka Ma’in thermal springs in Jordan. In, *Algae and cyanobacteria in extreme environments*. Springer, pp. 411–424.
- Ionescu, D., Oren, A., Levitan, O., Hindiyeh, M., Malkawi, H., and Berman-Frank, I. (2009) The cyanobacterial community of the Zerka Ma’in hot springs, Jordan: morphological and molecular diversity and nitrogen fixation. *Arch. Hydrobiol. Suppl. Algol. Stud.* **130**: 109–124.
- Ionescu, D., Siebert, C., Polerecky, L., Munwes, Y.Y., Lott, C., Haeusler, S., et al. (2012) Microbial and Chemical Characterization of Underwater Fresh Water Springs in the Dead Sea. *PLoS One* **7**: 21.
-

- 
- Jonkers, H.M., Koh, I.-O., Behrend, P., Muyzer, G., and De Beer, D. (2005) Aerobic organic carbon mineralization by sulfate-reducing bacteria in the oxygen-saturated photic zone of a hypersaline microbial mat. *Microb. Ecol.* **49**: 291–300.
- Jørgensen, B.B. and Des Marais, D.J. (1986) Competition for sulfide among colorless and purple sulfur bacteria in cyanobacterial mats. *FEMS Microbiol. Lett.* **38**: 179–186.
- Jørgensen, B.B. and Nelson, D.C. (1988) Bacterial zonation, photosynthesis, and spectral light distribution in hot spring microbial mats of Iceland. *Microb. Ecol.* **16**: 133–147.
- Jørgensen, B.B., Nelson, D.C., and Ward, D.M. (1992) Chemotrophy and decomposition in modern microbial mats. *Proterozoic Biosph. A Multidiscip. Study. Cambridge Univ. Press. Cambridge* 287–293.
- Jørgensen, B.B., Revsbech, N.P., Blackburn, T.H., and Cohen, Y. (1979) Diurnal cycle of oxygen and sulfide microgradients and microbial photosynthesis in a cyanobacterial mat sediment. *Appl. Environ. Microbiol.* **38**: 46–58.
- Katz, A. and Starinsky, A. (2009) Geochemical History of the Dead Sea. *Aquat. Geochemistry* **15**: 159–194.
- Kaufman, A., Yechieli, Y., and Gardosh, M. (1992) Reevaluation of the lake-sediment chronology in the Dead Sea basin, Israel, based on new  $^{230}\text{Th}/^{232}\text{Th}$  dates. *Quat. Res.* **38**: 292–304.
- Kjeldsen, K.U., Jakobsen, T.F., Glastrup, J., and Ingvorsen, K. (2010) *Desulfosalsimonas propionica* gen. nov., sp. nov., a halophilic, sulfate-reducing member of the family Desulfobacteraceae isolated from a salt-lake sediment. *Int. J. Syst. Evol. Microbiol.* **60**: 1060–1065.
-



- 
- Kohls, K., Abed, R.M.M., Polerecky, L., Weber, M., and De Beer, D. (2010) Halotaxis of cyanobacteria in an intertidal hypersaline microbial mat. *Environ. Microbiol.* **12**: 567–575.
- Koops, H.-P., Böttcher, B., Möller, U.C., Pommerening-Röser, A., and Stehr, G. (1990) Description of a new species of *Nitrosococcus*. *Arch. Microbiol.* **154**: 244–248.
- Kushner, D.J. (1978) Life in high salt and solute concentrations: halophilic bacteria. *Microb. life Extrem. Environ.* 317–368.
- Kushner, D.J. (1985) The halobacteriaceae. In, *The Bacteria: a Treatise on Structure and Function*, New York. pp. 171-214.
- Lanyi, J.K. (1974) Salt-dependent properties of proteins from extremely halophilic bacteria. *Bacteriol. Rev.* **38**: 272.
- De Lourdes Moreno, M., Pérez, D., García, M.T., and Mellado, E. (2013) Halophilic bacteria as a source of novel hydrolytic enzymes. *Life* **3**: 38–51.
- Lozupone, C.A. and Knight, R. (2007) Global patterns in bacterial diversity. *Proc. Natl. Acad. Sci.* **104**: 11436–11440.
- Madern, D., Ebel, C., and Zaccai, G. (2000) Halophilic adaptation of enzymes. *Extremophiles* **4**: 91–98.
- Des Marais, D.J. (2003) Biogeochemistry of hypersaline microbial mats illustrates the dynamics of modern microbial ecosystems and the early evolution of the biosphere. *Biol. Bull.* **204**: 160–167.
- Des Marais, D.J. (1995) The biogeochemistry of hypersaline microbial mats. *Adv. Microb. Ecol.* **14**: 251.
-

- 
- Marion, G.M., Fritsen, C.H., Eicken, H., and Payne, M.C. (2003) The search for life on Europa: limiting environmental factors, potential habitats, and Earth analogues. *Astrobiology* **3**: 785–811.
- McEwen, A.S., Ojha, L., Dundas, C.M., Mattson, S.S., Byrne, S., Wray, J.J., et al. (2011) Seasonal flows on warm Martian slopes. *Science* **333**: 740–743.
- Mesbah, N.M. and Wiegel, J. (2008) Life at Extreme Limits. *Ann. N. Y. Acad. Sci.* **1125**: 44–57.
- Mevarech, M., Frolow, F., and Gloss, L.M. (2000) Halophilic enzymes: proteins with a grain of salt. *Biophys. Chem.* **86**: 155–164.
- Mullakhanbhai, M.F. and Larsen, H. (1975) *Halobacterium volcanii* spec. nov., a Dead Sea halobacterium with a moderate salt requirement. *Arch. Microbiol.* **104**: 207–214.
- Nissenbaum, A. (1975) The microbiology and biogeochemistry of the Dead Sea. *Microb. Ecol.* **2**: 139–161.
- Oren, A. (1983a) *Halobacterium sodomense* sp. nov., a Dead Sea halobacterium with an extremely high magnesium requirement. *Int. J. Syst. Bacteriol.* **33**: 381–386.
- Oren, A. (1983b) Population dynamics of halobacteria in the Dead Sea water column. *Limnol. Oceanogr.* **28**: 1094–1103.
- Oren, A. (1999) Bioenergetic aspects of halophilism. *Microbiol. Mol. Biol. Rev.* **63**: 334–348.
- Oren, A. (2002a) Molecular ecology of extremely halophilic Archaea and Bacteria. *FEMS Microbiol. Ecol.* **39**: 1–7.
- Oren, A. (2002b) Diversity of halophilic microorganisms: environments, phylogeny, physiology, and applications. *J. Ind. Microbiol. Biotechnol.* **28**: 56–63.
-

- 
- Oren, A. (2005) A hundred years of Dunaliella research: 1905–2005. *Saline Systems* **1**: 1–14.
- Oren, A. (2006a) The genera *Rhodothermus*, *Thermonema*, *Hymenobacter* and *Salinibacter*. In, *The prokaryotes*. Springer, New York. Springer, New York, pp. 712–738.
- Oren, A. (2006b) The order Haloanaerobiales. In, *The prokaryotes*. Springer, New York, pp. 809–822.
- Oren, A. (2006c) The order halobacteriales. In, *The prokaryotes*. Springer, New York, pp. 113–164.
- Oren, A. (2007) Diversity of Organic Osmotic Compounds and Osmotic Adaptation in cyanobacteria and algae. In, *Algae and Cyanobacteria in Extreme Environments*. Springer, pp. 639–655.
- Oren, A. (2010a) The dying Dead Sea: The microbiology of an increasingly extreme environment. *Lakes Reserv. Res. Manag.* **15**: 215–222.
- Oren, A (2010b) Industrial and environmental applications of halophilic microorganisms. *Environ. Technol.* **31**: 825–834.
- Oren, A. (2011) Thermodynamic limits to microbial life at high salt concentrations. *Environ. Microbiol.* **13**: 1908–1923.
- Oren, A. (2013a) Life at High Salt Concentrations. In, *The Prokaryotes-Prokaryotic Communities and Ecophysiology*. Springer Verlag - Berlin Heidelberg, pp. 421–440.
- Oren, A. (2013b) Life at high salt concentrations, intracellular KCl concentrations, and acidic proteomes. *Front. Microbiol.* **4**:
-

- 
- Oren, A. (2013c) Life in Magnesium-and Calcium-Rich Hypersaline Environments: Salt Stress by Chaotropic Ions. In, *Polyextremophiles*. Springer, pp. 215–232.
- Oren, A. and Gurevich, P. (1995) Dynamics of a bloom of halophilic archaea in the Dead Sea. *Hydrobiologia* **315**: 149–158.
- Oren, A., Larimer, F., Richardson, P., Lapidus, A., and Csonka, L.N. (2005) How to be moderately halophilic with broad salt tolerance: clues from the genome of *Chromohalobacter salexigens*. *Extremophiles* **9**: 275–279.
- Oren, A. and Shilo, M. (1985) Factors determining the development of algal and bacterial blooms in the Dead Sea: a study of simulation experiments in outdoor ponds. *FEMS Microbiol. Lett.* **31**: 229–237.
- Oren, A. and Shilo, M. (1982) Population dynamics of *Dunaliella parva* in the Dead Sea. *Limnology* **27**:
- Reed, R. (1986) Halotolerant and halophilic microbes. In, *Microbes in extreme environments*. Academic, London, pp. 55–81.
- Revsbech, N.P. and Jørgensen, B.B. (1986) Microelectrodes: their use in microbial ecology. *Adv. Microb. Ecol* **9**: 293–352.
- Revsbech, N.P., Jørgensen, B.B., and Brix, O. (1981) Primary production of microalgae in sediments measured by oxygen microprofile,  $\text{H}_4\text{CO}_3$  fixation, and oxygen exchange methods. *Limnol. Ocean.* **26**: 717–730.
- Roberts, M.F. (2006) Characterization of Organic Compatible Solutes of Halotolerant and Halophilic Microorganisms. *Methods Microbiol.* **35**: 615–647.
- Roberts, M.F. (2005) Organic compatible solutes of halotolerant and halophilic microorganisms. *Saline Systems* **1**: 1–30.
-

- 
- Schramm, A., Stein, M., and Goldstein, S.L. (2000) Calibration of the  $^{14}\text{C}$  time scale to 40 ka by  $^{234}\text{U}/^{230}\text{Th}$  dating of Lake Lisan sediments (last glacial Dead Sea). *Earth Planet. Sci. Lett.* **175**: 27–40.
- Sorokin, D.Y., Tourova, T.P., Muyzer, G., and Kuenen, G.J. (2008) *Thiohalospira halophila* gen. nov., sp. nov. and *Thiohalospira alkaliphila* sp. nov., novel obligately chemolithoautotrophic, halophilic, sulfur-oxidizing gammaproteobacteria from hypersaline habitats. *Int. J. Syst. Evol. Microbiol.* **58**: 1685–1692.
- Steinhorn, I., Assaf, G., Gat, J.R., Nishry, A., Nissenbaum, A., Stiller, M., et al. (1979) Dead Sea - Deepening of the mixolimnion signifies the overture to overturn of the water column. *Science* **206**: 55–57.
- Ventosa, A., Arahal, D.R., and Volcani, B.E. (1999) Studies on the microbiota of the Dead Sea — 50 years later. *Microbiol. Biogeochem. Hypersaline Environ.* 139–147.
- Ventosa, A., Nieto, J.J., and Oren, A. (1998) Biology of moderately halophilic aerobic bacteria. *Microbiol. Mol. Biol. Rev.* **62**: 504–544.
- Vreeland, R.H., Litchfield, C.D., Martin, E.L., and Elliot, E. (1980) *Halomonas elongata*, a new genus and species of extremely salt-tolerant bacteria. *Int. J. Syst. Bacteriol.* **30**: 485–495.
- Wieland, A. and Kühl, M. (2000) Short-term temperature effects on oxygen and sulfide cycling in a hypersaline cyanobacterial mat (Solar Lake, Egypt). *Mar. Ecol. Prog. Ser.* **196**: 87–102.
- Wilkansky, B. (1936) Life in the Dead Sea. *Nature* **138**: 467
-



## Overview of enclosed manuscripts

### *Chapter 2:*

#### **Microbial and Chemical Characterization of Underwater freshwater springs in the Dead Sea**

Danny Ionescu, Christian Siebert, Lubos Polerecky, Yaniv Y. Munwes, Christian Lott, Stefan Häusler, Mina Bižić-Ionescu, Christian Quast, Jörg Peplies, Frank Oliver Glöckner, Alban Ramette, Tino Rödiger, Thorsten Dittmar, Aharon Oren, Stefan Geyer, Hans-Joachim Stärk, Martin Sauter, Tobias Licha, Jonathan B. Laronne, Dirk de Beer

**Author contributions:** Experimental design: DI CS. Conducted experiments: DI CS YYM CL SH MBI TR TD. Data analysis: SH DI CS LP CQ. Contributed reagents/materials/analysis tools: CQ JP FOG AR AO SG HJS MS TL JBL DdB. Wrote the manuscript: DI CS LP CQ JP AR DdB.

Specifically, my main contribution to this manuscript involved the determination of general and phylum specific cell numbers in the spring waters and the Dead Sea. For this I performed fluorescence *in-situ* hybridization (FISH) and DNA staining. I have extensively analyzed the 454 sequencing data to choose appropriate FISH probes. Although, only little data is presented in the manuscript the adjustment of the protocol took 2 to 3 month due to extensive autofluorescence of the sediment. Additionally, I contributed in the cluster analysis of the 454 data. I performed hyperspectral imaging scans and analyzed the data obtained. During the fieldwork I preserved the spring water samples for dissolved organic matter extraction and took part in DNA extraction. Furthermore I took samples for phosphate, nitrate, and sulfide which I analyzed later. I wrote the method section of FISH and cell count analysis. Due to my extensive contribution to this manuscript it was included in this thesis.

**Published in PLoS ONE 7(6): e38319. doi:10.1371/journal.pone.0038319**

*Chapter 3:*

**Micoenvironments of reduced salinity harbour biofilms in Dead Sea underwater springs**

Stefan Häusler, Beatriz E. Noriega, Lubos Polerecky, Volker Meyer, Dirk De Beer, Danny Ionescu

**Author contributions:** Experimental design: SH DI. Conducted Experiments: SH BN. Data analysis: SH LP. Contributed reagents/materials/analysis tools: VM DdB LP. Wrote the manuscript: SH DI LP DdB.

**Published in Environmental Microbiology Reports (2014) 6: 152–158  
doi: 10.1111/1758-2229.12140**

*Chapter 4:*

**Spatial distribution of diatom and cyanobacterial microbial mats in the Dead Sea is determined by response to rapid salinity fluctuations**

Stefan Häusler, Miriam Weber, Dirk De Beer, Danny Ionescu

**Author contributions:** Experimental design: SH DI. Conducted experiments: SH MW DI. Data analysis: SH DI. Contributed reagents/materials/analysis tools: DdB. Wrote the manuscript: SH DI MW DdB.

**In preparation for submission to Extremophiles**



*Chapter 5:*

**Sulfate reduction and sulfide oxidation in extremely steep salinity gradients formed by freshwater springs emerging into the Dead Sea**

Stefan Häusler, Christian Siebert, Miriam Weber, Moritz Holtappels, Beatriz E. Noriega, Dirk De Beer, Danny Ionescu

**Author contributions:** Experimental design: SH DI. Conducted experiments: SH MW DI BN. Data analysis: SH DI MH CS BN. Contributed reagents/materials/analysis tools: CS MH DdB. Wrote the manuscript: SH DI CS MW DdB.

**Prepared for submission to FEMS Microbiology Ecology**



## Chapter 2

### Microbial and chemical characterization of underwater fresh water springs in the Dead Sea

Danny Ionescu<sup>1</sup>, Christian Siebert<sup>2</sup>, Lubos Polerecky<sup>1</sup>, Yaniv Y. Munwes<sup>3</sup>, Christian Lott<sup>1,4</sup>, Stefan Häusler<sup>1</sup>, Mina Bižić-Ionescu<sup>1,5</sup>, Christian Quast<sup>1</sup>, Jörg Peplies<sup>6</sup>, Frank Oliver Glöckner<sup>1,7</sup>, Alban Ramette<sup>1</sup>, Tino Rödiger<sup>2</sup>, Thorsten Dittmar<sup>1,8</sup>, Aharon Oren<sup>9</sup>, Stefan Geyer<sup>2</sup>, Hans-Joachim Stärk<sup>10</sup>, Martin Sauter<sup>11</sup>, Tobias Licha<sup>11</sup>, Jonathan B. Laronne<sup>3</sup>, Dirk de Beer<sup>1</sup>

<sup>1</sup>Max Planck Institute for Marine Microbiology, Bremen, Germany

<sup>2</sup>Department of Catchment Hydrology, Helmholtz-Centre for Environmental Research – UFZ, Halle / Saale, Germany

<sup>3</sup>Department of Geography & Environmental Development, Ben Gurion University of the Negev, Beer Sheva, Israel

<sup>4</sup>HYDRA Institute for Marine Sciences, Elba Field Station, Campo nell'Elba (LI), Italy

<sup>5</sup>Department of Stratified Lakes, Leibniz Institute of Freshwater Ecology and Inland Fisheries Berlin (IGB), Stechlin, Germany

<sup>6</sup>Ribocon GmbH, Bremen, Germany

<sup>7</sup>Jacobs University Bremen GmbH, Bremen, Germany

<sup>8</sup>Institute for Chemistry and Biology of the Marine Environment (ICBM), Carl von Ossietzky University, Oldenburg, Germany

<sup>9</sup>Department of Plant and Environmental Sciences, Institute of Life Sciences, The Hebrew University of Jerusalem, Jerusalem, Israel

<sup>10</sup>Department of Analytical Chemistry, Helmholtz-Centre for Environmental Research – UFZ, Leipzig, Germany

<sup>11</sup>Geoscientific Centre, University of Göttingen, Göttingen, Germany.

**Published in PLoS ONE 7(6): e38319.**

---

## **Abstract**

Due to its extreme salinity and high  $Mg^{2+}$  concentration the Dead Sea is characterized by a very low density of cells most of which are Archaea. We discovered several underwater fresh to brackish water springs in the Dead Sea harboring dense microbial communities. We provide the first characterization of these communities, discuss their possible origin, hydrochemical environment, energetic resources and the putative biogeochemical pathways they are mediating. Pyrosequencing of the 16S rRNA gene and community fingerprinting methods showed that the spring community originates from the Dead Sea sediments and not from the aquifer. Furthermore, it suggested that there is a dense Archaeal community in the shoreline pore water of the lake. Sequences of bacterial sulfate reducers, nitrifiers, iron oxidizers and iron reducers were identified as well. Analysis of white and green biofilms suggested that sulfide oxidation through chemolithotrophy and phototrophy is highly significant. Hyperspectral analysis showed a tight association between abundant green sulfur bacteria and cyanobacteria in the green biofilms. Together, our findings show that the Dead Sea floor harbors diverse microbial communities, part of which is not known from other hypersaline environments. Analysis of the water's chemistry shows evidence of microbial activity along the path and suggests that the springs supply nitrogen, phosphorus and organic matter to the microbial communities in the Dead Sea. The underwater springs are a newly recognized water source for the Dead Sea. Their input of microorganisms and nutrients needs to be considered in the assessment of possible impact of dilution events of the lake surface waters, such as those that will occur in the future due to the intended establishment of the Red Sea–Dead Sea water conduit.

## Introduction

The Dead Sea is a terminal lake located on the border between Jordan, the Palestinian Authority and Israel, and is part of a larger geological system known as the Jordan Dead Sea Rift. The lake consists of a deeper northern basin (deepest point at ~725 m below sea level) and a southern basin, which has dried out but is kept shallow by continuous transfer of water from the northern basin as it is used for commercial mineral production. Until 1979 the Dead Sea was a meromictic lake with hypersaline, anoxic and sulfidic deep waters and a seasonally varying mixolimnion (Anati et al., 1987). Since the beginning of the 20th century the water budget of the Dead Sea has been negative, leading to a continuous decrease in the water level (Anati et al., 1987; Oren, 2010). The extensive evaporation in the absence of major water input led to an increase in the density of the upper water layer, which caused the lake to overturn in 1979 (Steinhorn et al., 1979). Since then, except after two rainy seasons in 1980 and 1992, the Dead Sea remained holomictic and has been characterized by a NaCl supersaturation and halite deposition on the lake bottom, with total dissolved salt concentrations reaching 347 g L<sup>-1</sup>. Due to the continuous evaporation of the Dead Sea, Na<sup>+</sup> precipitates out as halite while Mg<sup>2+</sup>, whose salts are more soluble, is further concentrated and has become the dominant cation (Oren, 2010).

The increased salinity and the elevated concentration of divalent ions make the Dead Sea an extreme environment that is not tolerated by most organisms. This is reflected in a generally low diversity and very low abundance of microorganisms. The microbiology of the lake has been subject for research since the 1930s when Benjamin Elazari-Volcani (Wilkansky at the time) isolated the first microorganisms from the sediment of the Dead Sea (Wilkansky, 1936). Besides Bacteria and Archaea (Elazari-Volcani, 1940) these isolates included algae (Elazari-Volcani, 1943b), protozoa (Elazari-Volcani, 1943a) and ciliates (Elazari-Volcani, 1944). Since then, several Bacterial and Archaeal isolates have been obtained in culture, both from the sediment and from the water body (Oren, 2010). The general cell abundance in the Dead Sea water is very low (< 5 x 10<sup>4</sup> cells mL<sup>-1</sup>; this study), except for two blooms in 1980 and 1992, when after severe winters the upper meter

of the water column was diluted by 15-30%, floods provided an input of phosphate, and the cell concentrations reached  $20\text{-}35 \times 10^6$  cells mL<sup>-1</sup> (Oren and Gurevich, 1995).

Recently, we discovered a complex system of underwater springs in the Dead Sea. A more detailed exploration revealed that these springs harbor microbial communities with much higher diversity and cell density than reported to date for the Dead Sea, including dense biofilms covering sediments and rocks around the springs. In this study we provide the first description of these habitats and the associated microbial communities. Based on comparative analyses of the community structure and geochemical reconstruction of the spring water sources, we propose hypotheses about the main energy resources and metabolic pathways that drive these microbial ecosystems, as well as discuss their possible origins and environmental adaptations.

## **Material and Methods**

### **Site description**

The underwater springs are located in the Darga area on the western coast of the Dead Sea, and are divided into two systems (Fig. 1). The northern system (springs 1-5) consists of one or more springs at the bottom of deep steep-walled shafts (Fig. 2A). Often several such shafts are connected and form a large system that extends from shallow (~10 m) to deeper (~30 m) waters. The diameter and depth of each shaft can reach up to 15 and 20 m, respectively. The walls of the shafts are finely laminated (Fig. S1A). Groundwater emerges from either small seeps (~20 cm in diameter, Fig. S1B) or deeper shafts that are hidden within deeper cavities (Fig. S1C). The springs in the southern system (springs 10-12) do not form shafts. Instead, they are located at the bottom of steep walls descending directly from the water surface, and are covered by cobble (Fig. S1D). Uniquely in the southern system and in addition to the described springs, large water seeps without clear boundaries were also found, mostly at depths of more than 15 m. Detailed hydrological and geological maps of the area can be found in Laronne Ben-Itzhak and Gvritzman, (2005).

---

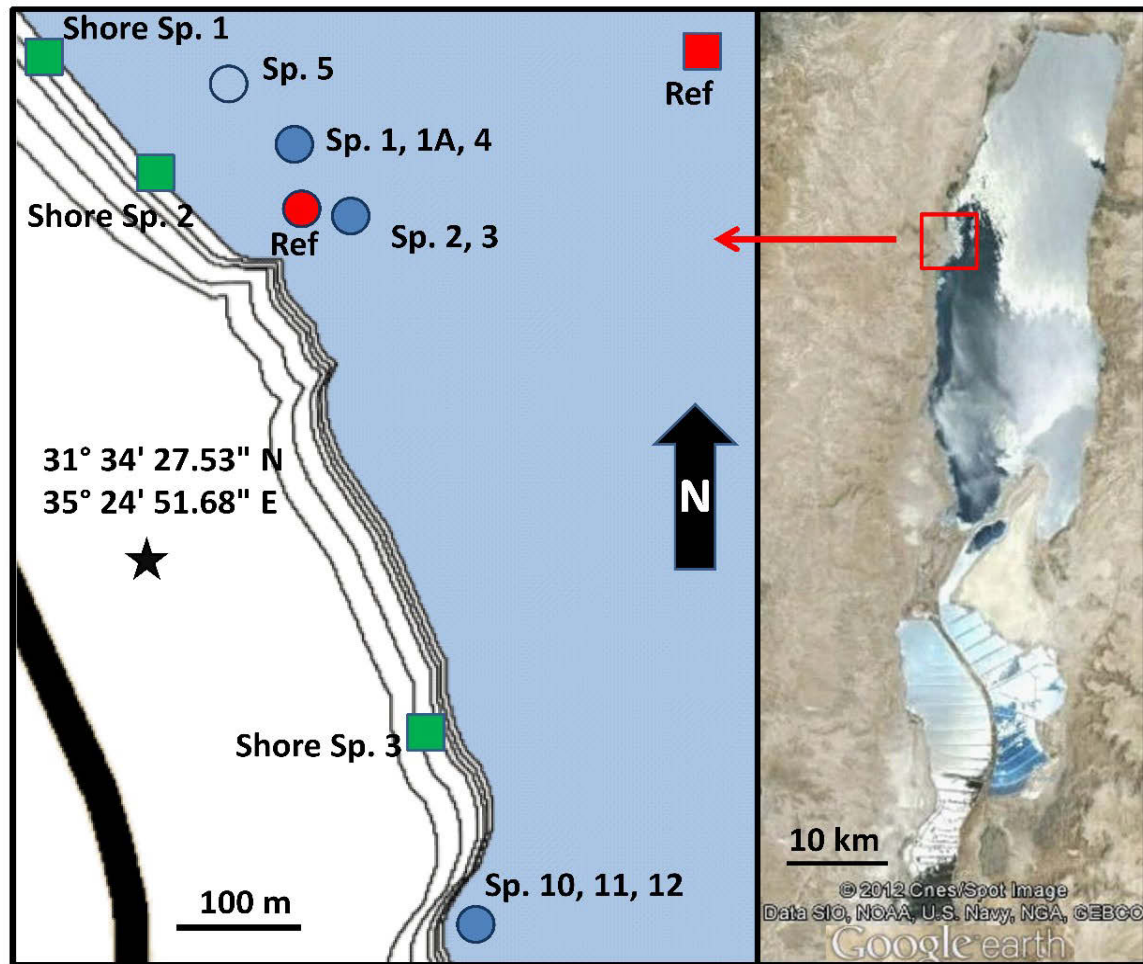


**Figure 1.** Locations of the sampling sites on the west coast of the Dead Sea, showing the northern and southern spring systems. Underwater springs with the corresponding reference site are marked with blue and red circles, whereas shore springs together with their reference site are marked with green and red squares, respectively. The open-water reference site for the shore springs was used only for comparison of dissolved organic matter (DOM) and total dissolved nitrogen (TDN). The open blue circle is located in the center of an underwater spring upwelling and was sampled for DOM and TDN analysis. The contour lines on the left panel represent the yearly drop in the lake level and are a close approximation of the areal topography. The satellite image was created using Google Earth.

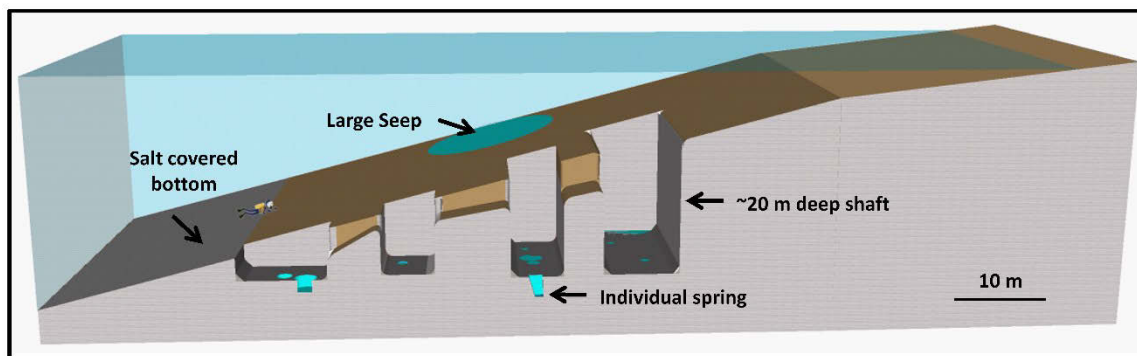


**Figure 2.** Sketch of the northern spring system. The water seep shown on the slope of the sketch is found only in deeper parts of the southern system where water seeps through the sediment surface over a large area without defined boundaries. The shafts have steep, laminated walls (see Fig. S1A) and contain one or more springs (blue). Localized water sources are either directly visible on the shaft bottom (Fig S1B) or are hidden within deeper cavities (Fig. S1C). In the southern spring system (not shown in the sketch) springs do not form shafts and are covered by cobbles (Fig. S1 D).

## Sampling

Sampling of underwater springs for the analysis of microbial diversity, cell counts, pigments and water chemistry took place in June 2010 (Table 1). Samples for sulfide, ammonium, and phosphate quantification as well as for the analysis of dissolved organic carbon (DOC) and total dissolved nitrogen (TDN) were additionally collected from the same springs in October 2011. Prior to sampling, springs were marked by SCUBA divers based on light refraction in the mixing zone of the groundwater and the ambient Dead Sea water. Sediment and microbial mat samples were collected by SCUBA divers in cores and sterile 50 mL tubes. Water samples from all springs except spring 5 were collected using a 40 m long hose connected to a peristaltic pump. A type K thermocouple cable was attached on the hose and connected to a thermometer (TM-747D, Tenmars, Taiwan) on the boat. Based on the difference in temperature, the submerged end of the pumping hose was placed into the spring by a SCUBA diver. Samples were collected once the density of the pumped water was stable and significantly lower than that of the Dead Sea, allowing several minutes (2-3 hose volumes) for washing of the hose with the spring water to minimize chemical and bacterial cross contamination. The pumping speed was kept low to prevent



uptake of sediments or of the ambient Dead Sea water. Approximately 10 L of water were pumped from each spring. A water sample from the underwater spring 5 was collected from the surface of the Dead Sea where the emerging spring water formed an upwelling due to its low density compared to the Dead Sea water. This sample is therefore to an unknown extent mixed with ambient Dead Sea water. To allow a comparison between the native Dead Sea microbial communities and those associated with the underwater springs, reference sediment samples were additionally collected from an area without groundwater seepage (Fig. 1, Red Circle).

To reveal the possible origin of the underwater spring water, samples for water chemistry analysis were collected from these auxiliary sites (Table 1): freshwater wells from the Upper and Lower Judea Group Aquifer (JGA); brackish springs emerging at the shore close to the sampling site at distances 1–90 m from the Dead Sea shore line (shore sp. 1-3 in Fig. 1); and shore springs in the Qedem area south of the sampling site, discharging hot brines from Lower Cretaceous or even Jurassic strata (Gvirtzman and Stanislavsky, 2000). Pore water from the Dead Sea Group (DSG) sediment next to the shore spring 3 was sampled at depth of 0.7 m, which was 0.3 m above the 2010 Dead Sea water level. The pore water was squeezed from a sediment core on site using a mechanical, stainless steel, screw press. Thus the pore water represents interstitial waters transported by gravity from the exposed DSG sediments towards the Dead Sea. The term Dead Sea Group sediments will be used here on to describe all sediments which at some point throughout the history of the Dead Sea, were covered by its water.

Dead Sea water for dissolved organic matter (DOC) and total dissolved nitrogen (TDN) analysis was sampled away from the shore (Fig. 1, Square ref). To prevent influence of coastal and underwater spring waters, the samples were collected from a depth of 5 m.

All samples were kept at 4 °C until further processing. Water samples for DNA extraction were filtered within 12 h, and the filters were kept at -20 °C until further analysis, whereas sediments and microbial mats were transferred to -20 °C within 24 h. The samples were transferred to Germany on dry ice for further processing.

---

Samples for water chemistry analysis were transported within 10 h of sampling to storage and 4 °C; however, brine samples were stored at ambient conditions to prevent salt crystallization. Storage conditions were maintained during shipping to Germany for further analysis. Samples for cation analysis were pre acidified on site.

**Table 1** Type of samples collected from the different underwater springs and auxiliary sites, and of analyses performed.

Site	Type of samples collected			Type of analysis			
	Water	Sediment	Biofilm	Pigments	FISH	Community*	Chemistry
Spring 1	+	+	–	–	+	+/+	+
Spring 1A	+	+	–	–	+	+/+	+
Spring 2	+	+	+	–	+	+/+	+
Spring 3	+	+	+	–	+	+/+	+
Spring 4	–	+	–	–	–	–/+	–
Spring 5	+	–	–	–	–	–	+
Spring 10	+	+	+	–	+	+/+	+
Spring 11	+	+	+	–	+	+/+	+
Spring 12	–	–	+	+	–	+/+	–
Shore Spring 1, 2, 3	+	–	–	–	–	–	+
Dead Sea Reference	–	+	–	–	–	+	–
Dead Sea Water	+	–	–	–	–	–	+
Auja 2, 4	+	–	–	–	–	–	+
Jericho 2, 5	+	–	–	–	–	–	+
Mitzpe Jericho 2	+	–	–	–	–	–	+
EinQilt 1, 2	+	–	–	–	–	–	+
Qedem brine	+	–	–	–	–	–	+
Porewater	+	–	–	–	–	–	+
Sample Code	W_SP#	S_SP#	(W/G)B_SP#				

The northern system (springs 1–5), southern system (springs 10–12) and auxiliary sites are shaded in light and dark grey respectively. Community analysis refers to 454 pyrosequencing and Automated Ribosomal Intergenic Spacer Analysis (ARISA), pigment analysis was done by hyper-spectral imaging. Auja and Jericho 5 wells represent waters from the Lower Judea Group Aquifer (Mekorot Co., personal comm.), whereas Mitzpe Jericho 2 and Qilt springs represent waters originating from the marly sequences of the Upper Judea Group Aquifer (Mekorot Co., personal comm.). Qedem brine represents ascending water from the deep thermal aquifer south of the sampling area [10]. Pore water was sampled at a depth of 0.7 m below surface next to shore spring 3. The sample code field refers to the naming of the respective sample in subsequent analyses. W, S, B stand for water, sediment and biofilm respectively; w/g refers to white/green biofilms; SP# refers to the identification number of the spring.

doi:10.1371/journal.pone.0038319.t001

### **Water chemistry analysis**

Water (4 L) and pore water (0.6 L) sample were filtered on site through 0.22  $\mu\text{m}$  cellulose-acetate filters and filled into separate bottles for cation and anion analyses. Cation analysis was conducted as previously described (Dulski, 1994). Shortly, the samples were additionally acidified by adding 0.3 mL of 6M HCl. Determination of Mg, Ca, Sr, Rb, Cs, Mn was done by ICP-MS (Elan-DRC, Perkin Elmer, Germany), whereas Na, K, Ba, B, Li, Si were analyzed with ICP-AES (Spectro Ciros CCD, Spectro Analytical Instruments, Germany). Both analyses were calibrated with matrix-adjusted standard solutions. Cl, Br and  $\text{SO}_4$  were analyzed by ion chromatography.  $\text{HCO}_3^-$  was Gran-titrated adjusting the waters to pH 4.3 with  $\text{H}_2\text{SO}_4$ . For interpretation, ion concentrations were normalized to those in seawater, since seawater is a major source of brines and evaporates.  $\text{H}_2\text{S}$  was analyzed colorimetrically using the methylene blue method (Cline, 1969). pH temperature and Eh were measured on site, with a SenTix41 gel and SenTix platinum electrode, respectively connected to a WTW 350i field meter.

### **Analysis of dissolved organic carbon (DOC) and total dissolved nitrogen (TDN)**

DOC and TDN were analyzed in samples (250 mL) collected in acid-cleaned polycarbonate bottles, which were stored at  $-20\text{ }^\circ\text{C}$  until analysis at the Max Planck Research Group for Marine Geochemistry (Oldenburg, Germany). Samples were thawed, acidified with HCl (p.a. quality) to pH=2 and purged with ultrapure synthetic air to remove inorganic carbon. DOC and TDN were measured with a total organic carbon analyzer (TOC-VCPH, Shimadzu) equipped with a TNM-1 module for nitrogen analyses and an ASI-V auto-sampler. A subset of samples was also filtered through pre-combusted Whatman GF/F filters. Because there was no detectable difference between filtered and non-filtered samples, our analyses of total dissolved organic carbon and nitrogen represents DOC and TDN. To test for possible matrix effects of the high salt content, a standard addition experiment was performed by adding  $\text{NH}_4\text{Cl}$  and potassium phthalate to a subset of samples. The added amounts of DOC and TDN could be reproduced with an external

---

calibration, demonstrating that the Dead Sea water matrix did not affect our analyses. Additionally the catalysts of the TOC analyzer were optically controlled for signs of chlorine breakthrough. The analyses of DOC and TDN were validated with consensus deep-sea reference material (CRM Program, <http://yyy.rsmas.miami.edu/groups/biogeochem/CRM.html>) provided by the University of Miami.

### **Rare earth elements and yttrium (REY)**

REY were measured using ICP-MS (Elan-DRC, Perkin Elmer, Germany) as previously described (Dulski, 2001). Low concentrations of REY in the water made pre-concentration necessary. Approximately 3 L of filtrated water (0.22  $\mu\text{m}$ , cellulose acetate Sartobran capsule filter, Sartorius, Germany) were spiked with a Tm-spike for recovery analysis and adjusted to pH 2 by using sub-boiled suprapure HCl ( $\text{HCl}_{\text{sp}}$  Merck, Germany) and within 2h passed through a pre-conditioned C18 Sep-Pak cartridge (waters, USA) at a rate of 1 L  $\text{h}^{-1}$ . Cartridges were pre-conditioned in the laboratory by cleaning them with 10 mL of 6 M sub-boiled  $\text{HCl}_{\text{sp}}$ , rinsing in ultra-pure water (Merck Millipore, Germany) to neutral pH and loading with a liquid ion exchanger (a mixture of two different ethylhexylphosphates, Merck, Germany). The REY-loaded cartridges were washed with 50 mL of 0.01 M sub-boiled  $\text{HCl}_{\text{sp}}$  and eluted by 40 mL of 6 M sub-boiled  $\text{HCl}_{\text{sp}}$  at a rate of 3 mL  $\text{min}^{-1}$ . The eluates were evaporated to incipient dryness and the residues dissolved in 3 mL of sub-boiled suprapure  $\text{HNO}_3$  (Merck, Germany) and spiked with a Ru-Re mixture that was later used to correct the internal drift of the response factors in the ICP-MS measurements, if necessary. The interference of molecular ions with the desired mono-charged ions of the REY were routinely corrected as previously described (Dulski, 1994). REY values are given in Table S1.

### **DNA extraction**

Based on preliminary cell counts, 4 L of water and 25 g of spring sediments were used for DNA extraction as previously described (Ionescu et al., 2009). All samples were incubated for 30 min in lysis buffer (0.1 M Tris, 0.05 M EDTA, 100 mM NaCl, 1% SDS, pH 8) at 100 °C in a dry heating block or a water bath depending on sample size. Phenol was added (half of total volume) and samples were incubated at 60 °C for 15 min. An identical volume of chloroform was added and, following 10 min of incubation at room temperature (RT) and 10 min of centrifugation, the aqueous phase was transferred. After a second chloroform extraction the DNA was precipitated overnight at -20 °C with 1 volume of isopropanol and 0.05 volume of 5 M Sodium Acetate (pH 5.0). After a 20 min centrifugation the pellet was washed in 75% ethanol, recollected by centrifugation, and dissolved in 50 µL of molecular grade water. Due to the high salt content the DNA from the sediment samples was desalted using the Qiaex II gel extraction kit (Cat: 20021, Qiagen). DNA was quantified using a Nanodrop (Thermo Scientific) and subsamples of equal concentration were used for further analysis.

### **Pyrosequencing**

DNA extracts from a total of 18 samples were analyzed by 454 pyrosequencing for Bacterial and Archaeal diversity. Primer sets 28F and 519R (Lane, 1991) were used for Bacterial sequences and 341F (Ovreas et al., 1997) and 958R (DeLong, 1992) for Archaeal sequences. Pyrosequencing was done by Research and Testing Laboratories, Lubbock, Texas, using a Roche 454 FLX Genome Sequencer system. Shortly, Tag-encoded FLX amplicon pyrosequencing (bTEFAP) was carried out as previously described by Dowd et al.,(2008). A 20 ng (1 µl) aliquot of each DNA sample was used for a 25 µl PCR reaction. A 30 cycle PCR using HotStarTaq Plus Master Mix Kit (Qiagen, USA) were used under the following conditions: 94 °C for 3 minutes, followed by 30 cycles of 94 °C for 30 seconds; 55 °C for 40 seconds and 72 °C for 1 minute; and a final elongation step at 72 °C for 5 minutes. Following PCR, all amplicon products from different samples were mixed

---

in equal volumes and purified using Agencourt Ampure beads (Agencourt Bioscience Corporation, USA).

### **Sequence analysis**

Diversity and community structure analyses were performed on 90,320 Bacterial and 41,111 Archaeal sequences obtained from samples of spring waters and sediments, biofilms and reference sediment. Sequence reads from PCR amplicon pyrosequencing were preprocessed (aligned and quality-controlled) by the bioinformatics pipeline of the SILVA rRNA gene database project (Pruesse et al., 2007). Briefly, all reads were aligned using the SILVA Incremental Aligner against the SILVA SSU rRNA seed (Pruesse et al., 2007). Non-aligned reads (putative contaminations/artifacts) have not been considered for further downstream analysis. Additionally, all remaining reads shorter than 50 aligned nucleotides and reads with more than 2% of ambiguities or 2% of homopolymers, respectively, were removed. Subsequently, reads of the filtered datasets were dereplicated, clustered and classified in parallel on a sample by sample basis. Dereplication (identification of identical reads ignoring overhangs) and clustering (OTU definition based on a non-redundant subset of reads) was done using *cd-hit-est* (<http://www.bioinformatics.org/cd-hit>) applying identity criteria of 1.00 and 0.98, respectively, both times with a wordsize of 8. For each OTU/cluster, the longest read was then used as a reference of this cluster for taxonomic classification. The classification was performed by a local nucleotide BLAST search against the non-redundant version of the SILVA SSURef dataset (release 106; <http://www.arb-silva.de>) using *blast-2.2.22+* (<http://blast.ncbi.nlm.nih.gov/Blast.cgi>) with standard settings. To filter out low identity and artificial BLAST hits, hits for which the function  $(\% \text{ sequence identity} + \% \text{ alignment coverage})/2$  did not exceed the value of 93.0 were discarded. For the analyzed reads with sufficiently good BLAST hits, the taxonomic classification of the best BLAST hit according to the SILVA taxonomy has been assigned to the read. Reads without any BLAST hits, or reads with weak BLAST hits only, were classified as 'No Relatives'. Finally, the taxonomic path of each cluster reference was mapped to all reads within the corresponding cluster as well as to their corresponding

---

replicates. This last step allowed to obtain quantitative information (number of individual reads representing a taxonomic path), within the bounds of PCR and pyrosequencing biases. To confirm the taxonomic affiliation of the sequences, all cluster references were imported into ARB (Ludwig et al., 2004) and inserted into the guide tree of the SILVA SSURef dataset (release 108).

A detailed summary of the 16S rRNA gene pyrosequencing data analysis process for each sample, including the total number of reads and length distribution, as well as the results of quality management, dereplication, and clustering, can be found in Table S2. A detailed list of the final taxonomic affiliation of all analyzed sequences together with their relative abundances within the amplicon pool are given in Tables S3 (Bacteria) and S4 (Archaea). The sequences were deposited at the Sequences Read Archive (SRA) under study accession number ERA116549.

### **Rarefaction analysis**

Rarefaction curves (Gart et al., 1982) were calculated for each sample. For each curve 100 data points were calculated choosing random sub sets of classified reads from the sample. Reads excluded by the aligner or the quality control, were not considered for the calculation of rarefaction curves. The first calculated data point always used a sample size of 1, while the last data point included all reads from the sample. The simulated sample sizes for the remaining 98 data points were evenly distributed between 1 and the size of the sample.

### **Automated ribosomal intergenic spacer analysis (ARISA)**

ARISA was done as previously described (Ramette, 2009) using 3 replicates for each DNA extract. Several sediment samples from each spring were used as biological replicates. No biological replicates are available for the water samples.

### **Fluorescence in situ hybridization (FISH)**

Samples for FISH were fixed within minutes of sampling termination using fresh formaldehyde (1% final concentration), and stored at 4 °C. Several replicates of 100 mL were filtered from each spring. Prior to permeabilization filters were embedded in low-gelling-point agarose (0.2% [wt/vol] in Milli-Q water), dried for 15 minutes at 37 °C and dehydrated in 95% (vol/vol) ethanol. Subsequently, filter pieces were incubated in lysozyme solution (10 mg/ml lysozyme in 0.1 M Tris-HCL [pH 7.4] and 0.05 M EDTA [pH 8] for 1 hour at 37 °C. After two washing steps in Milli-Q water, a second permeabilization step was carried out using achromopeptidase (30 U mL<sup>-1</sup> achromopeptidase in 0.01 M NaCl and 0.05 Tris-HCl [pH 7.4]) for 30 minutes at 37 °C. For inactivation of intracellular peroxidases, filters were incubated for 30 minutes at RT in methanol containing 0.15% H<sub>2</sub>O<sub>2</sub>, washed in Milli-Q water, dehydrated for 1 minute in 95% (vol/vol) ethanol, and air dried at room temperature. Filters were cut in sections and hybridized with the oligonucleotide probes EUB338 I-III (Amann et al., 1990), Arch915a and NON338 (Amann et al., 1995). Formamide concentration in the hybridization buffers was 35% (vol/vol) for all probes used.

Hybridization and amplification was performed as described by Tujula et al., (2006), with the following modifications. Hybridization was performed overnight (12-15 h) at 46 °C. Amplification was increased by adding 3 parts of Alexa 488 (1 mg mL<sup>-1</sup>) labeled tyramides to 1000 parts of amplification buffer. The amplification time was elongated to 30 minutes at 46 °C. The filters were counter-stained and mounted using a DAPI (4',6-diamidino-2-phenylindole) mix as described by Teira et al., (2004).

The samples were examined with a Zeiss Axioplan microscope with a 100-W Hg lamp and filter sets for DAPI and Alexa488. From each filter 5 to 10 different fields of view (around 1000 to 5000 cells) were enumerated using the ACME software by Michael Zeder (<http://www.technobiology.ch>).



### **Hyper-spectral imaging**

High spatial resolution distributions of pigments in green biofilms covering cobble from spring 12 were measured using hyper-spectral imaging (Polerecky et al., 2009). This method provides full spectral data per pixel of acquired image thus enabling a non-intrusive study of pigment distribution across the sample. Undisturbed biofilm samples were illuminated with a halogen lamp emitting in visible and near-infrared regions (400-1000 nm), and scanned with a hyper-spectral camera (Pika II, Resonon) from a distance of ~5 cm at velocity  $200 \mu\text{m s}^{-1}$ . Subsequently, a biofilm subsample was placed on a microscope slide and scanned in a transmission mode under a Zeiss Axiophot microscope at velocity  $2 \mu\text{m s}^{-1}$ . Pigments were identified based on their *in vivo* absorption maxima (676 nm for chlorophyll *a*, 625 nm for phycocyanin, and 740 nm for bacteriochlorophyll *c*), and localized by calculating in every pixel of the image the second derivative of the spectral reflectance at the corresponding maximal absorption (Polerecky et al., 2009).

### **Cluster Analysis**

The different samples of the water and sediment microbial communities were compared by cluster analysis. The clustering was done using the DICE algorithm as implemented in the PAST software (Hammer et al., 2009), using stress factors 13% and 7% for the 454 data and ARISA data, respectively.

## Results

### Water chemistry

Compared to the Dead Sea water (data taken from Möller et al., 2003), underwater springs were significantly less saline and had a higher pH (Table 2). The southern springs were more saline and had a lower pH than the northern ones, with the exception of spring 1A, which was inactive at the beginning of the campaign and was sampled after it became active. All underwater springs except spring 2 had negative redox potential. Sulfide was detected in springs from both systems and ranged between 50-130  $\mu\text{M}$  DIC concentrations in the shore and underwater springs were 3-5 times higher than in the Dead Sea. DOC and TDN concentrations in underwater and shore springs as well as in the mixture of waters from the underwater spring 5 and the Dead Sea were also higher, however the DOC:TDN ratios were about 4 times lower than in the Dead Sea (Table 2).

Concentrations of major ions (Table 2) and trace elements (Table S6) varied significantly amongst the underwater springs. Seawater-normalized concentrations (hereafter denoted by subscript SW) exhibited sub-parallel patterns that were similar for all underwater springs (Fig. 3A). These patterns resembled those found in the shore springs from the area as well as in locally occurring brines, such as the pore water from the exposed Dead Sea Group (DSG) sediment or the thermal brines from the Qedem area (Fig. 3B). Both spring waters and local brines had higher  $\text{Br}_{\text{sw}}$  and  $\text{B}_{\text{sw}}$  compared to  $\text{Cl}_{\text{sw}}$  and  $\text{SO}_{4\text{sw}}$ , and depleted  $\text{Na}_{\text{sw}}$  and  $\text{SO}_{4\text{sw}}$ . The chemical similarity of the spring waters and brines led to the assumption that spring waters emerging on the shore and underwater are the result of (i) mixing of brines with the fresh groundwater component available from the mountain aquifers and (ii) dissolution and precipitation of evaporates which are abundant in the surrounding of the Dead Sea.

Table 2 Water chemistry of underwater springs and auxiliary sites

	Na <sup>+</sup>	K	Mg <sup>2+</sup>	Ca <sup>2+</sup>	Cl <sup>-</sup>	SO <sub>4</sub> <sup>2-</sup>	Br <sup>-</sup>	TDS	Density	pH	Eh	H <sub>2</sub> S	DiC	TA	DOC	TDN	DOC/ TDN	NH <sub>4</sub> <sup>+</sup>	NO <sub>3</sub> <sup>-</sup>	PO <sub>4</sub> <sup>3-</sup>	Mixing (%)	
	mM	mM	mM	mM	mM	mM	mM	g/L	g/cm <sup>3</sup>		mV	mM	mM	mM	μM	μM		μM	μM	μM	PW/Q	
Dead Sea	1460	201	1952	508	6147	139	81.3	338	1.240	6.16	293	-	1.05*	4.1-4.7†	185	20	9.2	600 <sup>§</sup>	3-8 <sup>§</sup>	0.2 <sup>§</sup>	-	
L Spring 1	429	5.23	34.8	12.6	127	5.00	5.10	7.58	1.003	7.44	-9	-	3.56	2.84	-	-	-	-	-	-	2.0/-	/4.0
D <sub>1</sub> Spring 1A	464	56.7	502	137	1693	25.5	18.0	88.4	1.069	6.75	-86	-	3.40	3.44	-	-	-	-	-	-	25.3/-	/8.0
N <sub>1</sub> D <sub>2</sub> Spring 2	102	9.86	62.1	21.3	259	6.73	2.29	9.40	1.005	7.38	+38	0.127	4.15	3.98	728	77	9.4	78	0.8	0.25	-	-
L Spring 3	62.6	6.67	41.1	12.9	164	3.20	1.49	16.8	1.010	7.43	-83	0.127	5.27	5.1	213	24	8.9	20	4.5	0.42	2.7/-	-/5.2
L Spring 4	37.0	5.00	29.0	8.00	108	2.00	1.00	6.07	1.002	-	-	-	-	-	-	-	-	-	-	-	1.9/-	-/3.6
S <sub>1</sub> D <sub>1</sub> Spring 10	277	31.0	222	59.0	858	5.00	9.00	44.7	1.031	6.76	-38	0.048	-	-	518	158	3.2	131	1.47	0.81	13.3/-	-
D <sub>1</sub> Spring 11	270	30.6	218	64.0	818	4.22	8.26	44.0	1.031	6.76	-40	0.063	-	-	473	170	2.7	181	1.01	0.69	12.9/-	-
D <sub>2</sub> Spring 1	29.5	3.72	22.7	7.91	80.5	1.03	0.70	4.96	-	7.17	52	-	4.67	4.28	729	323	2.3	-	-	-	1.4/-	-/2.6
L Spring 2	30.8	4.23	22.9	7.72	84.7	1.20	0.74	5.20	-	7.22	128	-	4.97	4.6	1445	593	2.4	-	-	-	1.5/-	-/2.9
D <sub>1</sub> Spring 3	103	4.36	30.9	11.9	166	1.67	0.84	10.4	-	7.16	-47	-	5.80	5.32	1386	584	2.4	-	-	-	2.1/-	-/4.2
L Spring 5	-	-	-	-	-	-	-	-	-	-	-	-	-	-	736	394	1.9	-	-	-	-	-
Porewater (PW)	1508	233	2132	508	6365	2.89	62.3	348	-	5.66	247	-	6.20	1.80	-	-	-	-	-	-	-	-
Qedembrine (Q)	1254	110	965	367	3532	9.3	26.2	198	-	6.31	-97	-	4.35	2.76	-	-	-	-	-	-	-	-
Jericho 5 well (JGA)	3.67	0.14	2.09	2.28	8.04	0.8	0.05	0.82	-	7.20	368	-	4.78	4.32	-	-	-	-	-	-	-	-

\*Taken from Stein et al. (93);

†Taken from Gross (47);

‡Taken from Stiller and Nissenbaum (76);

§Classification based on REV: L- Limestone group(D1- Dead Sea group, subgroup 1(D2- Dead Sea group, subgroup 2.

Chemical composition and other characteristics of the waters from the Dead Sea, underwater springs, shore springs and additional auxiliary sites. Mixing coefficients represent the calculated percentages of brine (either porewater or the Qedem brine) admixed to the freshwater from the Jericho 5 well that best explain the measured concentrations of K, Cl and Br as well as the ratios of Cl/Br and Ca/Mg. PW/- denotes mixture of the porewater and freshwater. -/Q denotes mixture of the Qedem brine and freshwater.

doi:10.1371/journal.pone.0038319.t002

To assess the contribution of mixing, we used a two-component mixing model to calculate the ionic composition of the spring waters. The local brine (either pore water or the Qedem brine) was used as the first component, whereas freshwater from the Lower JGA (represented by the Jericho 5 well) was used as the second component. The latter is justified based on the hydraulic studies of Laronne Ben-Itzhak and Gvirtzman (2005), which modeled the flow from the buried Lower JGA to Darga, and of Möller et al. (Möller et al., 2003), which proved a considerable supply of freshwater from the northwest to the Darga region. The calculation revealed that springs 1A, 10 and 11 contained between 12.9% and 25.3% of pore water admixed to the JGA freshwater, whereas spring 2 was better explained as a mixture of 8% Qedem brine and JGA freshwater (Table 2). The composition of the less saline underwater springs 1, 3 and 4 and shore springs 1-3 was equally well explained by mixing the JGA freshwater with either 1.4–2.7% of pore water or 2.6–5.2% of the Qedem brine (Table 2).

These mixing coefficients could explain measured concentrations for most but not all components (Fig. 3C). For example, the measured concentrations of  $\text{SO}_4$  and Ba were clearly higher (4–25 fold for  $\text{SO}_4$ , 1.5–5.5 fold for Ba) than the calculated ones in all springs, whereas the measured Sr content was slightly higher in springs 2 and 3 and lower in springs 1A and 11 than calculated.

The shore and underwater spring waters were characterized by distinct REY patterns, which allowed their classification into two groups (Fig. 4, Table 2, Table S1). In the “Limestone” group, which included underwater springs 1 and 3 and shore spring 2, the REY pattern continuously decreased from La to Lu, with positive Ce-, small positive Y- and small negative Eu-anomalies (Fig. 4A). These patterns resembled those found in waters from the Lower JGA (Auja and Jericho 5 wells) and in the whole Judea Group limestone (Möller et al., 2003; Siebert et al., 2009). In the “Dead Sea” group, which included springs 1A, 11, 2 and shore springs 1 and 3, REY patterns had a patelliform shape. The subgroup that included springs 1A and 11 was characterized by significantly decreased medium REE resulting in a patelliform shaped pattern and positive Ce- and Y-anomalies (Fig. 4B), similar to the pattern found in the Qedem brine and the Cretaceous marl from the Judea

---

Mountains (Möller et al., 2003; Siebert et al., 2009). The second subgroup, which included spring 2 and shore spring 1 (Fig. 4C), was characterized by a gentler decrease from La to Gd and a stronger increase towards Lu. Such patterns are typical for waters coming from marly sequences of the Upper JGA, as represented by the Mitzpe Jericho 2 and Qilt springs, and similar to the whole rock composition of a Cretaceous marl from the Judea Mountains.

## **Biofilms**

Dense white biofilms covered sediments around the underwater springs at all sites. The biofilms around the northern springs 1-5 formed small thin patches adjacent to the water outlet (Fig. S2A). In contrast, biofilms around the southern springs covered relatively large (2-10 m<sup>2</sup>) patches of sediment next to areas where water seeped out without clear boundaries (Fig. S2B). Large areas covered with biofilms were also found on sediments with no detectable water seepage, such as on slopes below springs 10 and 11 at depth ~20 m (Fig. S2C). Thickest white biofilms covering an area of several square meters were found around spring 12 (Fig. S2B). Microscopic analysis revealed that large, sulfur-storing filamentous bacteria, which are typical for sulfidic environments, were not present in the white biofilms.

In addition to white biofilms, rocks around the southern springs (particularly around spring 12) were covered by thick green biofilms. The white and green biofilms covered exclusively the lower and upper sides of the rocks, respectively. Microscopic observations of the green biofilms revealed the presence of diatoms and unicellular cyanobacteria (Fig. S3). The latter was confirmed by hyper-spectral imaging, which revealed high concentrations of chlorophyll *a* and phycocyanin, characteristic pigments of this functional group (Fig. 5A). Hyper-spectral imaging additionally revealed a high abundance of bacteriochlorophyll *c*, a pigment characteristic for green sulfur bacteria, which was tightly associated with chlorophyll *a* (Fig. 5B). Microscopic observations showed that this association had a specific spatial structure, with patches of cyanobacteria surrounded by or co-localized with green sulfur bacteria (Fig. 5C).

---

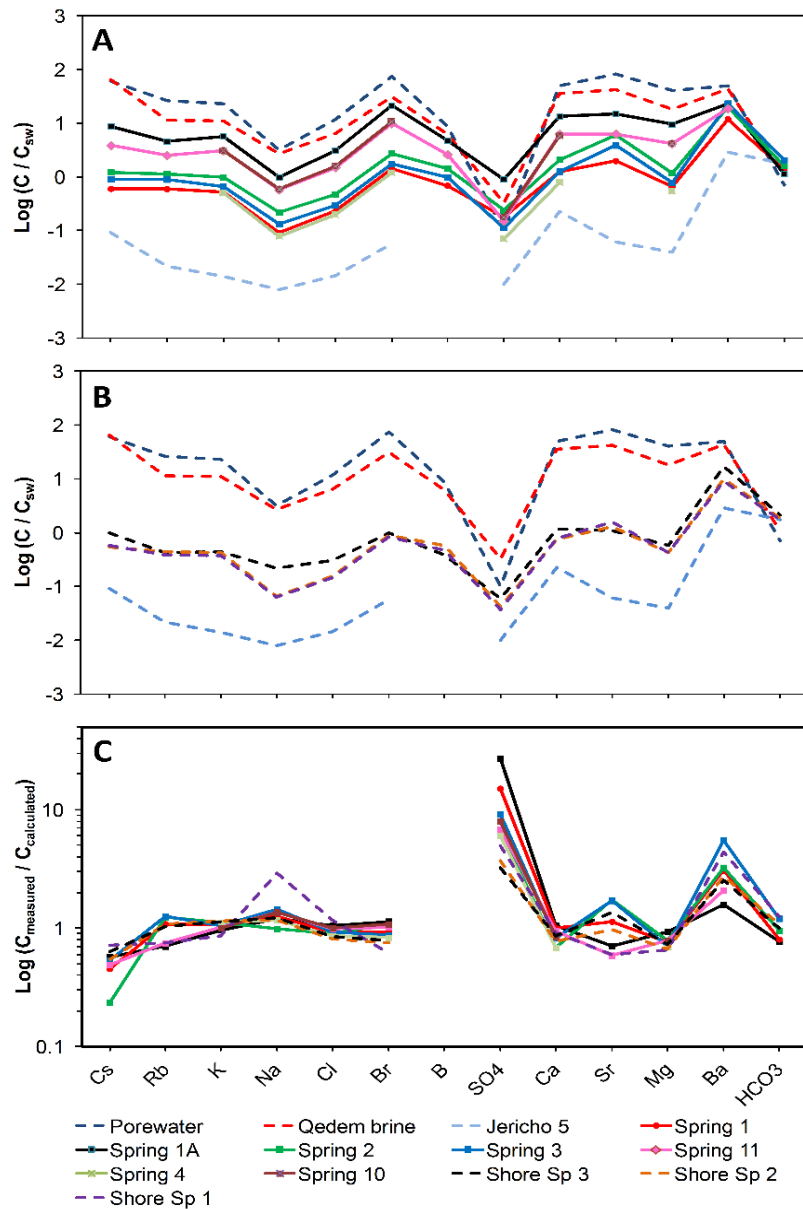


**Figure 3** Seawater normalized ( $C_{sw}$ ) concentrations of major ions in waters from the underwater springs (A) and from reference sites (B). The concentrations are listed in Table 2 and in supplementary Table 1. The ions are arranged along the x-axis based on their natural behavior: heavy alkalis Cs and Rb are mainly controlled by surfaces such as those of clay minerals; K, Na, Cl and Br stand for brines and salt minerals (halides); SO<sub>4</sub>, Ca, Sr, Mg, Ba and HCO<sub>3</sub> represent dissolved species from carbonate-sulfate minerals (e.g., anhydrite/gypsum, aragonite and barite). All these minerals are abundant in the Dead Sea sediments. (C) Ratios between the measured ion concentrations and those calculated by a two-component mixing model (see Table 2 for the estimated mixing coefficients) using the Jericho 5 freshwater and either the Dead Sea pore water or the Qedem brine as end-members.

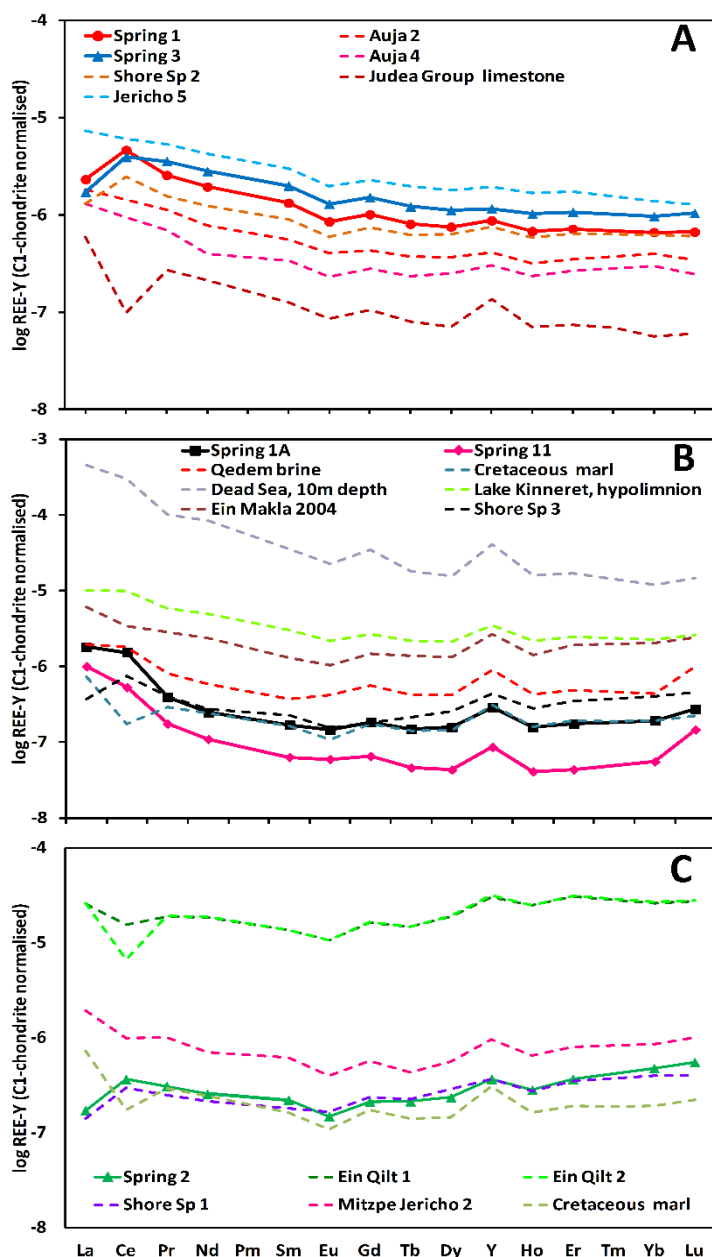


**Figure 4** Rare Earth elements and Yttrium (REY) pattern in underwater springs (solid lines with symbols) and in diverse ground waters from the local area with comparable patterns (dashed lines). The origin of the different waters is explained in Table 1, the REY concentrations are given in supplementary Table 2. Whole-rock REY patterns for the Judea Group limestone and the Cretaceous marl are also presented (data taken from Möller et al., 2003). Their normalized values are shifted by  $10^{-7}$  (limestone) and  $10^{-8}$  (marl) to ease the comparison. The fractionation patterns separate the springs into two major groups, the “Limestone” group (A) and the “Dead Sea” group, which is divided into two subgroups (B-C). Note logarithmic scale in all panels

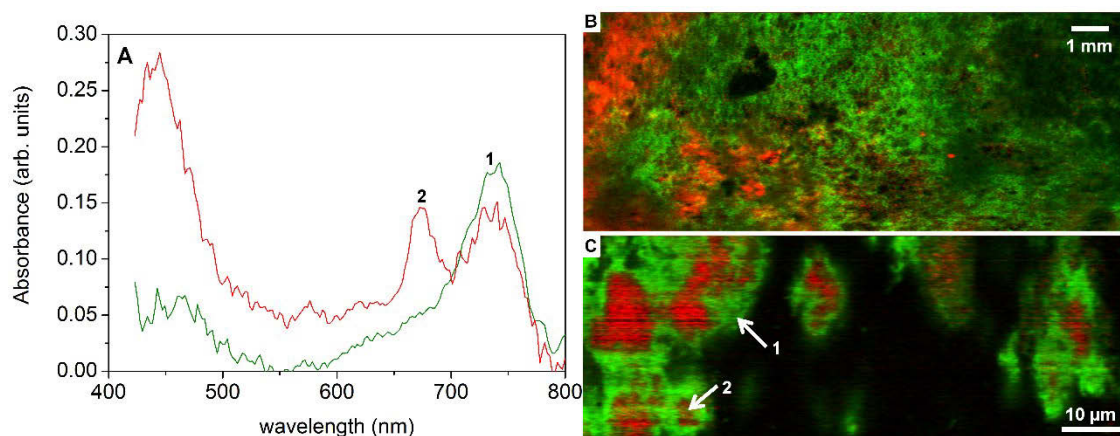


**Figure 5** (A) Examples of absorption spectra of green biofilm samples from spring 12. Locations where these spectra were taken are shown by arrows in panel C. Major peaks at 675 nm and 740 nm correspond to in vivo absorption maxima of chlorophyll a and bacteriochlorophyll c, respectively. (B-C) Distributions of pigments in whole-biofilm samples (B) and in biofilm samples under the microscope (C). Pigments characteristic for cyanobacteria (chlorophyll a and phycocyanin) are shown in red, whereas the pigment characteristic for green sulfur bacteria (bacteriochlorophyll c) is shown in green. Cyanobacteria were always co-localized with the green sulfur bacteria and never detected alone

### Microbial community analysis

Cell densities in the spring waters ranged between  $7 \times 10^5$  and  $10^7$  cells  $\text{mL}^{-1}$ , and were between 10 to 100 times higher than in the ambient Dead Sea water (Fig. 6A). Bacteria made 30-50% of the total cell counts (Fig. 6B), whereas in ambient Dead Sea water where bacteria could not be detected (Bodaker et al., 2010). Cell densities in sediment and biofilm samples could not be quantified in this study due to technical complications.

Rarefaction curves showed that the species richness was largest in the spring water samples (with the exception of spring 1A and 3) and progressively decreased in samples from the green biofilms, spring sediments and white biofilms (Fig. S4). Diversity in the spring sediments was similar to that in the reference DSG sediment. Both pyrosequencing and ARISA analyses showed clearly that the microbial communities in the spring waters and spring sediments are different (Fig. 7; Table S5).



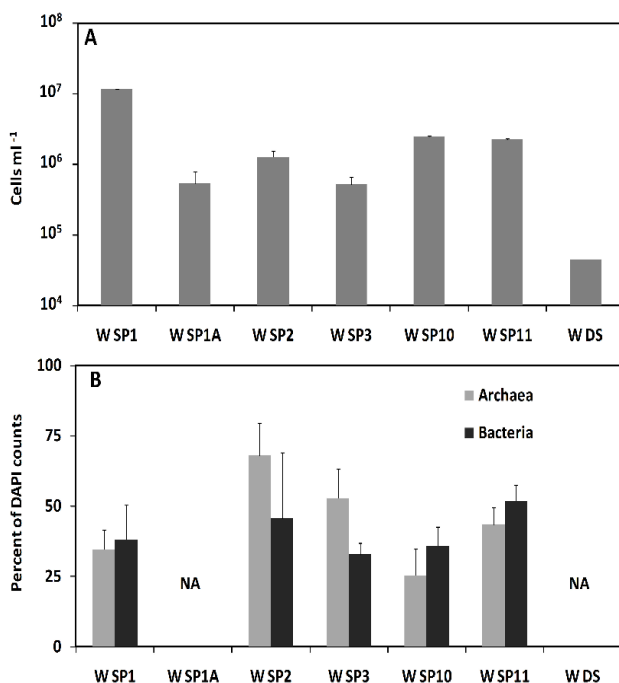


**Figure 6 (A)** Total counts of DAPI-stained cells and (B) percentage abundance of Archaea and Bacteria within the total cell counts in water samples collected from different underwater springs and from the reference Dead Sea water. Wn denotes water sample from spring n. Error-bars indicate standard error (N=10); NA = data not available.

Furthermore, the communities from the reference DSG sediment were much more similar to those in the spring sediments than those in the spring waters. The different replicate sediment samples used for the ARISA analysis showed no spring-specific clustering. The microbial communities in the green and white biofilms are closer to the spring water. Thus, the communities in the spring water and the biofilms differ from the Dead Sea communities but the sediments near the springs are colonized largely by normal Dead Sea microbial communities.

Based on species composition, with the exception of spring 11, the sediment samples share 45-50% similarity among themselves. A similar trend is observed among the biofilm samples; however, the sediment, biofilm and water sample clusters samples, were only 10% similar. When sequence frequency was additionally taken into account these values changed to 50-70% vs. 5% respectively (Fig. S5). All spring-associated communities were very different (maximum 10% similarity based on species composition) from the residual Dead Sea communities described by Bodaker et al., (2010) as well as from the communities identified during the 1992 bloom linked to the dilution of the upper water layer of the Dead Sea (Rhodes et al., 2010; Fig. S5). When comparing spring waters

only, the communities in springs 1A and 3 stood out in both analyses. This difference was, however, more pronounced in the pyrosequencing data, presumably due to a lower number of sequences obtained from these samples. Pyrosequencing indicated that the microbial communities in the white biofilms covering cobble around spring 12 were much more similar to the water-borne communities from springs 1, 2, 10 and 11 than to the white biofilm communities from springs 2 and 3. This similarity was, however, not evident in the ARISA data.

The major classes of detected Bacterial sequences varied between the samples from the springs' water phase, spring sediment and biofilm samples (Fig. 8A). Hereafter only the taxonomic name will be used when referring to sequence data. In spring water samples, *Epsilon*-, *Gamma*- and *Deltaproteobacteria* were detected in highest numbers, with *Epsilonproteobacteria* being especially dominant in southern springs 10 and 11, where they made up 75% and 47% of the total number of sequences, respectively. With the

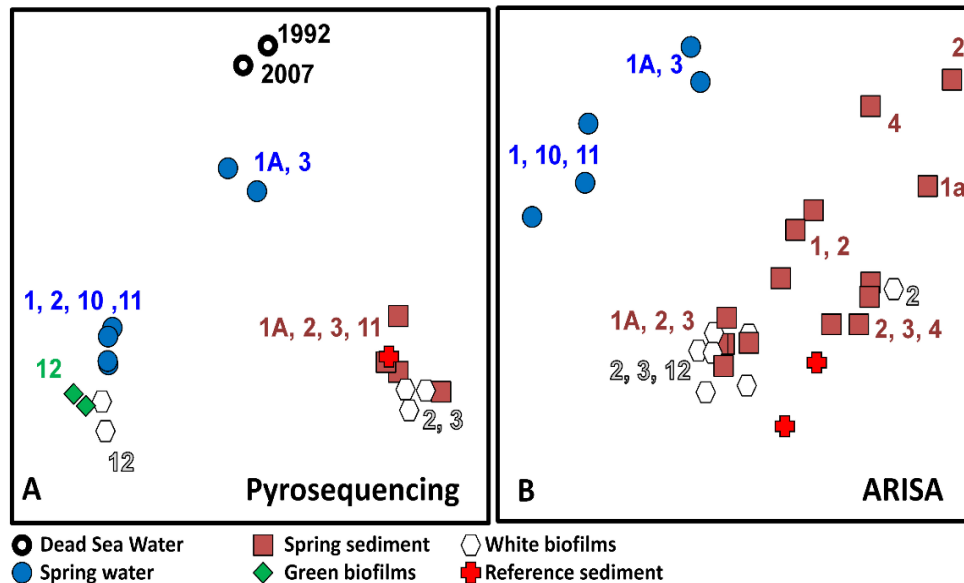


**Figure 7** Non Metric Multidimensional Scaling (NMDS) plots derived by the DICE algorithm from the (A) 454 pyrosequencing and (B) ARISA data, using stress values of 13% and 7%, respectively. Clustering of the pyrosequencing data was performed on the data matrix produced by the NGS system at a taxonomic depth of 5 (Family level). Duplicate samples represent biological replicates. Data for the 1992 and 2007 analyses were obtained from Rhodes et al., (2010) and Bodaker et al., 2010, respectively.

exception of springs 1A and 3, the spring water samples exhibited a large diversity within the *Chloroflexi* phylum. This was in contrast to sediment samples, where many classes from this phylum were absent, except for the *Chloroflexi* class itself, which was found exclusively in spring sediments. Another major difference was that the sediment samples contained many more sequences of *Deinococci*, *Clostridia*, *Nitrospira*, *Betaproteobacteria* and *Actinobacteria*. Except for *Clostridia*, these classes were frequent also in white biofilms from the northern springs 2 and 3. Sequences detected in the white biofilms from the southern springs were very different from those in the northern springs. They were dominated by *Epsilon*- and *Deltaproteobacteria* (on average 73% and 10%, respectively) and contained *Bacteroidia* (1.9%) and *Anaerolineae* (2.9%), unlike in other samples where these groups were not detected. Similar classes were detected also in the green biofilms from these springs, with *Gammaproteobacteria* and *Sphingobacteria* being additionally relatively abundant (25% and 1.5% on average, respectively).

Archaeal sequences were amplified successfully from only 11 out of the 18 samples. They contained a significant number of Bacterial false-positives (Table S4), which were excluded from the final analysis. Compared to Bacteria, the diversity of Archaea detected in the spring-associated samples was much lower, though in many samples (especially in spring sediments) no Archea were detected (Fig. 8B). *Crenarchaea* were detected in significant amounts only in one sample and clustered with sequences of uncultured deep subsurface *Crenarchaea* (Waddell et al., 2010) within the Marine Group 1 *Crenarchaea*. The *Euryarchaea* comprised mainly *Halobacteria* and *Thermoplasmata*. Both of these groups clustered with sequences found in deep-sea hydrothermal vents (Fig. 8C), and their possible significance will be discussed later. The *Euryarchaeal* community from the more saline spring 1A differed from the communities found in the other northern springs. While *Euryarchaea* were detected only in water samples from the northern springs, in southern springs they were detected only in the green biofilms.

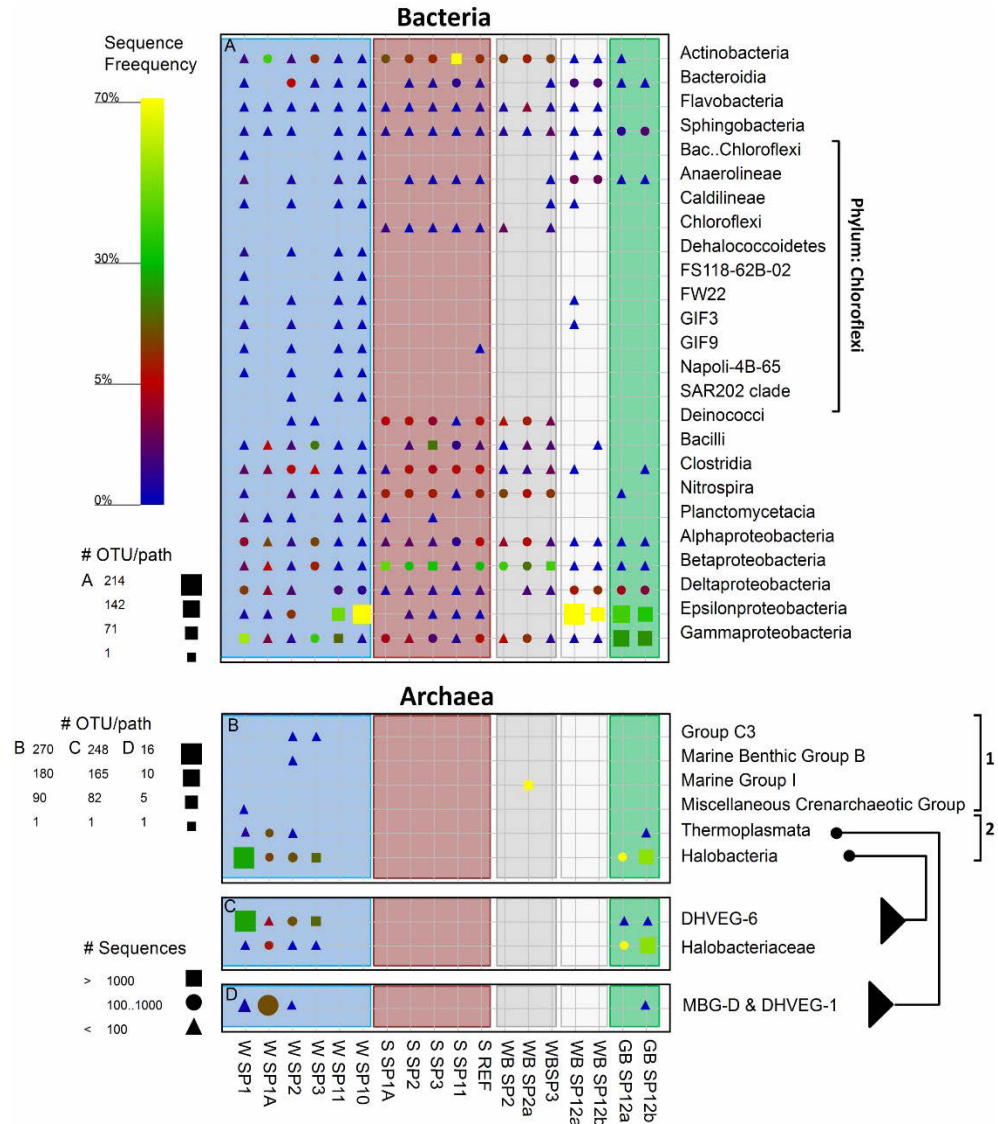


**Figure 8** Graphical representation of the sequence frequency in the studied Dead Sea samples, showing major detected classes within the Bacterial and Archaeal domains. Classes belonging to *Crenarchaea* and *Euryarchaea* are marked by brackets 1 and 2, respectively. The *Halobacteria* and *Thermoplasmata* classes are shown also at the family level to facilitate a more specific sample comparison. The color of the symbol represents the relative frequency of the taxonomic path within the sample. The size of the symbol represents the number of OTUs at deeper phylogenetic levels within that taxonomic path (see Methods for the definition of OTU). The shape of the symbol represents the number of sequences in the specific taxonomic path. Columns are shaded according to the sample type: blue=spring water, brown=spring sediment, grey=white biofilms from northern springs, white=white biofilms from southern springs, green=green biofilms from southern springs. Abbreviations in sample names: W=spring water. S=spring sediment, WB=white biofilm, GB=green biofilm, S-REF=reference sediment from the Dead Sea.

The studied samples differed also in functional groups of Bacteria (Fig. 9). Phototrophic bacteria were detected in large numbers in green biofilms from spring 12 and in lower amounts elsewhere. Cyanobacterial sequences were detected in most samples usually making up less than 1% of the sequences. Only water from spring 1A and the sediment of spring 3 comprised 20% and 3.6% cyanobacterial sequences respectively (Fig. 9A). Although cyanobacterial pigments, as detected by hyper-spectral imaging, were often detected in the green biofilms of spring 12, only few cyanobacterial sequences were obtained from these samples. Attempts to use different sets of cyanobacteria-specific primers to identify these organisms resulted always in non-related sequences (*Halanoerobiales*). Most abundant phototrophs in the green biofilms were green sulfur bacteria (25%), consistent with the presence of bacteriochlorophyll *c* (Fig 6), and purple sulfur bacteria (10%) (Fig. 9B-C). Purple non-sulfur bacteria and *Chloroflexaceae* were common in sediment samples, but not in biofilms and spring water.

Chemolithotrophic sulfide oxidizers from the class *Epsilonproteobacteria* were very frequent and diverse in the green and white biofilms from spring 12 (on average 37% and 72%, respectively; Fig. 9D). The high abundance of this group was shown also by FISH analysis (Fig. S6). The water of the nearby springs 10 and 11 contained *Epsilonproteobacteria* as well; however, only from the *Sulfurimonas* genus and almost no sequences of *Sulfurovum* or the *Campylobacteraceae* (Fig. 9E). Few (<3%) *Acidithiobacillaceae* and *Thiotrichaceae* (recently renamed as *Beggiatoaceae* (Salman et al., 2011)) were found around most springs, except around spring 11.

Sulfate reducers were found at relatively higher numbers mainly in the water samples and in the biofilms from spring 12 (Fig. 9F). Within this group, *Desulfobacteraceae* were dominant in the water samples (0.4-8%) while *Desulfobulbaceae* were dominant in the biofilms (2.7-9%). The sulfate reducers in the spring water were more diverse but 4-8 times less frequent than in the biofilms associated with spring 12.

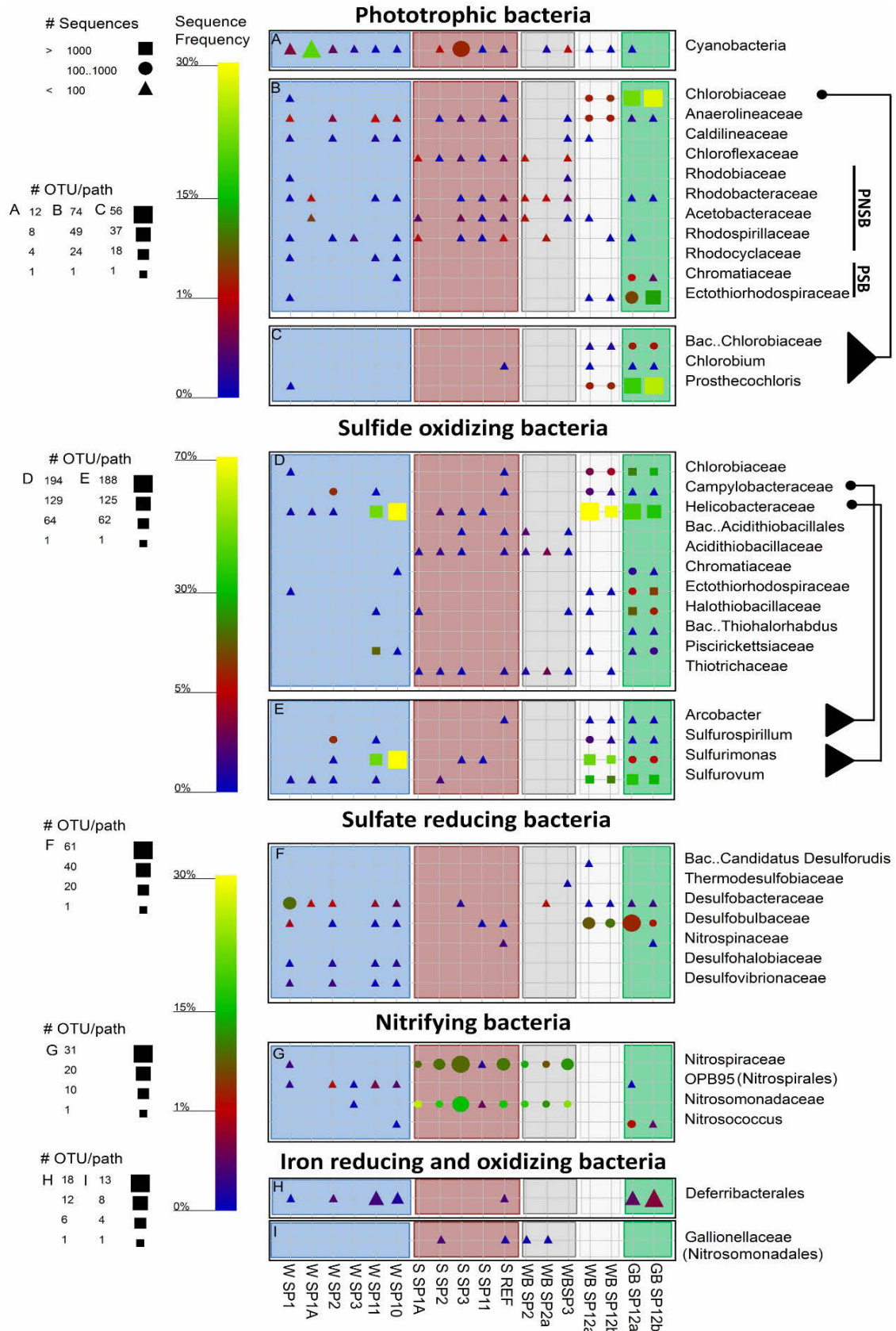
Nitrifying bacteria were highly abundant in the spring sediments from the northern system (11-27%) and in lower amounts in spring waters (<2%; Fig. 9G). The water samples contained mainly an unnamed family of *Nitrospirales* (OPB95), whereas *Nitrospiraceae*

---

and *Nitrosomonadaceae* were abundant in the sediment samples and white biofilms around springs 2 and 3. *Nitrosococcus* were identified in the green biofilms of spring 12 (0.5-1.2%). Remarkably, nitrifiers were found with an equally high frequency in the Dead Sea reference sample as well. The ammonia oxidizing bacteria from the family *Nitrospinaceae* (*Deltaproteobacteria*) were found exclusively in the reference sediments (0.4%; not shown in Fig. 9G).

*Deferribacterales* (iron and nitrate reducing bacteria) were found in the green biofilms of spring 12 (0.6%), in the reference sediments (0.4%), and in all spring water samples (<0.41%) except for springs 1A and 3 (Fig. 9H). A low amount of sequences of iron oxidizing bacteria belonging to the *Gallionellaceae* (<0.1%) was detected in sediments and white biofilms around spring 2 and in the Dead Sea sediment (Fig. 9).

**Figure 9** Graphical representation of the sequence frequency in the studied Dead Sea samples, showing major detected phyla and families of different functional groups of Bacteria. PSB and PNSB in panel B refer to purple sulfur and non sulfur bacteria, respectively. The different genera within the families *Chlorobiaceae*, *Campylobacteraceae* and *Helicobacteraceae* are shown to facilitate a more specific sample comparison. The symbols and sample naming are explained in detail in Fig. 8. Note different legends for OTU/path for each panel, and scale-bars for relative sequence frequency for several combined panels.



## **Discussion**

This study provides the first description of dense microbial communities in the Dead Sea. It shows that these communities are exclusively linked to groundwater seepage at the lake floor. Here we discuss the possible source of these organisms and the putative biogeochemical pathways they are mediating. Furthermore we discuss the origin and chemical properties of the spring waters and their importance for the microbial communities.

### **Origin and properties of the underwater springs**

The major elements composition as well as the rare earth elements and yttrium (REY) patterns are markers of biotic and abiotic processes that occur along the flowpath of the groundwaters before they emerge as springs at the Dead Sea floor. We combine these data with the results of the bacterial community analysis to identify these processes.

Generally, in groundwater systems, REY are mainly released from accessory minerals, among which phosphates and carbonates predominate (Hannigan and Sholkovitz, 2001). After dissolution of REY-bearing minerals, the majority becomes immediately adsorbed onto mineral surfaces (Johannesson et al., 1999). Consequently, along the flow path, mineral surfaces in contact with passing water are continuously equilibrated to the concentration of REY in the water. Once a hydrological system is well established, changes in REY no longer occur or they are at least insignificant. Hence, REY patterns of such waters represent the initial water-rock interaction in the recharge area of the aquifer that defines the primary REY pattern of the groundwater (Möller et al., 2003; Siebert et al., 2009).

The REY patterns of the studied springs are evidence of freshwater running from the Judea Group Aquifer (JGA) to the Dead Sea. However, they show distinct features from which their contact with the DSG sediment can be inferred. Waters from the “Limestone” group springs show similar REY pattern as freshwaters pumped from the Lower JGA (wells Auja 2 and 4, Jericho 5). We therefore assume that these waters flow from the

---



limestone aquifer to the Dead Sea through well-developed open cracks with negligible contact to the unconsolidated DSG sediments. By flushing through these cracks and by admixing of interstitial brines, the waters are further enriched with dissolved and suspended minerals, as well as species such as H<sub>2</sub>S, but only in marginal amounts.

In contrast, we suggest that waters in the “Dead Sea” group springs migrate from the JGA through small fissures and less open cracks, with their flow paths through the DSG sediment possibly still developing. Consequently, their interaction with DSG minerals and interstitial brines is much more intense. This is supported by the similarity of their “soup-bowl”-like REY pattern to that of the Qedem brine, for which the intense contact with DSG sediments has been shown (Gavrieli et al., 2001a). However, this similarity cannot be explained by simple admixing of the local brines to the JGA freshwater. If the mixing coefficients estimated from the major ion composition (Table 2) were used, the resulting REY patterns would be much closer to that of the JGA than those of the pore water or Qedem brines (Fig. S7). Therefore, additional processes need to be considered. First, the pattern with considerably decreased medium REE's (MREE) and positive Y-anomalies can be the result of long-term leaching of phosphates and sulfates. This process releases predominantly MREE (Hannigan and Sholkovitz, 2001); thus, if it occurred in the past, the MREE would now be lacking and thus lead to MREE depletion in the passing water. Second, the observed pattern can be due to FeOOH precipitation (Bau, 1999) and subsequent weathering. If FeOOH complexes at pH>6, a relevant value for these springs, Ce, Nd and Sm as well as heavy REE have a higher affinity to co-precipitate than the rest of the REE and Y (Bau, 1999). Therefore, the remaining waters show depletion in medium REE and slight increase towards Lu with a positive Y-anomaly. However, if FeOOH become reduced, heavy REE and Ce are predominantly released and become enriched in the water (Tujula et al., 2006). Indeed, spring waters 1A and 11 are reducing (Table 2) and show patterns with positive Ce-anomalies, which are comparable to those in waters from the anoxic hypolimnion in Lake Kinneret and from strongly reducing Ein Makla spring in Hammat Gader (Fig. 4B), where redox-cycling of Fe plays an important role (Siebert, 2006; Siebert et al., 2009). Water of spring 2 interacts with FeOOH as well. However, in contrast to the other “Dead Sea” group members, recycling of Fe-oxihydroxides is unlikely in this

---

spring due to its oxidizing conditions (Table 2). Instead, FeOOH precipitated along the flow path is weathered and not reduced, releasing heavy REE first and preventing Ce-anomalies, the latter because Ce is still in an oxidized state (Ce(IV)) and therefore more stably fixed in the Fe complexes (Moeller et al., 2007). Hence the REY pattern for spring 2 shows a less decreasing trend from La to Eu than the pattern of springs 1A and 11 (compare Figs. 4B and 4C). The initial source of iron, which is necessary for complexation of FeOOH, may be the weathering of Fe-bearing cherts. These are abundant in the Senonian rocks of the Judea Mountains (Gross, 1977) and in the eroded wadi debris, therefore also in the DSG-sediments (Nissenbaum et al., 1972).

The ionic composition of the spring waters indicates that the JGA freshwaters are affected by mixing at different proportions with the locally occurring brines (either the Dead Sea pore water or the ascending Qedem brine) before they emerge at the Dead Sea floor. The estimated pore water content in the more saline springs 1A, 10 and 11 was relatively high (13-25%). The less saline springs 1-4 could be equally well explained by mixing of JGA water with either 1.4-4.1% of pore water or with 2.6-8.0% of Qedem brine. This uncertainty was due to the relative similarity of the two brines with respect to their major ion composition. However, it could be resolved by considering molar Mg/Ca-ratios, which were quite distinct for the two brines (4.11 in the pore water, 2.6 in the Qedem brines). Since spring waters mainly comprise JGA freshwater with molar Mg/Ca<1, their high molar Mg/Ca ratios (2.76 to 3.76), which are higher than that for the Qedem brine, must be the result of a significant Mg-source. This could be either the admixed pore water or dissolved Mg-rich minerals. Such minerals (e.g. carnallite, bischofite) have been described for sinkholes (Katz and Starinsky, 2009) and most probably exist also within the thin DSG-sediment crust (Yecheili and Ronen, 1997), where evaporation lead to the precipitation of such minerals. However, they cannot be found in depths where the groundwater emerging in the studied springs is assumed to flow. Hence, the high molar Mg/Ca ratios in the spring waters indicate a significant contribution of the Mg-rich pore water as the preferential mixing partner, but do not exclude the contribution of Qedem brines as a possible third component.

---

The ionic composition additionally indicates that the groundwaters are affected by interactions with clays and by dissolution of evaporates such as aragonite, gypsum, anhydrite and halite, all of which are present in DSG-sediments (Barkan et al., 2001). Since Cs and Rb are highly controlled by surfaces, intense clay-water interaction is suggested by the marked differences between the measured Cs and Rb concentrations and those calculated by the mixing model (Fig. 3C). The moderately high DIC in the spring waters is predominantly in the form of  $\text{HCO}_3^-$ , suggesting dissolution of calcite (in the JGA) and aragonite (in the DSG sediment). The  $\text{HCO}_3^-$  content in the brines stays stable suggesting the high DIC (up to  $6.2 \text{ mmol L}^{-1}$ ) is not a result of additional mineral dissolution. Instead, the higher DIC concentration is due to increased  $\text{CO}_2$ , originating probably from bacterial decomposition of organic matter in the DSG-sediment.

The DOC in the underwater springs is high. This is probably due to mixing of the spring water with the pore water (see above), which is rich in organics (Siebert, unpublished data) due to continuous burial of terrestrial organic material during the sedimentation process of the Dead Sea sediments (Nissenbaum et al., 1972). High DOC was also detectable in the buoyancy-forced flow of underwater spring 5 as sampled on the surface. This suggests the underwater springs are a source of organic matter input into the Dead Sea. The low DOC:TDN ratios ( $<3$ ) in the majority of the springs suggest that most of the dissolved nitrogen is inorganic (Hansell and Carlson, 2002). The high concentration of ammonium is derived probably from the oxidation of organic matter during the process of sulfate reduction, as described for other subsurface aquifers in the Dead Sea area (Gavrieli et al., 2001b). Although exhibiting the same major ions and REY patterns, the underwater springs in the northern system (2 and 3) have a higher DOC/TDN ratio compared to the other springs; however, as most of the N is accounted for as ammonium we suggest that a large part of it was consumed as a nutrient by the microbial community along the aquifer flow path through the DSG sediments.

In some underwater springs,  $\text{H}_2\text{S}$  was detected in relatively high concentrations. This  $\text{H}_2\text{S}$  possibly originates from bacterial sulfate reduction that occurs along the flow path of the spring water, as shown for other sulfidic spring systems (Gavrieli et al., 2001b;

---

Macalady et al., 2007). This process requires organics and dissolved  $\text{SO}_4$ . The latter may be provided to the hydro-biological system by mineral dissolution, or by active bacterial leaching of anhydrite from the DSG sediment, as indicated by the high  $B_{\text{SW}}/\text{SO}_{4\text{SW}}$  ratios. The dissolution of anhydrite and gypsum is possible, since spring waters are undersaturated with respect to these minerals (Table S6). Indeed, spring waters show elevated  $\text{SO}_{4\text{SW}}$  concentrations, which exceed those in the Dead Sea, the pore water and the JGA groundwater, but are lower than in the Qedem brine (except for spring 1A). Accompanying the dissolution of anhydrite ( $\text{CaSO}_4$ ) is the release of Ca. However, enrichment in Ca-ions in spring waters is prevented by simultaneous precipitation of aragonite, supported by the fact that, in their outlets, all spring waters are supersaturated with respect to calcite and aragonite (Table S6).

Underwater spring waters showed remarkably high  $\text{Sr}_{\text{SW}}/\text{Ca}_{\text{SW}}$  ratios ( $>1$ ). These can be explained by several processes, such as (i) dissolution of celestite (Table S6), which is found among the precipitated minerals in the Dead Sea (Katz et al., 2009; Reznik et al., 2009), (ii) dissolution of Sr-containing anhydrite (Moeller et al., 2007), or (iii) release of Sr during transformation of aragonite to calcite (Usdowski, 1973).

In conclusion, the freshwater input in the brackish underwater springs originates from the Judea Group Aquifer (JGA). However, as suggested by our water chemistry data and argued in detail above, the JGA waters are affected by a number of processes before they emerge at the Dead Sea floor. These include interaction with clay minerals, fine clastics and  $\text{FeOOH}$  complexes, dissolution or precipitation of different types of evaporates (e.g., aragonite, gypsum, anhydrite, halite, celestite, barite), bacterial degradation of organic matter (by sulfate reduction), and mixing with interstitial and ascending brines in the Dead Sea Group sediment. The sum of these processes results in water with high concentrations of dissolved ammonium and organic matter, sulfide, sulfate and phosphorus; all of which are necessary to support the microbial communities at the springs outlets in the Dead Sea, as discussed below. Although the springs emerge over a relatively small area at the Dead Sea floor, our data indicate that their flow between the graben shoulders and the lake occurs through pathways of different hydraulic conductivities. This

---

leads to various residence times, which in turn results in a variable extent to which the above processes affect the spring waters' chemical composition. Overall, spring waters in the "Limestone" group (springs 1, 3, shore spring 2, and likely also spring 4) probably flow through well-developed open cracks, allowing marginal water-mineral interaction. In contrast, waters in the "Dead Sea" group (springs 1A, 2, 11, shore springs 1 and 3, and likely also spring 10) are likely to flow from the JGA through smaller fissures and less open cracks, with their flow paths through the DSG sediment possibly still developing. Consequently, their interaction with minerals and interstitial brines is much more intense.

### **Source of microorganisms in spring waters**

Microbial communities in the spring waters contained high cell densities. The close match between the total cell counts obtained by FISH and DAPI staining is a good indication that the majority of these cells were alive at the time of sampling (DeLong et al., 1999; Ravenschlag et al., 2000). Although the microbial community in the Judea Group Aquifer has not been studied yet, pristine aquifers always have very low numbers of microbial cells (Pedersen, 1990; Goldscheider et al., 2006; Haveman and Pedersen, 2010). Therefore, we suggest that these cells detected in the spring waters grew and were collected along the path of the groundwater flow from the aquifer to the Dead Sea and did not grow in the aquifer itself.

This conclusion is supported by the fact that the spring waters contain solutes that can be utilized or produced by microbial metabolisms. The sulfide in the spring waters probably originates from sulfate reduction, which is a feasible process as both sulfate and DOC are available. The high ammonium concentrations are probably the result of organic matter oxidation and are a further support for microbial activity along the aquifer's flow path. The REY patterns further suggest that redox cycling of Fe occurs along the flow path of the "Dead Sea" group springs. The requirements for Fe reduction are met by the availability of DOC and FeOOH, while Fe oxidation may occur anaerobically (Straub et al., 1996; Clement et al., 2005) or in parts of the aquifer that are still oxygenated. Oxidation of organic matter is further supported by the high concentration of inorganic nitrogen.

---

The source of microorganisms in the spring waters by collection along the path is further supported by the relatively high fraction of detected Archaea, which was much higher than in other groundwater aquifers and freshwater bodies (Keough et al., 2003; O'Connell et al., 2003). These Archaea may originate from two different possible sources. Shoreline pore water can be the first source as suggested by the fact that majority of the detected Archaeal sequences were from the halophilic group *Halobacteria*, which usually require a minimum salinity of 15%. The pore water of the Dead Sea shoreline is saturated with brine and contains organic matter from flood carried debris (C. Siebert, unpublished), which provides suitable conditions for *Halobacteria*. Furthermore, no *Halobacteria* were detected in springs far from the sandy shoreline, i.e. at the bottom of a steep cliff (springs 10 and 11).

An additional or alternative origin of the Archaea could be a second water source. This is suggested by the fact that the majority of *Halobacteria* detected in the spring water fall within a cluster of organisms associated with deep hydrothermal vents and differ from the *Halobacteraceae* found in the spring sediments (Fig. 8C). It has been shown before that this deep sea group of the *Halobacteria* can thrive in less saline environments (Gracas et al.; Elshahed et al., 2004). The *Thermoplasmata*-associated sequences from the springs cluster with samples from deep hydrothermal vents as well. The Dead Sea is located in a tectonically active environment (Lazar and Ben-Avraham, 2002) and ascending hydrothermal brines are often observed as thermal springs (e.g. Ein Gedi and Mitzpe Shalem; Swarieh, 2000; Shalev et al., 2008; Vengosh et al., 1991; Moeller et al., 2007). From their REY patterns and composition of major ions it cannot be excluded that ascending hydrothermal brines, as observed in the Qedem area, are intruding into the waters of the studied spring system.

### **Source of microorganisms in spring sediments**

Our data show that majority of organisms brought in by the springs do not colonize the sediments around them. Instead, the dense and diverse microbial communities found in the sediments around the springs consist largely of organisms that are resident in the Dead Sea sediments. This conclusion follows from a detailed comparison between the microbial communities detected in spring waters, spring sediments, Dead Sea water column (Bodaker et al., 2010) and the Dead Sea during a bloom (Rhodes et al., 2010). First, microbial communities in spring sediments were much more similar to those found in the ambient Dead Sea sediment than to those detected in the spring waters. The larger spread of sediment samples in the ARISA analysis could be a result of the higher number of samples, compared to the 454 analysis, as well as of the higher resolution of an ITS based method in comparison with partial sequencing of the 16S rRNA gene. The spread away from, rather than around, the Dead Sea reference sediments is probably due to an uneven number samples of Dead Sea reference sediments as compared to spring sediments. Second, microbial communities associated with springs differed from those induced by freshwater input into the Dead Sea during surface floods. Bodaker et al., (2010) showed that the bloom community of the Dead Sea differed from the residual community in the water column. Our data shows that these two communities resemble each other more than they resemble the communities associated with spring waters or sediments. Whether the dense microbial communities found associated with the springs on the lake's bottom are a result of lowered salinity or an input of nutrients dissolved in the spring water needs to be further investigated.

### **Putative biogeochemical pathways**

The importance of a certain metabolic pathway is linked to the abundance and activity of the cells involved. Therefore, solid data on the actual abundance of cells (obtained by FISH), as well as direct evidence that the cells detected by FISH actually perform this metabolism *in situ*, is required. As we at present do not have all this information, we base the following discussion on the assumption that the importance of a given metabolism is

---

approximated by the relative frequency of detected sequences that are closely related to species for which the metabolism in question was proven. Exceptions to this approach are phototrophy and sulfide oxidation, whose importance is further supported by our pigment analyses and visual *in-situ* observations of thick white biofilms, respectively. Overall, our complete dataset suggests that photosynthesis, sulfide oxidation, sulfate reduction, nitrification, and iron reduction most probably occur in the underwater spring ecosystems.

Phototrophy appears to be of significance only in the vicinity of spring 12, as thick green biofilms were found only there, mostly adhered to cobble. Between 30-40% of the sequences obtained from these biofilms are of known phototrophs. Spring 12 is shallower (12-14 m below water level, on a slope), not located within a crater structure, and the water flows through pebbles and cobble, thus not creating clouds of fine sediments. This was probably the only site where the light intensity (up to 45  $\mu\text{mol photons m}^{-2} \text{s}^{-1}$  in mid-day) was sufficient to fuel a dense phototrophic community. The dominant phototrophs in these biofilms were green sulfur bacteria, which are known to adapt well to low light intensities (Overmann, 2006). Sequences of purple sulfur bacteria, mainly represented by the *Ectothiorhodospiraceae*, were also highly abundant, making up 6-12% of the sequences. Though we could identify cyanobacteria microscopically (based on specific absorption and autofluorescence of their pigments), we obtained only a few sequences of a *Chroococciopsis*-like organism.

Hyper-spectral imaging showed a peculiar association between the green sulfur bacteria and the cyanobacteria, with patches of cyanobacteria surrounded by or co-localized with green sulfur bacteria. A co-localization of cyanobacteria and green sulfur bacteria was not described before. Green sulfur bacteria are usually strictly anaerobic organisms, and contain a quenching mechanism for protection against oxidation (Frigaard and Bryant, 2004). On the other hand, although cyanobacteria that are able to switch to anoxygenic photosynthesis are also known (Cohen et al., 1986; Oren et al., 2005), cyanobacteria are oxygenic phototrophs. The nature of the association found in this study is unclear and will be the subject of future studies.

---



Sulfide oxidation appears to be the key metabolism in this ecosystem, as suggested by the presence of a large variety of sulfide oxidizing bacteria. In the biofilms from the southern system 75-85% of the sequences are associated with known sulfide oxidizing bacteria. In the northern system the percentage is much lower (1.5-4.5%). Hydrogen sulfide ( $\text{H}_2\text{S}$ ) was measured in significant concentrations in the underwater springs (Table 2) and could be often smelled from the freshly retrieved sediment cores and from shore springs. Oxygen is present in the Dead Sea waters (20-40  $\mu\text{M}$ ; Shatkay et al., 1993); thus the process of aerobic sulfide oxidation is feasible. The sulfide oxidizing communities in the southern springs are different from those in the northern springs. The southern springs consist mainly of *Epsilonproteobacteria* and phototrophic sulfide oxidizers, while the *Thiotrichaceae* and *Acidithiobacillaceae* inhabit sediments and biofilms around the northern springs. The difference in sequence abundance between these spring sites suggests that sulfide plays a more important role in the southern system. This is also evident by the significantly larger size of white biofilms in the southern springs. Interestingly, sulfide oxidizers were not found in the water of all springs. The large number of sequences obtained from the water of springs 10 and 11 suggests a thriving community of sulfide oxidizing bacteria along the path of the water flow. The genera of sulfide oxidizing *Epsilonproteobacteria* found in the water of springs 10 and 11 differ from those found in the biofilms of spring 12. This supports the hypothesis mentioned above that only a few of the organisms found in the spring-associated biofilms and sediments, originate from the spring water. *Epsilonproteobacteria* are common among the non-phototrophic sulfide oxidizing bacteria in moderate saline environments (Benlloch et al., 2002) and were found to be main players in salt gradient systems such as the deep sea Mediterranean brines (La Cono et al.; van der Wielen et al., 2005).

Sulfate reduction is probably the source of the sulfide both in the spring waters and in the biofilms. This is consistent with the presence of diverse groups of sulfate reducers detected in most water samples. In the green and white biofilms of spring 12 sequences of sulfate reducers make 4% and 11% of total sequences respectively. The latter was confirmed by FISH using a specific probe for *Deltaproteobacteria* (Fig. S2). Along the water flow path sulfate necessary for the process originates from gypsum and anhydrite

---

dissolution. In the biofilms, the co-existence of sulfate reducers with sulfide oxidizers suggests that an internal sulfur cycle exists in these communities.

Sulfate reducers are generally missing from the sediments of the northern springs. Sulfate reduction was never convincingly measured in the Dead Sea sediments (Oren A, unpublished results), and to date no extreme halophilic sulfate reducers are known. The fluctuating water flow, observed in the northern system, may not allow halotolerant sulfate reducers to develop there, as the salinity is regularly too high. In turn, the lack of sulfate reducers, the fluctuating water flow and the sediment instability are probably the reasons for the low abundance of sulfide oxidizers in the northern springs.

Nitrification appears to be significant in the sediments and biofilms of the northern springs and is absent in the southern system. Nitrogen is not limiting in the Dead Sea or in the underwater springs (Table 2). Furthermore, up to 400  $\mu\text{M}$  of ammonia were measured previously in the Dead Sea water column (Stiller and Nissenbaum, 1999). As nitrogen is plentiful, the reason for the absence of this group from the southern springs cannot be explained at this moment.

Reduction of iron, and possibly of other metals, may also be significant in the spring system. The *Acidithiobacillaceae* sequences (0.9-3%) from the northern springs are affiliated with the genus *Acidithiobacillus* and more specifically with *Acidithiobacillus thiooxidans* and *Acidithiobacillus caldus*, which are both known for dissolution of metal sulfides (Sand et al., 1995; Bosecker, 1997; Semenza et al., 2002). There are several other groups of organisms detected that suggest the role of metal reducing and oxidizing bacteria in the system. For example, members of the phylum *Deferribacteres* (Caccavo et al., 1996; Greene et al., 1997; Huber and Stetter, K, 2002) were found in most of the water samples and in the green biofilms of spring 12. Sequences affiliated with *Gallionella* sp. were found uniquely in samples from spring 2, which is the only spring with favorable chemical conditions for iron oxidation ( $E_h > 0$  mV). Additionally, several species of the genus *Pelobacter*, sequences of which were found in higher frequency in the biofilms of spring 12 (0.4-1.5%), are known as  $S^0$  as well as iron reducers (Lovley et al., 1995; Schink, 2006).

---

Microbial iron reduction is further supported by the detection of reduced Fe in the deeper parts of the lake prior to its overturn. Nishri and Stiller, (1984) reported up to 4  $\mu\text{M}$   $\text{Fe}^{2+}$  in the water column prior to the 1979 Dead Sea overturn and up to 1200  $\mu\text{M}$   $\text{Fe}^{2+}$  in the pore water of the Dead Sea. During 1978-1980, following the oxygenation of the water column, reduced Fe was not detected and only particulate Fe was reported. This suggests that oxidized iron as a substrate for iron reduction is abundant in the Dead Sea sediment. Due to the abundant supply of DOC from the spring water, a community of iron reducing bacteria can be sustained.

The majority of the microbial lineages described here are known from environments of various salinities (Oren, 2002) usually in well-established microbial mats or in overlaying waters with a constant salinity. The fluctuating nature of the Dead Sea spring system does not permit the establishment of neither a constant salinity nor a permanent gradient. Hence, a full comparison between the microbial communities in this system to those in any other system is difficult. We believe that the described flow regime prevents the growth of organisms which are adapted to a narrow range of salinities but leading to a specialized community that can cope with drastic salinity shifts.

### **Environmental fitness**

Although adaptation to salinity was not investigated in this study, we expect to find two types of organisms in these environments: moderate halophiles and extreme halophiles. This is based on our underwater observations, which indicate constant and fluctuating water flow regimes. Springs 10, 11, and 12 are characterized by a continuous flow with occasional changes in flow intensity. Therefore we can expect moderate halophiles to be able to grow in such a system. Indeed, the cultured green sulfur bacteria, whose 16S rRNA sequence is identical with the partial sequence of the dominant green sulfur bacteria in the biofilms of spring 12, grew best at seawater salinity (data not shown). Spring 1A, as were the large, borderless, seeping areas on the slopes below springs 10, 11, and 12, were inactive for part of the time. In the center of the spring the fresher water flows directly to the surface; however, the water often seeps through the sediments at the periphery or

---

through larger undefined areas. This suggests that the organisms in the spring sediment are exposed directly to these waters. Sudden and drastic changes in salinity, such as those induced by the onset and offset of the water flow, would call for an extreme halophile with rapidly responding osmoregulation and the ability to survive in a broad spectrum of salinities. Our data suggests that the organisms in the spring sediments are naturally found in the Dead Sea sediments; therefore an extreme halophile that can withstand freshwater would be an intriguing finding.

### **Significance of the springs for the Dead Sea**

The underwater springs described here are part of one system of springs. To this date there is no information available on the number of similar spring systems on both coasts of the Dead Sea, nor about their contribution to the water budget of the Dead Sea. This is partly because deeper springs, such as those in the northern system, cannot be detected from the shore. Recent findings of Siebert and Mallast (unpublished data) indicate that thermal infrared imaging allows indirect localization of underwater springs, even deeper ones. Additional, remote sensing studies have shown that similar systems exist on the eastern coast of the Dead Sea (Akawwi et al., 2008). However, further direct underwater exploration is necessary to collect information regarding their distribution, size, and the input of water and the accompanying microbiota that these systems provide for the Dead Sea.

The economic significance of the Dead Sea lies in mineral harvesting and tourism. Both industries can suffer due to changes in the microbiology of the Dead Sea. The information about the microbial input from the springs is especially relevant in the light of the currently discussed Red Sea–Dead Sea canal. The possible outcome of diluting the Dead Sea with the Red Sea water has recently been investigated (Oren et al., 2004). These predictions took into consideration insufficient factors: a) mixing of only two microbial communities, the residual community in the Dead Sea water column and the microbial community in the water of the Gulf of Aqaba; b) the nutrient input from the planned desalination plant. If such a water connection will be formed and the brine of the proposed

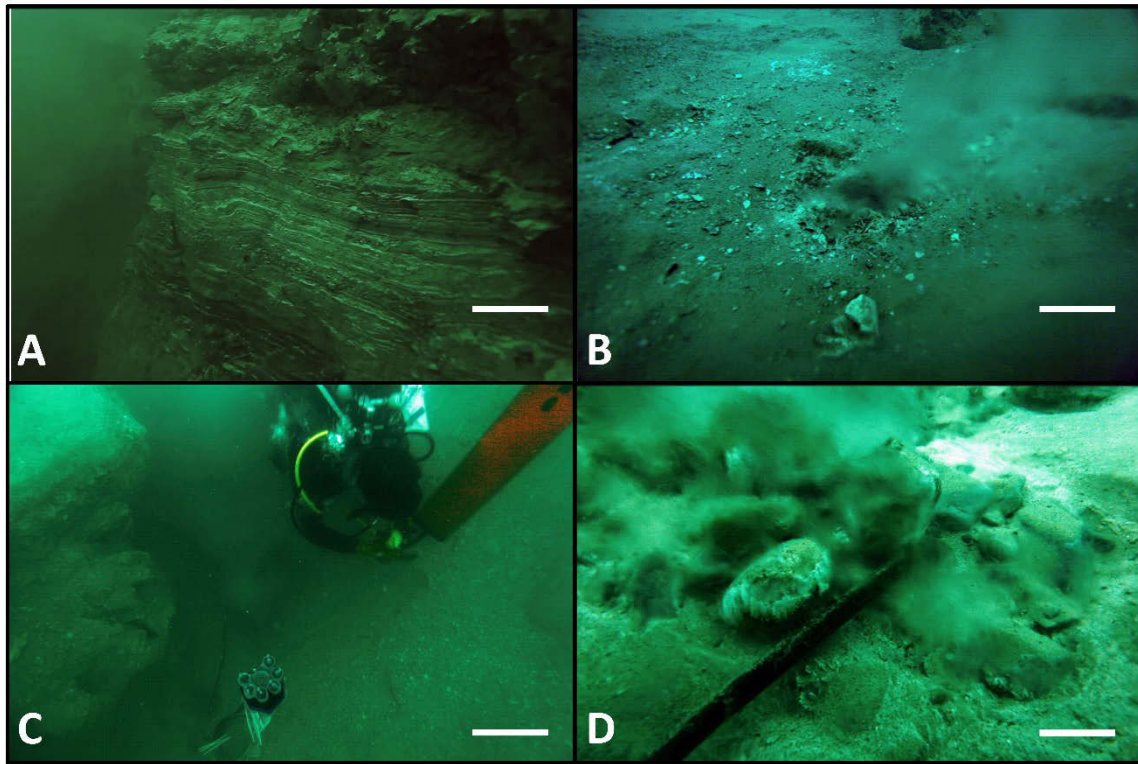
---

desalination plant will flow into the Dead Sea, a water lens with a relatively low salinity will form on the surface of the Dead Sea. Bacteria, organic matter and other nutrients from the underwater springs are rapidly transported to the less saline water layer at the surface. This may lead to massive blooms of either spring or Dead Sea bacteria. Such blooms will alter the visual appearance of the water thus directly affecting its touristic value. Furthermore, the lowered salinity and increased microbial activity may promote biofilm growth and thus lead to biofouling of the equipment used by the Dead Sea Works company to pump water from the northern basin to the southern basin. We suggest that the previously conducted experiments [74] be complemented with the addition of spring water as part of the assessment of the environmental impact of the proposed Dead Sea-Red Sea water canal.

We hypothesize that the dense hydrogeochemical network of channels and the associated microbial communities in association play an important role in the overall land stability in the area. It is likely that mineral dissolution by freshwater alone is not solely responsible for the formation of the large sinkholes on the coasts of the Dead Sea (Closson and Karaki, 2009). Microbial activity such as sulfate reduction and oxidation leads to faster dissolution of gypsum and carbonate layers via processes known from sulfuric acid speleogenesis (Engel et al., 2004). Sulfate released from anhydrite either by dissolution or by bacterial leaching (Engel et al., 2004; Shen and Buick, 2004) is used for sulfate reduction. The produced sulfide is oxidized by bacteria into sulfuric acid which leads to the dissolution of carbonate minerals (Engel et al., 2004). Sulfide oxidizing *Epsilonproteobacteria* as found in the water of springs 10 and 11 were suggested to be involved in sulfuric acid speleogenesis (Engel et al., 2003; Macalady et al., 2007). Our data indicates that dense microbial communities may exist in the area between the graben shoulder and the Dead Sea. The bacterial activity coupled with the freshwater flow may lead to the enlargement of channels and the formation of underground cavities, locations where the overlaying soil may become unstable.

## Conclusions and outlook

We have found a new microbial ecosystem in the Dead Sea, tightly associated with underwater springs that emerge at the lake floor at depths between 10-30 m. The ecosystem is diverse, and the presence of multiple major biogeochemical pathways is indicated. However, as demonstrated by our data, the springs do not serve as an input of this diversity, but more likely as a source of nourishment for the native Dead Sea community. The dominant microorganisms in the ecosystem as implicated by our microbial community and water chemistry data are phototrophs, sulfide oxidizers, sulfate reducers, nitrifiers and iron reducers. However, direct measurements of the rates of these processes are necessary to better understand the function of this microbial ecosystem and its impact on the Dead Sea ecosystem as a whole. Also detailed measurements of salinity, iron, nutrients, oxygen and stable isotopes of  $\delta^{34}\text{S}$  and  $\delta^{18}\text{O}$  in sulfate and sulfides in water as well as in and near the benthic communities are needed to elucidate the nature of the biogeochemical processes. Our data further suggest the existence of a dense microbial community within the DSG sediments and mineral bed located between the former and current Dead Sea water level line. However, the activity of this community and their role in the dissolution of minerals in these sediments remain to be determined. The underwater system of springs described here is the first out of several in the Dead Sea. Together, they are an unknown factor in its water budget as well as an unknown source of diversity and metabolic potential.

**Supplementary information**

**Figure S1** A) Lamination on the walls of the shafts created by the springs in the northern system. B) An example of a single water source out of several at the bottom of a shaft in the northern system. C) An example of an in-shaft cavity from which water springs out. D) Cobble covered spring in the southern system. Biofilms are visible on the cobble. Scale bar 0.2 m.

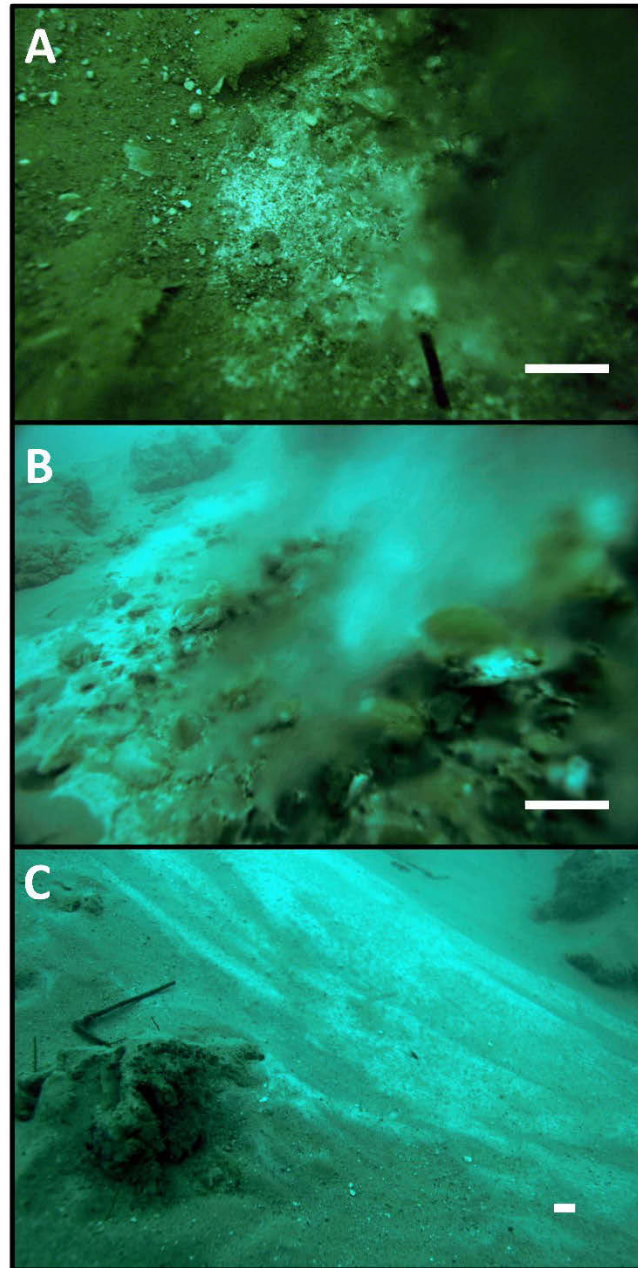


**Figure S2** Different types of biofilms found near the underwater springs. (A) Small patches of thin white biofilms covered sediments adjacent to the water source in springs 1-5. (B) Thick white biofilms covered sediments around spring 12, whereas top and bottom surfaces of rocks found within this spring were covered with green and white biofilms, respectively. (C) Large white biofilms covered slopes below springs 10 and 11 at depths ca. 20 m, although no water seepage was detected. Scale bar: 0.2 m



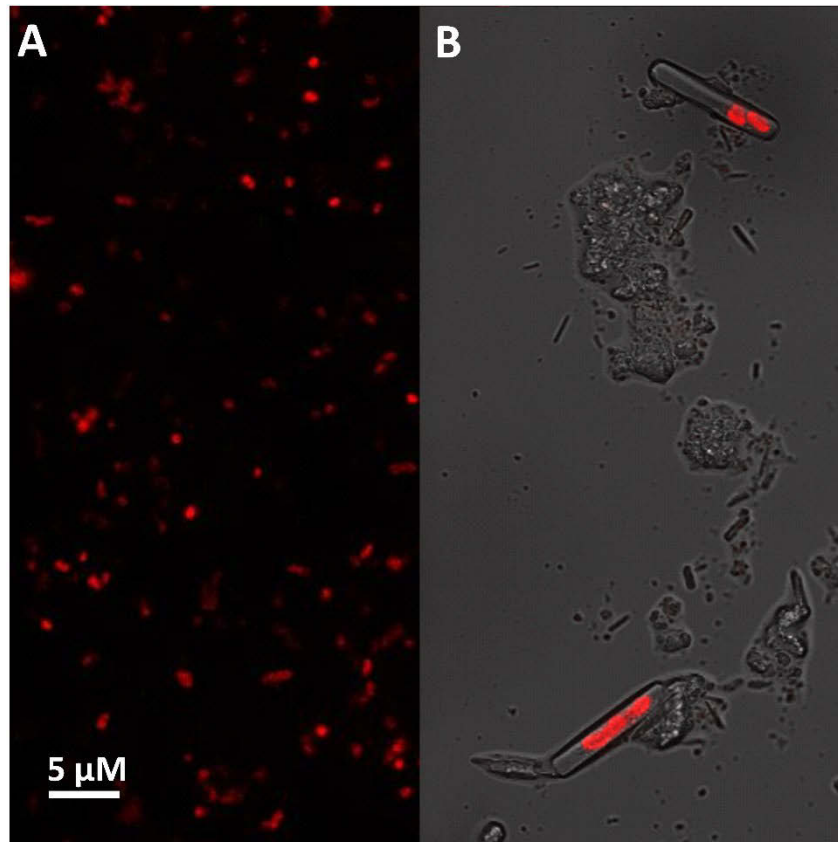


**Figure S3** Chlorophyll a autofluorescence confocal laser scanning microscopy of samples from the green biofilms of spring 12 showing small unicellular cyanobacteria (A) and diatoms (B). The images were acquired by Mr. Assaf Lowenthal.

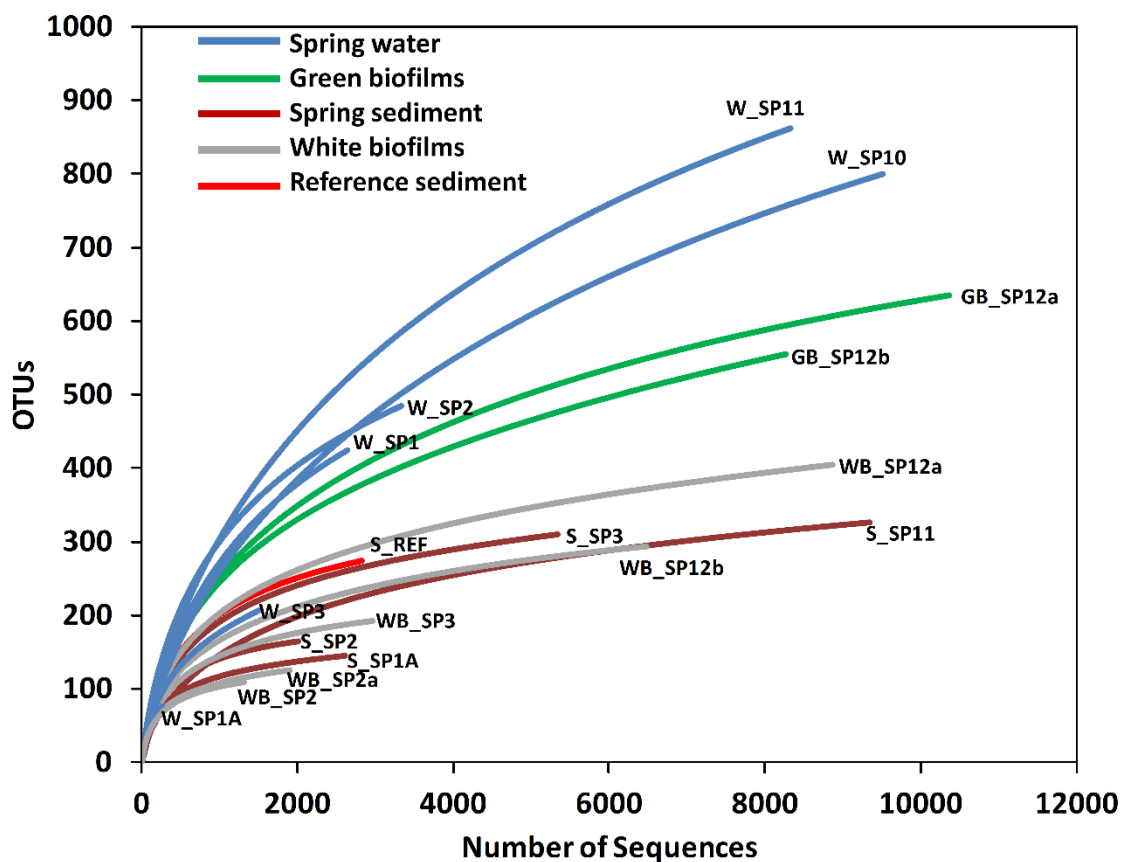


**Figure S4** Rarefaction curves for the different sediment, biofilm and water samples, as derived from the pyrosequencing data by the NGS pipeline. Samples names are given at the end of the curve: W, S, WB, GB stand for water, sediment, white biofilm and green biofilm respectively, followed by the spring number.

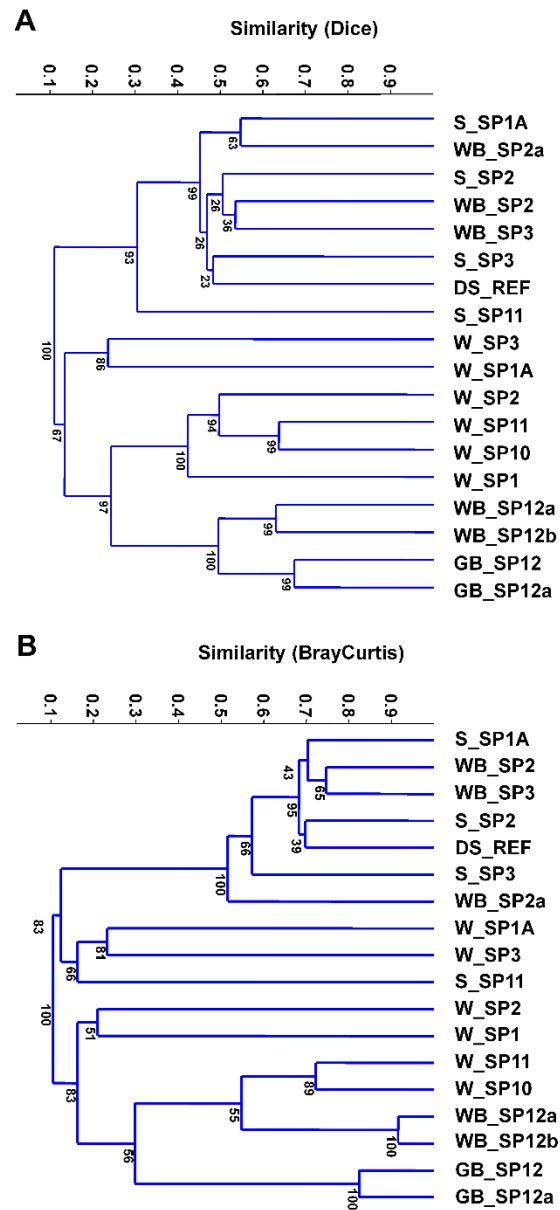


**Figure S5** Comparison of underwater spring waters, sediments and biofilms based on the taxonomy assigned to the pyrosequencing results at the 6th taxonomic depth. Panel A considers only sequence identity, whereas panel B takes additionally into account sequence frequency. The diagrams show that the reference microbial community shared 45% of the taxa with the spring sediments (except of spring 11) as opposed to 10% with the spring waters. The similarity between the reference sediments and springs sediments increased 50%-70% when sequence frequency was additionally taken into account, with the exception of spring 11. The reference Dead Sea sediments were collected in the northern spring system, whereas spring 11 belongs to the southern system.

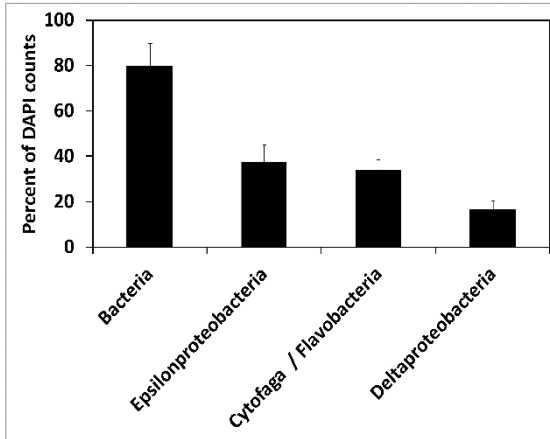


**Figure S7** Percent abundance of total Bacteria, Epsilonproteobacteria, Cytofaga/ Flavobacteria and Deltaproteobacteria out of total DAPI stained cells as obtained by Fluorescent In-Situ Hybridization on a white biofilm from spring 12. FISH was conducted using the EUBI, II, II, Eps404, CF119a and Delta\* 495a, b, c probes. \*Competitor probes were used. Total cell number as calculated from the cell counts is  $2.8 \times 10^{10}$  cells g<sup>-1</sup>.

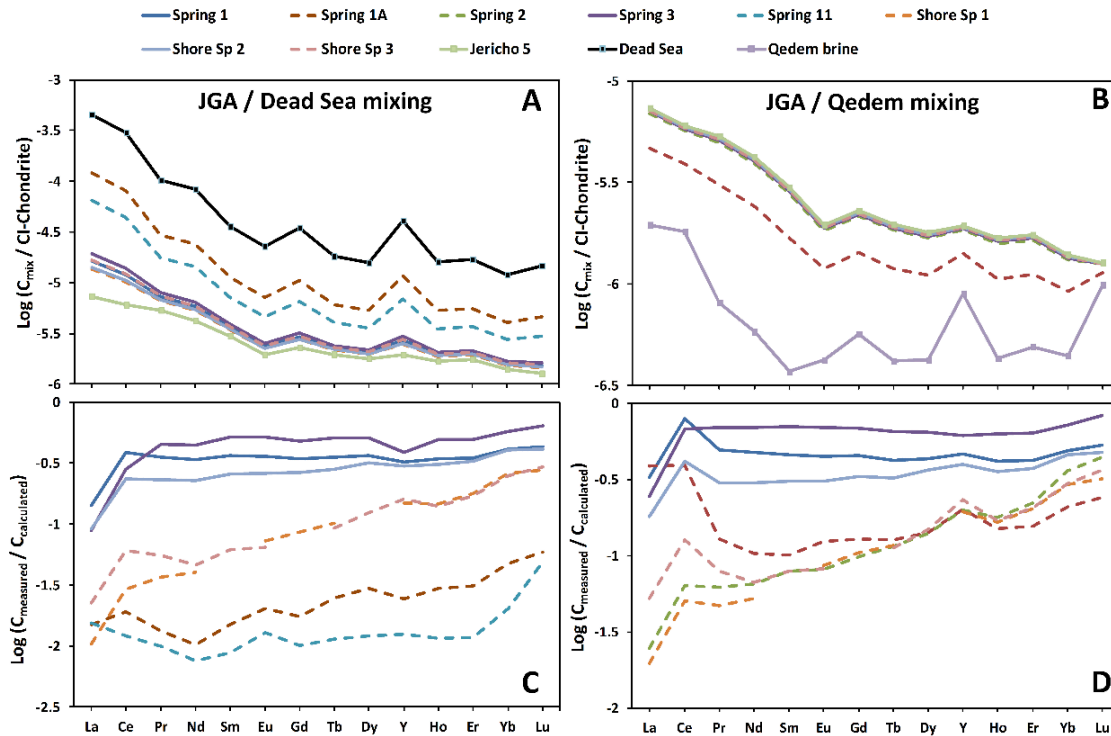


**Table S1** REY concentration in sampled waters and whole rock analyses. Tm is not listed, since it was added as spike.

pmol/L	La	Ce	Pr	Nd	Sm	Eu	Gd	Tb	Dy	Y	Ho	Er	Yb	Lu
Spring 1	3.06	6.59	0.25	0.78	0.17	0.05	0.23	0.03	0.23	5.00	0.05	0.17	0.18	0.04
Spring 1A	3.92	20.0	1.62	6.09	1.30	0.31	1.27	0.18	1.13	15.4	0.23	0.68	0.62	0.09
Spring 2	0.29	1.56	0.19	0.80	0.22	0.05	0.27	0.05	0.35	6.43	0.10	0.35	0.45	0.08
Spring 3	2.91	16.9	2.25	8.79	1.95	0.48	1.89	0.28	1.66	20.4	0.35	1.02	0.91	0.14
Spring 11	1.70	2.29	0.11	0.34	0.06	0.02	0.08	0.01	0.06	1.52	0.01	0.04	0.05	0.02
Shore Spr. 1	0.66	2.23	0.20	0.73	0.19	0.05	BDL*	0.05	0.40	7.10	0.10	0.32	0.38	0.06
Shore Spr. 2	2.18	10.6	0.99	3.86	0.87	0.22	0.93	0.14	0.95	13.2	0.20	0.61	0.59	0.08
Shore Spr. 3	3.65	16.1	2.15	8.59	2.03	0.50	2.12	0.34	1.90	22.7	0.39	1.11	1.00	0.15
Qedem Brine	3.30	7.78	0.51	1.82	0.36	0.16	0.71	0.09	0.63	15.7	0.15	0.46	0.42	0.14
Auja 2	3.08	6.11	0.71	2.45	0.54	0.15	0.54	0.08	0.55	7.20	0.11	0.33	0.37	0.05
Auja 4	2.18	4.03	0.44	1.24	0.33	0.08	0.35	0.05	0.38	5.30	0.08	0.25	0.28	0.03
Jericho 5	12.4	25.9	3.37	13.2	2.92	0.72	2.87	0.44	2.67	34.0	0.57	1.66	1.31	0.17
Mitzpe Jericho 2	3.26	4.29	0.63	2.19	0.60	0.15	0.72	0.10	0.83	16.8	0.22	0.75	0.81	0.14
HammatGader: EinMakla	10.3	14.7	1.81	7.43	1.28	0.38	1.83	0.31	1.99	47.0	0.48	1.84	1.92	0.33
EinQilt 1	43.5	66.5	11.9	58.3	13.3	3.94	20.2	3.32	28.0	530	8.36	29.1	24.7	3.76
EinQilt 2	43.7	28.7	12.1	59.1	13.2	3.92	20.6	3.35	28.4	552	8.46	29.6	25.2	3.82
Lake Kinneret, hypolimnion	17.1	42.9	3.68	15.4	2.93	0.80	3.38	0.49	3.18	61.8	0.74	2.35	2.15	0.36
µg/g														
Limestone (JGA)	17.1	10.5	2.59	11.0	2.39	0.61	3.43	0.51	3.54	48.1	0.90	3.04	3.12	0.53
Marlstone (JGA)	1.39	0.59	0.24	0.96	0.18	0.05	0.21	0.03	0.17	2.11	0.04	0.12	0.09	0.01

Table S 2 Sequence statistics per sample as obtained from the NGS analysis

Sample Name	#Seqs	Min	Average	Max	General						Classified		Unclassified		Good's coverage
					Reflected	Homopolymer	Clustered	Replicate	False hits	OTUs	OTUs	#Seqs	OTUs	#Seqs	
W SP1	2895	200	432,5988	561	0	0	1822	427	0	446	446	2895	0	0	0.977
W SP1A	262	200	444,3701	536	0	0	147	37	0	78	78	262	0	0	0.969
W SP2	3632	201	450,493	537	0	3	2651	372	0	606	603	3629	3	3	0.933
W SP9	1328	200	348,9996	539	0	0	1145	171	0	212	212	1328	0	0	0.948
W SP10	10073	200	469,3248	561	0	6	7252	1728	0	1087	1078	10033	9	40	0.949
W SP11	6811	200	469,1671	559	2	8	6663	1072	0	1066	1056	6771	10	40	0.926
5 SP1A	2633	150	324,3404	499	0	8	1676	814	0	133	150	2649	3	4	0.961
5 SP2	2076	150	417,9216	547	3	26	1310	562	0	175	170	2046	5	30	0.961
5 SP3	5449	150	421,0319	651	0	51	3251	1604	0	343	327	5423	16	26	0.961
BACTERIA	5 SP11	8426	361,9789	545	0	6	4337	4922	0	359	300	9187	59	239	0.990
W BSF2	1363	150	416,2406	541	0	16	656	371	0	150	119	1362	1	1	0.979
W BSF3	3060	150	416,7566	555	0	36	1650	959	0	215	204	3025	11	35	0.961
W BSF2a	1840	150	331,1103	491	0	9	1103	569	0	159	156	1837	3	3	0.961
W BSF12b	6973	200	469,4033	545	0	0	7096	1423	0	454	454	6973	0	0	0.964
W BSF11b	6241	200	468,6862	545	0	0	5997	1115	0	329	329	6241	0	0	0.955
GB SP12b	10909	200	435,5848	539	0	0	7536	2273	0	688	697	10506	1	3	0.972
5 OS	8408	200	431,6204	543	2	1	6226	1554	0	623	621	8401	2	7	0.971
W SP1	2819	151	418,5074	545	3	32	1601	766	0	295	288	2806	7	11	0.930
W SP1	6313	200	416,7973	569	1	15	4703	521	1245	1073	1064	6299	9	14	0.965
W SP1A	1864	201	422,2135	487	0	1	1333	195	626	135	135	1864	0	0	0.966
W SP2	6200	200	413,0065	514	1	54	5025	497	974	623	620	6195	3	5	0.964
W SP3	6734	200	413,712	536	1	56	5566	637	1432	482	487	6747	5	7	0.966
5 SP1A	1336	154	432,5157	496	0	0	908	393	416	33	33	1336	0	0	0.996
5 SP2	3148	150	417,6796	486	0	0	1672	1404	2765	72	71	3147	1	1	0.994
5 SP3	1665	152	419,6248	496	0	0	969	631	0	45	45	1665	0	0	0.996
W BSF2a	1696	150	387,3479	452	0	0	1153	710	1603	35	35	1696	0	0	0.966
GB SP12b	928	206	407,578	475	0	0	683	201	21	43	43	928	0	0	0.990
GB SP12b	10423	200	414,6996	529	0	0	6136	3945	2302	340	340	10423	0	0	0.990
5 OS ARCH	561	153	427,3963	492	0	0	490	129	576	22	22	561	0	0	0.969
ARCHAEA															

**Table S2:** #Seqs :The number of reads in this sample; Min: The shortest read in this sample (number of nucleotides); Max: The longest read in this sample (number of nucleotides); Average: The average length of a read in this sample (number of nucleotides); Rejected: Number of reads rejected by the aligner (possible contamination); Homopolymer: Number of reads rejected by the quality control because of a problematic amount of homopolymeric stretches in the read; Clustered: The number of reads assigned to a cluster within the same sample (98% identity); Replicates: The number of reads identical to another read within the the sample sample (100% identity); False Hit: The number of reads outside the target group of the used primers; OTUs (total): The total number of unique reads, at 98% sequence similarity, in each sample; OTUs (class.): The number of unique reads with an assigned taxonomic classification; #Seqs (class.): The total number of reads with an assigned taxonomic classification; OTUs (unclass.): The number of unique reads without an assigned taxonomic classification; #Seqs (unclass.): The total number of reads without an assigned taxonomic classification. Good's coverage [94] was calculated as  $1 - (n_i/N)$  where  $n_i$  is the number of OTUs containing only one sequence and  $N$  is the total number of sequences. The false positive Bacterial sequences obtained while using Archaea specific primers, were not used for the calculation.

**Table S3** (A list of Bacterial taxonomic paths and their relative abundance in the samples.) and **Table S4** (A list of Archaeal taxonomic paths and their relative abundance in the samples) can be downloaded from <http://www.plosone.org/article/info%3Adoi%2F10.1371%2Fjournal.pone.0038319>

**Table S4** R and p values are shown in the lower and upper half of the square matrix respectively. An R value of 1 between two groups represents total dissimilarity, whereas values closer to 0 suggest a high similarity. The significance of the similarity analysis (p) was done by permutation of group memberships using 10,000 replicates. P values of significance are marked in bold and italics.

**A**

R \ P	Water North	Water South	Sediment	WB North	WB South	GB South
Water North		0.1327	<i>0.0151</i>	<i>0.0295</i>	0.0684	0.0657
Water South	<b>0.2143</b>		<i>0.0503</i>	0.0949	0.3327	0.3302
Sediment	<b>0.7625</b>	<b>1</b>		0.6028	<i>0.0466</i>	<i>0.0454</i>
WB North	<b>1</b>	<b>1</b>	<b>0.09744</b>		0.103	0.104
WB South	<b>0.5893</b>	<b>1</b>	<b>1</b>	<b>1</b>		0.338
GB South	<b>0.4286</b>	<b>1</b>	<b>1</b>	<b>1</b>	<b>1</b>	

**B**

R \ P	Sediments	Water 1A, 3	Water 1, 10, 11
Sediments		<i>0.0032</i>	<i>0.0006</i>
Water 1A, 3	<b>0.9335</b>		0.6029
Water 1, 10, 11	<b>0.993</b>	<b>0</b>	



**Table S6** Trace element concentrations in sampled waters. Si\* is the sum of Si(II) and Si(III). \*\* Mn is the total sum of all Mn-species. Saturation indices were calculated by Geochemist's Workbench (using LLNL thermo database and Harvie-Möller-Ware activity model, as implemented in the USGS program PHREEQPTZ)

	Saturation Indices (SI)																
	Cs <sup>+</sup>	Rb <sup>+</sup>	Ba <sup>2+</sup>	B <sup>3+</sup>	Sr <sup>2+</sup>	Li <sup>+</sup>	Si*	Mn**	Anhy-drite	Argo-nite	Bar-ite	Cal-cite	Celes-tine	Dolo-mite	Gyp-sum	Ha-lite	Stronti-anite
Dead Sea	87.4	26.6	16.2	3.11	3.89	2.04	0.08	50.0	0.657	0.91	-	1.09	-	3.41	0.516	0.758	-
Spring 1	1.30	0.84	1.82	0.28	0.18	0.06	0.66	0	-1.28	0.769	0.524	0.934	-0.939	3.34	-1.13	-4.84	1.90
Spring 1A	18.8	6.44	3.57	1.94	1.37	0.70	0.61	30.0	-0.172	0.202	-	0.386	-	1.71	0.0365	2.63	-
Spring 2	2.62	1.61	3.06	0.60	0.35	0.14	0.72	0	-1.18	0.840	0.652	1.00	-0.564	3.55	1.04	-4.31	2.24
Spring 3	1.94	1.25	3.50	0.40	0.55	0.08	0.69	0	-1.47	1.00	0.439	1.17	-0.923	3.93	1.40	-4.65	2.31
Spring 4	-	-	-	-	-	-	-	-	-	-	-	-	-	-	-	-	-
Spring 10	-	-	-	-	-	-	-	-	-	-	-	-	-	-	-	-	-
Spring 11#	8.28	3.51	2.84	1.06	0.58	0.43	0.49	10	-1.4	-	0.0333	-	-1.17	-	-1.29	-3.41	-1.40
Sh Spring 1	2.11	0.60	2.62	0.16	0.10	0.03	0.31	0	-1.71	0.550	0.223	0.715	-1.52	2.90	-1.56	-5.14	1.53
Sh Spring 2	1.17	0.62	1.52	0.24	0.12	0.04	0.47	0	-1.89	0.756	0.189	0.920	-1.69	3.32	-1.73	-5.04	1.75
Sh Spring 3	1.25	0.54	1.38	0.20	0.15	BDL	0.37	0	-1.76	0.501	0.301	0.665	-1.68	2.82	-1.61	-4.90	1.38
Pore water	130.2	36.3	7.60	3.57	7.61	2.38	0.22	460	0.225	0.0262	-	0.156	-	1.64	0.0099	-0.537	-
Qedem brine	138.5	15.9	6.70	2.56	3.94	1.30	0.58	0.06	0.205	0.615	-	0.439	-	0.0954	0.118	1.78	-
Jericho 5	0.99	0.031	0.89	BDL	0.01	BDL	BDL	BDL	-2.53	0.276	0.527	0.441	-2.96	1.79	2.36	-7.44	0.642

**References**

- Akawwi, E., Al-zouabi, A., Kakish, M., Koehn, F., Sauter, M., Engineering, F., et al. (2008) Using Thermal Infrared Imagery (TIR) for Illustrating the Submarine Groundwater Discharge into the Eastern Shoreline of the Dead Sea-Jordan. *Am. J. Environ. Sci.* **4**: 693–700.
- Amann, R.I., Ludwig, W., and Schleifer, K.H. (1995) Phylogenetic identification and in situ detection of individual microbial cells without cultivation. *Microbiol. Rev.* **59**: 143–69.
- Amann, Rudolf, I., Krumholz, L., and Stahl, David, A. (1990) Fluorescent-oligonucleotide probing of whole cells for determinative, phylogenetic, and environmental studies in microbiology. *J. Bacteriol.* **172**: 762–770.
- Anati, D.A., Stiller, M., Shasha, S., and Gat, J.R. (1987) Changes in the thermo-haline structure of the Dead Sea 1979-1984. *Earth Planet. Sci. Lett.* **84**: 109–121.
- Anati, David, A., Stiller, M., Shasha, S., and Gat, Joel, R. (1987) Changes in the thermo-haline structure of the Dead Sea : 1979-1984. *Earth Planet. Sci. Lett.* **84**: 109–121.
- Barkan, E., Luz, B., and Lazar, B. (2001) Dynamics of the carbon dioxide system in the Dead Sea. *Geochim. Cosmochim. Acta* **65**: 355–368.
- Bau, M. (1999) Scavenging of dissolved yttrium and rare earths by precipitating iron oxyhydroxide : Experimental evidence for Ce oxidation, Y-Ho fractionation, and lanthanide tetrad effect. *Geobiology* **63**: 67–77.
- Benlloch, S., López-López, A., Casamayor, E.O., Øvreås, L., Goddard, V., Daae, F.L., et al. (2002) Prokaryotic genetic diversity throughout the salinity gradient of a coastal solar saltern. *Environ. Microbiol.* **4**: 349–60.
-

- Bodaker, I., Sharon, I., Suzuki, M.T., Feingersch, R., Shmoish, M., Andreishcheva, E., et al. (2010) Comparative community genomics in the Dead Sea: an increasingly extreme environment. *Isme J.* **4**: 399–407.
- Bosecker, K. (1997) Bioleaching: Metal solubilization by microorganisms. *Fems Microbiol. Rev.* **20**: 591–604.
- Caccavo, F.J., Coates, J.D., Rossello-Mora, R.A., Ludwig, W., Schleifer, K.-H., Lovley Derek R, and McInerney, M.J. (1996) *Geovibrio ferrireducens*, a phylogenetically distinct dissimilatory Fe (III)-reducing bacterium. *Arch. Microbiol.* **165**: 370–376.
- Cline, J.D. (1969) Spectrophotometric determination of hydrogen sulfide in natural waters. *Limnol. Oceanogr.* **14**: 454–458.
- Closson, D. and Karaki, N.A. (2009) Salt karst and tectonics: sinkholes development along tension cracks between parallel strike-slip faults, Dead Sea, Jordan. *Earth Surf. Process. Landforms* **34**: 1408–1421.
- Cohen, Y., Jørgensen, B.B., Revsbech, N.P., and Poplawski, R. (1986) Adaptation to Hydrogen Sulfide of Oxygenic and Anoxygenic Photosynthesis among Cyanobacteria. *Appl. Environ. Microbiol.* **51**: 398–407.
- La Cono, V., Smedile, F., Bortoluzzi, G., Arcadi, E., Maimone, G., Messina, E., et al. Unveiling microbial life in new deep-sea hypersaline Lake Thetis. Part I: Prokaryotes and environmental settings. *Environ. Microbiol.* **13**: 2250–2268.
- Delong, E.F. (1992) Archaea in coastal marine environments. *Proc. Natl. Acad. Sci. U. S. A.* **89**: 5685–5689.
- DeLong, E.F., Taylor, L.T., Marsh, T.L., and Preston, C.M. (1999) Visualization and enumeration of marine planktonic archaea and bacteria by using polyribonucleotide
-

probes and fluorescent in situ hybridization. *Appl. Environ. Microbiol.* **65**: 5554–5563.

Dowd, S.F., Sun, Y., Wolcott, R.D., Domingo, A., and Carroll, J.A. (2008) Bacterial tag-encoded FLX amplicon pyrosequencing (bTEFAP) for microbiome studies: Bacterial diversity in the ileum of newly weaned Salmonella-infected pigs. *Foodborne Pathog. Dis.* **5**: 459–472.

Dulski, P. (1994) Interferences of oxide, hydroxide and chloride analyte species in the determination of rare earth elements in geological samples by inductively coupled plasma-mass spectrometry. *Fresenius J. Anal. Chem.* **350**: 194–203.

Dulski, P. (2001) Reference Materials for Geochemical Studies : New Analytical Data by ICP-MS and Critical Discussion of Reference Values. *Geostand. Newsl.* **25**: 87–125.

Elazari-Volcani, B. (1944) A ciliate from the Dead Sea. *Nature* **154**: 355.

Elazari-Volcani, B. (1943a) A dimastigamoeba in the bed of the Dead Sea. *Nature* **152**: 301–302.

Elazari-Volcani, B. (1940) Algae in the bed of the Dead Sea. *Nature* **145**: 975.

Elazari-Volcani, B. (1943b) Bacteria in the bottom sediments of the Dead Sea. *Nature* **152**: 274–275.

Elshahed, M.S., Najar, F.Z., Roe, B.A., Oren, A., Dewers, T.A., and Krumholz, L.R. (2004) Survey of archaeal diversity reveals an abundance of halophilic Archaea in a low-salt, sulfide-and sulfur-rich spring. *Appl. Environ. Microbiol.* **70**: 2230–2239.

Engel, A.S., Lee, N., Porter, M.L., Stern, L.A., Bennett, P.C., and Wagner, M. (2003) Filamentous “Epsilonproteobacteria” dominate microbial mats from sulfidic cave springs. *Appl. Environ. Microbiol.* **69**: 5503–5511.

---

- Engel, A.S., Stern, L.A., and Bennett, P.C. (2004) Microbial contributions to cave formation: New insights into sulfuric acid speleogenesis. *Geology* **32**: 369.
- Frigaard, N.U. and Bryant, D. (2004) Seeing green bacteria in a new light: genomics-enabled studies of the photosynthetic apparatus in green sulfur bacteria and filamentous anoxygenic phototrophic bacteria. *Arch. Microbiol.* **182**: 265–276.
- Gart, J.J., Siegel, A.F., and German, R.Z. (1982) Rarefaction and Taxonomic Diversity. *Int. biometric Soc.* **38**: 235–241.
- Gavrieli, I., Yechieli, Y., Halicz, L., Spiro, B., Bein, A., and Efron, D. (2001a) The sulfur system in anoxic subsurface brines and its implication in brine evolutionary pathways: the Ca-chloride brines in the Dead Sea area. *Earth Planet. Sci. Lett.* **186**: 199–213.
- Gavrieli, I., Yechieli, Y., Halicz, L., Spiro, B., Bein, A., and Efron, D. (2001b) The sulfur system in anoxic subsurface brines and its implication in brine evolutionary pathways: the Ca-chloride brines in the Dead Sea area. *Earth Planet. Sci. Lett.* **186**: 199–213.
- Goldscheider, N., Hunkeler, D., and Rossi, P. (2006) Review: Microbial biocenoses in pristine aquifers and an assessment of investigative methods. *Hydrogeol. J.* **14**: 926–941.
- Gracas, D.A., Miranda, P.R., Barauna, R.A., McCulloch, J.A., Ghilardi Jr., R., Schneider, M.P.C., and Silva, A. Microbial Diversity of an Anoxic Zone of a Hydroelectric Power Station Reservoir in Brazilian Amazonia. *Microb. Ecol.* **62**: 853–861.
- Greene, A.C., Patel, B.K.C., and Sheehy, A.J. (1997) *Deferribacter thermophilus* gen. nov., sp. nov., a novel thermophilic manganese- and iron-reducing bacterium isolated from a petroleum reservoir. *Int. J. Syst. Bacteriol.* **47**: 505–509.
- Gross, S. (1977) The mineralogy of the Haturim Formation, Israel. *Geol. Surv. Israel Bull.* **70**: 1–80.
-

- Gvirtzman, H. and Stanislavsky, E. (2000) Large-scale flow of geofluids at the Dead Sea Rift. *J. Geochemical Explor.* **69**: 207–211.
- Hammer, Ø., Harper, D.A.T., and Ryan, P.D. (2009) PAST: Paleontological Statistics Software Package for Education and Data Analysis. 2001. *Palaeontol Electron.* **4**:
- Hannigan, R.E. and Sholkovitz, E.R. (2001) The development of middle rare earth element enrichments in freshwaters: weathering of phosphate minerals. *Chem. Geol.* **175**: 495–508.
- Hansell, D.A. and Carlson, C.A. (2002) Biogeochemistry of marine dissolved organic matter, Academic Press, San Diego.
- Haveman, S.A. and Pedersen, K. (2010) Distribution and Metabolic Diversity of Microorganisms in Deep Igneous Rock Aquifers of Finland. *Mol. Biol.* 37–41.
- Huber, H. and Stetter, K. O. (2002) Class I. Deferribacteres class. nov. In, *Bergey's Manual of Systematic Bacteriology*. Springer-Verlag, New York, pp. 465-479.
- Ionescu, D., Penno, S., Haimovich, M., Rihtman, B., Goodwin, A., Schwartz, D., et al. (2009) Archaea in the Gulf of Aqaba. *Fems Microbiol. Ecol.* **69**: 425–438.
- Johannesson, K.H., Farnham, Irene, M., Guo, C., and Stetzenbach, Klus, J. (1999) Rare earth element fractionation and concentration variations along a groundwater flow path within a shallow , basin-fill aquifer, southern Nevada, USA. *Geochim. Cosmochim. Acta* **63**: 2697–2708.
- Katz, A., Agnon, A., and Marco, S. (2009) Earthquake-induced barium anomalies in the Lisan Formation, Dead Sea Rift valley, Israel. *Earth Planet. Sci. Lett.* **286**: 219–229.
- Katz, A. and Starinsky, A. (2009) Geochemical history of the Dead Sea. *Aquat. Geochemistry* **15**: 159–194.
-

- Keough, B.P., Schmidt, T.M., and Hicks, R.E. (2003) Archaeal nucleic acids in picoplankton from great lakes on three continents. *Microb. Ecol.* **46**: 238–248.
- Lane, D. J. (1991) 16S/23S rRNA sequencing. In, *Nucleic Acid Techniques in Bacterial Systematics*. John Wiley and Sons, New York, pp. 115–175.
- Laronne Ben-Itzhak, L. and Gvirtzman, H. (2005) Groundwater flow along and across structural folding: an example from the Judean Desert, Israel. *J. Hydrol.* **312**: 51–69.
- Lazar, M. and Ben-Avraham, Z. (2002) First images from the bottom of the Dead Sea-- Indications of recent tectonic activity. *Isr. J. Earth Sci.* **51**:
- Lovley, D.R., Phillips, E.J., Lonergan, D.J., and Widman, P.K. (1995) Fe(III) and S<sub>0</sub> reduction by *Pelobacter carbinolicus*. *Appl. Environ. Microbiol.* **61**: 2132–8.
- Ludwig, W., Strunk, O., Westram, R., Richter, L., Meier, H., Yadhukumar, et al. (2004) ARB: a software environment for sequence data. *Nucleic Acids Res.* **32**: 1363–71.
- Macalady, J.L., Jones, D.S., and Lyon, E.H. (2007) Extremely acidic, pendulous cave wall biofilms from the Frasassi cave system, Italy. *Environ. Microbiol.* **9**: 1402–1414.
- Moeller, P., Rosenthal, E., Geyer, S., Guttman, J., Dulski, P., Rybakov, M., et al. (2007) Hydrochemical processes in the lower Jordan valley and in the Dead Sea area. *Chem. Geol.* **239**: 27–49.
- Möller, P., Rosenthal, E., Dulski, P., Geyer, S., and Guttman, Y. (2003) Rare earths and yttrium hydrostratigraphy along the Lake Kinneret–Dead Sea–Arava transform fault, Israel and adjoining territories. *Appl. geochemistry* **18**: 1613–1628.
- Nishri, A. and Stiller, M. (1984) Iron in the Dead Sea. *Earth Planet. Sci. Lett.* **71**: 405–414.
- Nissenbaum, A., Baedeker, M.J., and Kaplan, I.R. (1972) Organic geochemistry of Dead Sea sediments. *Geochim. Cosmochim. Acta* **36**: 709–727.
-

O'Connell, S.P., Lehman, R.M., Snoeyenbos-West, O., Winston, V.D., Cummings, D.E., Watwood, M.E., and Colwell, F.S. (2003) Detection of Euryarchaeota and Crenarchaeota in an oxic basalt aquifer. *FEMS Microbiol. Ecol.* **44**: 165–73.

Oren, A. (2002) Halophilic microorganisms and their environments, Kluwer Academic Press, Dordrecht.

Oren, A. (2010) The dying Dead Sea: The microbiology of an increasingly extreme environment. *Lakes Reserv. Res. Manag.* **15**: 215–222.

Oren, A., Gavrieli, I., Gavrieli, J., Kohen, M., Lati, J., and Aharoni, M. (2004) Biological effects of dilution of Dead Sea brine with seawater: implications for the planning of the Red Sea–Dead Sea “Peace Conduit.” *J. Mar. Syst.* **46**: 121–131.

Oren, A. and Gurevich, P. (1995) Dynamics of a bloom of halophilic archaea in the Dead Sea. *Hydrobiologia* **315**: 149–158.

Oren, A., Ionescu, D., Lipski, A., and Altendorf, K. (2005) Fatty acid analysis of a layered community of cyanobacteria developing in a hypersaline gypsum crust. *Arch. Hydrobiol. Suppl. Algal. Stud.* **117**: 339–347.

Overmann, J. (2006) The family Chlorobiaceae. In, *The Prokaryotes*. Springer, Berlin-Heidelberg, pp. 359–378.

Ovreas, L., Forney, L., Daae, F.L., and Torsvik, V. (1997) Distribution of bacterioplankton in meromictic Lake Saelenvannet, as determined by denaturing gradient gel electrophoresis of PCR-amplified gene fragments coding for 16S rRNA. *Appl. Environ. Microbiol.* **63**: 3367–3373.

Pedersen, K. (1990) Distribution and activity of bacteria in deep granitic groundwaters of southeastern Sweden. *Microb. Ecol.* **20**: 37–52.



- Polerecky, L., Bissett, A., Al-Najjar, M., Faerber, P., Osmers, H., Suci, P.A., et al. (2009) Modular Spectral Imaging System for Discrimination of Pigments in Cells and Microbial Communities. *Appl. Environ. Microbiol.* **75**: 758–771.
- Pruesse, E., Quast, C., Knittel, K., Fuchs, B.M., Ludwig, W., Peplies, J., and Gloeckner, F.O. (2007) SILVA: a comprehensive online resource for quality checked and aligned ribosomal RNA sequence data compatible with ARB. *Nucleic Acids Res.* **35**: 7188–7196.
- Ramette, A. (2009) Quantitative Community Fingerprinting Methods for Estimating the Abundance of Operational Taxonomic Units in Natural Microbial Communities. *Appl. Environ. Microbiol.* **75**: 2495–2505.
- Ravenschlag, K., Sahm, K., Knoblauch, C., Jorgensen, B.B., and Amann, Rudolf, I. (2000) Community structure, cellular rRNA content, and activity of sulfate-reducing bacteria in marine Arctic sediments. *Appl. Environ. Microbiol.* **66**: 3592–3602.
- Reznik, I.J., Gavrieli, I., and Ganor, J. (2009) Kinetics of gypsum nucleation and crystal growth from Dead Sea brine. *Geochim. Cosmochim. Acta* **73**: 6218–6230.
- Rhodes, M.E., Fitz-Gibbon, S.T., Oren, A., and House, C.H. (2010) Amino acid signatures of salinity on an environmental scale with a focus on the Dead Sea. *Environ. Microbiol.* **12**: 2613–2623.
- Salman, V., Amann, R., Girth, A.-C., Polerecky, L., Bailey, J. V, Hogslund, S., et al. (2011) A single-cell sequencing approach to the classification of large, vacuolated sulfur bacteria. *Syst. Appl. Microbiol.* **34**: 243–259.
- Sand, W., Gerke, T., and Hallmann, R. (1995) Sulfur chemistry, biofilm, and the (in)direct attack mechanism — a critical evaluation of bacterial leaching. *Appl. Microbiol. Biotechnol.* **43**: 961–966.
-

- Schink, B. (2006) The genus *Pelobacter*. In, *The Prokaryotes*. Springer, New York, pp. 5–11.
- Semenza, M., Viera, M., and Curutchet, G. (2002) The role of *Acidithiobacillus Caldud* in the bioleaching of metal sulfides. *Lat. Am. Appl. Res.* **32**: 303–306.
- Shalev, E., Levitte, D., Gabay, R., and Zemach, E. (2008) Assessment of Geothermal Resources in Israel Geological Survey of Israel.
- Shatkay, M., Anati, D.A., and Gat, J.R. (1993) Dissolved oxygen in the Dead Sea - seasonal changes during the holomictic stage. *Int. J. salt lake Res.* **2**: 93–110.
- Shen, Y. and Buick, R. (2004) The antiquity of microbial sulfate reduction. *Earth-Science Rev.* **64**: 243–272.
- Siebert, C. (2006) Seasonal chemical variations of lake Genezareth, its inflows and their causation. Freiei Universitaet Berlin, Unpublished PhD Thesis.
- Siebert, C., Geyer, S., Möller, P., Berger, D., and Guttman, Y. (2009) Lake Tiberias and its dynamic hydrochemical environment. In, *The Water of The Jordan Valley*. Springer-Verlag, Berlin-Heidelberg, pp. 219–246.
- Steinhorn, I., Assaf, G., Gat, J.R., Nishry, A., Nissenbaum, A., Stiller, M., et al. (1979) Dead Sea - Deepening of the mixolimnion signifies the overture to overturn of the water column. *Science (80- )*. **206**: 55–57.
- Stiller, M. and Nissenbaum, A. (1999) Geochemical investigation of phosphorus and nitrogen in the hypersaline Dead Sea. *Geochim. Cosmochim. Acta* **63**: 3467–3475.
- Swarieh, A. (2000) Geothermal energy resources in Jordan, country update report. In, *Proceedings World Geothermal Geothermal Congress.*, pp. 469–474.
-

- Teira, E., Reinthaler, T., Pernthaler, A., Pernthaler, J., and Herndl, G.J. (2004) Combining Catalyzed Reporter Deposition-Fluorescence In Situ Hybridization and Microautoradiography To Detect Substrate Utilization by Bacteria and Archaea in the Deep Ocean. *Society* **70**: 4411–4414.
- Tujula, N.A., Holmstro, C., Mußmann, M., Amann, R., Kjelleberg, S., and Crocetti, G.R. (2006) A CARD – FISH protocol for the identification and enumeration of epiphytic bacteria on marine algae. *J. Microbiol. Methods* **65**: 604 – 607.
- Usdowski, E. (1973) Das geochemische Verhalten des Strontiums bei der Genese und Diagenese von Ca-Karbonat-und Ca-Sulfat-Mineralen. *Contrib. to Mineral. Petrol.* **38**: 177–195.
- Vengosh, A., Starinsky, A., Kolodny, Y., and Chivas, A.R. (1991) Boron isotope geochemistry as a tracer for the evolution of brines and associated hot springs from the Dead Sea , Israel. *Earth* **55**: 1689–1695.
- Waddell, E., Elliott, T., Vahrenkamp, J., Roggenthen, W., Sani, R., Anderson, C., and Bang, S. (2010) Phylogenetic evidence of noteworthy microflora from the subsurface of the former Homestake gold mine, Lead, South Dakota. *Environ. Technol.* **31**: 979–991.
- Van der Wielen, P.W.J.J., Bolhuis, H., Borin, S., Daffonchio, D., Corselli, C., Giuliano, L., et al. (2005) The enigma of prokaryotic life in deep hypersaline anoxic basins. *Science* **307**: 121–3.
- Wilkansky, B. (1936) Life in the Dead Sea. *Nature* **138**: 467.
- Yechieli, Y. and Ronen, D. (1997) Early diagenesis of highly saline lake sediments after exposure. *Chem. Geol.* **138**: 93–106.
-



## Chapter 3

### **Microenvironments of reduced salinity harbor biofilms in Dead Sea underwater springs**

Stefan Häusler<sup>1</sup>, Beatriz E. Noriega-Ortega<sup>1</sup>, Lubos Polerecky<sup>1,2</sup>, Volker Meyer<sup>1</sup>, Dirk de Beer<sup>1</sup>, Danny Ionescu<sup>1</sup>

<sup>1</sup> Max Planck Institute for Marine Microbiology, Celsiusstrasse 1, 28211 Bremen, Germany

<sup>2</sup> Department of Earth Sciences – Geochemistry, Faculty of Geosciences, Utrecht University, Budapestlaan 4, 3584 CD Utrecht, The Netherlands

**Published in Environmental Microbiology Reports (2014) 6: 152–158**

**Abstract**

The Dead Sea is a hypersaline lake where only few types of organisms can grow. Recently, abundant and diverse microbial life was discovered in biofilms covering rocks and permeable sediments around underwater freshwater springs and seeps. We used a newly developed salinity mini-sensor (spatial resolution 300  $\mu\text{m}$ ) to investigate the salinity environment around these biofilms in a flume that simulates an underwater spring. Compared to the hypersaline bulk water, salinity at the sediment surface decreased to zero at seeping velocities of 7  $\text{cm s}^{-1}$ . At similar flow velocities, salinity above rocks decreased to 100-200  $\text{g L}^{-1}$  at a distance of 300  $\mu\text{m}$  from the surface. This depended on the position on the rock, and coincided with locations of natural biofilms. The salinity reduction substantially diminished at flow velocities of 3.5  $\text{cm s}^{-1}$ . We suggest that locally decreased salinity due to freshwater input is one of the main factors that make areas around underwater freshwater springs and seeps in the Dead Sea more favorable for life. However, due to frequent fluctuations in the freshwater flow, the locally decreased salinity is unstable. Therefore, microorganisms that inhabit these environments must be capable of withstanding large and rapid salinity fluctuations.

## Introduction

The Dead Sea is a terminal desert lake located at the border between Jordan, Israel and the Palestinian authority. The lake is characterized by total dissolved salt (TDS) concentrations of up to 348 g L<sup>-1</sup>, which is about 10-fold higher than in sea water (Oren, 2010). Continuous evaporation and reduced water input leads to precipitation of NaCl as halite at the lake bottom, leaving behind the more soluble cations Mg<sup>2+</sup> and Ca<sup>2+</sup>, whose concentrations are about 2 M and 0.5 M, respectively. Such high concentrations of divalent cations make the Dead Sea water an extreme environment where only few types of microorganisms can grow (Oren, 2010). Cell densities in the water column are generally very low (<5x10<sup>4</sup> cells; Ionescu et al., 2012). However, during severe winters or heavy rainfall, such as in 1980 and 1992, the top layer of the Dead Sea becomes diluted by up to 70 %, leading to a succession of blooms of the unicellular alga *Dunaliella* and of halophilic archaea, during which cell densities reach up to 3.5 x 10<sup>7</sup> cells ml<sup>-1</sup> (Oren and Gurevich, 1995; Oren et al., 1995).

Recently, we discovered a series of underwater freshwater springs in the Dead Sea (Ionescu et al., 2012). They are fed by the Judea Group Aquifer and emerge at depths between 10 to 30 m. Their waters are characterized by 10 to 100-fold higher cell densities than in the ambient Dead Sea. In addition, sediments and rocks around the springs harbor dense microbial communities, composed mainly of diverse Bacterial lineages that are absent in the ambient Dead Sea water (Bodaker et al., 2010). For example, 1-2 mm thick biofilms develop on sediments where the spring water seeps out in a dispersed way (Fig. 1A) or on cobbles and rocks in localized freshwater streams (Fig. 1B). Biofilms on sediments in seeping areas can cover up to several square meters, and are formed mainly by *Epsilonproteobacteria* or *Halothiobacillus* depending on the spring location (Ionescu et al., 2012). Biofilms on rocks are mostly found around the equator and are usually absent at the very top (Fig. 1B and Fig. S2). The green biofilms on the light-exposed part of the surface contain mainly green sulfur bacteria and cyanobacteria, whereas colorless sulfur bacteria from the class *Epsilonproteobacteria* are mainly found in the white biofilms covering the lower parts of the rock surfaces (Ionescu et al., 2012). Archaea were detected

---

only in the spring water, rock biofilms and the ambient Dead Sea and not in the spring sediments (Ionescu et al., 2012).

The factors leading to the high microbial diversity and biomass on sediments and cobbles around the springs are still unclear. One factor could be the supply of nutrients and dissolved sources of chemical energy. In comparison to the Dead Sea, the spring water is anoxic and contains hydrogen sulfide and sulfate (Ionescu et al., 2012), as well as a broad spectrum of dissolved organic compounds (Noriega-Ortega, unpublished data), a similar situation as in deep sea hydrothermal vents or shallow-water cold seeps (Van Dover, 2000; Foucher et al., 2009).

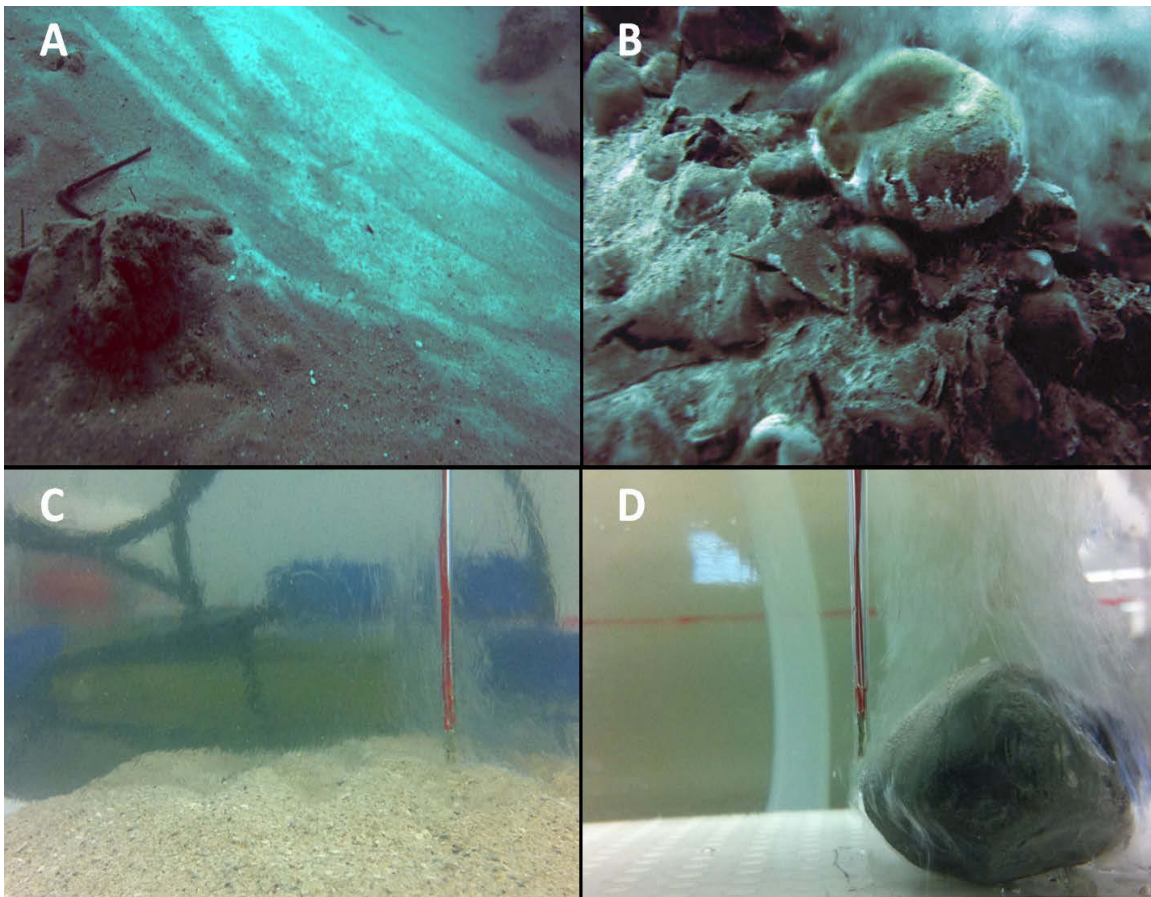


**Figure 1** Images of underwater freshwater springs in the Dead Sea (A and B) and of their laboratory mimics (C and D). Biofilms forming on the surfaces of sediments (A) and rocks (B) are also clearly visible.



An alternative or additional factor could be that the freshwater locally lowers the salinity of the Dead Sea and provides a less saline environment that can be inhabited by a higher diversity of organisms. The presence of such microenvironments is suggested from our *in situ* observations of clear fluctuations in the refractive index contrast at the sites of the freshwater input (Video S1). However, salinity measurements in water samples collected *in situ* close to the rock or sediment surface revealed no differences. Therefore, we developed a novel salinity mini-sensor to study the salinity microenvironment with a higher spatial resolution. Ideally, this sensor should be used *in situ* to provide direct salinity measurements above cobbles and sediments, which are necessary for testing the low salinity hypothesis. This was technically impossible since due to the water's unique ionic composition, the sensor could not resolve changes in salinity above 75% Dead Sea water. Therefore we tested the formation of microenvironments with a reduced salinity in a flume filled with a saturated NaCl brine to simulate the ambient hypersaline environment (320 g L<sup>-1</sup> NaCl; Fig. 1C and 1D). To mimic natural flow and water mixing conditions, freshwater input from below was introduced at flow rates that were in the range of those determined *in situ*.

## **Material and Methods**

### **Mimic of the Dead Sea underwater spring**

An aquarium (volume of 23 L) was filled with hypersaline NaCl brine, prepared by dissolving NaCl in distilled water to a final concentration of 300 to 320 g L<sup>-1</sup>. Higher salinities could not be reached by dissolution even if heating was applied. The dynamic viscosity of the NaCl brine was determined using a rotational rheometer CS10 (Bohlin) and compared to Dead Sea water. Freshwater (deionised) was introduced at the bottom through an array of 25 silicone tubes (2.5 mm diameter) connected to a peristaltic pump (Minipuls 3, Gilson). Dead Sea sediment from the seeping areas or cobble rocks from the streams were collected in October 2011 and placed at the bottom of the aquarium. In total

---

4 differently shaped cobble stones were analyzed (3 with biofilm growth and one without). The cobbles were oriented so that the green biofilm was facing upwards, similar to the *in situ* orientation. A 3 cm thick layer of Dead Sea sediment was placed on a mesh (0.1 mm mesh size) through which the freshwater was pumped. Due to rapid dilution of the brine reservoir the bulk salinity was reduced to 270 g L<sup>-1</sup> during the sediment measurements.

### **Salinity mini-sensor**

The salinity mini-sensor was built from two platinum wires separated by about 1 mm and enclosed in a glass housing (Fig. S1). The tip diameter was between 1.5 to 2 mm and was cut at an angle of 45°. The salinity measurement was achieved through the measurement of voltage. This is proportional to the resistance, which in turn is inversely proportional to the conductivity. The latter is proportional to salinity. The measuring circuit used a 20 kHz square voltage applied over a series resistor to the wires. The measured voltage across the sensor was galvanically separated and fed to an A/D converter, from which the signal could be read by a computer. The sensor was calibrated for salinity in the range between freshwater and the 320 g L<sup>-1</sup> NaCl solution at temperatures from 10 to 41°C.

### **Laboratory measurements**

Vertical salinity profiles were measured using a laboratory setup comprising a motorized stage (VT-80, Micos), a manual 3-axis micromanipulator (Märzhäuser), the salinity mini-sensor, and a data acquisition device (USB 6009, National Instruments). Measurements were automated and controlled by a computer using the program m-Profilier (Garching Innovation GmbH, developed by L. Polerecky). Before each measurement the sensor was calibrated using known salt solutions. All calibration solutions, the injected water and the aquarium water were kept at 25°C. Each profile was measured by first positioning the sensor about 300 µm above the sample-water interface while the freshwater flow was stopped. This minimum distance was required to avoid the influence of the sample surface on the resistance detected by the sensor. Subsequently, the freshwater flow was started and

---

the vertical profile was measured upwards in steps of 100  $\mu\text{m}$ . This was repeated at various locations over the rock surface separated by 1 mm. The influence of solid particles on the sensor signal was observed also when measuring salinity profiles inside sediments. This effect was corrected for by subtracting the change in the sensor signal under no flow conditions (assuming a homogeneous salinity in the pore water) from the signal under flow conditions.

### ***In situ* flow measurements**

Flow velocity was determined using an electromagnetic 3-axis velocity meter (ACM3-RS, ALEC electronics). Flow velocity was measured every 0.03 seconds over a time interval of >5 minutes and averaged over 1 s intervals.

### ***In situ* colour injection**

Commercially available blue food colorant (color based on brilliant blue E133; HaNamal, Israel) was mixed with Dead Sea water to ensure that when injected the dye would follow a trajectory of the freshwater flow rather than that determined by its own buoyancy. The mixture was injected in the spring water flow and recorded by an underwater video camera.

## Results and Discussion

The newly developed salinity mini-sensor was sensitive over the whole range of salinities encountered in our artificial flume setup (0-320 g L<sup>-1</sup>). Its sensitivity generally decreased with increasing salinity (Fig. 2). For example, at salinities above 200 g L<sup>-1</sup> it decreased up to 25-fold in comparison to the sensitivity at salinities below 75 g L<sup>-1</sup>. The sensor response depended also on temperature, exhibiting a lower signal range and a less curved dependence on salinity at lower temperatures (Fig. 2). At a distance of about 300 μm from a solid surface, the sensor signal decreased even in the absence of salinity gradients (see uncorrected profiles at no flow conditions in Fig. 3 and 4A). This is because the signal depends on the spatially integrated conductivity around the sensor tip, which decreases as the sensor tip approaches a solid surface.

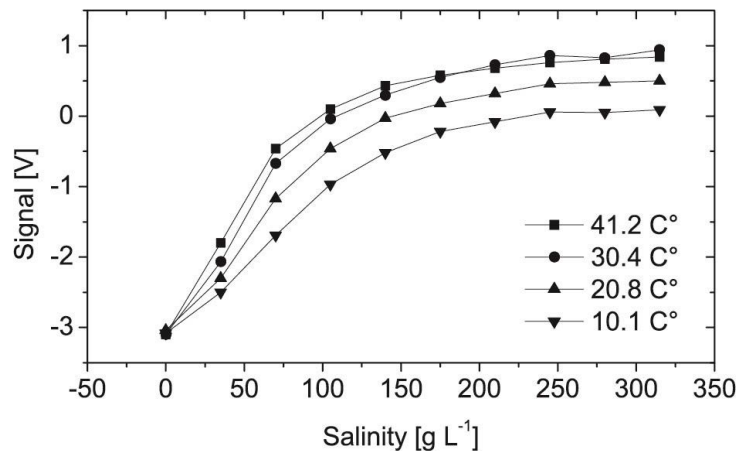


**Figure 2** Response of the newly developed salinity mini-sensor to salinity, as measured at different temperatures.

Thus, the spatial resolution of the sensor was about 300 μm. This limited meaningful salinity measurements above rocks to distances  $\geq 300$  μm, and implied that the salinity gradients reported hereafter are generally underestimated. Although similar mini-sensors were previously developed for studies of salinity gradients in microbial communities (see, e.g., Kohls et al., 2010), their sensitivity was adapted either for low or

high salinities. To the best of our knowledge this is the first description where the entire salinity range between 0 and 320 g L<sup>-1</sup> could be measured by a single sensor.

Freshwater flow velocities determined *in situ* by a 3-axis electromagnetic flow meter at a distance of about 2 cm above the lake bottom were highly variable, ranging from 2 to 5 cm s<sup>-1</sup> when measured above sediments in seeping areas and from 5 to 25 cm s<sup>-1</sup> above rocks in localised streams. Furthermore, the flow changed direction and magnitude on the scale of minutes (Fig. S3), or even stopped completely over extended time intervals (Ionescu et al., 2012). These fluctuations are presumably caused by changes in water input or by turbulent mixing in the free stream (Morton, 1959; List, 1982). The effect of changing flow velocity in the laboratory spring mimic was therefore tested by applying a high flow (7 cm s<sup>-1</sup>, maximal pump capacity) or low flow (3.5 cm s<sup>-1</sup>) velocity.

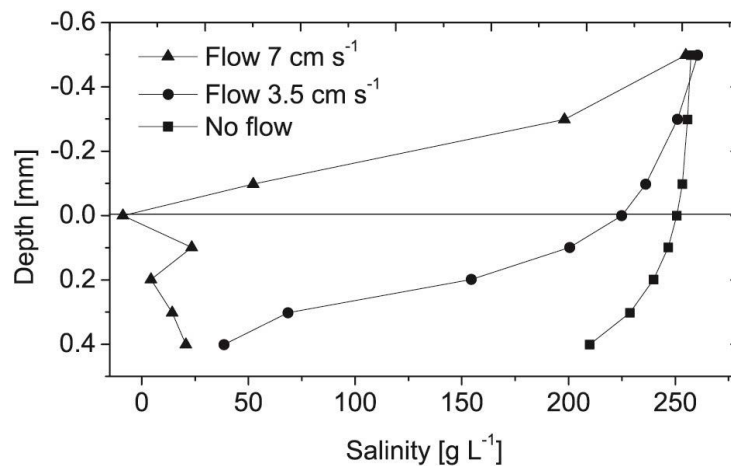


**Figure 3** Salinity distribution above and in sediments immersed in hypersaline water (270 g L<sup>-1</sup>) through which freshwater percolates at a vertical flow velocity of 7 cm s<sup>-1</sup> and 3.5 cm s<sup>-1</sup>. For comparison, a profile at no flow conditions is also shown to demonstrate the effect of the medium porosity on the sensor response. The sediment interference was accounted for in the two other profiles. Sediment-water interface is located at depth 0 mm.

For permeable sediments, the freshwater stream injected into the flume system resulted in water seepage through the sediment that manifested itself by similar fluctuations in the refractive index contrast as those observed *in situ* (Fig. 1C). At a vertical flow velocity of 7 cm s<sup>-1</sup>, salinity started to decrease steeply about 500 μm above the sediment-water interface and remained essentially zero inside the sediment (Fig. 3). For a lower flow

velocity ( $3.5 \text{ cm s}^{-1}$ ) the decrease was less steep; however, the salinity at depths of  $400 \text{ }\mu\text{m}$  inside the sediment was still significantly reduced (to about  $40 \text{ g L}^{-1}$ ).

For cobble stones located within a freshwater stream, the salinity distribution was more complex. At high flow velocities, salinity started to decrease about 1-1.2 mm above the cobble surface from the bulk water value of about  $320 \text{ g L}^{-1}$  and reached  $100\text{-}200 \text{ g L}^{-1}$  at a distance of  $300 \text{ }\mu\text{m}$  above the surface (Fig. 4A). Salinity directly at the cobble surface was likely even lower, although this could not be confirmed by direct measurements due to the limited spatial resolution of the sensor (see above). The locations of reduced salinity did not, however, extend over the entire cobble surface but were confined within a horizontal distance of about 6 mm from the cobble equator (Fig. 4B). This is consistent with models of flow around idealized spheres (Simpson, 1989; Johnson and Patel, 1999; Schlichting and Gersten, 2000), which suggest that the freshwater flow from below initially follows the bottom surface of the rock and separates from the rock surface (due to the upward buoyancy force) soon after it passes the blunt edge of the equator. Thus, the upward freshwater input creates a thin “envelope” of reduced salinity around the rock, with salinities gradually increasing from the lower side of the rock to levels equivalent to those in the ambient water across large parts of the upper side of the rock. The salinity decrease above rocks was minimal when the flow velocity was reduced by 50% (Fig. 4C), indicating similar sensitivity of the salinity gradients to the freshwater flow velocity as for sediments. The locations of reduced salinity coincided on three differently shaped cobbles with areas naturally overgrown by thick green biofilms (Fig. 4B; see Fig. S4A-B for more examples). In contrast, no natural biofilms were found on the top side of cobble surfaces where the salinity decrease was not observed. Furthermore, when the measurements were done on a cobble with a similar shape but with no natural biofilms, pronounced salinity decrease was again observed up to several millimetres above the cobble equator (Fig. S4C). Thus the salinity decrease was not due to the presence of the biofilm but due to the combined effects of mixing and flow of water around the rock surface.

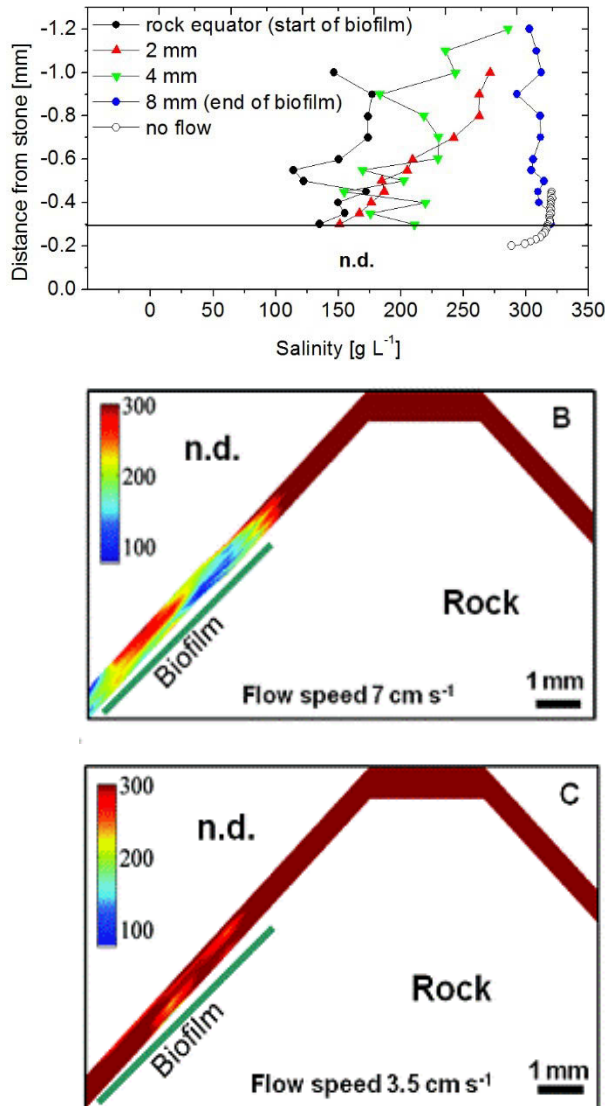


**Figure 4** Salinity distribution above the surface of a rock immersed in hypersaline water (320 g L<sup>-1</sup>) and exposed to freshwater flow from below. Panel A shows examples of vertical profiles at different horizontal positions from the rock equator, measured at a vertical flow velocity of 7 cm s<sup>-1</sup>. For comparison, a profile at no flow conditions is also shown to demonstrate the effect of a solid surface on the sensor response. Panels B and C show a comparison between the salinity distributions at high flow (7 cm s<sup>-1</sup>) and low flow (3.5 cm s<sup>-1</sup>) conditions. (n.d. = not determined); Colour bar values are in g L<sup>-1</sup>.

Taken together, our data strongly suggest that the microorganisms found in the natural biofilms on top of sediments and rocks around the freshwater underwater springs in the Dead Sea experience less extreme salinities than that of the ambient Dead Sea water. Furthermore, this local salinity reduction appears to be one of the factors that allows proliferation of a relatively abundant microbial biomass in an environment that is otherwise rather inhospitable due to extreme salinity and especially high concentrations of divalent cations. This interpretation is consistent with the commonly observed pattern of increasing diversity with decreasing salinity along salinity gradients (Jungblut et al., 2005; Rothrock and Garcia-Pichel, 2005; Abed et al., 2007). Additionally, it is consistent with our culturing experiments, which resulted in an isolation of a close relative of *Halothiobacillus* sp. (*Gammaproteobacteria*) from a cobble in the freshwater spring 10 in the Dead Sea (data not shown). This genus is known for its high salt tolerance (Kelly and Wood, 2000). In our cultures, no growth was observed on agar plates containing more than 278 g L<sup>-1</sup> of total dissolved salts (80% of the Dead Sea salinity), and best growth occurred at salinities between 26 to 43 g L<sup>-1</sup> (7.5-12.5% Dead Sea salinity). This suggests that the growth of this organism in the Dead Sea depends on the dilution effect by the spring water input, and supports the proposed existence of less saline microhabitats on rocks and sediments in the Dead Sea underwater spring system.

Although we have made a big effort to mimic the *in situ* flow and water mixing conditions, the salinity microenvironments observed above sediments and around cobbles in our flume experiments may differ from those present *in situ*. First, the NaCl brine used in our setup was 37% less viscous than Dead Sea water. However, larger viscosity differences between the ambient fluid and the spring water will likely lead to suppression of eddy formation and thus to lower entrainment of the ambient fluid at the interface of the rising buoyant jet (Mathur and Sreenivas, 2006). This will, in turn, result in less intense mixing of the two water masses and thus possibly larger salinity reduction if the cobble was to be placed in the more viscous Dead Sea water. Second, the flow in the Dead Sea spring system is often more complex than simulated in the flume. As indicated by the *in situ* colour injection experiment (Video S1), the flow around cobble stones can also be

---



deflected sideways as a result of massive entrainment from fast adjacent streams. This shows that although forced to rise because of the buoyancy force, freshwater can also flow around the top of a rock without flow separation. Thus, in certain locations of the springs the lower salinity envelope could cover the entire surface of a rock, allowing microbial growth also on the top. Indeed, rocks which are completely covered in biofilms are found around the underwater springs. However, such rocks are only rare and biofilm growth is mostly limited to areas along the rock equator that coincide with the experimentally observed salinity decrease.

An important finding of our experiments is the fact that the salinity microenvironment in sediments and above rocks is rather sensitive to the freshwater flow velocity. As indicated by our previous diving experience (Ionescu et al., 2012) and further demonstrated in this study (Fig. S3), the freshwater input fluctuates. Thus, based on our results, the *in situ* salinity microenvironments must fluctuate too, possibly over the full range of salinities in the system. Strategies to cope with salinity fluctuations have been investigated for microorganisms such as cyanobacteria and algae from other hypersaline systems like intertidal microbial mats or stromatolites. They include restoration of the cell volume by water channels, active extrusion of ions and the synthesis or uptake of organic compatible osmolytes (Kirst, 1990; Erdmann and Hagemann, 2001). However, in contrast to intertidal microbial systems, where the salinity fluctuations occur on the scale of hours to days (Abed et al., 2007; Kohls et al., 2010; Stal, 2012), salinity fluctuations in the underwater freshwater springs in the Dead Sea likely occur on the scale of minutes. Furthermore, the short term exposure to high concentrations of divalent cations present in the Dead Sea will pose another severe stress factor to the cells (Oren, 2013). The need to understand the mechanisms that enable the microorganisms in the Dead Sea freshwater springs to cope with the large and rapid osmotic and ionic fluctuations suggested by our measurements warrants further investigation.

It should be noted that the locally reduced salinity is suggested only as one possible factor contributing to the proliferation of microorganisms around the Dead Sea underwater springs. Previous measurements showed that the spring waters are anoxic and contain up

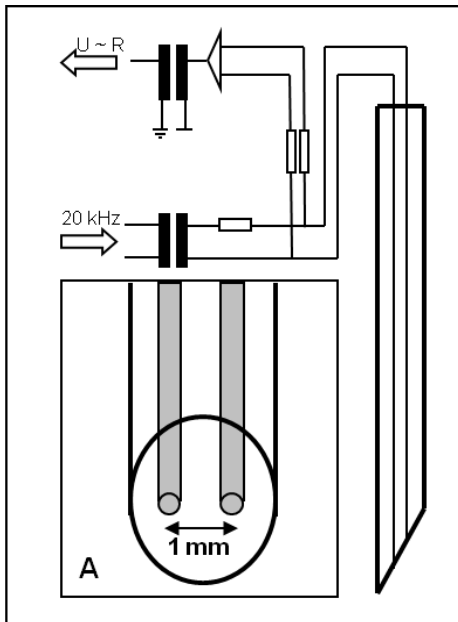
---

to 150  $\mu\text{M}$  of sulfide (Ionescu et al., 2009), whereas the ambient Dead Sea water contains on average 1.4  $\text{mg L}^{-1}$  of oxygen and no detectable sulfide since its overturn in 1979 (Shatkay et al., 1993). The locally increased availability of sulfide and oxygen as an electron donor and acceptor, respectively, is likely an additional critical factor that is responsible for the abundant microbial communities on the surfaces of sediments and rocks around the springs. This is consistent with the composition of the biofilms, which are generally dominated by close relatives of Bacteria involved in sulfur oxidation (Ionescu et al., 2012). Other substances brought in by the springs, such as dissolved organics, are also likely to play an important role.

In conclusion, we have shown that for rocks and permeable sediments submersed in a hypersaline ambient water, salinity close to their surfaces can be substantially reduced as a result of freshwater flow at bulk velocities in the range of a few centimetres per second. We suggest that this localized reduction in salinity is one of the main factors that allows microbial proliferation on sediments and rocks around underwater freshwater springs in the Dead Sea. Based on our indirect evidence that the microenvironments of reduced salinity are unstable due to fluctuating freshwater input from the underwater springs, we hypothesize that the microorganisms present in this environment possess as yet unidentified mechanisms that allow them to cope with large and rapid salinity fluctuations. Additional factors, including the input of reduced substances such as sulfide and organics, are also likely to play a role in these ecosystems. However, the assessment of their importance requires further investigation.

## **Acknowledgements**

This study was financially supported by the Max-Planck-Society. We would like to acknowledge the constructive discussions with Moritz Holtappels and Soeren Ahmerkamp. We thank the reviewers for their comments that greatly helped improving the manuscript. Furthermore we want to thank Christian Lott and Miriam Weber (HYDRA Institute, Elba, Italy) for their support during diving and underwater videography.

**Supplementary information**

**Figure S1** Schematic diagram of the newly developed salinity mini-sensor, showing the measuring principle and a close-up of the sensor tip (A).



**Figure S2** Image of rocks collected from the streams. Biofilm growth is mostly limited to the equator of the rocks. Green biofilms are located on the upper side.

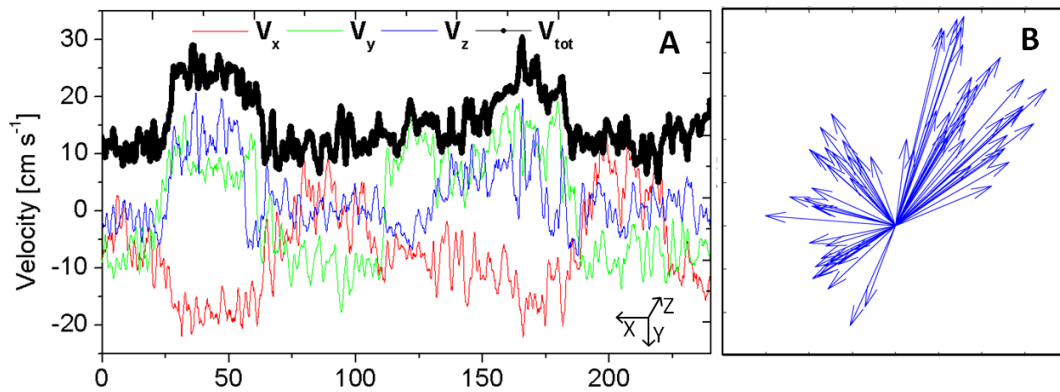


**Figure S3** Example of flow velocities measured *in situ* above a cobble at a vertical distance of 2 cm. Panel (A) shows all three cartesian components of the velocity vector ( $z$ -component corresponds to the vertical direction), as well as the vector magnitude, as a function of time. Panel (B) shows the projections of the velocity vector in the vertical plane (the time axis is collapsed).

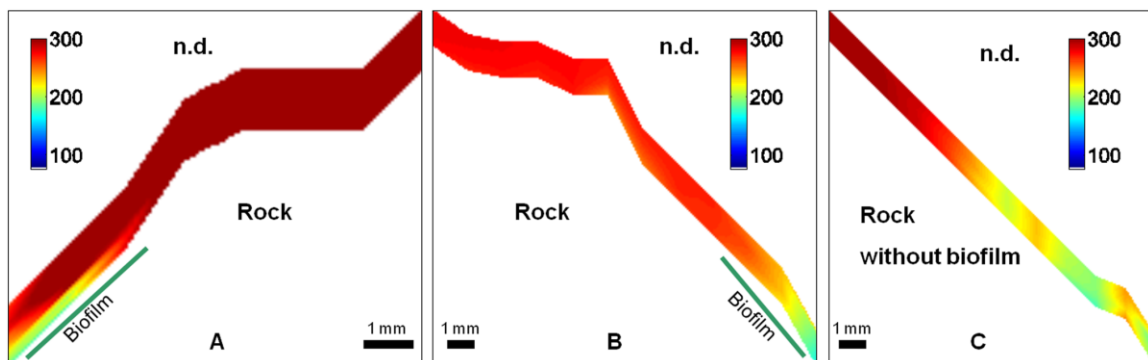


**Figure S4** Salinity distributions above the surface of rocks immersed in hypersaline water (300 g L<sup>-1</sup>) and exposed to freshwater flow from below at a vertical flow velocity of 7 cm s<sup>-1</sup>. Shown are examples for a rock without a biofilm and for two rocks partially covered with biofilms. Color bar values are in g L<sup>-1</sup>.

**Video S1** An *in situ* colour injection experiment showing the freshwater flow around a rock at the edge of a spring. The main flow of the spring is not visible in this close-up video. Can be downloaded from <http://onlinelibrary.wiley.com/doi/10.1111/1758-2229.12140/supinfo>

**References**

- Abed, R.M.M., Kohls, K., and De Beer, D. (2007) Effect of salinity changes on the bacterial diversity, photosynthesis and oxygen consumption of cyanobacterial mats from an intertidal flat of the Arabian Gulf. *Environ Microbiol* **9**: 1384–1392.
- Bodaker, I., Sharon, I., Suzuki, M.T., Feingersh, R., Shmoish, M., Andreishcheva, E., et al. (2010) Comparative community genomics in the Dead Sea: an increasingly extreme environment. *ISME J* **4**: 399–407.
- Erdmann, N. and Hagemann, M. (2001) Salt acclimation of algae and cyanobacteria: a comparison. In, *Algal Adaptation to Environmental Stresses*. Springer-Verlag, Berlin, pp. 323–361.
- Foucher, J.-P., Westbrook, G.K., Boetius, A., Ceramicola, S., Dupre, S., Mascle, J., et al. (2009) Structure and Drivers of Cold Seep Ecosystems. *Oceanography* **22**: 92–109.
- Ionescu, D., Penno, S., Haimovich, M., Rihtman, B., Goodwin, A., Schwartz, D., et al. (2009) Archaea in the Gulf of Aqaba. *FEMS Microbiol Ecol* **69**: 425–438.
- Ionescu, D., Siebert, C., Polerecky, L., Munwes, Y.Y., Lott, C., Haeusler, S., et al. (2012) Microbial and Chemical Characterization of Underwater Fresh Water Springs in the Dead Sea. *PLoS One* **7**: 21.
- Johnson, T.A. and Patel, V.C. (1999) Flow past a sphere up to a Reynolds number of 300. *J Fluid Mech* **378**: 19–70.
- Jungblut, A., Hawes, I., Mountfort, D., Hitzfeld, B., Dietrich, D.R., Burns, B.P., and Neilan, B.A. (2005) Diversity within cyanobacterial mat communities in variable salinity meltwater ponds of McMurdo Ice Shelf, Antarctica. *Environ Microbiol* **7**: 519–529.
-

- Kelly, D.P. and Wood, A.P. (2000) Reclassification of some species of *Thiobacillus* to the newly designated genera *Acidithiobacillus* gen. nov., *Halothiobacillus* gen. nov. and *Thermithiobacillus* gen. nov. *Int J Syst Evol Microbiol* **50**: 511–516.
- Kirst, G.O. (1990) Salinity tolerance of eukaryotic marine algae. *Annu Rev Plant Biol* **41**: 21–53.
- Kohls, K., Abed, R.M.M., Polerecky, L., Weber, M., and De Beer, D. (2010) Halotaxis of cyanobacteria in an intertidal hypersaline microbial mat. *Environ Microbiol* **12**: 567–575.
- List, E.J. (1982) Turbulent jets and plumes. *Annu Rev Fluid Mech* **14**: 189–212.
- Mathur, M. and Sreenivas, K.R. (2006) Effects of ambient viscosity on the entrainment and dynamics of a buoyant jet. In, *IUTAM Symposium on Laminar-Turbulent Transition*, Springer, The Netherlands pp. 219–224.
- Morton, B.R. (1959) Forced Plumes. *J Fluid Mech* **5**: 151–163.
- Oren, A. and Gurevich, P. (1995) Dynamics of a bloom of halophilic archaea in the Dead Sea. *Hydrobiologia* **315**: 149–158.
- Oren, A., Gurevich, P., Anati, D.A., Barkan, E., and Luz, B. (1995) A bloom of *Dunaliella parva* in the Dead Sea in 1992: biological and biogeochemical aspects. *Hydrobiologia* **297**: 173–185.
- Oren, A. (2010) The dying Dead Sea: The microbiology of an increasingly extreme environment. *Lakes Reserv Res Manag* **15**: 215–222.
- Oren, A. (2013) Life in Magnesium-and Calcium-Rich Hypersaline Environments: Salt Stress by Chaotropic Ions, Springer, Dordrecht pp. 215–232.
-

Rothrock, M.J. and Garcia-Pichel, F. (2005) Microbial diversity of benthic mats along a tidal desiccation gradient. *Environ Microbiol* **7**: 593–601.

Schlichting, H. and Gersten, K. (2000) *Boundary-layer theory*, Springer, Berlin.

Shatkay, M., Anati, D.A., and Gat, J.R. (1993) Dissolved oxygen in the Dead Sea—seasonal changes during the holomictic stage. *Int J Salt Lake Res* **2**: 93–110.

Simpson, R.L. (1989) Turbulent boundary-layer separation. *Annu Rev Fluid Mech* **21**: 205–232.

Stal, L.J. (2012) Cyanobacterial mats and stromatolites. In, *Ecology of Cyanobacteria II*, Springer, The Netherlands, pp.65-125

Van Dover, C.L. (2000) *The ecology of deep-sea hydrothermal vents*. Princeton University Press, New Jersey.





## **Chapter 4**

### **Spatial distribution of diatom and cyanobacterial microbial mats in the Dead Sea is determined by response to rapid salinity fluctuations**

Stefan Häusler<sup>1</sup>, Miriam Weber<sup>1,2</sup>, Dirk de Beer<sup>1</sup>, Danny Ionescu<sup>1</sup>

<sup>1</sup> Max Planck Institute for Marine Microbiology, Celsiusstrasse 1, 28211 Bremen, Germany

<sup>2</sup> HYDRA Institute for Marine Sciences, Elba Field Station, Campo nell'Elba (LI), Italy

**In preparation for Extremophiles**

## Abstract

Although cyanobacteria and diatoms are ubiquitous in hypersaline environments they have never been observed in the Dead Sea, one of the most hypersaline lakes on our planet. Here we report the discovery of phototrophic benthic microbial mats at subsurface freshwater seeps emerging into the Dead Sea. These mats are either dominated by diatoms or unicellular cyanobacteria and are spatially separated. Using *in situ* and *ex situ* oxygen microsensor measurements we show that these organisms are metabolically active in their natural habitat. We were able to enrich both phototrophic organisms and identify them. The diatoms, which are phylogenetically associated to the *Navicula* genus, grew in salinities up to 40% Dead Sea water (DSW) (14% total dissolved salts, TDS). The unicellular cyanobacteria belong to the extremely halotolerant *Euhalothece* genus and grew at salinities up to 70% DSW (24.5% TDS). As suggested by a variable oxygen penetration depth measured *in situ*, the organisms are exposed to drastic salinity fluctuations possibly ranging from brackish- to DSW salinity and vice versa within minutes to hours. We could demonstrate that both phototrophs are able to withstand such extreme short-term fluctuations. Nevertheless, while the diatoms recover their oxygen production activity faster from rapid fluctuations, the cyanobacteria recover faster from long term exposure to DSW. We conclude that the main reason for the development of these microbial mats is a local dilution of the hypersaline Dead Sea to levels allowing growth. Their spatial distribution in the seeping areas is a result of different recovery rates from short or long term fluctuation in salinity.

## Introduction

The Dead Sea is a hypersaline desert lake which is characterized by 348 g L<sup>-1</sup> TDS and an unusual ionic salt composition: The main components of the mineral salts are 1.98 M Mg<sup>2+</sup>, 1.54 M Na<sup>+</sup>, 0.42 M Ca<sup>2+</sup> and 0.21 M K<sup>+</sup> (Oren, 2010). Since the beginning of the 20<sup>th</sup> century the water budget of the lake has been negative leading to lake level drop of about 1 meter per year and an increasing salinity (Oren, 2010). Due to the high concentration of divalent cations which have a chaotropic (destabilizing) potential on biological macromolecules only highly adapted organisms can grow in this environment (Oren, 2010, 2013). Since the early 1940s a number of halophilic Bacteria, Achaea, unicellular algae of the genus *Dunaliella* and amoeboid and ciliate protozoa have been described and partly isolated from the lakes water column and sediment (Elazari-Volcani, 1940, 1943a, 1943b, 1944a; Oren, 2010). Nowadays, the resident microbial community being able to cope with the extreme conditions of the Dead Sea is mostly composed of *Archaea* (Bodaker et al., 2010). The algae *Dunaliella* is the only primary producer in the Dead Sea (Oren, 2010); however, it is not able to grow in pure Dead Sea water (DSW). Blooms only develop after heavy rainfall events and a resulting dilution of the upper water layer of the Dead Sea as was only observed twice in the recent past, once in 1980 and 1992-1994 (Oren et al., 1995).

Cyanobacteria and diatoms are phototrophic primary producers and are commonly found in a variety of hypersaline environments including hypersaline lagoons, salt lakes, solar salt ponds or hypersaline sulphur springs (Nübel et al., 1999, 2000; Wieland and Kühl, 2000; Ionescu et al., 2007; Oren, 2012; Fariás et al., 2013). Although some cyanobacterial and diatom strains from the Dead Sea were obtained in enrichment cultures at a time when the salinity of the lake was about 21% lower than today (Elazari-Volcani, 1940, 1944a), cyanobacteria have never been observed directly in the Dead Sea neither in the water nor in sediment samples (Oren, 2012).

Recently, a system of subsurface freshwater springs was discovered in the Dead Sea (Ionescu et al., 2012). These springs are located at the west coast of the lake and emerge at depths between 2 to 30 m and possibly even deeper. The salinity of the pure spring water

---

(4 to 88 g L<sup>-1</sup> TDS) is significantly less saline than the surrounding DSW. At certain locations where the spring water slowly seeps out of the sediment we discovered dense microbial mats which are visually dominated by either diatoms or unicellular cyanobacteria. We suggested earlier that one reason for their development is probably the formation of reduced salinity microenvironments on sediments (Häusler et al., 2014). However, variations in spring water flow velocity suggested that the organisms are exposed to substantial salinity fluctuations in the scale of minutes to hours (Häusler et al., 2014). So far we were not able to demonstrate under which condition these organisms are active and if they are indeed able to survive the proposed substantial short-term salinity fluctuations. Thus, using *in situ* and *ex situ* microsensor measurements we now show that these phototrophs are active in their natural environment and are able to survive substantial, fast salinity fluctuations. We partially describe their phylogenetic affiliation and speculate on the reasons for the spatial separation.

## **Material and Methods**

### **Location, spring water sampling and chemistry**

Measurements and sampling of a diatom and cyanobacterial microbial mat were performed in November 2012. Water sampling procedure and determination of the physico-chemical parameters of the spring water was done according to Ionescu et al. (2012), where also a detailed description of the system can be found.

### ***In situ* measurements**

*In situ* oxygen measurements in a diatom mat were conducted using a Clark-type oxygen microelectrode (tip diameter 20 µm) with a guard cathode (Revsbech and Jørgensen, 1986) connected to the Diver-Operated Microsensor System, DOMS (Weber et al., 2007). A set of 3 profiles was measured every 45 minutes over a period of 23 hours. The signal obtained

---

in air saturated DSW represented the oxygen concentration corresponding to 100 % air saturation and was determined using a modified Winkler protocol for Dead Sea water (Nishri and Ben-Yaakov, 1990) at *in situ* water temperature. The reading in anoxic Dead Sea water and anoxic fresh water (prepared by dissolution of 0.1 g Sodiumdisulfite in 50 ml water) as well as in the anoxic layers of the mat was the same, and taken as zero oxygen (Wieland et al., 2003). Each set of profiles obtained was visualized and interpolated using the sigma plot software (Systat software inc). Light intensity during the measurement was monitored with a photosynthetic active radiation (PAR) light logger (Odyssey, Data flow systems, Christchurch, New Zealand) located at the site of measurement. Spectral light availability was measured with a USB 4000 spectrometer (Ocean Optics, Duiven, The Netherlands) connected to the DOMS (Weber et al., 2007). A depth profile of spectral light was measured by recording spectra every meter according to the dive computer Elite T3 (Aeris, San Leonardo, USA). Depth was corrected for density related pressure differences.

Possible spring water fluctuations were determined by recording temperature in the diatom mat, using a Tidbit-v2 temperature logger (Onset, Burne, USA).

### ***Ex situ* microsensor measurements**

*Ex-situ* oxygen microsensor measurements were also conducted with the DOMS in the same way as described above on retrieved cores of a cyanobacterial and diatom mat. The pore- and overlying water salinity corresponded in both cores to 80% of DSW (determined by weighing a known volume and comparison to a calibration curve). During sampling the diatom mat got pushed approximately 1 cm into the sediment to the core wall. Nevertheless, illumination could be applied through the transparent core wall using a Schott lamp (KL 2500 LCD, SCHOTT) at an intensity of 30  $\mu\text{mol photons m}^2 \text{s}^{-1}$ .

### **Culture conditions and partial characterization**

The same cores used for *ex-situ* microsensor measurements served as inoculum for enrichment cultures. The culture medium was prepared on a basis of sterile filtered (0.2  $\mu\text{m}$  filter, Millipore) DSW diluted with deionized sterile water to a final concentration of 30% DSW. The cyanobacterial and diatom media were supplemented with all components of the BG 11 medium (Rippka et al., 1979) except  $\text{MgSO}_4$  and  $\text{CaCl}_2$  or of the f/2 medium (Guillard and Ryther, 1962), respectively. Cultures were grown at 28°C under white fluorescent light with an intensity of 30  $\mu\text{mol photons m}^2 \text{s}^{-1}$  (corresponding to in situ light intensity) with a light dark cycle of 12 h. Growth occurred within 3 to 4 weeks and each culture contained either unicellular cyanobacteria or diatoms with the same morphology as observed from *in situ* samples. To test growth in different salinities, the obtained enrichment cultures served as inoculum for media containing increasing concentrations of DSW between 5 to 100% DSW (tested in duplicates with a resolution of 10% between 10 to 100 % DSW media). pH ranged from 7.12 in 5% DSW to 5.95 in 100% DSW media. Artificial biofilms were obtained by placing sterile GFF filters (4 h at 400 C°) in the cultures until a unialgal microbial mat developed after 5 to 6 weeks. The ability to survive prolonged exposures to pure DSW was tested by incubation of the artificial biofilms in pure DSW for one week and afterwards transferring them to low saline media. Growth was always determined by visual observation after 4 to 6 weeks.

### **Light microscopy and scanning electron microscopy (SEM)**

Environmental and culture samples were examined using a Zeiss Axioplan light microscope with a 100 W Hg lamp and filter sets for detecting chlorophyll auto fluorescence. SEM images of the diatoms were obtained by filtration of the samples on Ag/Pd pre-coated filters (0.2  $\mu\text{m}$ , Millipore) and examination in a Quanta 250 FEG scanning electron microscope (FEI, Hillsboro, Oregon, USA).

### **16S rRNA gene clone libraries and phylogenetic analysis**

DNA was extracted from a 1.5 ml sample from the initial 30% DSW cultures of the cyanobacteria and diatoms using a phenol chloroform protocol identical to the one described in detail in Ionescu et al. (2012). Cyanobacterial 16S rRNA and diatom 18S rRNA genes were amplified by polymerase chain reaction (PCR) using the primer pairs CYA106F / CYA781R (Nübel et al., 1997) and EUK A/B (Medlin et al. 1988), respectively. The 50 µl PCR reaction contained 100 ng of template DNA, 0.5 µM of each primer, 0.2 mM of dNTPs, 0.5 units of DreamTaq DNA polymerase and the respective buffers (Thermo Scientific, Germany). PCR's were performed in a thermo cycler (Mastercycler, Eppendorf, Germany) using the following programs. For Cyanobacteria: 5 min at 94 °C, followed by 35 cycles of 45 sec at 94 °C, 45 sec at 60 °C and 45 sec at 72 °C; followed by 10 min final extension at 72 °C. For diatoms: 5 min at 94 °C, followed by 35 cycles of 1 min at 94 °C, 1 min at 55 °C and 2 min at 72 °C; followed by 10 min final extension at 72 °C and 1 cycle 10 min at 15°C. A clone library was prepared from the obtained PCR amplicons using the TOPO® TA Cloning® Kit (pCR4-TOPO, Invitrogen, Karlsruhe, Germany) followed by sequencing of the inserts using the BigDye Terminator v 3.1 Cycle sequencing Kit (Applied Biosystems, Foster City, USA) following the manufactures manual. The obtained sequences were analysed using the program Sequencher 4.6 (Gene Codes Corp.) and afterwards the sequences were compared to the NCBI database using BLAST (Altschul et al., 1990).

### **Short term salinity response on oxygenic photosynthesis**

To evaluate the short-term response of the organisms to changing DSW concentrations, oxygen production was taken as proxy for cell damage while manipulating the DSW concentrations in the media. Specifically, artificial biofilms were grown on GFF filters as described above and then transferred to a small flow chamber (1 cm x 0.5 cm) to which medium was continuously supplied using a peristaltic pump (MINIPULS® 3, Gilson). Light was provided in all experiments from a Schott lamp (KL 2500 LCD, SCHOTT) at an

---

intensity of  $30 \mu\text{mol photons m}^2 \text{ s}^{-1}$  (corresponding to maximum *in situ* light irradiance and growth conditions). A Clark-type oxygen microelectrode (tip diameter  $20 \mu\text{m}$ ) with a guard cathode (Revsbech and Jørgensen, 1986) was placed inside the biofilm at the  $\text{O}_2$  production peak and oxygen production was determined by the light-dark shift (LDS) method (Revsbech et al., 1981) in triplicates. The microsensor was calibrated for oxygen at each salinity using the reading obtained in the oxygenated water column of the flow chamber as the 100% value. The 0% value was determined using media bubbled with  $\text{N}_2$  gas. The corresponding oxygen concentration for the different media was calculated using empirical values determined from Winkler titration as was done for the *in situ* microsensor measurements.

Two experiments were conducted simulating short-term spring-water flow scenarios: (I) a gradual decrease in spring water flow and thus an increase in DSW concentration followed by a gradual increase in spring water flow to the initial salinity. (II) A sudden stop of spring water flow and thus an immediate exposure to pure DSW followed by an instant reestablishment of the original flow. The first scenario was simulated by increasing the concentration of DSW in the medium gradually over time in 10% DSW steps every 15 minutes to 100% DSW and then gradually decreased again to the starting salinity or lower. This was done using either a high saline grown artificial biofilm (40% DSW) or a low saline grown biofilm (5% DSW) of either diatoms or cyanobacteria. The second scenario was simulated by exposing biofilms of either cyanobacteria or diatoms which were grown at high salinity (40 % DSW), to a sudden shift from the starting salinity to 100% DSW for 15 minutes following an immediate downshift in salinity back to 40% DSW. The recovery was monitored over time. Although the fluctuations might be even more rapidly than 15 minutes, this was the minimum time required for medium exchange and microsensor signal stabilization. When the salinity was changed in both experiments, the old medium was removed by a syringe until only little medium was left. Then the flow cell was flushed at least 3 times with the new medium and gross photosynthesis was determined in the end of each shift to allow for microsensor signal stabilization. To ensure comparable rates the sensor was not moved during the experiment. All experiments were done in

---



duplicates with each replicate experiment conducted with a new biofilm which was previously not exposed to salinity shifts.

## Results

The diatom mat investigated *in situ* was roughly 0.5 to 1 mm thick and could be clearly distinguished from the sediment by a brownish color (Fig. 1A). It spread over several square meters on the sediment surface. In comparison to the diatom mats, the cyanobacterial mats were greenish in appearance and their distribution was limited to patches of a few square centimeters (Fig. 1B). These mats were either dominated by pennate diatoms (Fig. 1C) or unicellular cyanobacteria (Fig. 1D). Both microbial mat types

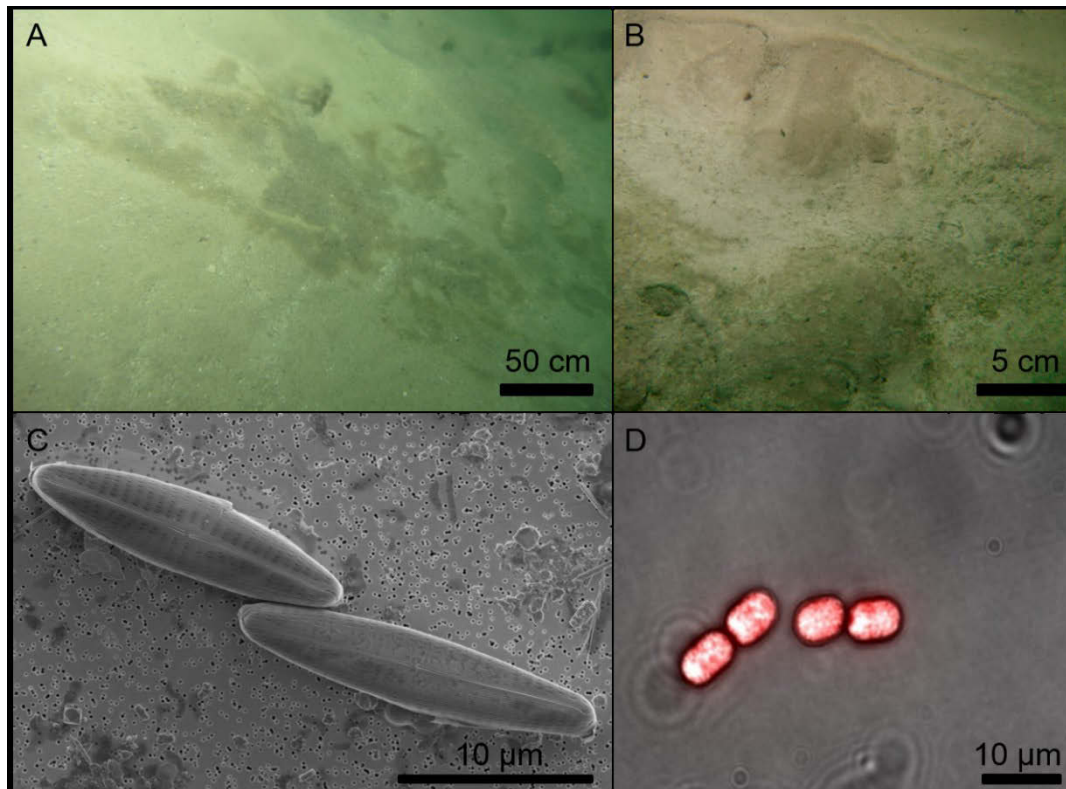


**Figure 1** A and B: *In situ* images of the two types of microbial mats observed in the Dead Sea where spring water seeps out of the sediment. The brownish microbial mats spreading over several square meters (A) are dominated by pennate diatoms with the main morphotype shown in a SEM image (C). The greenish mats only cover small patches of sediment (~5 cm in diameter) and are dominated by unicellular cyanobacteria as shown in a light microscope image (D; autofluorescent image).

could be found at similar water depths between 3 to 10 meters and only occurred where slow spring water seepage was observed.

The physical and chemical water properties of the pure spring water sampled from the diatom mat are summarized and compared to the Dead Sea in Table 1. The spring water is warmer and significantly less saline and less acidic than the DSW. Silica and dissolved inorganic carbon (DIC) concentration in the spring water were 4-5 times higher than in DSW whereas nitrate and phosphate were in the same range. Dissolved organic matter (DOM) could be detected in higher concentrations in the Dead Sea. Due to technical complexities, no pure spring water from the cyanobacterial mats could be obtained. Nevertheless, we expect no large differences between the pure spring waters in the diatom and cyanobacterial site since most springs sampled previously in the system had similar physico-chemical properties (Ionescu et al., 2012).

**Table 1** Physico-chemical parameters of the Dead Sea and the spring water seep were the diatom mat was observed. \* Values taken from Stiller and Nissenbaum (1999)

<b>Sample</b>	<b>Temp [C°]</b>	<b>pH</b>	<b>TDS [g l<sup>-1</sup>]</b>	<b>Si(II,III) [mM]</b>	<b>DOC [µM]</b>	<b>DIC [mM]</b>	<b>NO<sub>3</sub><sup>-</sup> [µM]</b>	<b>PO<sub>4</sub><sup>3-</sup> [µM]</b>
<b>Dead Sea</b>	24,9	6,16	338	0,08	1366	1,05	3-8*	0.2*
Diatom seep	29,1	6,93	59	0,34	330	5,56	1,29	0,23

Long term *in situ* oxygen profiling in the diatom mat, revealed a highly dynamic system (Fig. 2). Oxygen concentration decreased sharply at the mat surface from 49 µM in the overlying water to anoxic conditions inside the sediment. Oxygen penetration depth fluctuated between 0.1 to 0.2 mm with a single exception of 0.9 mm in the night. When incident light was above 25 µmol photons m<sup>-2</sup> s<sup>-1</sup>, oxygen was gradually detected up to 0.5 mm in the sediment. Ex-situ measurements conducted in less than 3 h of sampling on both mats showed extensive oxygen production upon illumination (Fig. 3) at a salinity corresponding to 80% of DSW.

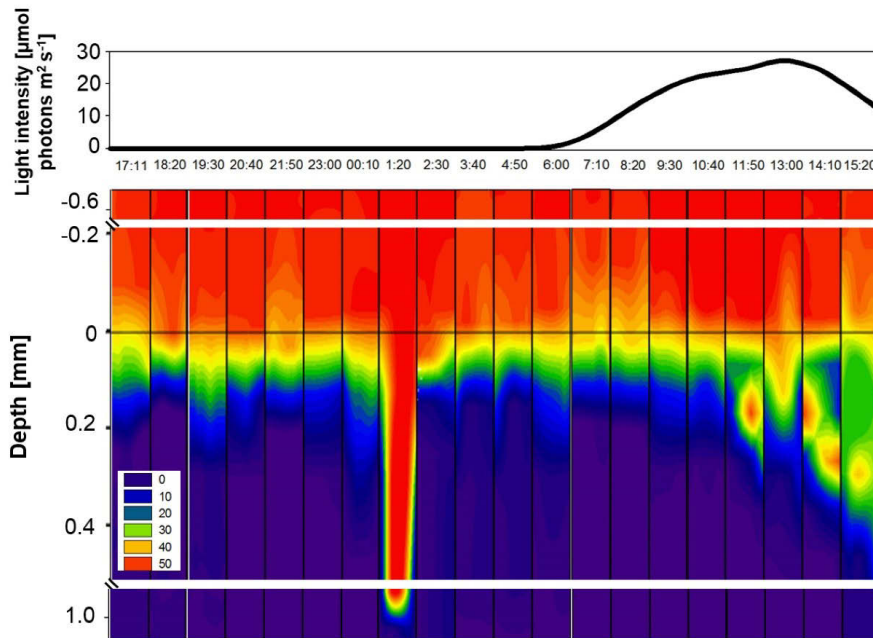


**Figure 2** *In situ* oxygen profiles measured in the diatom mat. Each panel represents a set of three subsequent profiles measured each hour. X and Y axis corresponds to time and depth, respectively.  $O_2$  concentrations are color-coded in  $\mu\text{M}$  (see color bar on the lower left). Fluctuating oxygen penetration depth indicates fluctuating spring water flow. Oxygen evolution is detected at high light in the upper mat surface as indicated by the incident light intensities shown in the top graph.

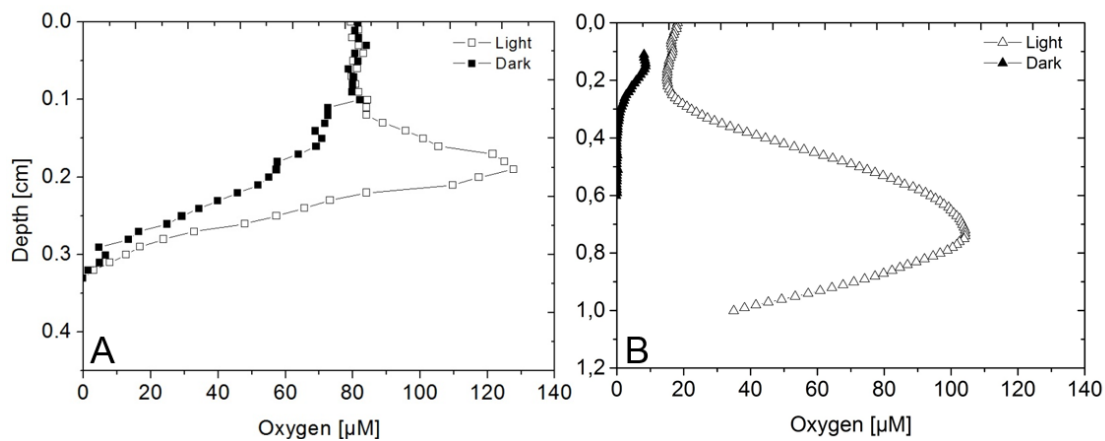


**Figure 3** Dark and light ( $30 \mu\text{mol photons m}^{-2} \text{s}^{-1}$ ) oxygen profiles measured *ex situ* in a cyanobacterial dominated microbial mat (A) and diatom dominated microbial mat (B). The salinity in the overlying water corresponded to 80% of Dead Sea water salinity. Extensive oxygen production could be detected in both microbial mats.

Both organisms could be enriched in culture. Although more diatom morphotypes were observed in the *in situ* sample, the dominating one had the same morphology as those in our enrichment cultures (Fig. S1). Only one cyanobacterial morphotype was present in the *in situ* sample and corresponded to the enrichment cultures. Limited growth was observed in diluted non-amended DSW and growth was strongly stimulated by the addition of nutrients. Diatoms grew between 5 to 40% DSW whereas cyanobacteria between 5 to 70% DSW. When high saline grown (40% DSW) artificial biofilms of both organisms were exposed for 1 week to 100% DSW and subsequently transferred back to the original growth medium only the cyanobacterial culture started to re-grow.

Partial 16S rRNA gene sequences obtained from the cyanobacterial culture were 97 to 98% identical to *Euhalothece* sp., strain MPI 96N304. The partial 18S rRNA gene sequences obtained from the diatom culture were 96-98% identical to *Navicula salinicola*. Morphological identification using the SEM images of the diatoms confirmed the classification to the *Navicula* genus (M. Edlund, personal communication).

O<sub>2</sub> evolution was linearly reduced in all artificial biofilms with increasing DSW concentrations in the media (Fig. 4A and B). Biofilms grown at high salinity (40% DSW) were able to perform photosynthesis over the complete salinity spectra; however, in pure DSW the cyanobacterial mat and the diatom mat reached only up to 3 and 0.5% of the initial value, respectively. Upon consequent exposures to lower DSW concentrations, oxygen evolution immediately recovered. When the starting salinity was reached, 90 minutes after the exposure to 100% DSW, the cyanobacterial photosynthetic activity recovered completely whereas the diatoms only reached between 40 to 60% of their initial value. When the salinity was further decreased down to 5% DSW in the medium, cyanobacterial activity decreased once more, whereas that of the diatoms stayed relatively constant between 60 to 80% of the initial value. In contrast to the high saline grown biofilms oxygen production in the low saline adapted biofilms (5% DSW) could only be detected until 60% of DSW in the media. Recovery of the photosynthetic potential was delayed in the diatom biofilm and no recovery was observed in the cyanobacterial biofilm (Fig. 3B) not even after 12 h.

---

A rapid salinity shift applied to both high saline adapted cultures resulted in an immediate inhibition of O<sub>2</sub> production in both organisms (Fig. 4C). Initial recovery of photosynthetic activity was equal in both cultures. However, within 90 minutes after the exposure to pure DSW the diatoms completely recovered their initial photosynthetic activity whereas the cyanobacterial activity only recovered to about 40% of the initial value in the same time frame.

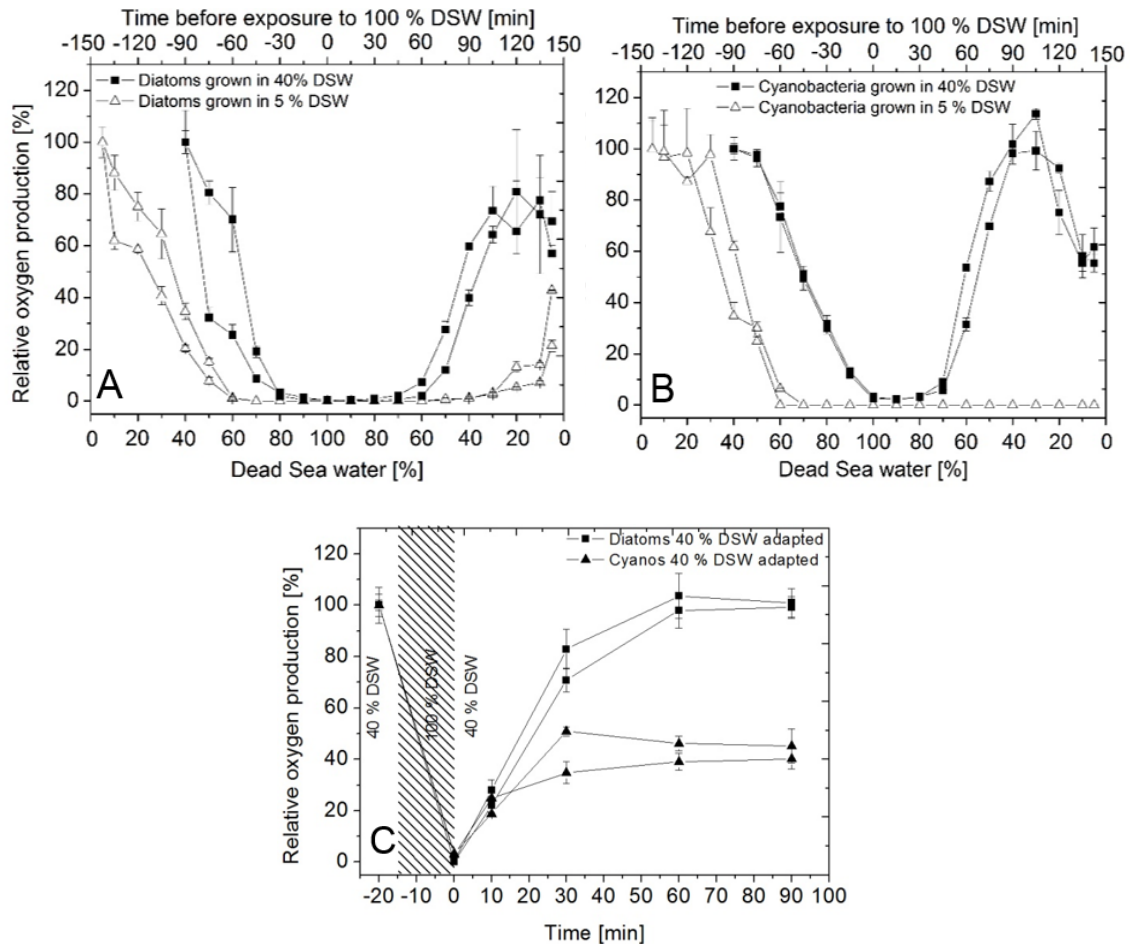


**Figure 4** Gross photosynthetic activity response of diatom (A) and cyanobacterial (B) artificial biofilms grown in 5% DSW media and 40% DSW media to stepwise (each step corresponds to 10% DSW for 15 min) increase in salinity to DSW levels and subsequent decrease to starting salinity. (C) Recovery of photosynthetic activity in 40% DSW media of 40% DSW grown artificial biofilms of cyanobacteria and diatoms exposed to 15 min pure DSW.

## Discussion

In this study we provide evidence for active cyanobacteria and diatoms in the Dead Sea. In addition to *in situ* measurements of oxygen production in the diatom mat under ambient light (Fig. 2), photosynthetic activity could be demonstrated for both mat forming organisms in freshly collected samples upon illumination (Fig. 3). We discuss here the possible reasons for the development of these dense phototrophic microbial mats in the Dead Sea and the ecological implications of the stress exerted on the organisms by the salinity fluctuations in this extreme environment.

The microbial mats were only found in areas where spring water seepage was observed. This strongly suggests that one reason for the development of these mats is a mean, local, salinity reduction of the Dead Sea water by the significantly less saline spring water (Table 1). The formation of such reduced salinity environments was recently demonstrated from flume experiments mimicking the spring water flow (Häusler et al., 2014). This is further supported by the fact that neither diatoms nor cyanobacteria could grow in pure DSW and only grew in diluted media. The salinity growth range observed for the diatoms between 5 to 40% DSW (1.75 to 14%, weight of TDS per volume) is in the range of the salinity tolerance observed for other halotolerant diatoms between 0.5 to 15% TDS (Clavero et al., 2000). In contrast to the diatoms, the cyanobacterial enrichments were more salt tolerant and grew in media containing 5 to 70% DSW (1.75 to 24.5% TDS). Garcia-Pichel et al. (1998) previously showed that cyanobacteria which are closely related to the *Euhalothece* cluster are able to grow at salinities between 1.5% to NaCl saturation (approximately 28-34 % TDS). Elevated concentration of  $Mg^{2+}$ , which is the main cation in pure Dead Sea water (Oren, 2010), is likely to be the reason why growth of the cyanobacteria is not observed at higher concentrations of Dead Sea water.  $MgCl_2$  is a highly chaotropic salt, known to denature cellular macromolecules at concentrations already below 1 M (Hallsworth et al. 2007).

Local salinity reduction is the main reason for the growth of the biofilms but the supply of nutrients by the spring water could be beneficial as well. Only limited growth of

---

both organisms could be observed in not-supplemented diluted DSW. The addition of nutrients to the same media increased the growth of both the diatoms and the cyanobacteria. The spring water is enriched in silica (Table 1) which is necessary for the synthesis of the diatom's frustules and is considered a major limiting nutrient for diatom growth (Martin - Jézéquel et al., 2000). Phosphate and nitrate are present in similar concentrations in the spring water and in the Dead Sea and thus extra supply by spring water does not play a role for the presence of mats at the springs. Many phototrophic organisms possess a carbon concentrating mechanisms (CCM) to achieve high intracellular CO<sub>2</sub> concentrations and prevent oxygenase activity of the RubisCo and thus can also thrive at low DIC concentrations (Kaplan and Reinhold, 1999; Giordano et al., 2005). However, the supply of high concentrations of DIC (5.5 mM, Table 1) from the spring water might also be beneficial, leading to energy saving by the down regulation of the CCM as suggested for diatoms (Hopkinson et al., 2011). The effects of the different nutrients supplied by the spring water were not investigated separately. Nevertheless, the reasons for the development of the phototrophic microbial mats in the underwater springs of the Dead Sea may not be substantially different from those leading to *Dunaliella* blooms in the water column, namely a reduction in salinity and the input of nutrients (Oren et al. 1995).

The proposed exposure of the microbial mats to fluctuating salinity, as indicated by previous variable flow measurements (Häusler et al., 2014) and observations by scuba divers (Ionescu et al., 2012), is also evident in the *in situ* microsensor measurements (Fig. 2). Oxygen penetration depth measured every hour in the diatom mat varied and even displayed a sudden deepening at night. Since the spring water is anoxic and photosynthesis is absent at night, the only explanation for the increased oxygen penetration into the sediment is a reduced spring water input and subsequent sinking of oxygenated heavier Dead Sea brine into the sediment. In addition, fluctuations in spring water input were confirmed by variation in temperature of up to 0.7 C°, recorded at the surface in the diatom mat (Fig. S2). Thus the organisms inhabiting the Dead Sea underwater springs have to deal with increasing and decreasing salinities in a matter of minutes to hours. From these measurements the degree of salinity fluctuations cannot be inferred but under the most

---

extreme case the salinity could occasionally increase to pure DSW as simulated in our experiment (Fig. 4).

Considering the different tolerance and response to changes in ambient salinity of the diatoms and cyanobacteria, a first picture emerges about their microenvironments allowing us to hypothesize about the observed distribution of the microbial mats in the Dead Sea. The average salinity the organisms are exposed to *in situ* is likely to be at the upper level that allows for growth, as only cells adapted to high salinity are acclimated to cope with extensive salinity fluctuations. This conclusion is further supported by the observation that both organisms could perform photosynthesis at 80% DSW shortly after collection (Fig. 2). This was only observed in artificial biofilms grown at high salinity (Fig. 4A and B). The absence of diatoms in the cyanobacterial microbial mats could result from a mean higher salinity which is too high to allow for diatom growth (50-70% DSW) or from long exposures (days to weeks) to DSW which can only be tolerated by the cyanobacteria. As will be discussed in the following paragraphs, one reason for the absence of cyanobacteria in the diatom mats could result from frequent, and sudden short-term fluctuations which are better tolerated by the diatoms and thus may allow them to outcompete the cyanobacteria in such areas.

The salinity fluctuations caused by the varying flow regime of the springs exert an extreme stress on the organisms in the mat as can be deduced from the decreasing photosynthetic activity measured in the artificial biofilms exposed to increasing DSW concentrations (Fig. 3). This is in accordance to the general stress effect observed for cyanobacteria and algae exposed to substantial increase in external salt concentrations using NaCl (for comprehensive reviews see Kirst, 1990; Sudhir and Murthy, 2004; Allakhverdiev and Murata, 2008). Osmotic water loss and an increase of intracellular ion concentration impair cellular processes like photosynthesis by the disturbance of the well-balanced intracellular water activity and ion homeostasis. This effect can be reversible upon exposures to low salinity whereas if the exposure to high salinity is too long, Na<sup>+</sup> ions can irreversibly damage photosystems (PS) I and II due to the dissociation of extrinsic proteins as shown for cyanobacteria (Allakhverdiev et al., 2000; Allakhverdiev and Murata,

---



2008). The effect of the unique salt composition of DSW with its high concentrations of  $Mg^{2+}$  and  $Ca^{2+}$  on PS I and II is unknown and warrants further investigations. Nevertheless, the observed reversibility of the photosynthetic inhibition only in high saline adapted cells (Fig. 3A and B) implies that protective measures against ionic damage were already present in these cells due to their growth salinity. Among these protective measures are likely an increased concentration of compatible organic osmolytes which are known to protect the photosystems from ionic damage (Murata et al., 1992; Papageorgiou and Murata, 1995; Ohnishi and Murata, 2006), unsaturation of fatty acids in membrane lipids (Allakhverdiev et al., 2001), which may lead to e.g. enhanced  $Na^+/H^+$  antiporter activity (Allakhverdiev and Murata, 2008), as well as changes in the proteome (Bhargava and Srivastava 2013). Hence, high saline adapted cells are better adapted to withstand salinity fluctuations.

Comparing the different response of the high saline grown cyanobacteria and diatoms to a gradual or rapid salinity change, it suggests that the cyanobacteria are able to withstand longer exposures to high DSW concentrations without damage (165 min in DSW concentrations higher than the adaptation salinity; Fig. 4A and B). This is further evident from the cyanobacterial biofilm which can re-grow in low saline media after being exposed 1 week to pure DSW whereas the diatoms do not. In contrast, the diatoms can recover faster than the cyanobacteria after a sudden exposure to DSW (Fig. 4C). When the cyanobacteria were exposed to a sudden increase in external salt concentration it probably led to a high intracellular ion concentration which inhibited ion export systems (e.g.  $Na^+/H^+$  antiporters; Allakhverdiev et al., 2000). The export systems may have been still functioning in the gradual salinity shift, thereby keeping the intracellular ionic concentration relatively low and thus preventing photosystem damage. This may explain why the cyanobacteria could recover completely their photosynthetic potential within 90 minutes after the exposure to pure DSW in the gradual salinity shift, but not in the same timeframe after the sudden DSW shock. In the case of diatoms, the exposure time of 15 minutes to pure DSW was too short to damage the photosynthetic machinery as occurred in the longer exposure to higher salinities resulting from the gradual shifts (Fig. 4B and C). The compartmentalisation of eukaryotic cells (chloroplasts, nucleolus, mitochondria etc.) and a different permeability to ions of the distinct membranes, could lead to a better protection against short-term

---

exposures to high salinities. Vacuoles, known to be present in *Navicula* species (Round et al., 1990), could also have a role in the recovery from a short extreme salinity shock by compartmentalizing  $\text{Na}^+$  from the cytoplasm as shown for red algae and plants (Mostaert et al. 1996; Parks et al. 2002). Thus, due to the more complex structure diatoms could have an advantage over the cyanobacteria in a spring environment exposed to sudden extreme short-term salinity shifts. In addition, the diatoms could have an advantage in hypoosmotic conditions where ionic damage does not occur (e.g. when the spring water flow is higher than average). No apparent additional loss of  $\text{O}_2$  production was observed when the high saline grown diatoms were subjected to hypoosmotic treatment (below 40% DSW in this case; Fig. 4A and B), whereas the cyanobacterial  $\text{O}_2$  production activity was again impaired during these conditions. A similar resistance of photosynthetic activity to hypoosmotic conditions was observed in microalgae with strong cell walls (Hellebust, 1985). Strong cell walls are likely to prevent bursting of the cells under hypoosmotic conditions (Bisson and Kirst 1995).

Growth of both organisms is limited to a water depth <10 meter, although springs are observed down to at least 30 meters (Ionescu et al., 2012). Light is strongly attenuated with depth in the spring's area (Fig. S2) reaching an intensity of about  $30 \mu\text{mol m}^2 \text{s}^{-1}$  at 10 meters (Fig. 2), although benthic diatoms were reported to thrive at much lower light levels at continental slopes (McGee et al., 2008). Thus, the light level or quality (Fig. S3) in deeper areas might not be sufficient to balance the high energy required for osmoregulation (e.g. osmolyte synthesis and energy consuming cation efflux systems) and/or protein synthesis (Allakhverdiev et al., 2005). Indeed, the diatoms seem to be light limited as *in situ* oxygen evolution was only detected close to the maximum *in situ* light intensity of  $30 \mu\text{mol photons m}^{-2} \text{s}^{-1}$  (Fig. 2). However, the role of light with respect to the salinity tolerance needs to be determined separately.

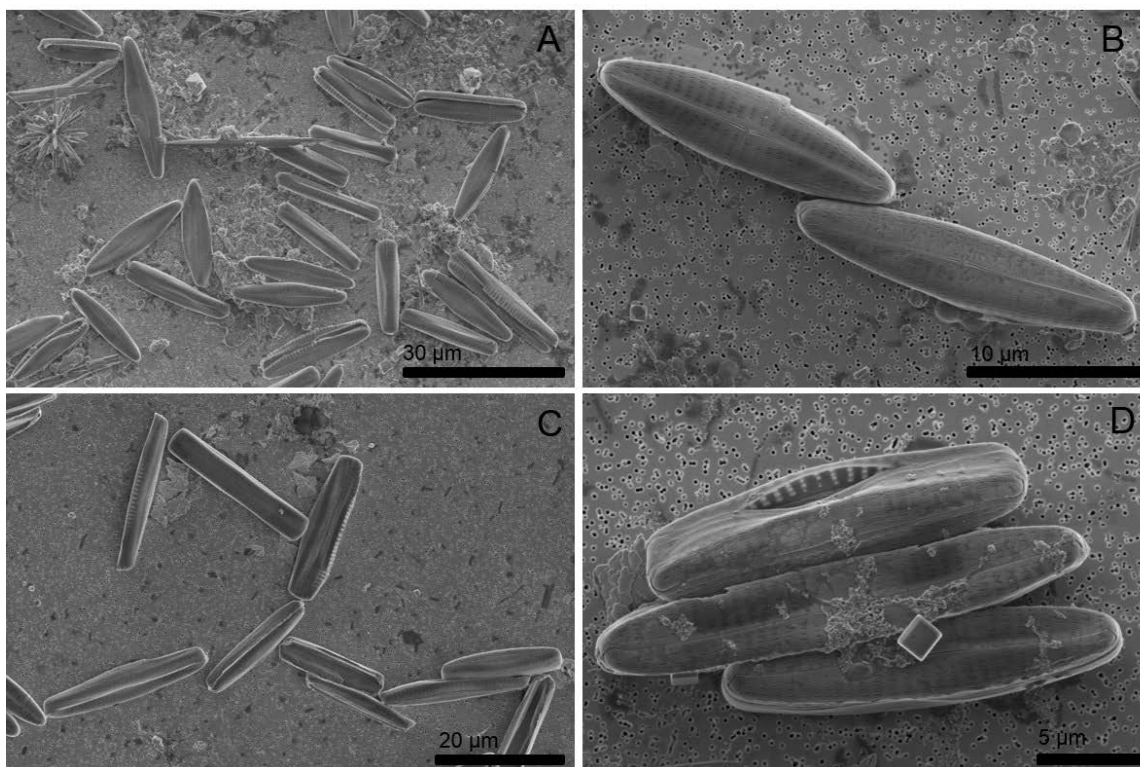
We here demonstrate the existence of active, extreme halotolerant phototrophic organisms inhabiting freshwater springs in the Dead Sea which can tolerate short-term exposures to an unusual salt composition beyond their growth tolerance and rapidly recover their photosynthetic potential. We presented evidence that the local regime of salinity

---

fluctuations determines which of the two types of organisms dominates. As compared to other microbial environments exhibiting salinity fluctuations in the orders of hours to days like intertidal microbial mats (Kohls et al., 2010; Stal, 2012), the fast and extreme salinity fluctuations in the spring system discovered in the Dead Sea are unique. Furthermore, the ability of these organisms to recover their photosynthetic potential after the exposure to pure DSW is remarkable. In addition to 1.5 M Na<sup>+</sup>, pure DSW contains high concentrations of divalent cations (2 M Mg<sup>2+</sup> and 0.5 M Ca<sup>2+</sup>) which have a more chaotropic (destabilising) potential on biological macromolecules than monovalent ions (Cacace et al., 1997; Hallsworth et al., 2007; Oren, 2013). Thus, the exposure to pure DSW must be even more damaging to cellular macromolecules than pure NaCl solutions which are used for all other studies mostly in moderate concentrations (Kirst, 1990; Sudhir and Murthy, 2004; Bhargava and Srivastava 2013 and references therein). It will be fascinating to explore the molecular salinity response of these organisms in detail. In addition, competition studies are needed to fully understand the distribution of the phototrophs in the Dead Sea springs in detail. Moreover, the role of light and the supply of organic matter from the springs needs to be addressed with respect to the spatial competition between the diatoms and cyanobacteria since it was shown that light conditions and organic-matter can affect the recovery or inhibition of PSII during salt stress (Allakhverdiev and Murata 2008).

## **Acknowledgements**

This study was financially supported by the Max-Planck-Society and the DAAD. We want to acknowledge Christian Lott from the HYDRA Institute (Elba) for his support during diving and underwater videography. Furthermore we want to thank Yaniv Y. Munwes for field assistance, Shiri Meshner for providing us with lab space in the Ein Gedi lab of The Dead Sea and Arava Science Center. We are also deeply grateful for the supply of lab equipment by Aharon Oren.

**Supplementary information**

**Figure S1** SEM images from the *in situ* Diatom mat (upper panel A and B) and from the Diatom enrichment cultures grown in 5% Dead Sea water (C) and 40 % Dead Sea water (D).

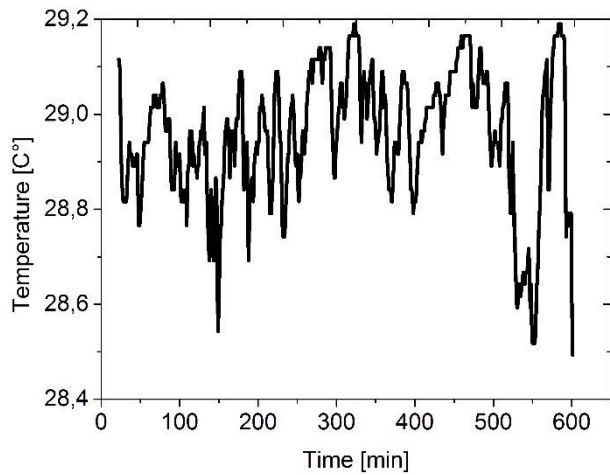


**Figure S2** Temperature recorded at the diatom mat surface shows extensive fluctuations of up to 0.7 C°.

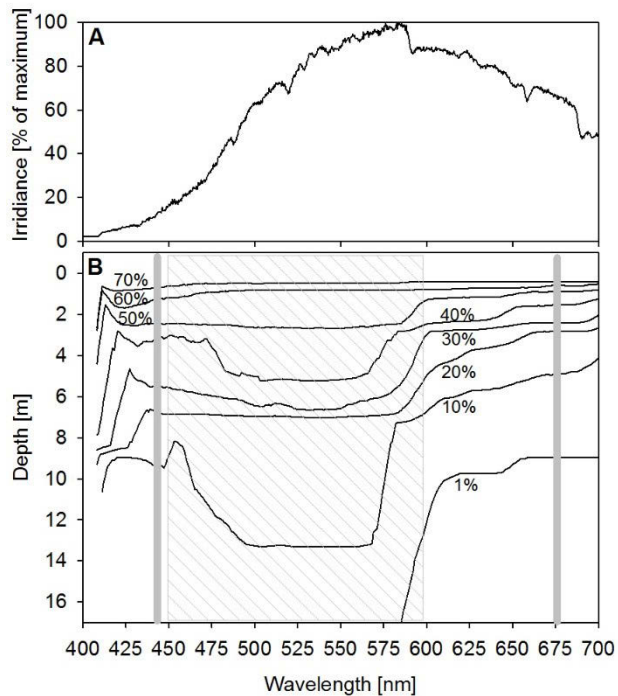


**Figure S3** Surface light (A) is strongly attenuated in the Dead Sea spring area as seen in the contour lines depicting the relative amount of light left at a certain depth (B). Slim grey bars indicate the *in vivo* absorption maxima of Chlorophyll a (440 and 675 nm; Bidigare et al. 1990), whereas the grey shaded area represents the range of absorption by auxiliary pigments including carotenoids (450-550 nm; Johnsen et al. 1994) and phycobiliprotein-dominated pigments (480-600 nm; Johnsen et al. 1994).

**References**

- Allakhverdiev, S.I., Sakamoto, A., Nishiyama, Y., Inaba, M., and Murata, N. (2000) Ionic and osmotic effects of NaCl-induced inactivation of photosystems I and II in *Synechococcus* sp. *Plant Physiol.* **123**: 1047–1056.
- Allakhverdiev, S.I., Kinoshita, M., Inaba, M., Suzuki, I., and Murata, N. (2001) Unsaturated Fatty Acids in Membrane Lipids Protect the Photosynthetic Machinery against Salt-Induced Damage in *Synechococcus*. *Plant Physiol.* **125**: 1842–1853.
- Allakhverdiev, S.I., Klimov, V. V, and Hagemann, M. (2005) Cellular energization protects the photosynthetic machinery against salt-induced inactivation in *Synechococcus*. *Biochim. Biophys. Acta (BBA)-Bioenergetics* **1708**: 201–208.
- Allakhverdiev, S.I. and Murata, N. (2008) Salt stress inhibits photosystems II and I in cyanobacteria. *Photosynth. Res.* **98**: 529–539.
- Altschul, S.F., Gish, W., Miller, W., Myers, E.W., and Lipman, D.J. (1990) Basic local alignment search tool. *J. Mol. Biol.* **215**: 403–410.
- Bhargava P, Srivastava A (2013) Salt Toxicity and Survival Strategies of Cyanobacteria. In, *Stress Biology of Cyanobacteria*. London, Routledge Chapman & Hall CRC Press, pp 171–188
- Bidigare, R.R., Ondrusek, M.E., Morrow, J.H., and Kiefer, D.A. (1990) In-vivo absorption properties of algal pigments. In, *Orlando '90, 16-20 April*. International Society for Optics and Photonics, pp. 290–302.
- Bodaker, I., Sharon, I., Suzuki, M.T., Feingersch, R., Shmoish, M., Andreishcheva, E., et al. (2010) Comparative community genomics in the Dead Sea: an increasingly extreme environment. *Isme J.* **4**: 399–407.
-

- Cacace, M.G., Landau, E.M., and Ramsden, J.J. (1997) The Hofmeister series: salt and solvent effects on interfacial phenomena. *Q. Rev. Biophys.* **30**: 241–277.
- Clavero, E., Hernández- Mariné, M., Grimalt, J.O., and Garcia- Pichel, F. (2000) Salinity tolerance of diatoms from thalassic hypersaline environments. *J. Phycol.* **36**: 1021–1034.
- Elazari-Volcani, B. (1940) Algae in the bed of the Dead Sea. *Nature* **145**: 975.
- Elazari-Volcani, B. (1943a) A dimastigamoeba in the bed of the Dead Sea. *Nature* **152**: 301–302.
- Elazari-Volcani, B. (1943b) Bacteria in the bottom sediments of the Dead Sea. *Nature* **152**: 274–275.
- Elazari-Volcani, B.E. (1944a) The microorganisms of the Dead Sea. *Pap. Collect. to Commem. 70th Anniv. Dr. Chaim Weizmann. Collect. Vol.* 71–85.
- Elazari-Volcani, B. (1944b) A ciliate from the Dead Sea. *Nature* **154**: 355.
- Erdmann, N. and Hagemann, M. (2001) Salt acclimation of algae and cyanobacteria: a comparison. In, *Algal Adaptation to Environmental Stresses*. Springer, Berlin-Heidelberg, pp. 323–361.
- Farías, M.E., Rascovan, N., Toneatti, D.M., Albarracín, V.H., Flores, M.R., Poiré, D.G., et al. (2013) The discovery of stromatolites developing at 3570 m above sea level in a high-altitude volcanic lake Socompa, Argentinean Andes. *PLoS One* **8**: e53497.
- Garcia-Pichel, F., Nübel, U., and Muyzer, G. (1998) The phylogeny of unicellular, extremely halotolerant cyanobacteria. *Arch. Microbiol.* **169**: 469–482.

- Giordano, M., Beardall, J., and Raven, J.A. (2005) CO<sub>2</sub> concentrating mechanisms in algae: mechanisms, environmental modulation, and evolution. *Annu. Rev. Plant Biol.* **56**: 99–131.
- Guillard, R.R.L. and Ryther, J.H. (1962) Studies of Marine planktonic diatoms: I. *Cyclotella Nana* Husted, and *Detonula confervacea* (Cleve) Grun. *Can. J. Microbiol.* **8**: 229–239.
- Hallsworth, J.E., Yakimov, M.M., Golyshin, P.N., Gillion, J.L.M., D’Auria, G., De Lima Alves, F., et al. (2007) Limits of life in MgCl<sub>2</sub> containing environments: chaotropy defines the window. *Environ. Microbiol.* **9**: 801–813.
- Häusler, S., Noriega-Ortega, B.E., Polerecky, L., Meyer, V., de Beer, D., and Ionescu, D. (2014) Microenvironments of reduced salinity harbour biofilms in Dead Sea underwater springs. *Environ. Microbiol. Rep.* **6**: 152–158.
- Hellebust, J.A. (1985) Mechanisms of response to salinity in halotolerant microalgae. *Plant Soil* **89**: 69–81.
- Hopkinson, B.M., Dupont, C.L., Allen, A.E., and Morel, F.M.M. (2011) Efficiency of the CO<sub>2</sub>-concentrating mechanism of diatoms. *Proc. Natl. Acad. Sci.* **108**: 3830–3837.
- Ionescu, D., Lipski, A., Altendorf, K., and Oren, A. (2007) Characterization of the endoevaporitic microbial communities in a hypersaline gypsum crust by fatty acid analysis. *Hydrobiologia* **576**: 15–26.
- Ionescu, D., Siebert, C., Polerecky, L., Munwes, Y.Y., Lott, C., Häusler, S., et al. (2012) Microbial and Chemical Characterization of Underwater Fresh Water Springs in the Dead Sea. *PLoS One* **7**: 21.
- Johnsen, G., Samset, O., Granskog, L., and Sakshaug, E. (1994) In-vivo absorption characteristics in 10 classes of bloom-forming phytoplankton-taxonomic
-



characteristics and responses to photoadaptation by means of discriminant and HPLC analysis. *Mar. Ecol. Prog. Ser.* **105**: 149–157.

Kaplan, A. and Reinhold, L. (1999) CO<sub>2</sub> concentrating mechanisms in photosynthetic microorganisms. *Annu. Rev. Plant Biol.* **50**: 539–570.

Kirst, G.O. (1990) Salinity tolerance of eukaryotic marine algae. *Annu. Rev. Plant Biol.* **41**: 21–53.

Kohls, K., Abed, R.M.M., Polerecky, L., Weber, M., and De Beer, D. (2010) Halotaxis of cyanobacteria in an intertidal hypersaline microbial mat. *Environ. Microbiol.* **12**: 567–575.

Martin- Jézéquel, V., Hildebrand, M., and Brzezinski, M.A. (2000) Silicon metabolism in diatoms: implications for growth. *J. Phycol.* **36**: 821–840.

McGee, D., Laws, R.A., and Cahoon, L.B. (2008) Live benthic diatoms from the upper continental slope: extending the limits of marine primary production. *Mar. Ecol. Ser.* **356**: 103.

Medlin, L., Elwood, H.J., Stickel, S., and Sogin, M.L. (1988) The characterization of enzymatically amplified eukaryotic 16S-like rRNA-coding regions. *Gene* **71**: 491–499.

Mostaert, AS, Orlovich DA, King RJ (1996) Ion compartmentation in the red alga *Caloglossa leprieurii* in response to salinity changes: freeze- substitution and X- ray microanalysis. *New Phytol* **132**:513–519.

Murata, N., Mohanty, P.S., Hayashi, H., and Papageorgiou, G.C. (1992) Glycinebetaine stabilizes the association of extrinsic proteins with the photosynthetic oxygen-evolving complex. *FEBS Lett.* **296**: 187–189.

---

- Nishri, A. and Ben-Yaakov, S. (1990) Solubility of oxygen in the Dead Sea brine. *Hydrobiologia* **197**: 99–104.
- Nübel, U., Garcia-Pichel, F., Clavero, E., and Muyzer, G. (2000) Matching molecular diversity and ecophysiology of benthic cyanobacteria and diatoms in communities along a salinity gradient. *Environ. Microbiol.* **2**: 217–226.
- Nübel, U., Garcia-Pichel, F., Köhl, M., and Muyzer, G. (1999) Spatial scale and the diversity of benthic cyanobacteria and diatoms in a salina. In, *Molecular Ecology of Aquatic Communities*. Springer, Berlin-Heidelberg pp. 199–206.
- Nübel, U., Garcia-Pichel, F., and Muyzer, G. (1997) PCR primers to amplify 16S rRNA genes from cyanobacteria. *Appl. Environ. Microbiol.* **63**: 3327–3332.
- Ohnishi, N. and Murata, N. (2006) Glycinebetaine counteracts the inhibitory effects of salt stress on the degradation and synthesis of D1 protein during photoinhibition in *Synechococcus* sp. PCC 7942. *Plant Physiol.* **141**: 758–765.
- Oren, A. (2010) The dying Dead Sea: The microbiology of an increasingly extreme environment. *Lakes Reserv. Res. Manag.* **15**: 215–222.
- Oren, A. (2012) Salts and brines. In, *Ecology of Cyanobacteria II*. Springer, Berlin-Heidelberg pp. 401–426.
- Oren, A. (2013) Life in Magnesium-and Calcium-Rich Hypersaline Environments: Salt Stress by Chaotropic Ions. In, *Polyextremophiles*. Springer, pp. 215–232.
- Oren, A., Gurevich, P., Anati, D.A., Barkan, E., and Luz, B. (1995) A bloom of *Dunaliella parva* in the Dead Sea in 1992: biological and biogeochemical aspects. *Hydrobiologia* **297**: 173–185.
-

- Papageorgiou, G.C. and Murata, N. (1995) The unusually strong stabilizing effects of glycine betaine on the structure and function of the oxygen-evolving photosystem II complex. *Photosynth. Res.* **44**: 243–252.
- Parks, G.E., Dietrich, M.A., and Schumaker, K.S. (2002) Increased vacuolar Na<sup>+</sup>/H<sup>+</sup> exchange activity in *Salicornia bigelovii* Torr. in response to NaCl. *J. Exp. Bot.* **53**: 1055–1065.
- Revsbech, N.P. and Jørgensen, B.B. (1986) Microelectrodes: their use in microbial ecology. *Adv. Microb. Ecol* **9**: 293–352.
- Revsbech, N.P., Jørgensen, B.B., and Brix, O. (1981) Primary production of microalgae in sediments measured by oxygen microprofile, H<sub>4</sub>CO<sub>3</sub> fixation, and oxygen exchange methods. *Limnol. Ocean.* **26**: 717–730.
- Rippka, R., Deruelles, J., Waterbury, J.B., Herdman, M., and Stanier, R.Y. (1979) Generic assignments, strain histories and properties of pure cultures of cyanobacteria. *J. Gen. Microbiol.* **111**: 1–61.
- Round, F.E., Crawford, R.M., and Mann, D.G. (1990) The diatoms: biology & morphology of the genera, Cambridge University Press, Cambridge.
- Stal, L.J. (2012) Cyanobacterial mats and stromatolites. In, *Ecology of Cyanobacteria II*. Springer, Berlin-Heidelberg pp. 65-125
- Sudhir, P. and Murthy, S.D.S. (2004) Effects of salt stress on basic processes of photosynthesis. *Photosynthetica* **42**: 481–486.
- Weber, M., Faerber, P., Meyer, V., Lott, C., Eickert, G., Fabricius, K.E., and De Beer, D. (2007) In situ applications of a new diver-operated motorized microsensor profiler. *Environ. Sci. Technol.* **41**: 6210–6215.
-

Wieland, A. and Kühl, M. (2000) Irradiance and temperature regulation of oxygenic photosynthesis and O<sub>2</sub> consumption in a hypersaline cyanobacterial mat (Solar Lake, Egypt). *Mar. Biol.* **137**: 71–85.

# Chapter 5

## **Sulfate reduction and sulfide oxidation in extremely steep salinity gradients formed by freshwater springs emerging into the Dead Sea**

Stefan Häusler<sup>1</sup>, Miriam Weber<sup>1,2</sup>, Christian Siebert<sup>3</sup>, Moritz Holtappels<sup>1</sup>, Beatriz E. Noriega-Ortega<sup>4</sup>, Dirk de Beer<sup>1</sup>, Danny Ionescu<sup>1</sup>

<sup>1</sup>Max Planck Institute for Marine Microbiology, Celsiusstrasse 1, 28211 Bremen, Germany

<sup>2</sup>HYDRA Institute for Marine Sciences, Elba Field Station, Campo nell'Elba (LI), Italy

<sup>3</sup> Helmholtz-Center for Environmental Research UFZ, Dept. of Catchment Hydrology, T. Lieser Str. 4, Halle/Saale, Germany

<sup>4</sup>ICBM-MPI Bridging Group for Marine Geochemistry Carl-von-Ossietzky-Str. 9-11  
26129 Oldenburg, Germany

**Prepared for submission to FEMS Microbiology Ecology**

## Abstract

Abundant and diverse microbial mats were recently discovered in freshwater springs emerging into the Dead Sea, an extremely hypersaline lake in which only few types of microorganisms can survive. Most of these microbial mats are dominated by sulfide oxidizing bacteria (SOB). We used a polyphasic approach to assess the activity of the SOB communities and link the source of sulfide to either local communities of sulfate reducing bacteria in the spring's surface sediment or distant communities along the flow path. Isotopic analysis of coexisting sulfide and sulfate in the spring water showed a fractionation of 39 to 50‰ indicating that the sulfate reducing community detected earlier in the spring waters by sequencing analysis is indeed active. Although the microbial mats were also shown to harbor various taxa of sulfate reducing bacteria (SRB), local sulfate reduction rates (SRR) of  $<2.8 \text{ nmol cm}^3 \text{ d}^{-1}$  determined in the spring surface sediment are too low to account for the sulfide flux determined by *in situ* microsensor measurements. Thus, the supply of reduced S-compounds produced along the subsurface flow path of the emerging groundwaters, in combination with a locally reduced salinity and  $\text{O}_2$  supply from the Dead Sea water column are the driving factors for the abundant microbial biomass encountered in the springs. Alternatingly fast and slow discharging springs are characterized by extreme changes in flow regimes, leading to environments with strongly variable salinities. We speculate that the development of microbial mats dominated by either SOB related to the *Sulfurimoas/Sulfurovum* genus or the *Thiobacillus/Acidithibacillus* genus is a result of the different mean salinities between the mats. A SRR of up to  $10 \text{ nmol cm}^3 \text{ d}^{-1}$  detected in the Dead Sea sediment is surprisingly higher than in the less-saline springs. While this shows the presence of an active, extremely halophilic SRB community in the Dead Sea sediments, we suggest that extensive salinity fluctuations limit the SRB populations in the springs due to the high energy demand of osmoregulation.

## Introduction

The Dead Sea located between Jordan, Israel and the Palestinian Authorities, is one of the most hypersaline lakes on our planet. It is the lowest exposed surface on earth ( $< -423$  meters mean sea level) and consists of a deep northern and a shallow southern basin. Since the middle of the 20<sup>th</sup> century the water budget of the Dead Sea has been negative due to the diversion of freshwater from its drainage basin and the use of the lake's brines for industrial salt production (Oren, 2010). As a result over the last decades there is a constant drop in the lake level of about  $1 \text{ m a}^{-1}$  (Lensky et al., 2005) and a continuous change of the physico-chemical properties of the water. The salinity and density of the brine increased resulting in an overturn in 1979 and ending a century long meromictic phase which was characterized by an anoxic, sulfidic bottom and an oxic surface water body (Steinhorn et al., 1979). Nowadays, the lake is holomictic with a total dissolved salt concentration of  $>340 \text{ g l}^{-1}$ . Supersaturation of NaCl in the water column led to continuous precipitation of halite. Thus, the more soluble  $\text{Mg}^{2+}$  and  $\text{Ca}^{2+}$  ions have become the dominant cations (about 2 M and 1.5 M, respectively, Oren 2010). The extreme salinity and especially the high concentrations of divalent cations, which have a high chaotropic (destabilizing) effect on biological macromolecules (Oren, 2013), make the Dead Sea an extreme environment.

These harsh conditions are only tolerated by a few types of microorganisms as reflected in the low microbial diversity. Generally the microbial community of the Dead Sea ecosystem seems to be dominated by Archaea (Bodaker et al., 2010). The only primary producer detected in the lake is the unicellular algae *Dunaliella* sp. (Oren, 2010). However, extensive blooms of the algae only develop during periods when the upper water layer of the lake gets sufficiently diluted after severe rainfall and subsequent runoff events. Such bloom events were monitored in 1980 and 1992 and were followed by blooms of Archaea living on the exudates of the autotrophic algae (Oren and Shilo, 1982, 1985; Oren, 1983; Oren et al., 1995). In addition to these microorganisms several Archaea and Bacteria species, as well as protozoa and ciliates have been isolated so far from the water column and the sediments of the lake (Elazari-Volcani, 1943a, 1943b, 1944; Oren, 2010). Sulfate reducing bacteria have never been isolated from the Dead Sea (Oren, 2010). However, at times when

---

the lake was still permanently stratified a difference of 35‰ in the  $\delta^{34}\text{S}$  value between dissolved sulfide and sulfate and the depletion in  $\delta^{34}\text{S}$  by 25 to 35‰ in iron sulfide in the sediment, indicated the presence of sulfate reducing activity in the lake (Nissenbaum, 1975).

Recently a large system of underwater freshwater springs emerging into the northern basin of the Dead Sea was discovered (Ionescu et al., 2012). The water originates from the Upper Cretaceous Aquifers and flows through the Quaternary sediments of the Dead Sea and its precursors until it emerges along the shoreline at depths of 2 to 30 meter into the lake. The discovered system is divided into a northern and a southern part. In the northern part the springs are located at the bottom of deep shafts (10 to 30 meters) whereas in the southern part these shafts are absent and the water emerges either as jets from distinct outlets or as widespread slow seeps from the Dead Sea sediments. Based on 16S rRNA gene analysis and microscopic observations, it was concluded that these springs harbor an unusual high and diverse biomass of microorganisms compared to the surrounding Dead Sea. For instance rocks and cobbles located in the jets of the southern system are covered with thick green and white biofilms mainly composed of phototrophic and chemolithotrophic sulfur oxidizing bacteria (SOB). At seeping sites on the other hand microbial mats are dominated by SOB belonging to the *Epsilonproteobacteria* (Ionescu et al., 2012). In addition, sequences of sulfate reducing bacteria (SRB) were detected in the spring sediments and the surrounding Dead Sea (Ionescu et al., 2012).

The main reason for the high microbial biomass is probably the development of microenvironments of reduced salinity on surfaces exposed to spring water discharge (Häusler et al. 2014). In addition, the springs deliver organic matter and sulfide (Ionescu et al., 2012) which could fuel the SRB and the SOB communities, respectively. Thus, the aim of this study was to investigate whether the sulfur related microbial community suggested from the sequencing analysis is indeed active. Furthermore, we aim at elucidating whether the sulfide in the spring water is produced locally in the spring sediments, or most likely along the subsurface passage through the Quaternary sediments, rich in organic matter and sulfate minerals, by sulfate reduction. To answer these questions we used a polyphasic

---



approach: First, we used the isotopic signature of coexisting sulfate and sulfide in the spring water to determine the source of sulfide. Second, we performed *in situ* microsensor measurements on two microbial mats to establish the activity of the SOB community, and third used radiolabeling experiments to determine sulfate reduction rates (SRR) in the spring- and the surrounding Dead Sea sediments. In combination with 16S rRNA gene sequences detected in the different microbial mats we furthermore speculate that differences in the community of SOB and SRB related sequences between distinct spring water outlets are a result of different spring water flow regimes leading to different mean salinities. Additionally we used ultra-high resolution mass spectrometry via the Fourier Transform Ion Cyclotron Resonance Mass Spectrometer (FT-ICR-MS) to characterize dissolved organic matter (DOM) present in the Dead Sea, as well as in the springs and aquifers.

## **Material and Methods**

### **Water sampling and analyses**

Spring water was sampled and the various chemical parameters were analyzed as described by Ionescu et al. (2012). In addition, for isotopic measurements of sulfide, 6 ml of spring water was collected in Exertainers prefilled with 100  $\mu$ l of 20% zinc acetate (w/v) to fix S(-II) as ZnS. The contents of the vials were then filtered by using a 0.2  $\mu$ m polycarbonate filter (Millipore). Subsequently, sulfate was precipitated as BaSO<sub>4</sub> in the filtrate by acidification with 1M HCL (to pH 3) following the addition of 150  $\mu$ l of 1.2 M BaCl<sub>2</sub>. The precipitate was recovered on a separate 0.2  $\mu$ m polycarbonate filter. All filters were dried at 60 °C for at least 12 hours. For measurements of  $\delta^{34}\text{S}$  the filters were placed in tin cups and about 400  $\mu$ g of Vanadium pentoxide was added as catalyst. The ratio of  $\delta^{34}\text{S}$  was determined using a FISIONS OPTIMA mass spectrometer (Fisons, Middlewich, Chessire, UK) coupled to a Carlo Erba elemental analyzer (CE Instruments, Milano, Italy). Data are reported in mean of duplicate samples in the standard  $\delta$ -notation versus the Vienna-Canon

---

Diabolo Troilite (V-CDT) standard according to:  $\delta^{34}\text{S} (\text{‰}) = (((^{34}\text{S}/^{32}\text{S})_{\text{sample}} / (^{34}\text{S}/^{32}\text{S})_{\text{V-CDT}}) - 1) \times 1000$

In addition, for fingerprint analysis of dissolved organic matter, Dead Sea water samples (n=43) were collected using Niskin entrapment bottles at different depths between 6 and 166 m along a transect from shore and up to 1000 m away. Samples were transferred directly into acid rinsed 1 l plastic bottle. Samples from the aquifers were collected from various wells (n=19). 30 samples of underwater springs were analysed.

### **DOM extraction and sample preparation**

46 samples of Dead Sea water were collected at different depths. DOM was extracted from the water samples by solid phase extraction (SPE) (Dittmar et al., 2008) with the following modifications; samples were not filtered prior to DOM extraction and 1l of sample was diluted 1:1 with ultrapure water. 16 samples from aquifers and wells, together with 7 samples from spring water were solid phase extracted as described by Dittmar and colleagues in 2008. The samples were acidified to pH 2 with HCl analytical grade and run through Varian Bond Elut PPL resins by gravity.

### **FT-ICR-MS data processing**

Ultrahigh-resolution mass spectrometry via the Fourier transform ion-cyclotron resonance (FT-ICR-MS) technique was performed on a Bruker Solarix 15 Tesla FT-ICR-MS. Electrospray ionization was in negative mode. 500 scans were accumulated. Samples were injected at a flow rate of  $120 \mu\text{l h}^{-1}$  and the mass range analyzed was from 180 to 2000 m/z. Molecular formulae were assigned for all samples using Data Analysis software (ESI Compass 1.3) from Bruker Daltonics with error limits below or equal to 0.5 ppm. More than 12,000 compounds were identified in the samples.

## **Community of Sulfate reducing and sulfide oxidizing bacteria**

Sediment and biofilm samples were taken in sterile falcon tubes. DNA extraction and data analysis was performed as described in detail by Ionescu et al. (2012). Tag pyrosequencing for bacterial diversity, using primer sets 28F and 519R (Lane, 1991), was done by MrDNA (Shallowater, Texas, USA), using a Roche 454 FLX Genome Sequencer (Branford, USA). The obtained sequences were screened for bacteria affiliated to sulfur oxidizing and sulfate reducing bacteria.

### ***In situ* microsensor measurements**

For *in situ* microsensor measurements Clark-type oxygen (Revsbech and Ward, 1983), H<sub>2</sub>S (Jeroschewski et al., 1996) and pH microelectrodes (Revsbech and Jørgensen, 1986) were used. The microsensors had a tip diameter between 20 to 50 µm. To obtain an estimation of salinity inside the microbial mat the profiler was additionally equipped with a salinity mini-sensor with a tip diameter of 1.5 mm using the measuring principle as described in detail in Häusler et al. (2014). This sensor is able to measure salinities of 0–350 g l<sup>-1</sup> NaCl (High range sensor). However, in Dead Sea water (DSW) a decrease in sensor signal is observed in liquids containing >75 % DSW due to its above described unique salt composition. Thus, accurate calibrations cannot be obtained and only the raw signal was qualitatively compared to the reference site. For accurate salinity determination a second salinity sensor was used (low range sensor) with the same measuring principle as the first, but adjusted to measure linearly in salinities from freshwater to 70 g l<sup>-1</sup> TDS. Above this value it was out of range (O.R) and showed a constant signal. All sensors were mounted on an autonomous profiling lander (Gundersen and Jørgensen, 1990; Wenzhöfer and Glud, 2002) to conduct measurements at the sediment-water interface in a white microbial mat located on a seepage area (hereafter WhMat1) and a Dead Sea reference site not influenced by emerging groundwater. Depth profiles were recorded with a spatial resolution of 100 µm. The sensors were allowed to equilibrate in each depth for 5 seconds before the signal was recorded. Triplicate readings were averaged from each depth. For another white

---

microbial mat located vertically on a cliff (hereafter WhMat2), the Diver-Operated Microsensor System (DOMS) was used (Weber et al., 2007). There the oxygen profile and sulfide profile were measured subsequently since this instrument allows the mounting of only one sensor at a time. The sensors were also allowed to equilibrate in each depth for 5 seconds and triplicate readings were recorded.

### **Microsensor calibration**

Oxygen microsensors were calibrated prior to the measurement using a linear two-point calibration. The signal obtained in aerated Dead Sea water at *in situ* temperature represented the concentration corresponding to 100 % air saturation. The concentration of oxygen was then determined at corresponding temperatures in triplicates using a modified Winkler protocol for Dead Sea water (Nishri and Ben-Yaakov, 1990). The reading in anoxic Dead Sea water and anoxic freshwater (both prepared by dissolution of 0.1 g Sodium dithionate in 10 ml) was the same as in the deeper sediment layers and thus taken as zero oxygen. The H<sub>2</sub>S sensor was calibrated at *in situ* temperature (28 C°) in acidified spring water (pH 2) by adding increasing amounts of NaS-solution. Aliquots were taken and fixed in 2% ZnAC solution (w/v) and determined afterwards with the colorimetric assay of Cline (1969). pH sensors were 2-point-calibrated using commercial buffer solutions (Mettler Toledo). The salinity sensors were calibrated using a dilution series of Dead Sea water with de-ionized water.

### **Flux calculations**

Diffusive fluxes were calculated according to Fick's first law of diffusion,

$$J = -\Phi D_{eff} \frac{\partial C_i}{\partial x} \quad (1)$$

where  $\Phi$  is the porosity of the microbial mat,  $D_{eff}$  is the effective diffusion coefficient in the microbial mat and  $dC/dx$  is the one-dimensional concentration gradient. Porosity in the microbial mat was assumed to be 0.9 (Jorgensen and Cohen, 1977; Jørgensen et al., 1979;

Wieland and Kühl, 2000).  $D_{eff}$  was determined with  $D_{eff} = D_0 / \theta^2$ , where  $D_0$  is the diffusion coefficient in water at the given salinity and temperature and  $\theta^2$  is tortuosity with  $\theta^2 = 1 - \ln(\Phi^2)$ , (Berner, 1980; Boudreau, 1996). Since the low range salinity sensor signal was constant at 60 ‰ inside the microbial mat, it is unlikely that temperature and salinity changed within the approximately 2 mm thick microbial mat. Thus,  $D_0$  was also assumed to be constant and  $D_0$  for oxygen and sulfide at 60 ‰ salinity and 28 C° was taken from the tables of Seawater and Gases (<https://www.unisense.com/support>). Total sulfide concentrations at each depth were calculated from the local H<sub>2</sub>S concentrations and pH values as described by Jeroschewski et al., (1996). For pKs estimation, the ionic strength at each point of the profile was calculated assuming linear mixing between the spring water source and Dead Sea water according to the salinity profile. pKs was then calculated according to the obtained ionic strength at each point of the profile using the formula for high ionic strength NaCl solutions at 28 C° provided by Hershey et al. (1988). For oxygen flux calculation in the reference site,  $D_0$  of Dead Sea water was according to Gat et al., 1991 estimated to be 0.36 of the diffusion coefficient of freshwater at *in situ* temperature was taken from the tables of Seawater and Gases (<https://www.unisense.com/support>)

### Consideration of porewater advection

In the presence of advective porewater flow the diffusive flux cannot be calculated from (1). Instead, a 1D numerical transport-reaction model was set up using the finite element program COMSOL Multiphysics® 4.3. Assuming steady state conditions, the governing equation is

$$-\Phi D_{eff} \frac{\partial^2 C_i}{\partial x^2} + u \frac{\partial C_i}{\partial x} = R_i \quad (2)$$

where  $u$  is the porewater velocity and  $R$  is the reaction rate of the compound  $i$  described by Michaelis-Menten kinetics (half saturation constant: 10  $\mu\text{mol L}^{-1}$ ). Since the WhMat1 was covered with a microbial mat of potential sulfide oxidizers, equation 2 was solved for concentrations of H<sub>2</sub>S and O<sub>2</sub> and the two equations were coupled assuming either

complete oxidation of sulfide ( $\text{H}_2\text{S} + 2 \text{O}_2 \rightarrow \text{SO}_4^{2-} + 2 \text{H}^+$ ) or oxidation of sulfide to elemental sulfur ( $2 \text{H}_2\text{S} + \text{O}_2 \rightarrow 2 \text{S} + 2 \text{H}_2\text{O}$ ), so that either  $R_{\text{O}_2} = 2 \times R_{\text{H}_2\text{S}}$  or  $2 \times R_{\text{O}_2} = R_{\text{H}_2\text{S}}$ . Subsequently, the porewater velocity in the model was adjusted until the best match of modeled and measured concentrations was found. Then, the total fluxes were extracted.

### **Sulfate reduction measurements**

To obtain a uniform salinity throughout each core, sulfate reduction rates (SRR) were measured in WhMat1 sediment using the percolation technique as described by de Beer et al. (2005). Intact cores were sampled by SCUBA divers at the different sites and transferred to the lab of the Hebrew University of Jerusalem within 12 h. Two replicate cores were then percolated with twice the core volume using anoxic water (bubbled 1 h with  $\text{N}_2$  gas) with either high salinity of  $276 \text{ g l}^{-1}$  total dissolved salts (TDS) obtained by mixing 20% spring water and 80% Dead Sea (v/v) or low salinity of  $90 \text{ g l}^{-1}$  (80% spring water and 20% Dead Sea water). Afterwards the percolation of each core was repeated with the same water containing  $25 \text{ kBq ml}^{-1}$  of  $\text{S}^{35}\text{O}_4^{2-}$ . The cores were then incubated for 6-8 hours at  $27 \text{ C}^\circ$ . The incubations were terminated by slicing the cores in 1 cm intervals and suspending the sediment into equal amounts of 20% (w/v) ZnAC.  $^{35}\text{S}$  reduction was determined and calculated by using the cold chromium distillation procedure after Kallmeyer et al. (2004). In sediment cores obtained from the Dead Sea and from a microbial mat which was dominated by diatoms (hereafter DMat), percolation was not possible and thus SRR were determined using the whole core injection method (Fossing and Jørgensen, 1989).  $25 \mu\text{l}$  of  $50 \text{ kBq } \mu\text{l}^{-1}$  of  $\text{S}^{35}\text{O}_4^{2-}$  solution was injected in 1 cm intervals into the cores. Afterwards the cores were incubated, sliced and incubation was terminated as described above.

A third experiment was conducted in sediment slurries from the top 3-4 cm surface sediment of WhMat1. The sediment was sampled with cores and stored for 1 week at  $4 \text{ C}^\circ$  before the measurements were performed. Sediment was homogenized under  $\text{N}_2$  atmosphere. Spring water ( $30 \text{ g l}^{-1}$  TDS) was mixed with DSW ( $338 \text{ g l}^{-1}$  TDS) to obtain a salinity gradient ranging from pure spring water to 100% DSW. Then the water mixtures were amended with lactate, acetate, propionate and butyrate each to a final concentration

---

of 0.1 mM. 4 ml of sediment and 16 ml of Spring-Dead Sea water mixture at the defined salinity were then added to serum bottles, perched with N<sub>2</sub> gas and vigorously shaken. Before adding 20 µl of 50 kBq µl<sup>-1</sup> of S<sup>35</sup>O<sub>4</sub><sup>2-</sup> the vials were incubated for 3 h at 27 C° to enable salinity adaptation. Incubation time ranged from 12-36 h. The incubations were terminated by injection of 5 ml 20% ZnAC and SRR were determined as described above.

### **Sediment porosity and porewater**

Efficient porosity of the sediment for calculation of SRR was determined by the weight loss of sediment after drying at 70 °C for 48 h. Porewater was collected from each site using core sections of 1 cm intervals and centrifuging each section 15 min at 10 000 rpm. Sulfate concentration in the pore water was determined in diluted samples using an ion chromatograph (761 Compact IC, Metrohm, Filderstadt, Germany). Salinity determination was done by gravimetric density measurement and calculation assuming linear mixing of pure groundwater from the springs and DSW.

## **Results**

### **Sulfur isotopes and physico-chemical parameters**

The physico-chemical parameters of the spring waters sampled in the northern and southern system, respectively, are summarized in Table 1. Compared to the Dead Sea, the springs contain up to 5 times more sulfate and are all significantly less saline, significantly sulfidic, and have a higher pH, compared to DSW. Total Dissolved organic carbon (DOC) and total dissolved nitrogen (TDN) are highest in the Dead Sea whereas inorganic carbon (DIC) is higher in the groundwaters. The DOC/TDN ratio is <3, indicating that most of the TDN exists in inorganic form fitting well to the high obtained ammonia values. δ<sup>34</sup>S signatures of sulfate in the spring water range from 19 to 20‰ whereas δ<sup>34</sup>S signatures

---

of sulfide range from -19 to -30 ‰ (Fig. 1). The overall fractionation  $\Delta^{34}\text{S}$  ( $\delta^{34}_{\text{sulfate}} - \delta^{34}_{\text{sulfide}}$ ) between sulfide and sulfate range from 39 to 50 ‰ in the various springs.

**Table 1** Physico-chemical properties of the Dead Sea and pure spring water

System	Sample	Temp [C°]	pH	Eh [mV]	TDS [g l <sup>-1</sup> ]	SO <sub>4</sub> <sup>2-</sup> [mM]	H <sub>2</sub> S <sub>tot</sub> [μM]	DIC [mM]	DOC [mM]	TDN [mM]	DOC/ TDN	NH <sub>4</sub> [mM]
	Dead Sea*	27,5	6,16	90	338,0	1,39	0	1,05	1,36	0,88	1,5	0,43
North springs	Spring 01	24	7,16	-180	12,8	3,50	NA	3,36	NA	NA	NA	NA
	Spring 07	29,3	7,08	-80	24,8	10,71	57,0	4,2	0,56	0,1	5,3	NA
South springs	WhMat1	28,2	6,91	NA	30,9	2,68	54,0	3,13	0,34	0,12	2,7	0,16
	DMat	29,1	6,93	NA	58,8	2,13	NA	5,56	0,33	0,12	2,6	0,68
	WhMat2	27,7	6,70	-130	50,2	3,04	63,0	2,77	0,43	0,2	2,1	0,16
	RockMat	28,7	6,70	-147	54,9	3,39	80,0	3,05	0,48	0,23	2,1	0,11

\*Data taken from Ionescu et al. 2012

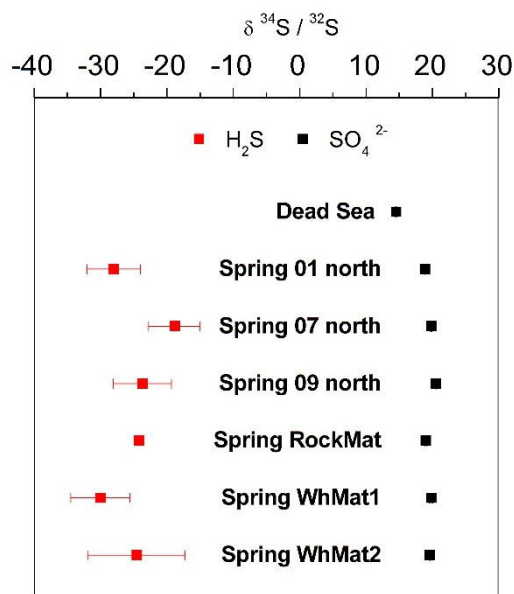


**Figure 1** Isotopic composition of Sulfide and Sulfate obtained from the Dead Sea and pure spring water samples



## Microbial mats and their respective sulfur metabolizing Bacterial community

Our sampling and measurements were focused on 4 microbial mats, all of which were exposed to spring water seepage. Two of the microbial mats spread over several square meters at spots where groundwater slowly seeps out of the sediment. At the first site, the sediment was covered by a 1-2 mm thick white microbial mat (WhMat1, Fig.2A), whereas the sediment at the second site was covered by a brownish mat, mainly formed by diatoms (hereafter DMat, Fig. 2B). A microbial mat similar to WhMat1 was found on a vertical cliff (WhMat2, Fig 1C). A fourth type of microbial mat was found on cobble located inside a fast flowing jet of 1-2 meter in diameter (RockMat, Fig.2 D).

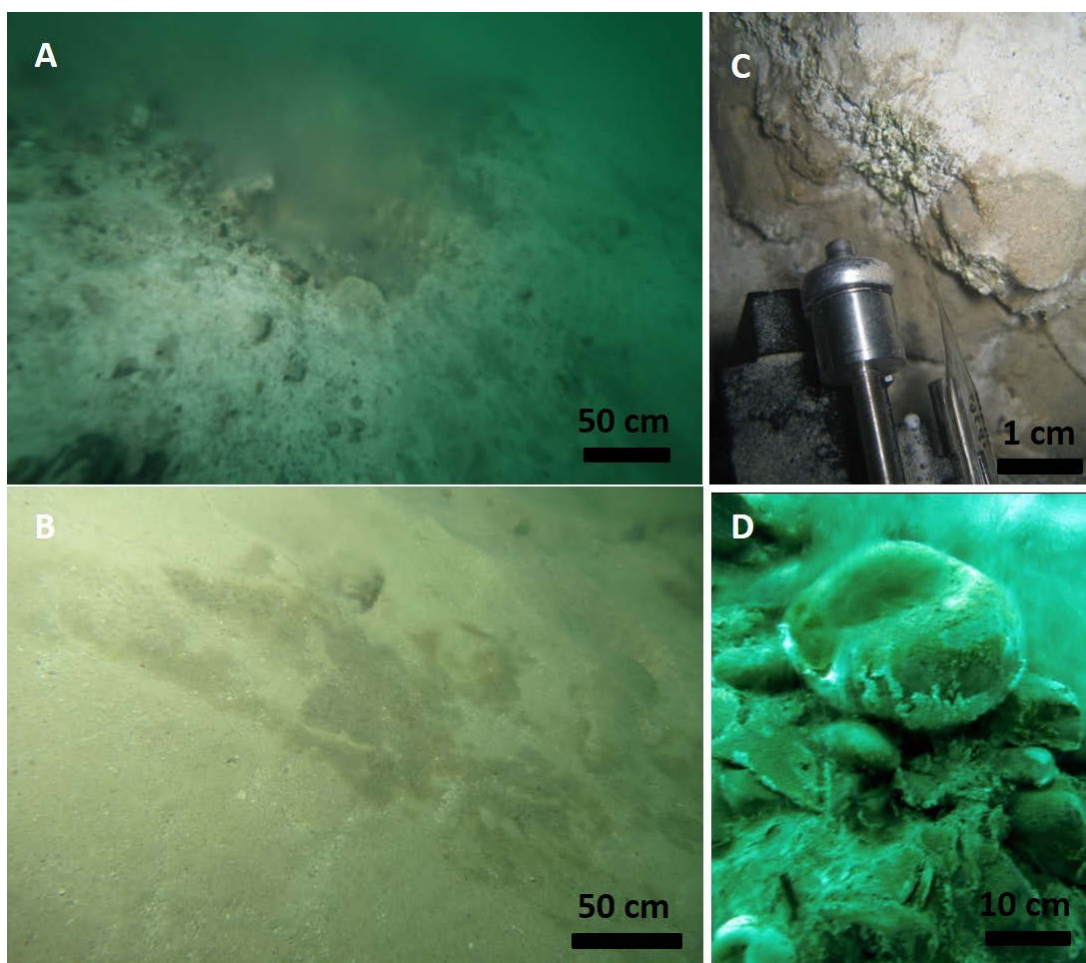


**Figure 2** Images showing the different microbial mats found in the underwater springs. WhMat1 (A) and Dmat (B) are covering several square meters of sediment, (C) WhMat2 and (D) Mat4.

Sequences matching the 16S rRNA gene of known sulfate reducing bacteria (SRB) and sulfide oxidizing bacteria (SOB) were detected in all microbial mats as well as in the Dead Sea (Fig. 3). Generally, sequence abundance of SRB and SOB was higher in the microbial mats as compared to the Dead Sea indicating that the conditions for both groups are more favorable in the spring environments. Comparing the springs with each other reveal that the highest SOB and SRB richness can be found in RockMat and WhMat1, which were clearly dominated by sequences related to SOB. Specifically, in WhMat1 the dominating SOB taxa are closely related to the *Sulfurimonas* and *Sulfurovum* genera, which are also found in RockMat, although sequences related to the green sulfur bacterium *Prosthecochloris* are most abundant in the latter. *Thiobacillus* like sequences represent the main SOB in both DMat and WhMat2 with *Acidithiobacillus* being additionally detected in the former. Among the SRB, WhMat1 and RockMat are dominated by a single genera MSBL7, which belongs to the *Desulfobulbaceae* family and has no cultured representatives. In contrast, sequence abundance and taxa numbers of SOB and SRB are remarkably reduced in DMat and WhMat2 where the sole sequences related to SRB cluster to the *Desufosporosinus*. The only SRB detected in the Dead Sea reference site clusters to the *Desulfobulbus* genus.

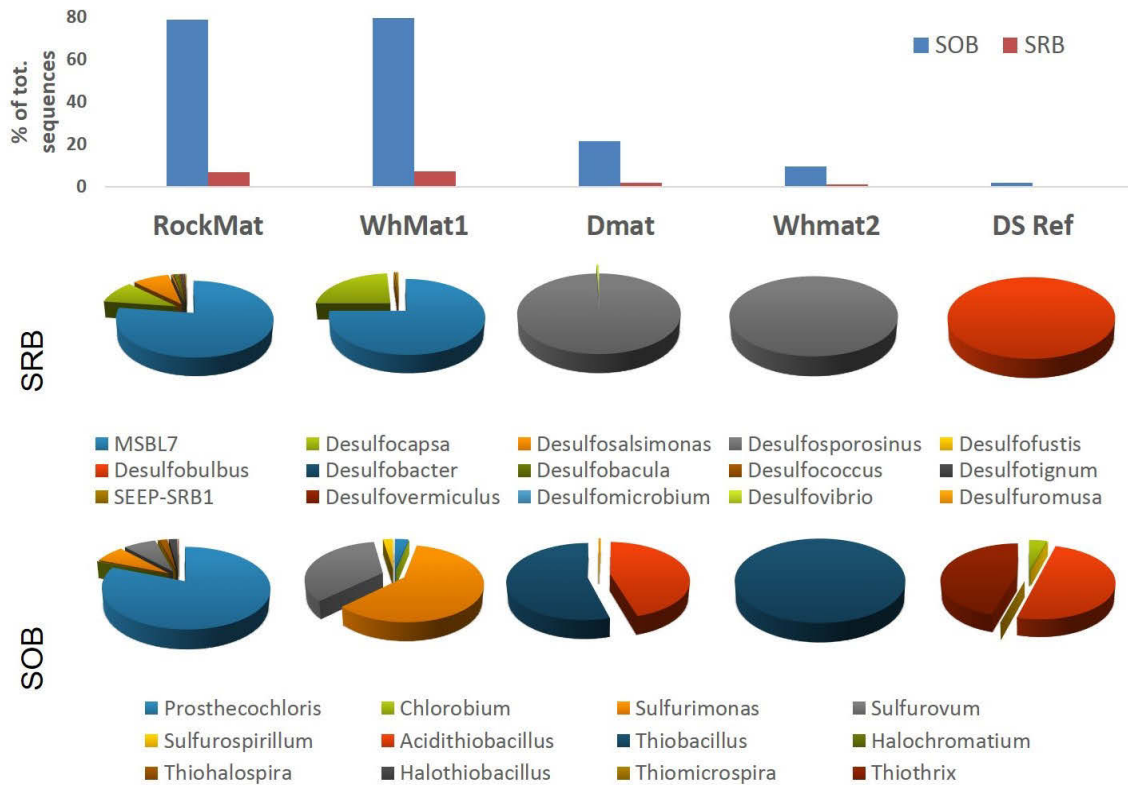


**Figure 3** Graphical representation of the sequence frequency of sulfate reducing (SRB) and sulfur oxidizing bacteria (SOB) in the studied microbial mats and the Dead Sea (DS Ref) sediment (upper panel). The lower panels show the relative sequence frequency of detected genera in each sample.

### ***In situ* microsensor measurements**

*In situ* microsensor measurements performed in WhMat1 (Fig. 4A and B) and at a reference site not exposed to spring water seepage (Figs. 4C and 4D) reveal clear differences. The impact of the spring water seepage at WhMat1 can be clearly seen by the sharp decrease in the signal of the high range salinity sensor (Fig. 4B). The short increase of sensor signal before its decrease is a result of the sensor response when exposed to pure DSW: with increasing salinity, it shows an increasing signal starting from fresh water to 75% DSW and decreases at higher TDS again. According to this, salinity starts to decrease already 4

mm above the microbial mat, which is also seen in the low range salinity profile when the sensor reached its maximum of detectable salinity (Fig 4 B). Salinity inside the microbial mat is constant at around  $60 \text{ g l}^{-1}$  and decrease inside the sediment to  $40 \text{ l}^{-1}$ , which is in agreement with the value measured in the pure spring water from this site ( $30 \text{ g l}^{-1}$ , Tab.1). The data from the reference site shows that the sediment does not interfere with the readings of the salinity sensor (Fig. 4C).

In WhMat1 pH increased from 6.1 to 6.6 and redox potential decreased steeply at the surface of the microbial mat. Oxygen concentrations followed the same shape as redox potential and decreased from  $49 \text{ }\mu\text{M}$  (Dead Sea water air saturation) to complete depletion at a depth of 2 mm inside the sediment (Fig.4 A). Sulfide was consumed in the 2 mm oxic zone indicating direct sulfide oxidation with oxygen as electron acceptor. Measured concentrations were compared to profiles calculated using a numerical model and a porewater flow out of the sediment of  $0.1 \text{ }\mu\text{m s}^{-1}$ . The complete oxidation of sulfide to sulfate ( $\text{H}_2\text{S} + 2 \text{ O}_2 \rightarrow \text{SO}_4^{2-} + 2 \text{ H}^+$ ) was found to have the best fit to the measured data (Fig. S1A). Total fluxes of oxygen and sulfide calculated considering both diffusion and advection, were  $12.12$  and  $6.06 \text{ mmol m}^{-2} \text{ d}^{-1}$ , respectively. When using alternative stoichiometry, i.e. the oxidation of sulfide to elemental sulfur ( $2 \text{ H}_2\text{S} + \text{O}_2 \rightarrow 2 \text{ S} + 2 \text{ H}_2\text{O}$ ), the modeled and measured  $\text{O}_2$  profiles matched if a porewater flow of  $20 \text{ }\mu\text{m s}^{-1}$  was used, however, the modeled  $\text{H}_2\text{S}$  concentrations significantly deviated from the measured values (Fig. S1B).

In WhMat2 oxygen got depleted within the first 0.2 mm of the mat (Fig. 5). Here, the overlapping  $\text{H}_2\text{S}$  and oxygen profile also indicates that sulfide was oxidized with oxygen, however since salinity and pH were not measured in this mat (due to technical limitations) we do not provide any flux calculations.

In contrast to WhMat1 and WhMat2, oxygen at the reference site penetrated around 1 cm into the sediment. Diffusive oxygen uptake was estimated to be  $0.46 \text{ mmol m}^{-2} \text{ d}^{-1}$  and thus 36 times lower than the oxygen consumption measured in the WhMat1. Sulfide was not detectable and pH was constant at 6.

---

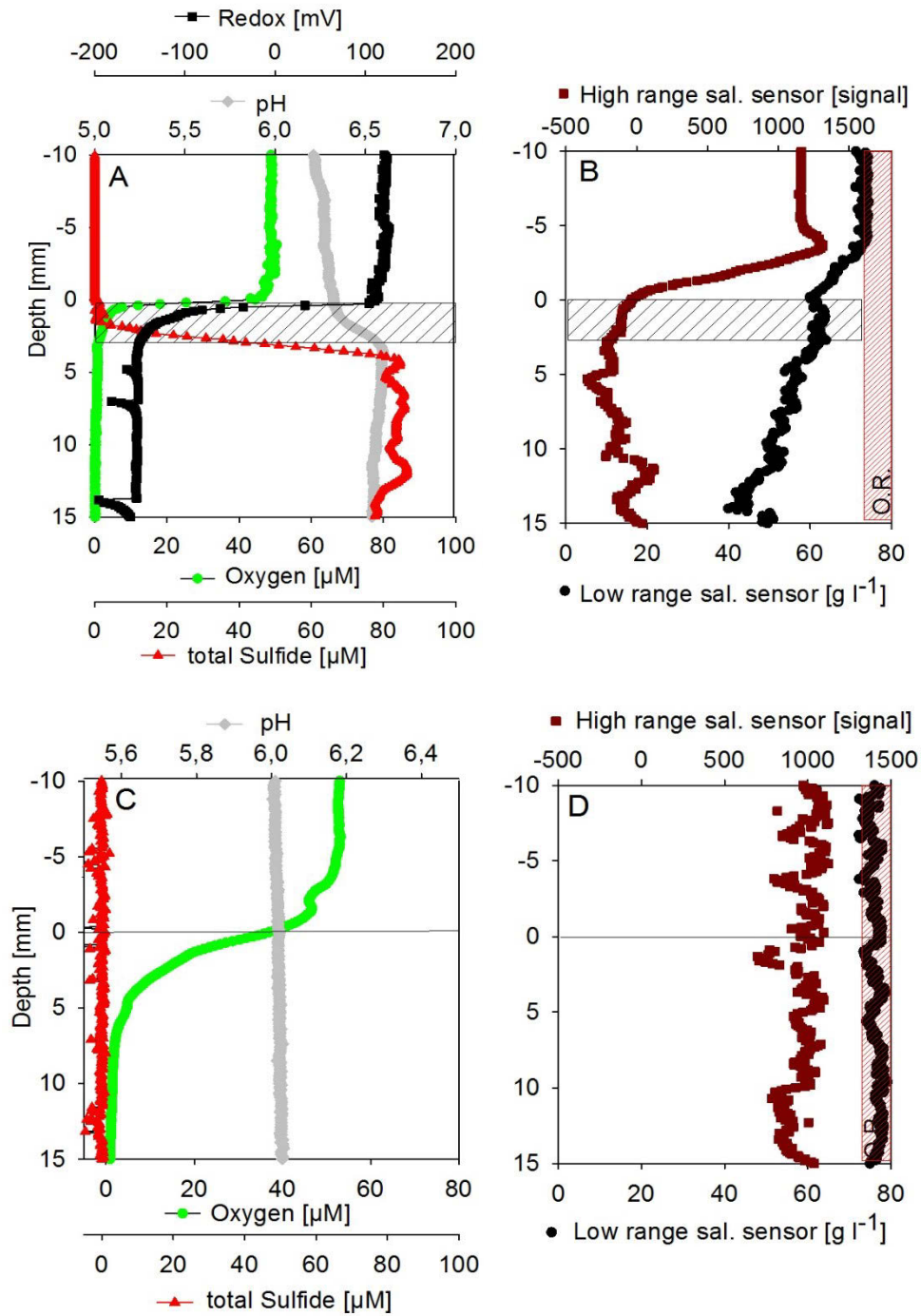


**Figure 4** Microsensor profiles measured *in situ* in the WhMat1 microbial mat (A and B) and the Dead Sea reference site (C and D). Shaded area in A and B corresponds to the location of the microbial mat whereas the line in C and D indicates the sediment surface. The low range salinity sensor is only able to measure until 70  $\text{g l}^{-1}$ , beyond this salinity it is out of range (O.R.).

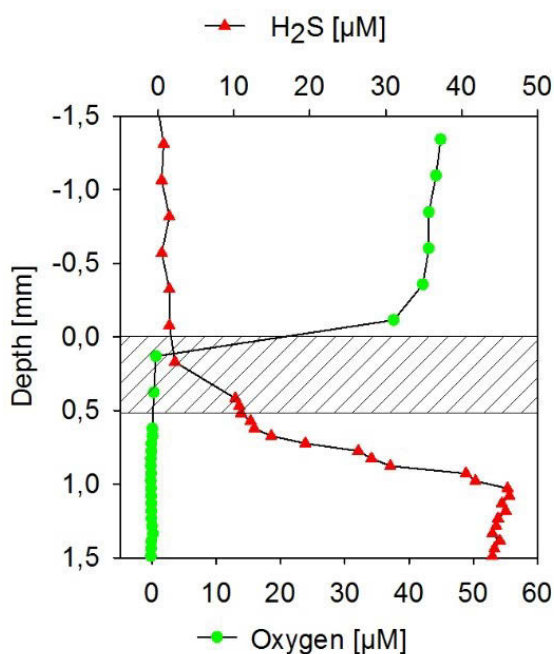


**Figure 5** H<sub>2</sub>S and oxygen microsensor profiles measured *in situ* in the WhMat2 microbial mat located vertically on a cliff where spring water flow passed parallel. Shaded area indicates position of the biofilm.

### Sulfate reduction activity

Sulfate reduction rates (SRR) in the cores collected from WhMat1 were extremely low at both 90 and 276 g l<sup>-1</sup> TDS and ranged from 0.02 to 1.21 and 0.001 to 1.06 nmol cm<sup>-3</sup> d<sup>-1</sup>, respectively (Fig. 6). In the core collected from DMat, the salinity was constant throughout the core at 186 g l<sup>-1</sup> as determined after the incubation. SRR in DMat was slightly higher than in WhMat1 cores and ranged from 0.006 to 2.8 nmol cm<sup>-3</sup> d<sup>-1</sup>. Highest SRR rates of up to 10.1 nmol cm<sup>-3</sup> d<sup>-1</sup> were detected in the Dead Sea reference site. Although care was taken to obtain replicate cores close to each other, no clear pattern SRR with depth could be observed indicating an extremely heterogeneous spatial distribution of sulfate reducing microorganisms in both the Dead Sea and spring water sediments. Cumulative, depth-integrated rates (0 to 10 cm) revealed no clear differences in the total SRA between high and low salinity in WhMat1 sediment (Fig. 6). Nevertheless, the highest depth integrated rates of 35.1 μmol m<sup>2</sup> d<sup>-1</sup> were 3 orders of magnitude lower than the total sulfide flux of 6.06 mmol m<sup>2</sup> d<sup>-1</sup> determined by microsensors from the same site.

The effect of salinity on SRA was further tested at a higher resolution in a slurry experiment performed with sediment collected from the upper 2-3 cm of WhMat1 (Fig. 7). To enhance SRA, lactate, acetate, propionate and butyrate (0.1 mM final concentration of each) were added to the slurries. Generally, the rates were in the lower range of those determined in the core incubations from this site, with a maximum of  $0.05 \text{ nmol cm}^{-3} \text{ d}^{-1}$ . Replicate incubations showed a similar pattern at low and intermediate salinities. Among the different salinities tested, the highest SRA were observed in samples incubated at 90 to 120  $\text{g l}^{-1}$  TDS, however in two incubations of 276 and 300  $\text{g l}^{-1}$  TDS, respectively, elevated activity was detected as well.

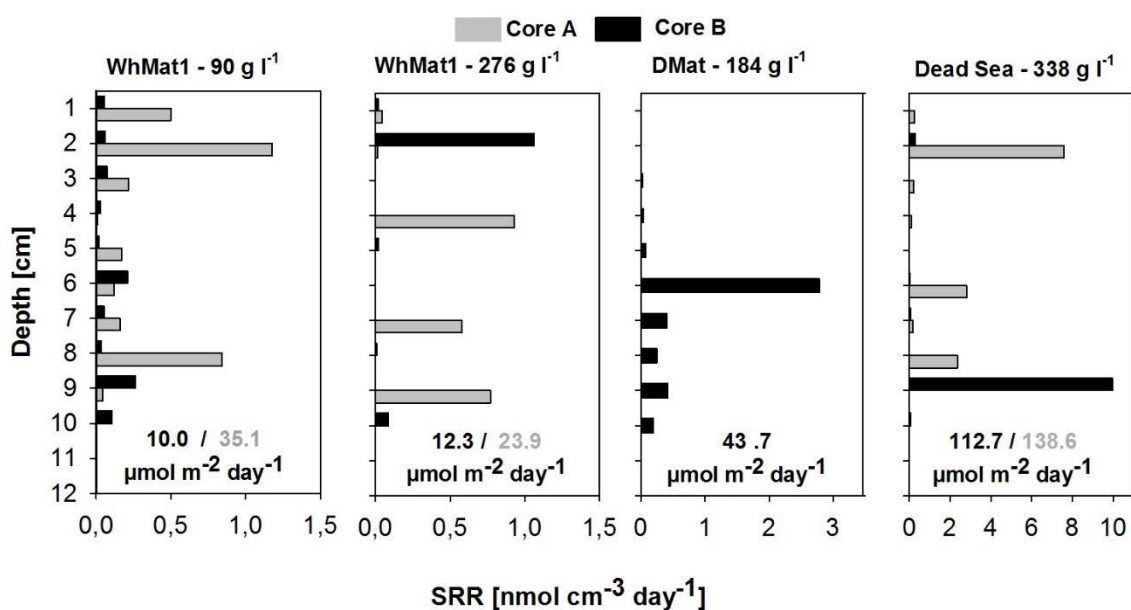


**Figure 6** Sulfate reduction rates (SRR) determined in cores from the WhMat1 site by percolation with low saline water (A) and high saline water (B). SRR in the Dmat site (C) and Dead Sea reference site (D) were determined by the injection technique. Gray and Black bars corresponds to the values obtained in the replicate cores from each site with the depth integrated rates shown in the respective color at the bottom of each graph.

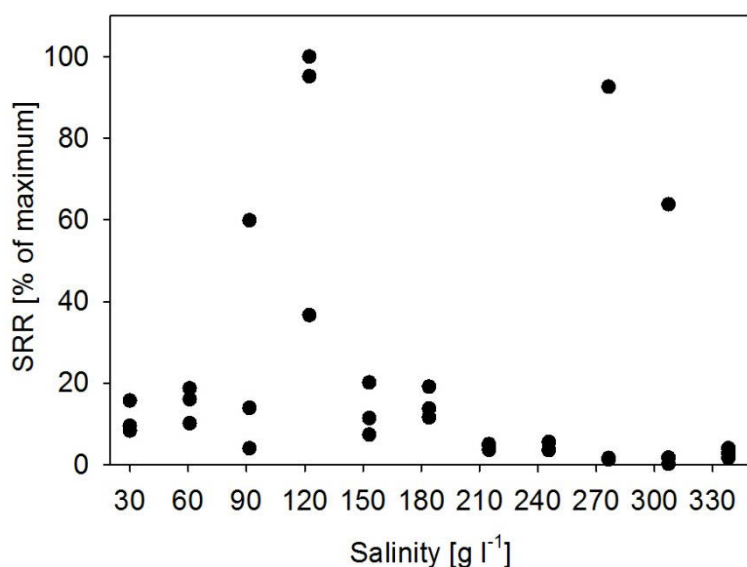


**Figure 7** Relative sulfate reduction rates determined in a slurry experiment in triplicates over a salinity range from pure spring water (30 g l<sup>-1</sup> TDS) to pure Dead Sea water (340 g l<sup>-1</sup> TDS). Slurries were amended with lactate, acetate, propionate and butyrate, 1 mM each.

## DOM analysis

The compounds identified by FT-ICR-MS were divided in categories according to where they were found (Fig S2). Unique compounds are those which were found only in the springs (1806), only in the aquifers (238) or only in the Dead Sea (89). Compounds identified in the three data sets (5711) are considered to be refractory, as they seem to be resistant to microbial degradation. 2575 compounds from the aquifers are also found in springs. 1563 compounds were originated in the springs and are also present in the Dead Sea.



## Discussion

Our results showed that the sulfide provided by the springs is of biological origin. This can be concluded from the high fractionations between coexisting sulfide and sulfate in the spring waters where  $\Delta^{34}\text{S}$  ( $\delta^{34}_{\text{sulfate}} - \delta^{34}_{\text{sulfide}}$ ) ranged from 39 to 50 ‰. Such high fractionations (and up to about 70 ‰ in other cases) usually only occur during bacterial sulfate reduction (Brunner & Bernasconi 2005; Canfield et al. 2010; Sim et al. 2011). Thermochemical sulfate reduction usually does not lead to high fractionations (Machel et al. 1995). Biological Sulfate reduction is further supported by the presence of organic matter alongside sulfate, in the spring waters (Table 1). The increased DIC concentrations as well as the high concentrations of ammonia in the spring waters (Table 1) also point to bacterial degradation of organic matter as was previously concluded (Ionescu et al., 2012). Biological sulfate reduction also occurs in the subsurface flow path of (thermal) springs elsewhere at the Dead Sea (Gavrieli et al., 2001). However, in these springs, isotope fractionation between sulfide and sulfate was only ~30‰ (Gavrieli et al. 2001, and references therein), whereas we measured up to 50‰ in the springs investigated here. The magnitude of sulfur isotope fractionations was suggested to be depended on microbial metabolism and carbon sources (Detmers et al., 2001; Sim et al., 2011), rate of sulfate reduction (Habicht and Canfield, 2001), temperature (Brüchert et al., 2001), amount of available sulfate (Habicht et al., 2002), as well as repeated cycles of sulfide oxidation followed by disproportionation (Canfield & Thamdrup 1994; Canfield et al. 1998). We believe the latter is the main cause for the high fractionation in the spring waters, given the abundance of SOB sequences in the water (Ionescu et al., 2012). While future measurements are needed to show the activity of SOB in the spring water, our results strongly support the activity of sulfate reducing microorganisms along the subsurface flow path of the springs through the Quaternary sediment body.

The SRR measurements conducted in this study (Fig. 6) indicated that the SRB community detected by 16S rRNA analysis (Fig. 3) is indeed active, both in the spring sediments and the Dead Sea. The SRR in the Dead Sea was with up to 10.1 nmol cm<sup>-3</sup> d<sup>-1</sup> in the lower range of those mentioned by Oren (1988) in the Quaternary Dead Sea sediment body of the

---

lake. Thus although no SRB have been isolated so far from the Dead Sea (Oren, 2010), our results confirm the existence of an active sulfate reducing community being adapted to the harsh conditions in the lake. Members of the *Desulfobulbus* genus were the only sequences detected in the Dead Sea sediment, which could be associated with known SRB (Fig. 3). Although members of the *Desulfobulbaceae* family are generally not halophilic (Kuever et al. 2005), sequences of this family were found on the floor of the extreme  $Mg^{2+}$  rich hypersaline Bannock Basin, Mediterranean Sea (Daffonchio et al. 2006). They were also detected in extremely hypersaline evaporation pans in South Africa (Roychoudhury et al. 2013). Furthermore, the *Desulfobulbaceae* family consists mostly of incomplete oxidizers (Kuever et al. 2005), which are generally observed to be more halotolerant than complete oxidizers (Oren 1999, 2011). Therefore, extreme halophilic members of the *Desulfobulbus* genus could indeed be responsible for the activity observed in the Dead Sea. However, the SRR in the Dead Sea were very low as compared to other extremely hypersaline environments such as lake Tanatar in the Kulunda Steppe ( $<475 \text{ g l}^{-1}$  TDS) where SRR of  $12\text{-}423 \text{ nmol cm}^{-3} \text{ d}^{-1}$  were measured (Foti et al. 2007). High SRR were also measured in a saltern pan systems in South Africa ( $422 \text{ g kg}^{-1}$  TDS,  $27\text{-}3,685 \text{ nmol cm}^{-3} \text{ d}^{-1}$ ; Porter et al. 2007). Thus assuming that the Dead Sea SRB are adapted to the unusual salt composition of the lake, the high salinity in the Dead Sea of  $340 \text{ g l}^{-1}$  TDS ( $274 \text{ g kg}^{-1}$  TDS) is unlikely to limit SRR. The low sulfate concentrations in the Dead Sea (above 1 mM, Table 1) should also not limit SRR (Roychoudhury et al., 1998). However, it is well known that organic matter (OM) availability and quality, strongly affects SRR in marine and hypersaline environments (Schubert et al. 2000; Niggemann et al. 2007; Glombitza et al. 2013). Therefore, the low SRR measured in the Dead Sea sediment could be a consequence of the general lack of primary production and thus low input of fresh organic carbon to the sediment. Extensive primary production by the algae *Dunaliella* was only observed twice in recent history, in 1980 and 1992 (Oren, 2010). The low carbon input from the water column to the sediment is further supported by the low oxygen consumption rates of  $0.46 \text{ mmol m}^{-2} \text{ d}^{-1}$  measured in the reference site. Such rates are comparable to deep sea environments where carbon flux to the sediment is low (Glud et al., 1994).

---

Interestingly, SRR were even lower in the spring sediment than in the Dead Sea sediment (Fig. 6). This was unexpected since the spring water locally reduces the extreme salinity of the Dead Sea (Fig. 4B; Häusler et al. 2013), which appears to allow for the proliferation of more taxa of SRB, especially seen in WhMat1 and RockMat (Fig. 3). Also, in contrast to the Dead Sea, SRR in the spring's sediment are most likely not limited by OM supply. Part of the OM delivered by the springs originates from the aquifer, or from the underwater flow path. Most of it cannot be traced back in the Dead Sea water column, suggesting that this OM is bioavailable and gets rapidly consumed either in the spring sediments or in the Dead Sea, very close to the sediment (Fig. S2). Furthermore, we were not able to enhance SRR by the addition of known substrates for SRBs (lactate, acetate, propionate and butyrate). We therefore propose that extreme spatio-temporal salinity fluctuations in the spring sediments can explain these low SRR. Such salinity fluctuations are indicated by measurements of variable flow in the spring system (Häusler et al., 2014), and are further supported by salinity profiles measured subsequently during several hours in the same spot of WhMat1 (Fig. S3). Due to the fluctuating spring flow, pressure induced convective circulation similar to other seeping systems (Wenzhöfer et al. 2000), or haline convection as modeled from estuarine environments (Webster et al., 1996) are also likely to occur, leading to invading of DSW into the sediment. This will lead to extreme spatio-temporal salinity fluctuations in the system allowing for the development of micro niches of different salinity in the spring sediment, which can be occupied by SRB possessing different salinity optima. Indeed, the SRB community in WhMat1 sediment appears to harbor two subpopulations with a low and high salinity optimum of 90-120 g l<sup>-1</sup> and 280-300 g l<sup>-1</sup> TDS, respectively (Fig. 7). A heterogeneous distribution of these SRB groups may be the reason for the heterogeneous SRR detected in the cores (Fig. 6). However, despite the availability of multiple environmental niches, continuous salinity fluctuations will require constant metabolic adjustment of the cells to the prevailing conditions. For example, upon salinity increase, the sulfate reducer *Desulfovibrio vulgaris* shows an up-regulation of the ATPase gene at the transcript and protein level (Mukhopadhyay et al., 2006), indicating a general higher energy demand in salt stressed SRB. The increase in energy demand is likely a consequence of cellular adjustments including the synthesis or uptake of organic solutes to

---

achieve osmotic equilibrium with the ambient medium, cell membrane changes as well as up-regulation of ion efflux systems (Mukhopadhyay et al., 2006). Constant salinity fluctuations thus dramatically increase the overall maintenance energy of the SRB population in the spring system, resulting in energy shortage for cell division and may limit the population size of SRB since this physiological group only obtains little energy from their metabolism (Oren 1999; 2011). An overall low population size may thus be responsible for the low SRR observed in the surface sediment of the springs (Fig. 6), and may also explain the extreme heterogeneity in the slurry experiment (Fig. 7).

The SOB community is independent of the local SRR in the spring surface sediment and relies of sulfide supplied by the spring water. This can be concluded from the low maximal depth integrated SRA of  $35.1 \mu\text{mol m}^2 \text{d}^{-1}$  which was three orders of magnitude lower than the sulfide flux of  $6.06 \text{ mmol m}^{-2} \text{d}^{-1}$  measured in the same area. The sulfide supplied by the spring water is aerobically oxidized by the SOB community at the interface between spring- and Dead Sea water (Figs. 4 and 5), where oxygen is present and an overall reduced salinity allows for their development. Since aerobic sulfide oxidation delivers far more energy than sulfate reduction (Oren 1999; 2011), the SOB community probably has sufficient energy to survive the salinity fluctuations in the spring system, and thus allows for the buildup of the high biomass. We suggest that the main driving factor for the development of the high biomass of SOB in the spring system of the Dead Sea is a local reduction in salinity and the external supply of sulfide which is aerobically consumed with oxygen supplied from the Dead Sea.

Although all springs may experience large spatio-temporal salinity fluctuations, we suggest that the observed differences between the community structures of SOB and SRB in the distinct microbial mats (Fig. 3) are likely to be a result of different mean salinities among them. On average the salinity is probably lowest around RockMat and in WhMat1 where most taxa are found, whereas salinity is on average higher in DMat and WhMat2 allowing only for the existence of specific, presumably more halotolerant SRB and SOB taxa of *Desulfosporosinus* and *Thiobacillus/Acidithiobacillus*, respectively. Percolation of the core obtained in the DMat was not possible, due to its low permeability. The lower permeability

---

leads to reduction in spring water flow velocity through the sediment, which in turn will result in higher salinities inside and above the sediment. Indeed, the pore water salinity of DMat was about 184 g l<sup>-1</sup> TDS throughout the core, much higher than the pore water salinity in WhMat1 (about 60 g l<sup>-1</sup> TDS, Fig. 4), which was dominated by SOB of the *Sulfurimonas* and *Sulfurovum* genera (Fig. 3). RockMat was located in a fast flowing stream where high spring water up-flow velocities of 5-25 cm s<sup>-1</sup> lead to an extensive salinity reduction around the rock surface (Häusler et al., 2014). The high salinity in DMat could explain the general absence of the *Sulfurimonas* and *Sulfurovum* like bacteria at this site. Isolates of the *Sulfurimonas* and *Sulfurovum* genera were shown to tolerate a maximum salinity of 60 g l<sup>-1</sup> TDS (Inagaki et al. 2003, 2004). It is therefore likely that also the SOB belonging to the *Acidithiobacillus*, *Thiobacillus* genera and the SRB belonging to the *Desulfosporosinus* genus detected solely in Dmat and WhMat2 may be more halotolerant than the SOB and SRB detected in WhMat1. Bacteria related to the genus *Acidithiobacillus* were previously enriched at 4 M NaCl from hypersaline habitats (Sorokin et al., 2006). Although species of the *Desulfosporosinus* (SRB) and *Thiobacillus* (SOB) genera are generally not halophilic (Kelly et al., 2005; Spring and Rosenzweig, 2006), our results suggests that these genera may harbor halophilic members. Thus, overall the community structure of SRB and SOB in the different microbial mats seems to be controlled by salinity which is in agreement with other studies showing a strong effect of salinity on community composition (Freitag et al., 2006; Abed et al., 2007). Differences in mean salinity are likely a result of different sediment permabilities in the distinct areas affecting spring water input and thus salinity reduction.

In conclusion we were able to demonstrate that most of the sulfide, which is aerobically consumed by sulfide oxidizing bacteria in WhMat1 and WhMat2 is produced along the subsurface flow path of the spring water and only little production occurs in the surface sediments of the springs, presumably due to extensive salinity fluctuations limiting local SRR. Thus, the main factors for the high abundance of SOB in the system are a local salinity reduction as already concluded earlier (Häusler et al., 2014), and the external supply of reduced substances from the spring water as shown here. We suggest that the reason for the different dominance of specific groups of SRB and SOB in the various

---

microbial mats is a consequence of different flow regimes of spring water in the system and thus differences in salinity. In addition, our results indicate that there is an active, extremely halophilic SRB community in the sediments of the Dead Sea, which are not affected by spring water seepage. The ability of the SRB in the Dead Sea as well as the microorganisms in the springs to tolerate continuous or temporal exposures to high concentrations of divalent cations ( $\sim 2$  M  $\text{Mg}^{2+}$  and  $0.5$  M  $\text{Ca}^{2+}$ ) warrants further investigations. More studies about the groundwater flow and the specific microenvironments are also needed to fully understand the dynamics of the system.

### **Acknowledgements**

This study was financially supported by the Max-Planck-Society and the SUMAR project (BMBF grant code: 02WM0848) as well as by the DAAD. We want to acknowledge Benjamin Brunner for the isotope analysis. We also want to thank Christian Lott from the HYDRA Institute (Elba) for his support during diving and underwater videography. Furthermore we want to thank Shiri Meshner for providing us with lab space in the Ein Gedi lab of The Dead Sea and Arava Science Center. We are also deeply grateful for field assistance by Yaniv Munwes as well as by the supply of lab equipment by Aharon Oren.

## Supplementary information

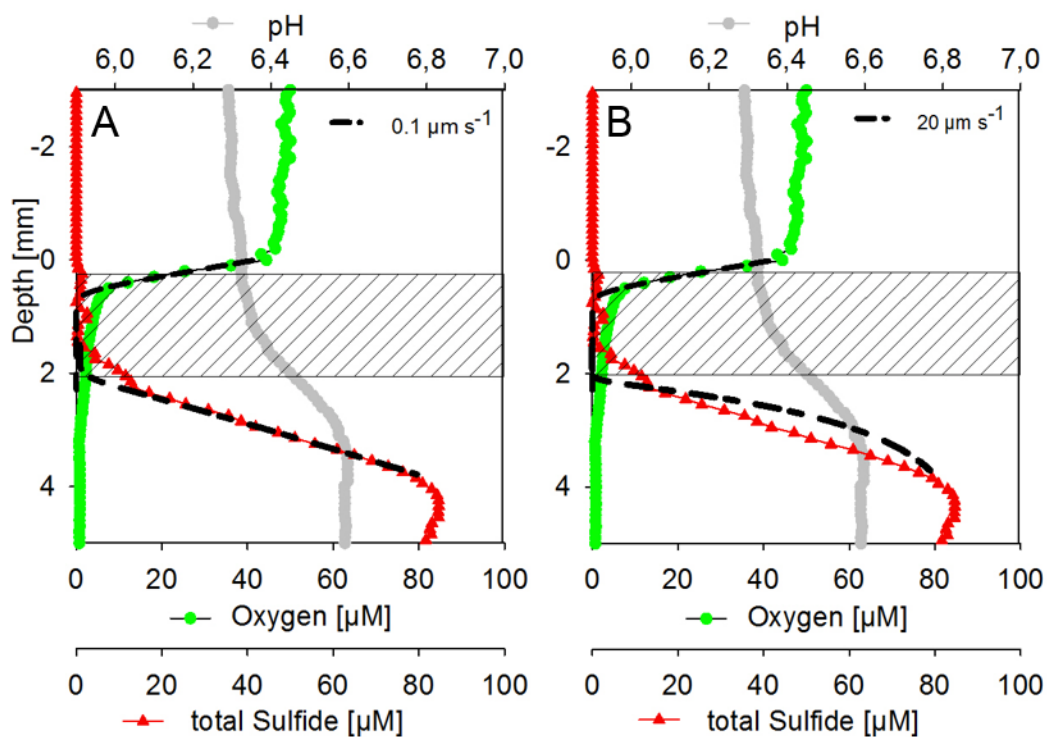


**Figure S1** Rescaled microsensors profiles from Figure 4 obtained in the WhMat1 showing the modeled (dashed line) sulfide and oxygen profiles. In (A) a  $\text{H}_2\text{S}:\text{O}_2$  stoichiometry of 1:2 (complete oxidation) with an advective up flow velocity of  $0.1 \mu\text{m s}^{-1}$  was used whereas in (B) a 2:1 ratio (incomplete oxidation) with an up flow of  $20 \mu\text{m s}^{-1}$  was used.

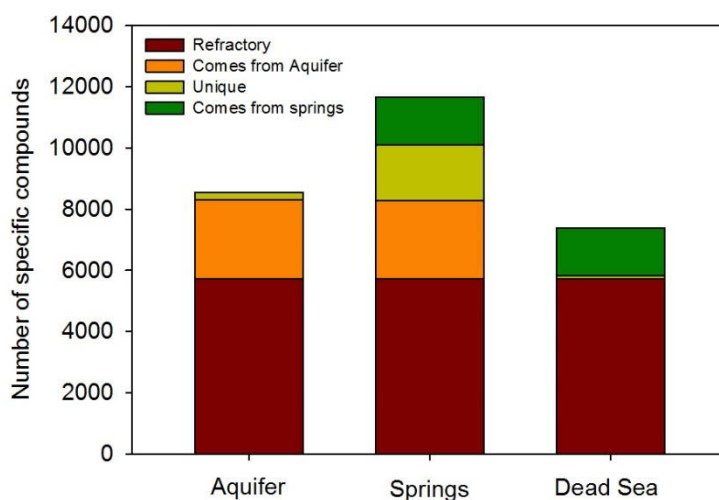


**Figure S2** Number of specific compounds detected in the Aquifer-, spring- and the Dead Sea water. A large fraction of the molecules are shared between the compartments indicating that these compounds are refractory. Part of the detected molecules originating from the aquifer and the springs are not present in the Dead Sea, implying that these compounds are bioavailable.

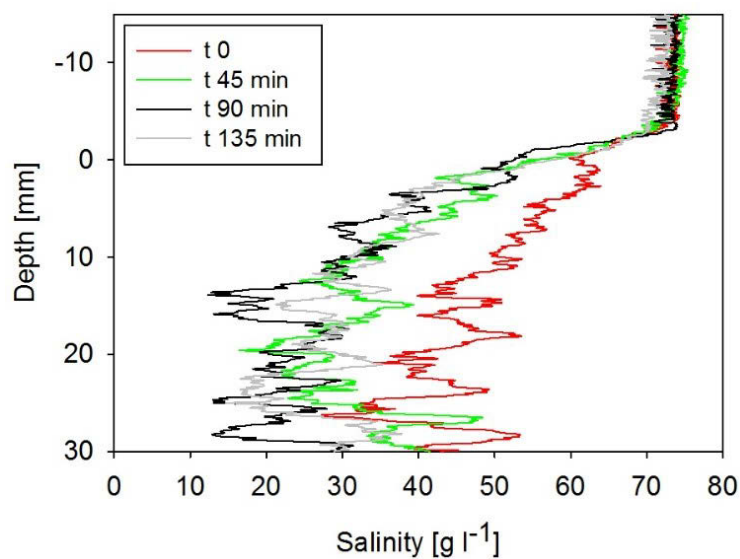


**Figure S3** Salinity sensor profiles measured subsequently with the low range salinity sensor in the WhMat1 microbial mat.



**References**

- Abed, R.M.M., Kohls, K., and De Beer, D. (2007) Effect of salinity changes on the bacterial diversity, photosynthesis and oxygen consumption of cyanobacterial mats from an intertidal flat of the Arabian Gulf. *Environ. Microbiol.* **9**: 1384–1392.
- De Beer, D., Wenzhöfer, F., Ferdelman, T.G., Boehme, S.E., Huettel, M., van Beusekom, J.E.E., et al. (2005) Transport and mineralization rates in north sea sandy intertidal sediments, Sylt-Rømø basin, Wadden sea. *Limnol. Ocean.* **50**: 113–127.
- Berner, R.A. (1980) Early diagenesis: A theoretical approach, Princeton University Press.
- Bodaker, I., Sharon, I., Suzuki, M.T., Feingersch, R., Shmoish, M., Andreishcheva, E., et al. (2010) Comparative community genomics in the Dead Sea: an increasingly extreme environment. *Isme J.* **4**: 399–407.
- Boudreau, B.P. (1996) The diffusive tortuosity of fine-grained unlithified sediments. *Geochim. Cosmochim. Acta* **60**: 3139–3142.
- Brüchert, V., Knoblauch, C., and Jørgensen, B.B. (2001) Controls on stable sulfur isotope fractionation during bacterial sulfate reduction in Arctic sediments. *Geochim. Cosmochim. Acta* **65**: 763–776.
- Brunner, B. and Bernasconi, S.M. (2005) A revised isotope fractionation model for dissimilatory sulfate reduction in sulfate reducing bacteria. *Geochim. Cosmochim. Acta* **69**: 4759–4771.
- Canfield, D.E., Farquhar, J., and Zerkle, A.L. (2010) High isotope fractionations during sulfate reduction in a low-sulfate euxinic ocean analog. *Geology* **38**: 415–418.
- Canfield, D.E. and Thamdrup, B. (1994) The production of <sup>34</sup>S-depleted sulfide during bacterial disproportionation of elemental sulfur. *Science* **266**: 1973–1975.
-

- Canfield, D.E., Thamdrup, B., and Fleischer, S. (1998) Isotope fractionation and sulfur metabolism by pure and enrichment cultures of elemental sulfur-disproportionating bacteria. *Limnol. Oceanogr.* **43**: 253–264.
- Cline, J.D. (1969) Spectrophotometric determination of hydrogen sulfide in natural waters. *Limnol. Oceanogr.* **14**: 454–458.
- Detmers, J., Brüchert, V., Habicht, K.S., and Kuever, J. (2001) Diversity of sulfur isotope fractionations by sulfate-reducing prokaryotes. *Appl. Environ. Microbiol.* **67**: 888–894.
- Dittmar, T., Koch, B., Hertkorn, N., and Kattner, G. (2008) A simple and efficient method for the solid-phase extraction of dissolved organic matter (SPE-DOM) from seawater. *Limnol. Ocean. Methods* **6**: 230–235.
- Elazari-Volcani, B. (1944) A ciliate from the Dead Sea. *Nature* **154**: 355.
- Elazari-Volcani, B. (1943a) A dimastigamoeba in the bed of the Dead Sea. *Nature* **152**: 301–302.
- Elazari-Volcani, B. (1943b) Bacteria in the bottom sediments of the Dead Sea. *Nature* **152**: 274–275.
- Fossing, H. and Jørgensen, B.B. (1989) Measurement of bacterial sulfate reduction in sediments: evaluation of a single-step chromium reduction method. *Biogeochemistry* **8**: 205–222.
- Freitag, T.E., Chang, L., and Prosser, J.I. (2006) Changes in the community structure and activity of betaproteobacterial ammonia-oxidizing sediment bacteria along a freshwater–marine gradient. *Environ. Microbiol.* **8**: 684–696.
-

- Gavrieli, I., Yechieli, Y., Halicz, L., Spiro, B., Bein, A., and Efron, D. (2001) The sulfur system in anoxic subsurface brines and its implication in brine evolutionary pathways: the Ca-chloride brines in the Dead Sea area. *Earth Planet. Sci. Lett.* **186**: 199–213.
- Glombitza, C., Stockhecke, M., Schubert, C.J., Vetter, A., and Kallmeyer, J. (2013) Sulfate reduction controlled by organic matter availability in deep sediment cores from the saline, alkaline Lake Van (Eastern Anatolia, Turkey). *Front. Microbiol.* **4**:
- Glud, R.N., Gundersen, J.K., Barker Jørgensen, B., Revsbech, N.P., and Schulz, H.D. (1994) Diffusive and total oxygen uptake of deep-sea sediments in the eastern South Atlantic Ocean: *in situ* and laboratory measurements. *Deep Sea Res. Part I Oceanogr. Res. Pap.* **41**: 1767–1788.
- Gundersen, J.K. and Jorgensen, B.B. (1990) Microstructure of diffusive boundary layers and the oxygen uptake of the sea floor. *Nature* **345**, 604 - 607
- Habicht, K.S. and Canfield, D.E. (2001) Isotope fractionation by sulfate-reducing natural populations and the isotopic composition of sulfide in marine sediments. *Geology* **29**: 555–558.
- Habicht, K.S., Gade, M., Thamdrup, B., Berg, P., and Canfield, D.E. (2002) Calibration of sulfate levels in the Archean ocean. *Science*. **298**: 2372–2374.
- Häusler, S., Noriega-Ortega, B.E., Polerecky, L., Meyer, V., de Beer, D., and Ionescu, D. (2014) Microenvironments of reduced salinity harbour biofilms in Dead Sea underwater springs. *Environ. Microbiol. Rep.* **6**: 152–158.
- Hershey, J.P., Plese, T., and Millero, F.J. (1988) The  $pK_1$  for the dissociation of  $H_2S$  in various ionic media. *Geochim. Cosmochim. Acta* **52**: 2047–2051.
- Inagaki, F., Takai, K., Kobayashi, H., Nealson, K.H., and Horikoshi, K. (2003) *Sulfurimonas autotrophica* gen. nov., sp. nov., a novel sulfur-oxidizing  $\epsilon$ -
-

proteobacterium isolated from hydrothermal sediments in the Mid-Okinawa Trough. *Int. J. Syst. Evol. Microbiol.* **53**: 1801–1805.

Inagaki, F., Takai, K., Nealson, K.H., and Horikoshi, K. (2004) *Sulfurovum lithotropicum* gen. nov., sp. nov., a novel sulfur-oxidizing chemolithoautotroph within the  $\epsilon$ -Proteobacteria isolated from Okinawa Trough hydrothermal sediments. *Int. J. Syst. Evol. Microbiol.* **54**: 1477–1482.

Ionescu, D., Siebert, C., Polerecky, L., Munwes, Y.Y., Lott, C., Haeusler, S., et al. (2012) Microbial and Chemical Characterization of Underwater Fresh Water Springs in the Dead Sea. *PLoS One* **7**: 21.

Jeroschewski, P., Steuckart, C., and Kühn, M. (1996) An amperometric microsensor for the determination of H<sub>2</sub>S in aquatic environments. *Anal. Chem.* **68**: 4351–4357.

Jørgensen, B.B. and Cohen, Y. (1977) The sulfur cycle of the benthic cyanobacterial mats. *Limnol. Ocean. States* **22**:

Jørgensen, B.B., Revsbech, N.P., Blackburn, T.H., and Cohen, Y. (1979) Diurnal cycle of oxygen and sulfide microgradients and microbial photosynthesis in a cyanobacterial mat sediment. *Appl. Environ. Microbiol.* **38**: 46–58.

Kallmeyer, J., Ferdelman, T.G., Weber, A., Fossing, H., and Jørgensen, B.B. (2004) A cold chromium distillation procedure for radiolabeled sulfide applied to sulfate reduction measurements. *Limnol. Ocean. Methods* **2**: 171–180.

Kelly, D.P., Wood, A.P., and Stackebrandt, E. (2005) *Thiobacillus Beijerinck* 1904b. In, *Bergey's Manual of Systematic Bacteriology*. Springer, New York pp. 764–769.

Kuever, J., Rainey, F.A., and Widdel, F. (2005) Family II. *Desulfobulbaceae* fam. nov. In, *Bergey's Manual of Systematic Bacteriology*, Springer, New York pp. 988-999

---

- Lane, D.J. (1991) 16S/23S rRNA sequencing. In, *Nucleic Acid Techniques in Bacterial Systematics*. John Wiley and Sons, New York, pp. 115–175
- Lensky, N.G., Dvorkin, Y., Lyakhovsky, V., Gertman, I., and Gavrieli, I. (2005) Water, salt, and energy balances of the Dead Sea. *Water Resour. Res.* **41**:
- Mukhopadhyay, A., He, Z., Alm, E.J., Arkin, A.P., Baidoo, E.E., Borglin, S.C., et al. (2006) Salt stress in *Desulfovibrio vulgaris* Hildenborough: an integrated genomics approach. *J. Bacteriol.* **188**: 4068–4078.
- Niggemann, J., Ferdelman, T.G., Lomstein, B.A., Kallmeyer, J., and Schubert, C.J. (2007) How depositional conditions control input, composition, and degradation of organic matter in sediments from the Chilean coastal upwelling region. *Geochim. Cosmochim. Acta* **71**: 1513–1527.
- Nishri, A. and Ben-Yaakov, S. (1990) Solubility of oxygen in the Dead Sea brine. *Hydrobiologia* **197**: 99–104.
- Nissenbaum, A. (1975) The microbiology and biogeochemistry of the Dead Sea. *Microb. Ecol.* **2**: 139–161.
- Oren, A. (1999) Bioenergetic aspects of halophilism. *Microbiol. Mol. Biol. Rev.* **63**: 334–348.
- Oren, A. (2013) Life in Magnesium-and Calcium-Rich Hypersaline Environments: Salt Stress by Chaotropic Ions. In, *Polyextremophiles*. Springer, pp. 215–232.
- Oren, A. (1983) Population dynamics of halobacteria in the Dead Sea water column. *Limnol. Oceanogr.* **28**: 1094–1103.
- Oren, A. (2010) The dying Dead Sea: The microbiology of an increasingly extreme environment. *Lakes Reserv. Res. Manag.* **15**: 215–222.
-

- Oren, A. (2011) Thermodynamic limits to microbial life at high salt concentrations. *Environ. Microbiol.* **13**: 1908–1923.
- Oren, A., Gurevich, P., Anati, D.A., Barkan, E., and Luz, B. (1995) A bloom of *Dunaliella parva* in the Dead Sea in 1992: biological and biogeochemical aspects. *Hydrobiologia* **297**: 173–185.
- Oren, A. and Shilo, M. (1985) Factors determining the development of algal and bacterial blooms in the Dead Sea: a study of simulation experiments in outdoor ponds. *FEMS Microbiol. Lett.* **31**: 229–237.
- Oren, A. and Shilo, M. (1982) Population dynamics of *Dunaliella parva* in the Dead Sea. *LIMNOLOGY* **27**:
- Revsbech, N.P. and Jørgensen, B.B. (1986) Microelectrodes: their use in microbial ecology. *Adv. Microb. Ecol* **9**: 293–352.
- Revsbech, N.P. and Ward, D.M. (1983) Oxygen microelectrode that is insensitive to medium chemical composition: use in an acid microbial mat dominated by *Cyanidium caldarium*. *Appl. Environ. Microbiol.* **45**: 755–759.
- Roychoudhury, A.N., Viollier, E., and Van Cappellen, P. (1998) A plug flow-through reactor for studying biogeochemical reactions in undisturbed aquatic sediments. *Appl. geochemistry* **13**: 269–280.
- Schubert, C.J., Ferdeman, T.G., and Strotmann, B. (2000) Organic matter composition and sulfate reduction rates in sediments off Chile. *Org. Geochem.* **31**: 351–361.
- Sim, M.S., Bosak, T., and Ono, S. (2011) Large sulfur isotope fractionation does not require disproportionation. *Science.* **333**: 74–77.
-

- Sorokin, D.Y., Tourova, T.P., Lysenko, A.M., and Muyzer, G. (2006) Diversity of culturable halophilic sulfur-oxidizing bacteria in hypersaline habitats. *Microbiology* **152**: 3013–3023.
- Spring, S. and Rosenzweig, F. (2006) The genera *Desulfitobacterium* and *Desulfosporosinus*: taxonomy. In, *The prokaryotes*. Springer, New York pp. 771–786.
- Steinhorn, I., Assaf, G., Gat, J.R., Nishry, A., Nissenbaum, A., Stiller, M., et al. (1979) Dead Sea - Deepening of the mixolimnion signifies the overture to overturn of the water column. *Science* **206**: 55–57.
- Weber, M., Faerber, P., Meyer, V., Lott, C., Eickert, G., Fabricius, K.E., and De Beer, D. (2007) *In situ* applications of a new diver-operated motorized microsensor profiler. *Environ. Sci. Technol.* **41**: 6210–6215.
- Webster, I.T., Norquay, S.J., Ross, F.C., and Wooding, R.A. (1996) Solute exchange by convection within estuarine sediments. *Estuar. Coast. Shelf Sci.* **42**: 171–183.
- Wenzhöfer, F. and Glud, R.N. (2002) Benthic carbon mineralization in the Atlantic: a synthesis based on *in situ* data from the last decade. *Deep Sea Res. Part I Oceanogr. Res. Pap.* **49**: 1255–1279.
- Wieland, A. and Kühl, M. (2000) Short-term temperature effects on oxygen and sulfide cycling in a hypersaline cyanobacterial mat (Solar Lake, Egypt). *Mar. Ecol. Prog. Ser.* **196**: 87–102.





# Chapter 6

## Conclusions and perspectives

### Conclusions

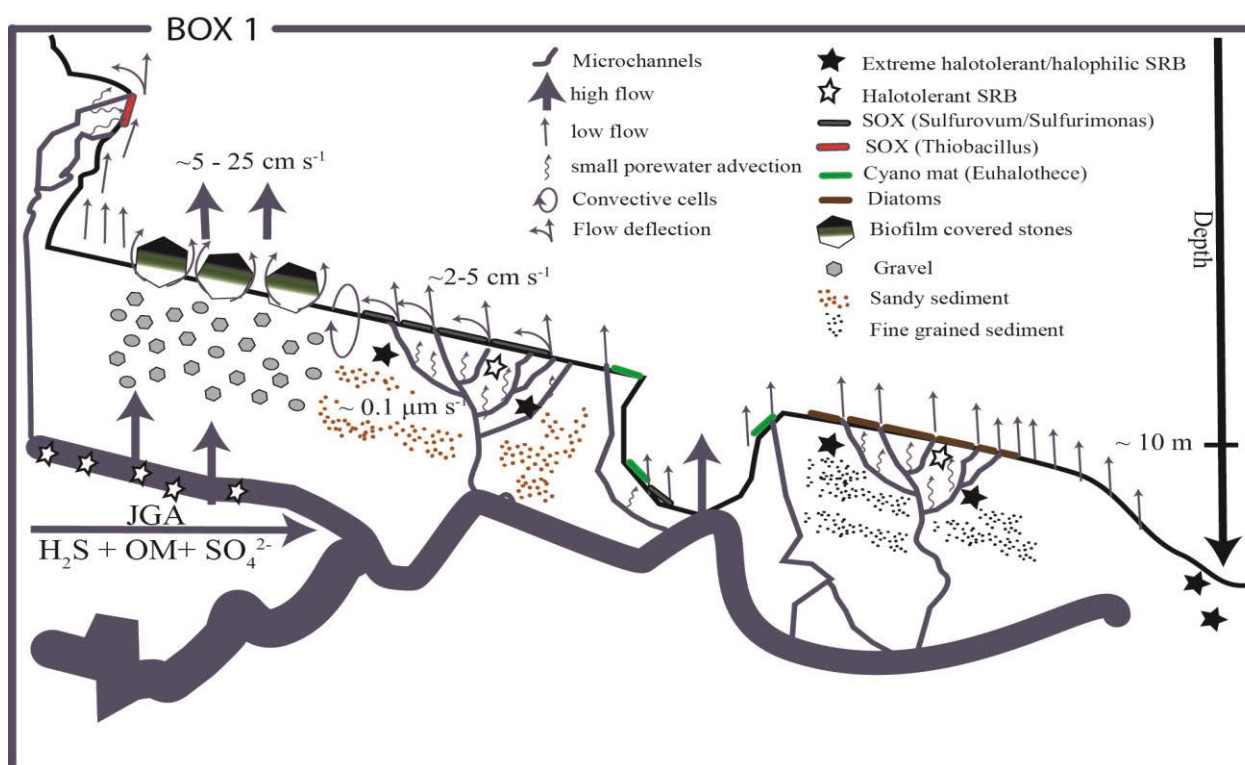
This thesis provides first insights into the microenvironments and microbial communities of a previously unknown ecosystem of subsurface fresh- and brackish water springs emerging into the Dead Sea. Although, the results presented here provide “snapshot” information about the system, a first picture emerges about the development of the microbial mats and their observed distribution in this unique ecosystem (Box 1). The main driving factor for the establishment of the abundant microbial mats observed in the system (Ionescu et al. 2012; Chapter 2) appears to be a local salinity reduction similar to that demonstrated in an artificial spring (Häusler et al. 2014; Chapter 3). *In situ* the formation of such low saline microenvironments was confirmed by microsensor measurements (Chapter 5). The reduction in salinity is sufficient to allow growth of diatoms and cyanobacteria into extensive mats (Chapter 4). The input of reduced substances produced along the flow path of the springs, additionally supports the development of a high biomass of sulfide oxidizing bacteria (Chapter 5). Despite the beneficial effects of the springs, fast and frequent fluctuations in the flow velocity of the springs create a salinity regime with high spatio-temporal complexity (Chapter 3). Accordingly, the spring microbiota is exposed to large fluctuations in salinity over the course of minutes to hours, which are by far more drastic than in other ecosystems where large salinity fluctuations normally occur over a diurnal cycle (i.e. intertidal microbial mats; Stal 2002; Abed et al. 2006). Nevertheless, as evident by the abundant microbial biomass, the organisms in the spring ecosystem are obviously capable of dealing with such fluctuations. However, the data shows that different flow regimes in distinct springs, lead to the dominance of different populations, with different salt tolerances. This is indicated by the phototroph distribution

and their different salt tolerance (chapter 4) as well as the distribution of sulfide oxidizing bacteria (chapter 5).

Life in hypersaline environments is energetically expensive (Oren, 1999, 2011). The springs in the Dead Sea provide a lower salinity environment for microorganisms, allowing moderate halophiles and less halotolerant organisms to thrive. However, the constant changes in salinity that have been documented in this thesis have their own energetic demands. Microorganisms respond to changes in salinity and thus osmotic stress with modifications of their cellular metabolism including e.g. active export of ions, cell membrane changes, accumulation or synthesis of organic osmolytes, as well as the expression of stress genes and changes in the proteome (Mukhopadhyay et al., 2006; Bhargava and Srivastava, 2013; Zhou et al., 2013). These cellular responses have a high energy demand which is apparent by the up regulation of ATPase synthesis in some bacteria (Mukhopadhyay et al., 2006) or the increase in activity of photosystem I and respiration in cyanobacteria and algae (Sudhir and Murthy, 2004). In addition to the stress of fluctuating salinity, survival in the Dead Sea springs is further hampered by the concurrent effects of frequent exposure to high concentrations of divalent cations ( $Mg^{2+}$  and  $Ca^{2+}$ ). These cations must be considered as an additional stress factor due to their chaotropic (destabilizing) potential on biological macromolecules (Hallsworth et al., 2007). This will require the constant repair of potentially damaged macromolecules or their de novo synthesis. Therefore, the overall maintenance energy needed by the organisms inhabiting the springs is presumably extremely high.

These energetic constraints may explain the measured sulfate reduction rates and the distribution of the phototrophic microorganisms. Aerobic sulfide oxidation delivers enough energy to balance the high energy demand of living in constant salinity fluctuations. Since sulfide is supplied from the springs and oxygen from the Dead Sea, sulfide oxidizers in the spring environment are not energetically limited, which explains their high biomass. In contrast, photosynthesis, which also has a high energy yield is dependent on light availability and quality, appears to be inadequate to provide enough energy for cellular adjustments deeper than 10 meters water depth. Since sulfate reduction only yields low

---



**Conceptual view of the southern part of the Darga spring system in the Dead Sea.** Spring water originating from the Judean Group Aquifer (JGA) flows via different pathways into the Dead Sea (Chapter 1). Along the flow path the chemical composition of the spring water is altered by mixing with interstitial brines in the Dead Sea Group sediment, evaporate and mineral interactions (e.g.  $\text{CaSO}_4$  dissolution) and microbial sulfate reduction (SRB) that is fueled by organic matter (OM) from the aquifer. The sulfidic spring water emerges into the Dead Sea through sediments with different permeabilities, leading to differences in up-flow velocities and thus different mean salinities between the distinct spring water outlets. This results in differences between dominating phototrophs (Diatoms and Cyanobacteria; Chapter 4) and sulfide oxidizing bacteria (SOX; Chapter 5) depending on their salinity tolerance. In areas where coarse gravel is found, high spring water velocities of  $5 - 25 \text{ cm s}^{-1}$  lead to salinity reduction around cobble stones. This allows for the development of microbial mats on the underside of cobble stones, but not at the top side, since the freshwater flow separates from the rock surface shortly after the rock equator (Chapter 3). Within sediments where the permeability is lower, spring water up-flow is only in the range of  $0.1 \mu\text{m s}^{-1}$  ( $3.1 \text{ m year}^{-1}$ ), as determined from modeling of microsensors profiles (Chapter 5). However, spring water up-flow velocities of  $2 - 5 \text{ cm s}^{-1}$  as determined 2 cm above these areas (Chapter 3) suggest the existence of micro channels similar to those found in simulated fluid venting systems (Mörz et al., 2007). Fluctuations in spring water input as indicated by fluctuating flow velocities (Chapter 3) and microsensors measurements (Chapter 4 and 5) would lead to pressure differences and thus result in convective circulations as described for other seep systems (Wenzhöfer et al., 2000). This leads to complex spatio-temporal salinity fluctuations in the system which probably results in a high energy demand overall required for cellular adjustments of the microorganisms. Furthermore, a population of extremely halotolerant/halophilic SRB also appears to thrive in the Dead Sea sediment not affected by spring water input.

energy as compared to the above mentioned processes (Oren, 1999, 2011), sulfate reducing bacteria can presumably only build up a low biomass in the spring system, which may explain the low rates measured in the spring sediments.

Although energetic considerations can explain much of the distribution of functional groups in the spring system, they fail to explain the occurrence of sulfate reduction in the hypersaline Dead Sea sediments. Due to the high energy demand of a constantly-high salinity, sulfate reducing organisms (which all appear to use the compatible solutes strategy for osmotic balance), were assumed to be absent at such extreme salinities (Oren, 1999, 2011). Therefore, it may be that the sulfate reducers in the Dead Sea use a different strategy to make a living. This can be, for instance, the energetically cheaper salt-in strategy (accumulation of KCl). Although, it was believed until recently that the salt-in strategy is confined to the family *Halobacteriaceae*, the order *Haloanaerobiales* and the genus *Salinibacter* (Oren, 2013a), the recent finding of the use of the salt-in strategy in an organism from the *Proteobacteria* domain (Deole et al., 2013), shows that this strategy may be more widespread than previously assumed. Accordingly, Oren (2013b) states that “We must rethink our concepts about the correlation between acidic proteomes, salt requirements and tolerance, accumulation of KCl, use of organic osmolytes, and microbial physiology and taxonomy”. Furthermore, recent insights into the salt adaptation mechanisms in Archaea involving the intracellular adjustments of proteomes by proteases and chaperones at low salinity (Vauclare et al., 2014), shows that we are only just beginning to understand the complexity of salt adaptation mechanisms. Thus, future research in the system is necessary to understand this interesting ecosystem in detail. This research may also provide insights into disturbance ecology and evolution of salt adaptation mechanisms.

## Perspectives and Outlook

It is known that the frequency and intensity of disturbances effects microbial communities compositionally and functionally (Miller et al., 2011; Berga et al., 2012). Thus, the underwater spring system in the Dead Sea is a suitable natural laboratory to investigate how the frequency and magnitude of salinity disturbances affects biodiversity, since such extreme disturbances appear to be one of the main characteristics of this system.

It is unclear what such frequent disturbances will have on genetic diversity. The role of disturbances as a driver of the patterns and distribution of genetic diversity is poorly understood (Banks et al., 2013 and references therein). Although the salt-in strategy is so far only known to be used by specific groups of microorganisms to obtain long term osmotic balance, cyanobacteria and algae carry out a similar strategy in the initial phase immediately after a salt shock; using ions to regain cellular volume (Erdmann and Hagemann, 2001; Hagemann, 2011). Subsequently, cyanobacteria and algae lower the concentration of ions by active ion export and long term osmotic balance is achieved by the accumulation of organic osmolytes. Since the organisms in the Dead Sea are constantly exposed to salt shocks, and thus may frequently experience high intracellular ions concentrations, it will be fascinating to investigate if these conditions eventually lead to alterations in the cellular machinery. The Dead Sea spring system is a perfect environment to study this question. For example, some microorganisms such as the diatoms or cyanobacteria may originate from surface springs that flush into the Dead Sea. The cyanobacteria can survive at least one week (and probably more) in pure Dead Sea water and are able to continue growing when the salinity is lowered again (Chapter 4). When exposed frequently to high salinities, have these organisms altered their osmoprotectant mechanisms? Conversely, the majority of the sediment microbial community originates from the Dead Sea (Chapter 2). These organisms may already be adapted to high saline conditions but how would their osmoregulation mechanisms change after colonizing the springs?

So far, the ecosystem investigated in this thesis seems to be unique. However, it is possible that similar disturbances in salinity occur in other subsurface spring water systems in hypersaline lakes. For example, within the Great Salt Lake (Utah, USA) subsurface low saline spring water discharge has recently been shown (Anderson et al., 2014). Thus, it would be intriguing to see whether small oases of microbial life are formed in other hypersaline lakes. Such systems may exhibit similar conditions as proposed for the Dead Sea spring system, namely a reduction in salinity that allows for the presence of less halotolerant taxa which are exposed to fast spatio-temporal salinity fluctuations. If life does exist in such environments, comparison of the systems may provide further insights into the evolutionary aspects mentioned above.

This thesis has focused mainly on the activity and function of photosynthetic and sulfur cycling organisms inhabiting the Dead Sea spring ecosystem (Chapter 4 and 5). However, other functional groups were also detected in the spring system by 454 pyrosequencing, including e.g. iron and nitrate reducing and ammonia and nitrite oxidizing bacteria (Chapter 2). So far, we know very little about whether these functional groups are active and what role they play in the biogeochemistry of the ecosystem. Preliminary data suggests that nitrification occurs in both the Dead Sea and the springs (Adeboyejo, 2013; Master thesis). These findings are unexpected due to the reduced pH in the Dead Sea (Beman et al. 2011, and references therein) and in light of thermodynamic considerations (Oren, 2011). Therefore, if future work can confirm that nitrification occurs, further interesting microbial adaptations to extreme environments could be identified.

If further isolation of microorganisms from the Dead Sea and spring environment is carried out, it could shed light on the specific adaptations required to survive the unusual salt composition and salinity fluctuations. Specifically the mechanisms regulating divalent cation tolerance would be of general interest since little is known about their regulating mechanisms (Oren, 2013c). If novel modes of salinity adaptation in the Dead Sea spring ecosystem can be elucidated, this could lead to the discovery of novel enzymes and subsequent development of new biotechnological applications.

## Testing hypotheses

This thesis provided first insights into the characteristics of the Dead Sea spring ecosystem. However, to confirm the conclusion that salinity fluctuations are responsible for energy limitation and to reveal the effects of constant salinity fluctuations on community structure and function, further experiments are needed. This should include a combination of *in situ* measurements as well as controlled lab experiments.

*In situ* measurements should be performed to directly target the magnitude and frequency of salinity fluctuations over time scales of weeks to months and need to be correlated with measurements of community structure, abundance and activity. Since the salinity sensor developed during the course of this work has limitations in accurately measuring in Dead Sea water (Chapter 3 and 5), we have developed a new sensor concept (in testing phase) using optical density measurements (which are unaffected by the salt composition and can be combined with oxygen optodes). This will allow direct quantification of the frequency and magnitude of salinity fluctuations, ideally in distinct springs. Simultaneously, proteomic and transcriptomic analysis should be performed on the natural communities to reveal the *in situ* response of the total spring communities to both short and long term salinity disturbances. Comparison of these meta-proteomic and genomic data to other datasets from e.g. intertidal microbial mats will allow insights into the effect of the magnitude and frequency of the salinity fluctuations on community structure and their response.

As part of the work presented here, we observed different sulfate reduction rates between the springs and the Dead Sea. To investigate how salinity and disturbance can structure the sulfate reducing community and affect rates, sulfate reduction rates should be measured along a gradient from the center of a spring to fully hypersaline Dead Sea sediments. Again this should be combined with assessments of community structure. For this, quantitative PCR may be an appropriate tool since quantification using fluorescent *in situ* hybridization was found to be challenging in the system due to extreme autofluorescence of the sediment. These sulfate reduction measurements need to be

---

correlated with lab experiments to further examine how the disturbance regime effects sulfate reduction activity, population size and community structure. This could be achieved using flow cells in which the frequency and magnitude of salinity fluctuations can be varied.

Similarly, such flow cell experiments using different light intensities and qualities could be conducted with the phototrophic organisms to confirm that their spatial distribution are a consequence of different salt tolerances and light limitations. This should be done with both diatoms and cyanobacteria separately, as well with mixed communities in competition experiments, where the physiological state and abundance of the organisms are monitored. Insights into physiological responses and abundance can be obtained non-invasively using microsensors or pulse amplitude modulated fluorometry (PAM) measurements and the hyper spectral imaging system, respectively.

In addition, to the measurements and experiments proposed, it will be valuable to obtain further enrichment cultures of different physiological groups in addition to the cyanobacterial, diatom, and green sulfur bacterial cultures obtained during this work. These cultures could be used to directly target the molecular response of distinct groups to the frequent salinity fluctuations and reveal new insights into the physiology of salt adaptation mechanisms.



## References

- Abed, R.M.M., Polerecky, L., Al Najjar, M., and De Beer, D. (2006) Effect of temperature on photosynthesis, oxygen consumption and sulfide production in an extremely hypersaline cyanobacterial mat. *Aquat. Microb. Ecol.* **44**: 21–30.
- Anderson, R.B., Naftz, D.L., Day-Lewis, F.D., Henderson, R.D., Rosenberry, D.O., Stolp, B.J., and Jewell, P. (2014) Quantity and quality of groundwater discharge in a hypersaline lake environment. *J. Hydrol.* **512**: 177–194.
- Banks, S.C., Cary, G.J., Smith, A.L., Davies, I.D., Driscoll, D.A., Gill, A.M., et al. (2013) How does ecological disturbance influence genetic diversity? *Trends Ecol. Evol.* **28**: 670–679.
- Beman, J.M., Chow, C.-E., King, A.L., Feng, Y., Fuhrman, J.A., Andersson, A., et al. (2011) Global declines in oceanic nitrification rates as a consequence of ocean acidification. *Proc. Natl. Acad. Sci.* **108**: 208–213.
- Berga, M., Székely, A.J., and Langenheder, S. (2012) Effects of disturbance intensity and frequency on bacterial community composition and function. *PLoS One* **7**: e36959.
- Bhargava, P. and Srivastava, A. (2013) Salt Toxicity and Survival Strategies of Cyanobacteria. In, *Stress Biology of Cyanobacteria*. CRC Press, pp. 171–188.
- Deole, R., Challacombe, J., Raiford, D.W., and Hoff, W.D. (2013) An extremely halophilic proteobacterium combines a highly acidic proteome with a low cytoplasmic potassium content. *J. Biol. Chem.* **288**: 581–588.
- Erdmann, N. and Hagemann, M. (2001) Salt acclimation of algae and cyanobacteria: a comparison. In, *Algal Adaptation to Environmental Stresses*. Springer, Berlin-Heidelberg, pp. 323–361.
-

- Hagemann, M. (2011) Molecular biology of cyanobacterial salt acclimation. *FEMS Microbiol. Rev.* **35**: 87–123.
- Hallsworth, J.E., Yakimov, M.M., Golyshin, P.N., Gillion, J.L.M., D’Auria, G., De Lima Alves, F., et al. (2007) Limits of life in MgCl<sub>2</sub> containing environments: chaotropicity defines the window. *Environ. Microbiol.* **9**: 801–813.
- Häusler, S., Noriega-Ortega, B.E., Polerecky, L., Meyer, V., de Beer, D., and Ionescu, D. (2014) Microenvironments of reduced salinity harbour biofilms in Dead Sea underwater springs. *Environ. Microbiol. Rep.* **6**: 152–158.
- Ionescu, D., Siebert, C., Polerecky, L., Munwes, Y.Y., Lott, C., Haeusler, S., et al. (2012) Microbial and Chemical Characterization of Underwater Fresh Water Springs in the Dead Sea. *PLoS One* **7**: 21.
- Miller, A.D., Roxburgh, S.H., and Shea, K. (2011) How frequency and intensity shape diversity–disturbance relationships. *Proc. Natl. Acad. Sci.* **108**: 5643–5648.
- Mörz, T., Karlik, E.A., Kreiter, S., and Kopf, A. (2007) An experimental setup for fluid venting in unconsolidated sediments: New insights to fluid mechanics and structures. *Sediment. Geol.* **196**: 251–267.
- Mukhopadhyay, A., He, Z., Alm, E.J., Arkin, A.P., Baidoo, E.E., Borglin, S.C., et al. (2006) Salt stress in *Desulfovibrio vulgaris* Hildenborough: an integrated genomics approach. *J. Bacteriol.* **188**: 4068–4078.
- Oren, A. (1999) Bioenergetic aspects of halophilism. *Microbiol. Mol. Biol. Rev.* **63**: 334–348.
- Oren, A. (2013a) Life at High Salt Concentrations. In, *The Prokaryotes-Prokaryotic Communities and Ecophysiology*. Springer Verlag - Berlin Heidelberg, pp. 421–440.
-

Oren, A. (2013b) Life at high salt concentrations, intracellular KCl concentrations, and acidic proteomes. *Front. Microbiol.* **4**:

Oren, A. (2013c) Life in Magnesium-and Calcium-Rich Hypersaline Environments: Salt Stress by Chaotropic Ions. In, *Polyextremophiles*. Springer, pp. 215–232.

Oren, A. (2011) Thermodynamic limits to microbial life at high salt concentrations. *Environ. Microbiol.* **13**: 1908–1923.

Stal, L.J. (2002) Cyanobacterial mats and stromatolites Springer.

Sudhir, P. and Murthy, S.D.S. (2004) Effects of salt stress on basic processes of photosynthesis. *Photosynthetica* **42**: 481–486.

Vauclare, P., Madern, D., Girard, E., Gabel, F., Zaccai, G., and Franzetti, B. (2014) New insights into microbial adaptation to extreme saline environments. In, *BIO Web of Conferences*. EDP Sciences, p. 2001.

Wenzhöfer, F., Holby, O., Glud, R.N., Nielsen, H.K., and Gundersen, J.K. (2000) In situ microsensor studies of a shallow water hydrothermal vent at Milos, Greece. *Mar. Chem.* **69**: 43–54.

Zhou, A., Baidoo, E., He, Z., Mukhopadhyay, A., Baumohl, J.K., Benke, P., et al. (2013) Characterization of NaCl tolerance in *Desulfovibrio vulgaris* Hildenborough through experimental evolution. *ISME J.* **7**: 1790–1802.



# **Oxygenic photosynthesis as a protection mechanism against iron-encrustation in environments with high Fe<sup>2+</sup> concentrations**

Ionescu Danny<sup>1</sup>, Buchmann Bettina<sup>1</sup>, Heim Christine<sup>3</sup>, Haeusler Stefan<sup>1</sup>, de Beer Dirk<sup>1</sup>,  
Polerecky Lubos<sup>1,2</sup>

<sup>1</sup>The Max Planck Institute for Marine Microbiology, Celsiusstr. 1, 28359, Bremen,  
Germany

<sup>2</sup>Department of Earth Sciences – Geochemistry, Faculty of Geosciences, Utrecht  
University Budapestlaan 4, 3584 CD, Utrecht, The Netherlands

<sup>3</sup>Geoscience Center, Georg-August University of Göttingen, Goldschmidtstr. 3, 37077  
Göttingen, Germany

**Submitted to:** The ISME Journal

**Keywords:** oxygenic phototrophs, Fe(II), iron-encrustation, banded iron formations

**Contribution:** SH contributed to microsensor measurements

## Abstract

If  $O_2$  is available at circumneutral pH,  $Fe^{2+}$  is rapidly oxidized to  $Fe^{3+}$ , which precipitates as  $FeO(OH)$ . Neutrophilic iron oxidizing bacteria have evolved mechanisms to prevent self-encrustation in iron. Hitherto, no mechanism has been proposed for cyanobacteria from  $Fe^{2+}$  rich environments; these produce  $O_2$  but are seldom found encrusted in iron. We connected sets of illuminated reactors to two groundwater aquifers with different  $Fe^{2+}$  concentrations (0.9  $\mu M$  vs. 26  $\mu M$ ) in the Äspö Hard Rock Laboratory, Sweden. Cyanobacterial mats developed in all reactors and were phylogenetically different between the reactors. Unexpectedly, cyanobacteria growing in the  $Fe^{2+}$ -poor reactors were encrusted in iron, whereas those in the  $Fe^{2+}$ -rich reactors were not. *In situ* microsensor measurements showed that  $O_2$  concentrations and pH near the surface of the cyanobacterial biofilms from the  $Fe^{2+}$ -rich reactors were much higher than in the overlying water. This was not the case for the biofilms growing at low  $Fe^{2+}$  concentrations. Measurements with enriched cultures showed that cyanobacteria from the  $Fe^{2+}$ -rich environment increased their photosynthesis with increasing  $Fe^{2+}$  concentrations, whereas those from the low  $Fe^{2+}$  environment were inhibited at  $Fe^{2+} > 5 \mu M$ . Modeling based on *in situ*  $O_2$  and pH profiles showed that cyanobacteria from the  $Fe^{2+}$ -rich reactor were not exposed to significant  $Fe^{2+}$  concentrations. We propose that, due to limited mass transfer, high photosynthetic activity in  $Fe^{2+}$  rich environments forms a protective zone where  $Fe^{2+}$  precipitates at a non-lethal distance from the cyanobacteria. This mechanism sheds new light on the possible role of cyanobacteria in precipitation of banded iron formations.

## **Diversity of iron oxidizing and reducing bacteria in flow reactors in the Äspö Hard Rock Laboratory**

Danny Ionescu<sup>1</sup>, Christine Heim<sup>2</sup>, Lubos Polerecky<sup>1,3</sup>, Alban Ramette<sup>1</sup>, Stefan Haeusler<sup>1</sup>, Mina Bizic-Ionescu<sup>1,4</sup>, Volker Thiel<sup>2</sup>, Dirk de Beer<sup>1</sup>

<sup>1</sup>The Max Planck Institute for Marine Microbiology, Celsiusstr. 1, 28359, Bremen, Germany

<sup>2</sup>Geoscience Center, Georg-August University of Göttingen, Goldschmidtstr. 3, 37077 Göttingen, Germany

<sup>3</sup>Department of Earth Sciences – Geochemistry, Faculty of Geosciences, Utrecht University, Budapestlaan 4, 3584 CD, Utrecht, The Netherlands

<sup>4</sup>Leibniz-Institute of Freshwater Ecology and Inland Fisheries, 16775 Stechlin, Germany

**Submitted to:** Geomicrobiology Journal

**Keywords:** : iron oxidation, iron reduction, subsurface microbiology, community structure, biogeochemical cycling

**Contribution:** SH contributed to microsensor measurements as well as to Fe<sup>2+</sup> profile analysis using a combination of a modified diffusive gel system and hyperspectral imaging

## Abstract

Processes of iron mineralization are of great significance to the understanding of Early-Earth geochemistry. Of specific interest are processes at circumneutral pH, where chemical oxidation of Fe can outcompete biological oxidation. To better understand microbially-induced mineral formation and the composition of the involved microbial communities, we set up a series of flow-reactors in the Äspö Hard Rock Laboratory, a 3.6 km tunnel that runs under the Baltic Sea. Various aquifers of Fe<sup>2+</sup>-rich brackish to saline waters penetrate the tunnel through a series of fractures. The reactors were set up with different combinations of light and aeration conditions, and were connected to three aquifers of differing chemical composition and age. Using a combination of 454 pyrosequencing and Catalyzed Reporter Deposition Fluorescent *In Situ* Hybridization we analyzed the bacterial community from these reactors in two consecutive seasons half a year apart. A general decrease in diversity was observed towards the deep part of the tunnel. Multivariate modeling of the community composition and environmental parameters shows that the overall diversity of the microbial community is controlled by salinity as well as carbon and nitrogen sources. However, the composition of iron oxidizing bacteria is driven by pH, O<sub>2</sub> and the availability of Fe<sup>2+</sup>. The latter is mostly supplied by Fe<sup>3+</sup> reduction in the reactors. Thus the reactors form a self-sustained ecosystem. Several genera of known aerobic and anaerobic iron oxidizing bacteria were found. *Mariprofundus* sp. was found to be dominant in many of the samples. This is the first description from groundwater of this marine species. The microbial community in the reactors is unique in each site while that in the exposed tunnel is more homogenous. Therefore we suggest that the flow reactors are a good model system to study the non-accessible microbial communities that are likely present in cracks and crevices of the surrounding bedrock.



# **Geochemistry driven trends in microbial diversity and function across a temperature transect of a shallow water hydrothermal system off Milos (Greece)**

Solveig I. Bühring<sup>1</sup>, Jan P. Amend<sup>2</sup>, Gonzalo V. Gómez Sáez<sup>2</sup>, Stefan Häusler<sup>3</sup>, Kai-Uwe Hinrichs<sup>4</sup>, Thomas Pichler<sup>5</sup>, Petra Pop Ristova<sup>5</sup>, Roy E. Price<sup>2</sup>, Ioulia Santi<sup>3</sup>, and Miriam Sollich<sup>1</sup>

<sup>1</sup> Young Investigator Group Hydrothermal Geomicrobiology, MARUM, University of Bremen, Bremen, Germany

<sup>2</sup> Department of Earth Sciences, Department of Biological Sciences, University of Southern California, Los Angeles, USA

<sup>3</sup> Max Planck Institute for Marine Microbiology, Bremen, Germany

<sup>4</sup> Organic Geochemistry Group, MARUM, University of Bremen, Bremen, Germany

<sup>5</sup> Geochemistry and Hydrogeology, University of Bremen, Bremen, Germany

**This manuscript is in preparation**

**Contribution:** SH performed *in situ* microsensor measurements

## Abstract

The shallow water hydrothermal vents off Milos Island, Greece, discharge hot, slightly acidic, reduced fluids into colder, slightly alkaline, oxygenated seawater. Gradients in temperature, pH, and geochemistry are established as the two fluids mix, leading to the formation of various microbial microniches. In contrast to deep-sea hydrothermal systems, the availability of sun light allows for a combination of photo- and chemotrophic carbon fixation. Despite the comparably easy accessibility of shallow water hydrothermal systems, little is known about their microbial diversity and functioning. We present data from a shallow hydrothermal system off Milos Island, one of the most hydrothermally active regions in the Mediterranean Sea. The physico-chemical changes from ambient seafloor to hydrothermal area were investigated and documented by *in situ* microsensor profiling of temperature, pH, total reduced sulfur and dissolved oxygen alongside porewater geochemistry. The spatial microbial diversity was determined using a combination of gene- and lipid-based approaches, whereas microbial functioning was assessed by stable isotope probing experiments targeting lipid biomarkers.

*In situ* microprofiles indicated an extreme environment with steep gradients, offering a variety of microniches for metabolically diverse microbial communities. We sampled a transect along a hydrothermal patch, following an increase in sediment surface temperature from background to 90 C°, including five sampling points up to 20 cm sediment depth. Investigation of the bacterial diversity using ARISA revealed differences in the community structure along the geochemical gradients, with the least similarity between the ambient and highly hydrothermally impacted sites. Furthermore, using multivariate statistical analyses it was shown that variations in the community structure could be attributed to differences in the sediment geochemistry and especially the sulfide content, and only indirectly to shifts in temperature.

Results from intact polar lipid analyses were consistent with the ARISA data and clearly differentiated those samples located close to the vent from those found in less affected areas. Changes from phospho- and betaine lipids within the top layer of the

unaffected area to glyco- and ornithine lipids in the hydrothermally influenced sediment layers reflected a change from photoautotrophic algae to a bacteria-dominated community as predominant lipid sources. A clear dominance of archaeal lipids indicated archaea as key players in the deeper, hotter layers of the hydrothermal sediment.

We performed stable isotope probing experiments with  $^{13}\text{C}$ -bicarbonate in the dark to investigate if chemolithotrophy, as opposed to phototrophy, plays any significant role for carbon fixation in shallow vent systems. Different amendments revealed that not only chemolithotrophy represents an important pathway for carbon fixation in these ecosystems, but that diverse ways of dark  $\text{CO}_2$  fixation exist, with hydrogen being the most effective electron donor under high temperature conditions.

## **Availability of light and chemical energy determines the structure of natural sulphide oxidizing biofilms**

Judith M. Klatt<sup>1</sup>, Steffi Meyer<sup>1</sup>, Stefan Häusler<sup>1</sup>, Jennifer L. Macalady<sup>2</sup>, Dirk de Beer<sup>1</sup>, Lubos Polerecky<sup>1,3</sup>

<sup>1</sup>Max Planck Institute for Marine Microbiology, Celsiusstr.1, D- 28359 Bremen, Germany

<sup>2</sup>Pennsylvania State University, University Park, Pennsylvania, USA

<sup>3</sup>Department of Earth Sciences – Geochemistry, Faculty of Geosciences, Utrecht University, Budapestlaan 4, 3584 CD, Utrecht, The Netherlands

**This manuscript is in preparation**

**Contribution:** SH contributed to microsensor measurements

## Abstract

We studied the interaction between phototrophic and chemolithoautotrophic sulphide oxidizing microorganisms in natural microbial biofilms forming in sulfidic streams exposed to daylight. Across the streams, the structure of these biofilms varied between two end-members: one characterized by a cyanobacterial layer on top of a distinct *Beggiatoa* layer (C/B biofilms) and the other with an inverted structure (B/C biofilms). We aimed to elucidate how this structure depends on the availability of energy for these two functional groups, and on their mutual interaction.

C/B biofilms formed where the availability of oxygen, and thus of chemical energy, from the water-column was limited ( $<5 \mu\text{M}$ ). Aerobic chemolithotrophic activity of *Beggiatoa* depended entirely on oxygen produced locally by cyanobacteria, which occurred only during intervals of high incident light intensity. In contrast, B/C biofilms formed at locations where oxygen in the water-column was comparatively abundant ( $>45 \mu\text{M}$ ) and continuously present. Here, *Beggiatoa* were independent of the local photosynthetic activity of cyanobacteria and outcompeted the cyanobacteria in the uppermost layer of the biofilm, i.e., closest to the energy sources for both functional groups. This outcompetition of photosynthetic microbes even in the presence of light was facilitated by the local decoupling of aerobic chemolithotrophy from oxygenic phototrophy.

We conclude that in the presence of uncoupled energy sources, the structure and activity of a long-term stable microbial community is primarily determined by a continuous rather than an intermittent source, even if the time-averaged energy supply from the latter one exceeds that from the former one.



## **Acknowledgements**

It would not have been possible to realize this thesis without the support and encouragement of a number of great colleagues, friends and of course my family.

First I want to thank Danny Ionescu. Danny, during the last years I learned so much from you, not only scientifically but also in terms of diving. Your door is always open for support, advice and good discussions, but not only scientifically but also for other life issues. I will never forget our fieldtrips to the Dead Sea where I experienced my physical and mental limits, but even in such situations you were always in a good mood and you found some encouraging words. Thank you so much for all the support you have given me. You are just the best supervisor ever.

I want to thank Christian Lott and Miriam Weber. Without you and the HYDRA Institute I would have never ended up at the MPI. I learned so much about SCUBA diving from you which helped me to survive and carry out the research in the Dead Sea. Also, thank you so much for your help and support during the first diving campaign in the Dead Sea.

Furthermore, I want to thank all the great people who helped us in the first diving and camping campaign at the Dead Sea shore, with lifting heavy stuff, including us and our diving equipment. Many thanks to Yaniv Munwes, Yuval Lorik, Itzik Califf, Nava Barshai, Boaz Mayzel. For all the help in the second campaign I want to thank Shiri Meshner, Iain Douglas, Beatriz Noriega and Lisa Schüler. Was great with you guys. And of course I want to thank Christian Siebert for the support and the good time we had in Israel. I am also grateful for all the support and lab equipment we got from Aharon Oren and Lily Man.

In particular I would also like to thank Dirk de Beer. Thank you Dirk for giving me the opportunity and of course the financial support to work independently on this topic. Thank you for your valuable input and good ideas. Also, I am so grateful that you have given me the opportunity to go on the fieldtrips to the hydrothermal vent systems in Milos and the cave trips in Frasassi. I learned a lot during this times and on top of it had a lot of fun climbing with you into the darkness.

## Acknowledgements

---

I am also very grateful for the support and advice I got from Tim Ferdelman. Thank you Tim for the discussions about sulfate reduction rates and Pitzer equations. I would also like to thank Marcel Kuypers and Thorsten Dittmar for valuable input during the PhD committee meetings and of course for being my reviewers.

Hannah M. we had a great time during the years at the MPI. Thank you so much for your help, without you I think I would have gone mad.

Mina, Duygu, Judith, Hannah B., Anna, Arjun, Kristina, I am so grateful for the amazing time in the Microsensor group with you guys. We always had good discussions about science or life in general.

A big THANK YOU also goes to the TA's in the Microsensor group for always helping out and building the amazing little microsensors I used throughout the years. The same holds true for Volker, Paul and Harald from the electronic workshop. Guys you are wizards, without your gadgets this thesis would not have been possible.

Finally I want to thank Lena. You went with me through the last three years, supported me throughout and especially in the final weeks of this thesis I do not know what I would have done without you. From the bottom of my heart I thank you so much.

Last but not least I want to thank my family for all the support they have given me and being there for me any time when I need encouragement.



Name: Stefan Häusler

Datum: 15 April 2014

Anschrift : Wielandstr, 30, 28203, Bremen

### **E r k l ä r u n g**

Hiermit versichere ich, dass ich

1. die Arbeit ohne fremde Hilfe angefertigt habe,
2. keine anderen als die von mir angegebenen Quellen und Hilfsmitteln benutzt habe und
3. die den benutzen Werken wörtlich oder inhaltlich entnommenen Stellen als solche kenntlich gemacht habe.

Bremen, den 15 April 2014

-----

(Unterschrift)